Naunyn-Schmiedeberg's Arch Pharmacol (2021) 394 (Suppl 1):S1–S61
DOI 10.1007/s00210-022-02205-7

GERMAN PHARM-TOX SUMMIT 2022

Abstracts
of the

88th Annual Meeting of the German Society for Experimental and Clinical Pharmacology and Toxicology (DGPT)

7 March – 10 March 2022

Digital

This supplement was not sponsored by outside commercial interests. It was funded entirely by the publisher.

Structure

Author Index

Please note that the abstracts are sorted by submission topic.
The submission ID has been kept and is reflected in the programme

Pharmacology – Cardiac pharmacology and treatment

24

Weight loss and gastrointestinal barrier function in high-fat died fed mice that were treated with an AT_1 receptor blocker

L. Nickel[1], A. Sünderhauf[2], E. Rawish[1], I. Stölting[1], S. Derer[2], C. Thorns[3], U. Matschl[4], A. Othman[5], C. Sina[2], **W. Raasch**[1]
[1]University of Lübeck, Institute of Experimental and Clinical Pharmacology and Toxicology, Lübeck, Germany
[2]University Hospital Schleswig-Holstein, Campus Lübeck, Institute of Nutritional Medicine, Lübeck, Germany
[3]University of Lübeck, Institute of Pathology, Lübeck, Germany
[4]Heinrich Pette Institute, Hamburg, Germany
[5]University Hospital Zürich, Institute for Clinical Chemistry, Zürich, Switzerland

Question: The angiotensin II (type 1) (AT_1) receptor blocker (ARB) telmisartan (TEL) is beneficial for the treatment of individuals suffering from metabolic syndrome. As we have recently identified that the anti-obese action of TEL is attributed to diet-independent alterations in gut microbiota, we investigated here whether TEL influences gut barrier function.

Methods*:* C57BL/6N mice were fed for 3 months with chow or high-fat diet (HFD) and treated with vehicle or TEL (8 mg/kg/day). Mucus thickness was determined by immunohistochemistry. Periodic acid-Schiff staining allowed the number of goblet cells to be counted. Using western blots, qPCR, and immunohistochemistry, factors related to mucus biosynthesis (*Muc2, St6galnac*), proliferation (*Ki-67*), or necroptosis (*Rip3*) were measured. The influence of the ARB losartan on cell viability was determined by using the mucus-producing cell line HT29MTX or small intestinal epithelial cells to investigate cell viability as solubility of TEL was too low for in-vitro experiments.

Results: In response to HFD, mice developed obesity as well as leptin and insulin resistance, which were prevented by chronic TEL treatment. While mucus thickness was lower, *Muc2* expression was only tendentially reduced in response to HFD feeding, and albumin excretion (as a sign of worsened intestinal permeability) was unchanged. Independent of feeding, TEL additionally reduced mucus thickness. Numbers of goblet cells were not affected by HFD feeding and TEL. *St6galnac* expression was increased by TEL. *Rip3* was increased in TEL-treated and HFD-fed mice, while *Ki-67* decreased. Cell viability was diminished by using >1 mM losartan.

Conclusions: The anti-obese effect of TEL was associated with a decrease in mucus thickness, which was likely not related to a lower expression of *Muc2* and goblet cells. A decrease in *Ki-67* and increase in *Rip3* indicates lower cell proliferation and necroptosis upon TEL. However, direct cell toxic effects are ruled out, as in-vivo concentrations are lower than 1 mM. This conclusion seems justified, as albumin excretion was not impaired in TEL-treated animals in our study. Nevertheless, follow-up studies are need to elucidate whether this detrimental TEL effect is relevant for gastrointestinal function.

29

Determination of COX-1-derived prostacyclin as a key mediator in bradykinin-induced dermal extravasation

M. Krybus[1], M. Sieradzki[1], E. Fahimi[1], S. Metry[1], R. Nüsing[2], G. Geisslinger[2], I. Steiner[3], T. Daldrup[3], M. Lehr[4], G. Kojda[1]
[1]Institute of Pharmacology and Clinical Pharmacology, Heinrich Heine University, Düsseldorf, Germany
[2]Institute of Clinical Pharmacology, Johann Wolfgang Goethe University, Frankfurt, Germany
[3]Institute of Forensic Medicine, Heinrich Heine University, Düsseldorf, Germany
[4]Institute of Pharmaceutical and Medicinal Chemistry, University of Münster, Münster, Germany

Introduction: Bradykinin (BK) is a key mediator in non-allergic angioedema (AE) such as hereditary AE or ACE inhibitor-induced AE. In small dermal blood vessels, signaling via the G_q-coupled BK receptor type 2 (B2) and subsequent COX activation seems to play an essential role.

Objectives: The aim was to determine which prostaglandins (PG) are the key mediators in B2 signaling and to find out which COX, COX-1 or COX-2, is predominantly involved.

Methods: We used the Miles assay to quantify dermal extravasation of the albumin binding dye Evans blue in dorsal skin of C57BL/6 (B6) and COX-1-deficient mice ($COX\text{-}1^{-/-}$) induced by i.d. injections of PBS, BK, the proteolytically stable BK-analogue labradimil (LD) and histamine (His) after i.p. pretreatment with inhibitors of COX or PG receptor antagonists. In addition, the stable metabolite of prostacyclin (PGI_2), 6-keto-$PGF_{1\alpha}$ (6K), was quantified as an indicator for PGI_2 production by ELISA in subcutaneous tissue from B6 and human dermal microvascular endothelial cells (HDMEC) treated with BK. In the latter, we also quantified and qualified 6K by LC-MS/MS.

Results: In B6, 2 nmol of BK induced an increase of extravasation reaching 4.26±0.07 (fold increase±SEM, n=6, P<0.0001) in comparison to PBS. Pretreatment of B6 with the unspecific COX inhibitor diclofenac reduced the extravasation to 2.26±0.28 (n=6, P<0.0001). A lesser reduction was observed using the more COX-2 specific etoricoxib before i.d. BK (n=5, to 3.03±0.14, P=0.0015). No significant effects could be observed for any COX inhibitor in $COX\text{-}1^{-/-}$ while extravasation in $COX\text{-}1^{-/-}$ was generally lower than in B6. Of the PG antagonists used, only the PGI_2 receptor antagonist RO1138452 showed a significant reduction of dermal extravasation induced by BK in B6 (n=6, to 2.94±0.13, P<0.0001) but not $COX\text{-}1^{-/-}$. Similar effects were observed for LD- but not His-induced dermal extravasations. Moreover, 6K concentrations were increased in the ELISA after BK treatment in subcutaneous tissue of B6 (n=6, from 0.21±0.08 pg mg^{-1} to 4.64±0.66 pg mg^{-1}, P<0.0001) as well as in HDMEC (n=6, from 29.15±6.64 pg mL^{-1} to 405.2±42.10 pg mL^{-1}, P<0.0001) and this increase was abolished by diclofenac. In HDMEC, this result could be verified by LC-MS/MS while also identifying 6K by its mass of 370 g mol^{-1}.

Conclusion: Our results suggest that the generation of PGI_2 predominantly formed by COX-1 most likely contributes to B2-mediated edema formation in small dermal blood vessels.

53

L-citrulline ameliorates pathophysiology in a rat model of superimposed preeclampsia

A. Man[1], Y. Zhou[1], U. Lam[1], G. Reifenberg[1], A. Werner[1], A. Habermeier[1], E. Closs[1], A. Daiber[1], T. Münzel [1], N. Xia[1], H. Li[1]
[1]Johannes Gutenberg University Medical Center, Pharmacology, Mainz, Germany

Question: Preeclampsia, characterized by hypertension, proteinuria, and fetal growth restriction, is one of the leading causes of maternal and perinatal mortality. By far, there is no effective pharmacological therapy for preeclampsia. The present study was conducted to investigate whether maternal f L-citrulline supplementation can amliorates the phenotype in preganant Dahl salt-sensitive rat, a model of superimposed preeclampsia.

Methods: Parental DSSR were treated with L-citrulline (2.5 g/L in drinking water) from the day of mating to the end of lactation period. Blood pressure of the rats was monitored throughout pregnancy and markers of preeclampsia were assessed. Endothelial function of the pregnant DSSR was assessed by wire myograph.

Results: L-citrulline supplementation significantly reduced maternal blood pressure, proteinuria, and levels of circulating soluble fms-like tyrosine kinase 1 in DSSR. L-citrulline improved maternal endothelial function by augmenting the production of nitric oxide in the aorta and improving endothelium-derived hyperpolarizing factor-mediated vasorelaxation in resistance arteries. L-citrulline supplementation improved placental insufficiency and fetal growth, which were associated with an enhancement of angiogenesis and reduction of fibrosis and senescence in the placentas. In addition, L-citrulline downregulated genes involved in the toll-like receptor 4 and nuclear factor-κB signaling pathway.

Conclusions: This study shows that L-citrulline supplementation reduces gestational hypertension, improves placentation and fetal growth in a rat model of superimposed preeclampsia. L-citrulline supplementation may represent an effective and safe therapeutic strategy for preeclampsia that benefit both the mother and the fetus.

77

Store-operated calcium entry differs between atrial and ventricular cardiomyocytes

J. Hermes[1], J. Kockskämper[1]
[1]Philipps-University Marburg, Institute for Pharmacology and Clinical Pharmacy, Marburg, Germany

Question: Nuclear calcium (Ca) regulation and store-operated Ca entry (SOCE) via plasma membrane channels (TRPC or Orai) have both been implicated in cardiac remodeling during hypertrophy and heart failure. It is not known, however, how SOCE might affect nuclear Ca in cardiomyocytes. Furthermore, potential differences in this regulation between atrial and ventricular myocytes have not been studied before. Hence, we set out to determine SOCE in atrial and ventricular myocytes and characterize its impact on nuclear Ca regulation.

Methods: Isolated atrial and ventricular myocytes from 12-16 weeks old rats were loaded with Fluo-4/AM (8µM, 20-30min) and electrically-stimulated at 1Hz. Cytoplasmic and nuclear Ca transients (CaTs) were imaged simultaneously using linescan confocal microscopy. SOCE was elicited by readdition of Ca (2mM) following depletion of the SR by zero Ca solution containing thapsigargin (0.5µM), verapamil (5µM), KB-R7943 (10µM) and bolus application of caffeine (20mM).

Results: There was a linear correlation between the amplitude of SOCE in the nucleus (nuc) and cytoplasm (cyto) with a slope close to 1 in both atrial and ventricular myocytes. SOCE amplitude amounted to a median of 0.45 (and 25 to 75 percentiles at 0.32 and 0.81) ΔF/Frest in cyto vs 0.56 (0.32/1.17) ΔF/Frest in nuc (P<0.01 vs cyto) in ventricular myocytes (n=39). It was significantly larger in atrial myocytes (n=21) with amplitudes of 0.98 (0.77/1.56) ΔF/Frest in cyto vs 1.09 (0.68/1.44) ΔF/Frest in nuc (P<0.01 vs cyto) (both P<0.05 vs ventricular). S66 (1µM, n=26) or BTP-2 (3µM, n=31), inhibitors of Orai/Stim, reduced SOCE in ventricular myocytes in cyto and nuc by ≈30-40%. SKF96365 (5µM, n=28), an inhibitor of TRPC channels, reduced SOCE in cyto and nuc by ≈35-40%. Combining S66 and SKF (n=20) had an additive effect reducing SOCE in cyto and nuc by ≈65%. By contrast, in

atrial myocytes, S66 (n=27) alone reduced SOCE in cyto and nuc by ≈70-80%, whereas combining S66 and SKF (n=28) had no additive effect (reduction of SOCE in cyto and nuc by ≈65-70%).

Conclusion: In both atrial and ventricular myocytes, nuclear SOCE depends on cytoplasmic SOCE. It is larger in atrial than in ventricular myocytes. In atrial myocytes, SOCE is driven mainly through Orai/Stim, whereas in ventricular myocytes both Orai/Stim and TRPC appear to contribute to SOCE.

78

Tunicamycin elicits proarrhythmic calcium release in electrically-stimulated rat cardiomyocytes

V. Hammer[1], J. Sommer[1], J. Kockskämper[1]
[1]Philipps-University, Institute for Pharmacology and Clinical Pharmacy, Marburg, Germany

Question: The sarco-/endoplasmic reticulum (SR/ER) is the major intracellular calcium (Ca) store in cardiomyocytes and also the major site of protein quality control. Disruption of ER homeostasis leads to accumulation of unfolded/misfolded proteins and ER stress. ER stress has been linked to physiological and pathophysiological conditions in the cardiovascular system. Using a well-known ER stress-inducing agent, Tunicamycin, we tested its acute effects on intracellular Ca regulation in rat ventricular myocytes.

Methodes: Cytoplasmic Ca (cytoCa) was measured in isolated rat ventricular myocytes loaded with Fluo-4-AM while electrically-stimulated at 1Hz for 12min in the absence (control) or presence of Tunicamycin (10 mg/ml). Confocal linescan imaging was employed to visualize Ca transients (CaTs). Sarcomere length was measured in unloaded cardiomyocytes.

Results: After stimulation for 12min, CaTs of control myocytes (n=13) showed no changes in diastolic Ca, but a decrease in systolic Ca and CaT amplitude (from 2.85±0.26 to 2.33±0.16 dF/Frest, p<0.01), while kinetic parameters were unchanged. By contrast, exposure to Tunicamycin (n=13) significantly increased diastolic Ca (from 1.03±0.01 to 1.16±0.04 F0/Frest, p<0.01), while systolic Ca and CaT amplitude remained unchanged. Moreover, Tunicamycin slowed down CaT decay time (from 330±19ms to 402±26ms, p<0.01). Furthermore, an increase of proarrhythmic Ca release was observed in Tunicamycin-treated cardiomyocytes mostly evident as Ca waves. While control cells showed no proarrhythmic Ca release (0 out of 13 cells), such events were observed in 9 out of 20 Tunicamycin-treated myocytes (p<0.01). Similarly, the fraction of cells exhibiting spontaneous contractions increased from 22% in control to 78% in the presence of Tunicamycin (p<0.0001).

Conclusion: Tunicamycin causes acute perturbations of Ca handling in ventricular cardiomyocytes by increasing diastolic Ca and CaT decay time as well as proarrhythmic Ca release and spontaneous contractions. The underlying mechanisms, however, remain to be determined.

105

Inactivation of HDAC2 attenuates atrial remodeling and delays the onset of atrial fibrillation in CREM-IbΔC-X transgenic mice

L. B. Tardio[1], J. P. Reinhardt[1], M. D. Seidl[1], U. Kirchhefer[1], F. U. Müller[1], J. S. Schulte[1]
[1]Institute of Pharmacology and Toxicology, UKM, University of Münster, Münster, Germany

Objectives: We recently demonstrated that valproic acid, an inhibitor of histone deacetylase (HDAC) isoforms 1, 2, 3 and 8 at therapeutic doses, is able to delay the development of atrial remodeling and the onset of atrial fibrillation (AF) in CREM-IbΔC-X transgenic mice (TG), a well-characterized model with extensive atrial remodeling and spontaneous onset of AF. Here we investigated the specific role of HDAC2 for atrial remodeling and intracellular Ca^{2+} dynamics in TG mice.

Material & methods: Mice with cardiomyocyte-specific knockout of HDAC2 (KO) were generated by crossbreeding $HDAC2^{loxP/loxP}$ and $\alpha MHC^{Cre+/-}$ mice and were then mated with TG mice. ECG recordings and estimations of atrial weights were performed on CTR ($FVB/N^{Cre+/-}$), KO, TG ($CREM\text{-}IbΔC\text{-}X^{Cre+/-}$) and TGxKO mice. Recordings of spontaneous intracellular Ca^{2+} (Ca^{2+}_i) releases with Fluo-4/AM and measurements of the cell size were performed in isolated atrial cardiomyocytes (ACMCs).

Results: TG mice (6 weeks, before onset of AF) developed atrial dilatation reflected by an increase in atrial weight. However, left atrial weight (LAW) was less increased in TGxKO mice compared to TG mice (LAW/body weight in mg/g±SD; CTR: 0.15±0.01, TG: 0.24±0.03$^{\#}$, TGxKO: 0.19±0.04; n=5-14) while right atrial weight was unaffected. Mean cell length and area were reduced in TGxKO mice compared to TG mice (Cell length in µm±SD: CTR: 96±7, TG: 153±15$^{\#}$, TGxKO: 132±10$^{*,\#}$; n=9-11, 25-52 cells per image). Spontaneous Ca^{2+}_i releases were recorded in ACMCs from 6 week old mice. The occurrence of spontaneous Ca^{2+}_i oscillations increased from 21% in CTR to 41%$^{\#}$ in TG while only 11%* of TGxKO ACMCs showed Ca^{2+}_i oscillations (n=9-12, 5-10 ACMCs/animal). Finally, the onset of AF was delayed in TGxKO vs TG mice (n=12-33). However, a detailed analysis showed that this could be observed almost exclusively in female mice. (*p<0.05 vs TG, $^{\#}$p<0.05 vs CTR).

Conclusion: Cardiomyocyte-specific inactivation of HDAC2 attenuated structural remodeling of atria and normalized increased spontaneous Ca^{2+}_i oscillations in ACMCs of CREM-IbΔC-X transgenic mice. However, it delayed the onset of AF exclusively in female mice. This demonstrates that HDAC2 plays an important role in Ca^{2+} dynamics and atrial remodeling. The impact of HDAC2 inactivation on gene and protein regulation and its alteration due to sex differences needs to be investigated in future studies.

Supported by the DFG

107

Heart-on-a-Chip: Microphysiometric monitoring of cardiomyocytes differentiated from human induced pluripotent stem cells

S. Eggert[1], K. Hariharan[2], **J. Wiest**[1]
[1]cellasys GmbH, Kronburg, Germany
[2]Fraunhofer-Institute for Biomedical Engineering (IBMT), Fraunhofer Project Center for Stem Cell Process Engineering, Würzburg, Germany

Microphysiometry is the measurement of the functions and activities of life or of living matter and of the physical and chemical phenomena involved [1]. It allows label-free monitoring of cellular metabolism and morphology of living cells and enables new applications in fields such as pharmacology or toxicology. Recently, we were able to extend the method toward monitoring of 3D cellular models, referred to as Organ-on-a-Chip [3-5]. To demonstrate the applicability of microphysiometry with human cardiomyocytes, a cellasys #8 assay [2] was performed via label-free and non-destructive monitoring of metabolic and morphological changes. IBMT cardiomyocytes from human induced pluripotent stem cells (hiPSCs) were cultivated on BioChips from day 22 to day 30. After transportation of the BioChips from Würzburg to Munich and overnight incubation, the cardiomyocytes were successfully checked optically for their beating activity. Then, a cellasys #8 assay was performed to identify changes after the transition from a serum-based to a chemically defined media without serum. During the 24h cellasys #8 assay, the extracellular acidification and changes in impedance of the cells were monitored in real-time. The FBS-free medium caused a decrease in the metabolic activity; however, the impedance values did not change essentially. The results indicate that the FBS-free test medium is a candidate for further use in more defined experiments using hiPSCs. The proof-of-principle measurement with human induced pluripotent stem cells demonstrated that microphysiometry is a promising tool for use in pharmacology and toxicology. In addition, it was possible to show that hiPSCs keep their functionality after a half day transportation between laboratories.

[1] Brischwein, M., Wiest, J.: Microphysiometry. In: Bioanalytical Reviews, Springer, 2018, doi:10.1007/11663_2018_2

[2] https://www.cellasys.com/downloads/cellasys-8/

[3] Alexander, F., Eggert, S., Wiest, J.: A novel lab-on-a-chip platform for spheroid metabolism monitoring, Cytotechnology, 2018, 70/1, 375-386, doi:10.1007/s10616-017-0152-x

[4] Alexander, F., Eggert, S., Wiest, J.: Skin-on-a-chip: Transepithelial electrical resistance and extracellular ..., Genes, 2018, 9/2, 114, doi:10.3390/genes9020114

[5] Schmidt, C. Markus, J. Kandarova, H., Wiest, J.: Tissue-on-a-Chip: Microphysiometry with human 3D-models on transwell inserts, Frontiers in Bioengineering and Biotechnology, 2020, 8:760, doi: 10.3389/fbioe.2020.00760

140

Evaluation of ERK^{T188} phosphorylation on inflammatory cells and their responses

J. N. Herbel[1], N. Amézaga Solé[2], K. Lorenz[1,3], A. Zernecke-Madsen[2]
[1]Universität Würzburg, Pharmakologie und Toxikologie, Würzburg, Germany
[2]Uniklinikum Würzburg, Experimentelle Biomedizin, Würzburg, Germany
[3]Leibniz-Institut für Analytische Wissenschaften, ISAS e.V., Dortmund, Germany

Background and hypothesis: The extracellular signal-regulated kinases 1 and 2 (ERK1/2) are part of a central signaling cascade in which various extracellular signals converge. ERK1/2 are involved in physiological and pathological effects such as cardiac hypertrophy, heart failure and cancer. An autophosphorylation at threonine 188 in ERK2 (pERKT188) has been shown to trigger nuclear ERK translocation and target activation and has thus far only been associated with pathological conditions, i.e. cardiac hypertrophy. Since cardiac hypertrophy and cancer can include inflammatory processes and since pERKT188 appears to act at the patho-physiological interface, it could be of great relevance in inflammation and heart failure. This study evaluates the impact of pERKT188 in immune cells like antigen-presenting cells (APC) and T cells.

Methods and results: To assess a potential induction of pERKT188 in inflammatory cells, we isolated APC including dendritic cells and macrophages and stimulated these cells with inflammatory triggers, i.e. LPS and TNFα. Western blot analyses of pERKT188 indeed revealed a significant increase.

To evaluate whether pERKT188 impacts on T-cell polarization, we co-cultured APC isolated from mice with ubiquitous expression of an ERK2 mutant simulating pERKT188, i.e. CAG-ERK2T188D (T188D), of a mutant that cannot be phosphorylated at this site, i.e. CAG-ERK2T188A (T188A), or of wild type (WT) littermates, with naïve CD4+ T cells from mice expressing a T cell receptor which is specific for ovalbumin 323-339 (OT-II mice). Indeed, APCs of T188D mice pulsed with ovalbumin 323-339 influenced the polarization of these CD4+ T cells towards a pro-inflammatory (Th1 T cells) phenotype as detected by flow cytometry. In contrast to this, APC derived from T188A mice triggered a more anti-inflammatory T-cell phenotype (Treg T cells). Also, flow cytometric analyses of spleen and lymph nodes of these mice revealed an increase of activated CD8+ T cells in T188D compared to WT and T188A mice. Of note, IFNy producing CD8+ T cells were increased in T188D, while CD8+ T cells of T188A mice showed an increased expression of PD-1, an immune checkpoint that plays a pivotal role in immune-regulation and is a target in cancer therapy.

Conclusion: Taken together, $pERK^{T188}$ seems to be involved in immune cell signaling and responses. Future analyses will help to clarify the (patho)physiological impact of $pERK^{T188}$ in the development of cancer and heart diseases.

143

Cardiac function in PP2CxPP5 overexpressing mice

R. Schwarz[1], U. Gergs[1], J. Neumann[1]
[1]Institute for Pharmacology and Toxicology, Medical Faculty, Martin Luther University Halle-Wittenberg, Halle (Saale), Germany

Question: Overexpression of the serine/threonine protein phosphatase (PP) 2C (PP2C) in cardiomyocytes is already known to lead to cardiac hypertrophy and dysfunction (Bollmann et al., Front Pharmacol. 2021;11:591773). The effects of cardiac PP5 overexpression are more subtle but an interaction with, for example PP2A, is known (Dörner et al., Int J Mol Sci. 2021;22(17):9448). We hypothetized that there is also an interaction between PP2C and PP5, because they are both present in human cardiomyocytes. To study signaling pathways of both protein phosphatases, we crossbred mice with cardiac overexpression of PP2C (PP2C-TG) and those with overexpression of PP5 (PP5-TG) to generate double transgenic (DT) mice.

Methods: The relative heart weight was measured in about six months old wild type (WT), PP2C-TG, PP5-TG and DT mice. Left ventricular force of contraction was measured in isolated spontaneously beating Langendorff-perfused hearts.

Results: Compared to WT mice the relative heart weight was increased in PP2C-TG and DT mice (7.40 ± 0.47 mg/g vs. 8.88 ± 0.97 mg/g and 10.13 ± 1.46 mg/g, $p < 0.05$). Relative heart weight was also increased in DT compared to PP5-TG mice (10.13 ± 1.46 mg/g vs. 8.06 ± 1.25 mg/g, $p < 0.05$, n= 4-8). The basal force in PP2C and DT mice was decreased compared to WT (7.87 ± 2.79 mN and 9.27 ± 2.65 mN vs. 13.91 ± 3.50 mN, $p < 0.05$, n= 6-8). The spontaneous frequency was decreased in DT mice compared to WT and PP2C (308.03 ± 49.82 bpm vs. 378.64 ± 52.15 bpm and 411.34 ± 40.27 bpm, $p < 0.05$, n= 6-8).

Conclusion: Co-overexpression of PP2C and PP5 leads to enhanced cardiac hypertrophy and further impaired cardiac function compared to overexpression of these PPs alone.

145

Functional evidence for phosphodiesterase inhibitory effects of levosimendan in mouse and human atrium

L. M. Rayo Abella[1], B. Hofmann[2], U. Gergs[1], J. Neumann[1]
[1]Institute for Pharmacology and Toxicology, Medical Faculty, Martin Luther University Halle-Wittenberg, Halle (Saale), Germany
[2]Department of Cardiac Surgery, Mid-German Heart Center, University Hospital Halle, Halle (Saale), Germany

Question: Levosimendan can increase the force of contraction in isolated atrial and ventricular preparations from guinea pig heart and from human ventricle. Initial data argued that levosimendan increased force of contraction only by increasing the sensitivity of myofilaments for calcium cations. Others presented experimental evidence that an inhibition of the activity of phosphodiesterases in the rat and human heart can alone explain the positive inotropic effect of levosimendan in these tissues. Hence, it remains controversial which mechanism(s) of action are utilized by levosimendan in the human heart.

Methods: Therefore, we studied the contractile effects of levosimendan in isolated electrically stimulated (1 Hz) muscle preparations from the human atrium. For comparison, we studied the inotropic and chronotropic effects of levosimendan in electrically stimulated (1 Hz) left atrial and spontaneously beating right atrial preparations from wild type mice using the same experimental setup.

Results: In human atrium, we detected a concentration and time dependent positive inotropic effect of levosimendan that reached plateau at 1 µM levosimendan with an EC50 value of about 7.2 nM for levosimendan. Levosimendan (0.3 µM and higher) shortened time to peak tension, time of relaxation, rate of force development and rate of relaxation in these human atria. Cilostamide (1 µM), an inhibitor a phosphodiesterase III, blocked the positive inotropic effect of levosimendan and propranolol (10 µM) reversed the positive inotropic effect of 10 µM levosimendan in isolated human atrial preparations. In contrast to the human atrium, in isolated mouse atrium in the organ bath, levosimendan (up to 10 µM) given alone failed to increase force of contraction or beating rate. Only in the additional presence of 0.1 µM rolipram, an inhibitor of the activity of phosphodiesterase IV, additionally applied levosimendan increased force of contraction and beating rate in isolated left or right atrial preparations from mice. The inotropic and chronotropic effects of levosimendan in the presence of rolipram in isolated mouse left or right atrial cardiac preparations were abolished by previously or subsequently applied propranolol.

Conclusion: In conclusion, we present evidence that levosimendan acts via phosphodiesterase inhibition in the human atrium and mouse atrium.

146

Effects of phosphoglycolate phosphatase inhibitors on the contractility and beating rate of mouse atrial preparations

C. Höhm[1], U. Gergs[1], J. Neumann[1], A. Gohla[2]
[1]Institute for Pharmacology and Toxicology, Medical Faculty, Martin Luther University Halle-Wittenberg, Halle (Saale), Germany
[2]Institute of Pharmacology and Toxicology, University of Würzburg, Würzburg, Germany

Question: Phosphoglycolate phosphatase, a member of the haloacid dehalogenase superfamily of hydrolases, is broadly expressed in mammalian tissues. Phosphoglycolate phosphatase can affect several metabolic pathways such as glycolysis and fat metabolism. Furthermore, phosphoglycolate phosphatase (PGP) might be relevant to regulating cardiac contractility.

Methods: We tested PGP-specific inhibitors, here called Compound 1 and Compound 2, in electrically stimulated left atrial preparations (1 Hz) and spontaneously beating right atrial preparations from wild type mice. We constructed cumulative concentration response curves to Compound 1 alone or Compound 2 alone from 100 nM up to 10 µM, under which conditions no inotropic or chronotropic effect was visible ($p>0.05$, n=5-7). Therefore, we studied 10 µM of Compound 1 or 2 in presence of 10 nM of the β_1 and β_2-adrenoceptor agonist isoprenaline and measured their effects on the force of contraction and spontaneous beating rate for 30 minutes.

Results: Under the latter experimental conditions, a maximum effect was observed after five minutes. Compound 1 attenuated the positive inotropic effect of isoprenaline by 21.4% ± 1% ($p<0.05$, n=8). In contrast, Compound 2 was slightly less effective and attenuated the positive inotropic effect by 20.6% ± 1.6% ($p<0.05$, n=8). In comparison to Compound 1 and Compound 2, their solvent namely dimethyl sulfoxide, decreased the positive inotropic effect only by 13% ± 0.7%, n=13). Both compounds as well as dimethyl sulfoxide did not alter the isoprenaline-induced positive chronotropic effect in mouse right atrial preparations.

Conclusion: We conclude that if compound 1 and 2 only affect PGP under our experimental conditions, one might speculate that PGP amplify the β-adrenoceptor-mediated positive inotropic effects in mammalian hearts and thus affect cardiac contractility. PGP does not seem to act on the sinus node in the mouse heart.

150

smRNA-FISH-based visualization of spatial mRNA expression upon right heart failure in whole heart sections

L. Jurida[1], S. Werner[1], F. Knapp[2], S. Rohrbach[2], M. Kracht[1]
[1]Justus-Liebig-Universität Giessen, Rudolf-Buchheim-Institut für Pharmakologie, Gießen, Germany
[2]Justus-Liebig-Universität Giessen, Institut für Physiologie, Giessen, Germany

Question: Heart failure is a leading cause of death worldwide. Right ventricular failure develops as a consequence of pulmonary arterial hypertension (PAH) with no specific treatment options available. The right ventricle (RV) differs developmentally, anatomically and functionally from the left ventricle (LV), which limits direct application of the substantial knowledge concerning LV failure for improving RV function. Therefore, a deeper understanding of the molecular, right ventricle-specific events in cardiac hypertrophy and subsequent failure is urgently needed. This includes the adaption of methods that allow visualizing gene expression in the heart directly with spatial and single cell resolution.

Methods: To identify molecular signatures and mechanisms of heart failure (HF) specific to the RV, we have established an animal model based on weanling rats, which develop two clearly distinguishable, slowly forming stages of disease (compensated and decompensated) in response to aortic or pulmonary artery banding (AOB, PAB). We performed a systematic comparison of functional and transcriptomic changes (RNAseq) occurring in rats undergoing AOB and PAB during compensated and decompensated states of progressive HF. The RNAseq data revealed a list of differentially expressed genes with potential roles in right heart hypertrophy and failure. We prepared 7 µm transverse sections of whole hearts from frozen tissue of sham treated and PAB rats from the decompensated stage. Fluorophore-labelled probes against 15 genes were hybridized to these sections. Using LAX and ICY software individual mRNA spots were quantified by scanning entire sections.

Results & Conclusion: Our data show that smRNA-FISH confirms differential gene expression upon PAB. The data reveal that basal and PAB-induced mRNA expression can differ substantially between left and right ventricle (e.g. Nppa). Moreover, while

some genes (e.g. Myh6) are abundantly and evenly expressed across the heart tissue, some inducible genes such as NppA are expressed in a highly localized fashion. The smRNA-FISH can now be further used to validate RNAseq data and identify regions in the heart that respond differentially to PAB or AOB.

182

Collagen expression in human cardiac fibroblasts is closely regulated by the unfolded protein response mediator PERK

A. DeGrave[1], T. Doan[1], S. Weinbrenner[1], S. Lutz[1]
[1]Institute of Pharmacology and Toxicology, Goettingen, Germany

Upon cardiac injury, cardiac fibroblasts (CF) transition into myofibroblasts, which display a higher secretory activity. This process involves an adaptation of the endoplasmic reticulum (ER) to the enhanced cargo load. Accordingly, we found that mechanical stress induces a variety of folding proteins and ER regulators in 3D engineered connective tissues (ECT), made of human CF and collagen. Amongst these was the protein kinase RNA-like ER kinase (PERK), which is one of the three master regulators of the unfolded protein response (UPR). We hypothesized that interference with PERK could prevent ER adaptation and thus the fibrotic response. We demonstrate that the PERK inhibitor GSK-2656157 indeed reduced the COL1A1 transcript level in ECT, which encodes the main cargo molecule Pro-collagen 1 in CF. Consequently, the tissue stiffness was reduced. Surprisingly, signs of moderate ER stress were found upon treatment, exemplified by the up-regulation of the UPR target DDIT3. To further understand the molecular mechanism behind this regulation, we treated 2D-cultured CF with the PERK inhibitors GSK-2656157 and AMG PERK 44 in the presence and absence of the ER stress inducer Thapsigargin (Tg). Without Tg, both inhibitors reduced the amounts of intracellular and secreted Pro-collagen 1 in a concentration-dependent manner. Tg alone resulted in a complete loss of Pro-collagen 1 and the combination of the PERK inhibitors with Tg partly restored the Pro-collagen 1 levels. The latter effect was expected as during high ER stress, PERK induces a translational blockade. Based on the only partial restoration of Pro-collagen 1 levels, we hypothesized that the second UPR master regulator IRE1α-induced RNA decay (RIDD) could be involved in this process. To test this, we used 4μ8C, which is an inhibitor of the RNAse activity of IRE1α. Contrary to our hypothesis, 4μ8C treatment resulted similarly to the PERK inhibitors in a concentration-dependent loss of Pro-collagen 1 and in no restoration in the presence of Tg. Interestingly, PERK expression was similarly regulated as Pro-collagen 1 in all investigated conditions. Taken together, our data demonstrates that in CF collagen expression is closely controlled by the unfolded protein response mediator PERK, which could therefore serve as an interesting target for an anti-fibrotic therapy.

190

microRNA-21 inhibition as a treatment for preventing adverse cardiac remodelling and dysfunction following myocardial infarction.

I. Duran Fernandez[1], D. Ramanujam[1], C. Beck[1], P. Vaccarello[1], S. Engelhardt[1]
[1]Institute of Pharmacology and Toxicology, Technical University of Munich, Munich, Germany

The default response to myocardial injury is fibrosis, where the infarct necrotic tissue is replaced with a fibrotic scar, causing loss of cardiac contractility and progressive heart failure. MicroRNA-21 is a central regulator of cardiac inflammation and fibrosis in cardiac disease, and it is highly expressed in cardiac cells after myocardial injury. miR-21 inhibition using small inhibitors prevented myocardial dysfunction in small and large animal models of heart failure. A previous study on a pig model of ischemia reperfusion revealed that miR-21 inhibition attenuated cardiac remodelling and dysfunction primarily through modifying myocardial macrophages and fibroblasts. Here, we aimed to determine the in vivo targetome of miR-21 in macrophages and fibroblasts using Argonaute2-ribonucleoprotein immunoprecipitation (AGO-RIP) in the presence of an antimiR specific for this microRNA.

Wild type mice were subjected to myocardial infarction (MI) by ligation of the left anterior descending artery and a synthetic inhibitor of miR-21 was injected for three consecutive days, starting at day 7 after the injury. Two days after the last antimiR injection (day 11), the hearts were harvested and the main cardiac cell types isolated. AGO-RIP followed by next generation sequencing was carried out to identify miR-21 targets related to ischemia-induced heart failure by means of their de-enrichment in the AGO2-bound transcriptome and de-repression in the mRNA transcriptome. Echocardiography was carried out to evaluate cardiac function before surgery and at days 7 and 11 after surgery.

Mice administered with antimiR-21 were protected from cardiac dysfunction induced by MI, measured globally by ejection fraction, and regionally by longitudinal train of the heart. Bioinformatic analysis of the transcriptomes and the corresponding targetomes revealed a strong de-enrichment (AGO2-RIP) and de-repression (input) of miR-21 targets in macrophages isolated from antimiR-21-treated hearts as compared to antimiR-control-treated hearts. Gene ontology analysis indicated a strong repression of genes associated with extracellular matrix organization in line with the recently established pro-fibrotic role of cardiac macrophages in cardiac remodelling.

Taken together, our data indicate macrophage miR-21 as an important regulator of ischemia-induced cardiac dysfunction and a potential target for therapeutic intervention in cardiac ischemia.

200

Monitoring beta1-adrenoceptor phosphorylation in human heart

A. Ahles[1], L. Hinz[1], J. Herrmann[1], S. Meunier[1], R. Feederle[2], H. Milting[3], A. Dendorfer[4], S. Engelhardt[1,5]
[1]Technische Universität München, Institut für Pharmakologie und Toxikologie, München, Germany
[2]Helmholtz Zentrum München, München, Germany
[3]Herz- und Diabeteszentrum NRW, Universitätsklinik der Ruhr-Universität Bochum, Bad Oeynhausen, Germany
[4]Ludwig-Maximilians-Universität München, Biomedizinisches Centrum München, München, Germany
[5]German Center for Cardiovascular Research (DZHK), Partner Site Munich Heart Alliance, München, Germany

Beta-blockers display one of the major classes of drugs to treat cardiovascular disorders. Treatment outcome is supposed to depend on genetic variation as well as on specific intracellular signaling properties of specific beta-blockers. In this regard, carvedilol is known to block classical adenylyl cyclase activation, yet it promotes intracellular phosphorylation of beta-adrenoceptors by G protein-coupled receptor kinases in cell culture studies. The resulting phosphorylation pattern is proposed to trigger arrestin recruitment and receptor desensitization and thus defines receptor activity.

Using mass spectrometry, we have previously determined the exact sites of intracellular phosphorylation of the human beta1-adrenoceptor (ADRB1) and identified a specific site in the distal C-terminus of the ADRB1 to become phosphorylated upon agonist stimulation, and to determine β-arrestin2 recruitment to the ADRB1 and receptor internalization. To monitor receptor phosphorylation at this site in humans, we generated monoclonal phosphosite-specific antibodies. The specificity of these antibodies was verified in HEK293 cells overexpressing the wild-type receptor or a phosphorylation-deficient receptor mutant. We next assessed ADRB1 phosphorylation in human heart samples of patients with dilated cardiomyopathy (DCM) and healthy controls. Phosphorylation was significantly increased in DCM patients, and this correlated with an increase in MAP kinase phosphorylation. The extent of phosphorylation was dependent on beta-blocker treatment as well as on the most common polymorphism in the ADRB1 - p.Arg389Gly.

We propose that monitoring ADRB1 phosphorylation might mirror ADRB1 activity. Our approach may prove useful to delineate pivotal and previously undetectable differences among clinically used beta-blockers and thereby improve their clinical application.

241

A novel direct inducible non-genetic murine model of diabetes-accelerated atherosclerosis

S. Gaul[1], K. Shahzad[2], **R. Medert**[3], B. Isermann[2], U. Laufs[1], M. Freichel[3]
[1]Universitätsklinikum Leipzig, Klinik und Poliklinik für Kardiologie, Leipzig, Germany
[2]Institute of Laboratory Medicine, Clinical Chemistry and Molecular Diagnostics, Department of Diagnostics, University Hospital Leipzig, Leipzig, Germany
[3]Heidelberg University, Institute of Pharmacology, Heidelberg, Germany

Background and Aims: Atherosclerosis is accelerated in diabetic patients. Genetic mouse models of atherosclerosis require breeding efforts which are time-consuming and costly and often display alterations in lipoprotein metabolism and inflammatory processes. This study aimed to establish a new non-genetic model of inducible metabolic risk factors mimicking hyperlipidemia and hyperglycemia and allowing to detect phenotypic differences dependent on the metabolic stressor(s).

Methods and Results: Wild type mice were injected with gain-of-function PCSK9D377Y (proprotein convertase subtilisin/kexin type 9) mutant adeno-associated viral particles (AAV) and streptozotocin (STZ) and fed either a high-fat diet (HFD) or high-cholesterol/high fat-diet (Paigen diet, PD) for 12 and 20 weeks. Combined hyperlipidemic and hyperglycemic mice, but not hyperlipidemia alone, display characteristic features of accelerated atherosclerosis characterized by larger and less stable plaques which contained more macrophages (MOMA-2 in diabetic HFD: 27% vs non-diabetic HFD: 19% area/plaque, after 20 weeks, $p< 0.05$) and less smooth muscle cells (α-SMA in diabetic HFD: 4% vs non-diabetic HFD: 6% area/plaque, after 20 weeks, $p< 0.05$), on both HFD or PD diet. Diabetic atherosclerotic mice fed a HFD showed 37% plaque area (of total lumen) compared to 16% plaque area in non-diabetic mice after 12 weeks; and 43% (diabetic HFD) vs. 29% area (non-diabetic HFD) after 20 weeks. Differences between the diabetic and non-diabetic atherosclerotic mice were confirmed using RNAseq analysis revealing that significantly more genes are dysregulated in mice with combined hyperlipidemia and hyperglycemia (2341 genes) as compared to the hyperlipidemia only group (424 genes). Those genes were related to pathways regulating inflammation, cellular metabolism and collagen degradation. Mice that were fed a PD showed accelerated atherosclerosis compared to HFD mice indicated by rapid plaque formation already after 8 weeks (diabetic PD: 48% plaque area vs. non-diabetic PD: 30% plaque area), therefore, representing a fast direct inducible hyperglycemic atherosclerosis model.

Conclusion: We established a non-genetic direct inducible mouse model of diabetes-accelerated atherosclerosis allowing comparative analyses of atherosclerosis in diabetic and non-diabetic conditions and revealing novel genetic pathways being involved (https://www.biorxiv.org/content/10.1101/2021.11.11.468191v1).

256

Effect of Plasma Dialysate from healthy volunteers after Remote Ischemic Conditioning on cardiomyocyte calcium cycling

T. Srivastava[1], F. Funk[1], P. Tüller[2], P. Kleinbongard[2], G. Heusch[2], J. Schmitt[1]
[1]Düsseldorf University Hospital, Institute of Pharmacology and Clinical Pharmacology, Düsseldorf, Germany
[2]Essen University Hospital, Institute of Pathophysiology, Essen, Germany

Introduction: Transient ischemia-reperfusion protects the heart from subsequent ischemia-reperfusion injury (I/R), even if applied to tissue remote from the heart (remote ischemic conditioning, RIC). The RIC signal from remote tissue to the heart involves neuronal and humoral pathways. In the heart, RIC not only reduces infarct size but also improves contractile function after I/R. Since cardiac contraction and relaxation are closely regulated by rapid changes of Ca^{2+} concentrations within myocytes, we hypothesized that RIC-induced humoral signals may affect cardiomyocyte Ca^{2+} cycling.

Objective: To analyze Ca^{2+} transients of cardiomyocytes treated with plasma dialysates from humans before and after RIC.

Material & methods: Healthy volunteers were subjected to RIC by 3 cycles of 5 min forearm ischemia/5 min reperfusion (blood pressure cuff inflation/deflation). Venous blood samples were taken before and 30 min after the RIC protocol, and a plasma-dialysate was prepared (12-14 kDa dialysis tubing; dialysis over night at 4°C against sample buffer in a 1:5 volume ratio). Isolated mouse cardiomyocytes (C57BL/6) were exposed to the dialysates for 30 min before 50 min hypoxia. Next, cardiomyocytes were loaded with the fluorescent Ca^{2+} indicator Fura-2 and paced to measure cytosolic Ca^{2+} and sarcomere length during contractile cycles.

Results: Ca^{2+} transients of cardiomyocytes incubated with RIC dialysates were higher compared to respective controls in 10 out of 10 sample pairs, indicating a more pronounced cytosolic Ca^{2+} increase (P<0.001; average increase by 39±7%, mean±SEM). RIC dialysates also enhanced the speed of Ca^{2+} rise by 43±6% (P<0.001) and the speed of Ca^{2+} decline by 50±10% (P<0.01). Intriguingly, this increase of Ca^{2+} parameters was of comparable magnitude to that of their decrease due to 50 min hypoxia in untreated myocytes. Isoproterenol (10^{-7} M) enhanced myocyte Ca^{2+} cycling in all groups. However, RIC-induced differences were observed to a similar extent as without isoproterenol, suggesting that RIC dialysates alter myocyte Ca^{2+} handling independently of beta-adrenergic receptor stimulation and PKA-dependent phosphorylation of Ca^{2+} regulatory proteins. RIC also increased the amplitude (23±14%) and velocity of sarcomere contraction (27±15%) and relaxation (25±19%) by trend.

Conclusion: Humoral factors released by RIC enhance cardiomyocyte Ca^{2+} cycling, which may play a role in cardioprotection from hypoxic/ischemic damage.

265

Transcriptomic changes in rat cardiac myocytes undergoing right and left ventricular failure

S. Werner[1], L. Jurida[1], O. Dittrich-Breiholz[2], F. Knapp[3], B. Niemann[4], S. Rohrbach[3], M. Kracht[1]
[1]Justus Liebig University Giessen, Rudolf Buchheim Institute of Pharmacology, Gießen, Germany
[2]Medizinische Hochschule, RFU Transcriptomics, Hannover, Germany
[3]Justus Liebig University Giessen, Institute of Physiology, Gießen, Germany
[4]Universitätsklinikum Gießen-Marburg, Herz-, Kinderherz- und Gefäßchirurgie, Gießen, Germany

Question: Cardiovascular diseases are the leading cause of death globally. Among these is ventricular failure, a progressive disorder going through a hypertrophic compensation of additional load and leading to failure by rapid decompensation. Several known treatment options for left ventricular failure proof to be ineffective in the right ventricle.

The establishment of animal models displaying (I) the progressive mode of compensation/decompensation (II) in both ventricles to allow for comparative analyses between stage and ventricle is therefore critical to describe right heart specific mechanisms of disease and develop treatments.

Methods: Non-restrictive clips around the pulmonary artery (PAB) or the aorta (AOB) were surgically implanted into weanling rats. Upon animal growth the clips become increasingly constricting, leading to compensation by 6 weeks and heart failure by 22 (PAB) or 26 weeks (AOB). Disease progression was monitored functionally and by imaging.

From both phases of AOB and PAB, as well as from matching sham animals, isolated cardiac myocytes were isolated and total RNA was extracted. Then, total RNAseq was performed followed by multi-dimensional bioinformatics analyses to identify differentially regulated genes, pathways and inferred protein interaction networks. The data were also compared to previous mRNAseq analyses obtained from total heart samples under the same conditions.

Results & Conclusion: While whole heart samples only showed slight deregulation in both treatments during compensation, failure resulted in strong ventricle specific expression patterns with markers for pathological remodelling. Isolated cardiac myocytes showed stronger effects upon compensation, which increased upon heart failure. While almost all genes expressed in cardiac myocytes were found in whole heart, differential expression showed differing patterns.

The differential expression patterns in left and right heart failure were ventricle specific in all sample types. Additionally both treatments lead to similar deregulations in the right ventricle upon heart failure, suggesting a reaction of the right ventricle to left heart failure with a specific program. Protein interaction analyses of the transcriptomic data showed ventricle specific co-regulation of known interactors. Combined, the rat model data allowed identifying profound molecular differences between right and left heart failure and show similarity to observations in human disease.

266

Effects of ephedrine and congeners on contractility of mouse atrial preparations with 5-HT_4-receptor overexpression

U. Gergs[1], C. Höhm[1], J. Neumann[1]
[1]Institute for Pharmacology and Toxicology, Medical Faculty, Martin Luther University Halle-Wittenberg, Halle (Saale), Germany

Question: Typical indirect sympathomimetic drugs like ephedrine, norephedrine, mescaline, and 3,4-methylenedioxymethamphetamine (MDMA; commonly known as ecstasy) might not only release noradrenaline but also raise serotonin levels in the heart. In principle, increased cardiac serotonin levels can be monitored by increase in contractility in 5-HT_4-receptor overexpressing mice (TG) compared to wild type mice (WT) where serotonin is ineffective.

Methods: We tested contractile effects of ephedrine, norephedrine, mescaline, and MDMA in isolated electrically stimulated left atrial preparations (1 Hz) and spontaneously beating right atrial preparations from WT and TG. We constructed cumulative concentration response curves to ephedrine, norephedrine, mescaline, and MDMA (10 nM to 10 µM) alone or in the additional presence of cocaine (10 µM).

Results: Under these experimental conditions, ephedrine, norephedrine and MDMA but not mescaline increased force of contraction by at most 53 %. Moreover, ephedrine, norephedrine and MDMA increased the beating rate by at most 45 % (n=3-4). The effects started at about 3 µM and reached a maximum at 10 µM, the highest concentration tested. The contractile effects of ephedrine, norephedrine and MDMA were antagonized by cocaine pre-treatment. All above mentioned effects were present in TG as well as in WT. Inotropic effects to mescaline were missing in TG and WT.

Conclusion:. We conclude that ephedrine, norephedrine and MDMA but not mescaline act probably via release of noradrenaline but not serotonin from intracellular stores in the mouse heart.

268

An optimized engineered heart tissue model to study pro-fibrotic enhancers

A. Stoter[1], B. Pan[1], J. Krause[2], G. Höppner[1], D. Lindner[2], K. Wrona[1], M. Hirt[1], T. Eschenhagen[1], J. Stenzig[1]
[1]Institut für Experimentelle Pharmakologie und Toxikologie, Hamburg, Germany
[2]Universitäres Herz- und Gefäßzentrum UKE Hamburg, Klinik und Poliklinik für Kardiologie, Hamburg, Germany

Introduction: Fibrosis is a common problem in heart disease. It promotes myocardial wall stiffness and arrhythmia and reduces cardiac output. Extracellular matrix is mainly deposited by activated resident fibroblasts. Genetically encoded enhancer sequences are necessary for fibroblast activation and could be disease-specific treatment targets. Engineered heart tissue (EHT) from human induced pluripotent stem cell (hiPSC)-derived fibroblasts and cardiomyocytes could be an advanced tool to study enhancer function in a human, physiological heart tissue environment.

Objectives: We aimed to test the feasibility of the EHT model for studying the consequences of CRISPR-Cas9 mediated genetic deletion of potentially pro-fibrotic enhancer sequences.

Material & methods: We evaluated concentrations 10, 15, 20 and 48 ng/mL TGF-β1 for fibroblast activation and 1, 5 and 10 µM of the TGF-β1 receptor inhibitor SB43152 (SB) for maintaining quiescence, starting at d1 or >d7 of culture in CF-EHT (90% hiPSC-derived cardiomyocytes, 10% quiescent hiPSC-derived fibroblasts). To prevent activation by undefined serum components, we assessed the tolerance of the model to serum reduction from 10% to 0.5%. We performed morphological and contractility analysis and expression analysis of fibrosis-associated genes.

Results: All concentrations of TGF-β1 and SB had no negative impact on CF-EHT force. Contraction rate in TGF-β1-treated CF-EHTs was lower than in controls (52 vs 68 bpm, n≥8/group at d13). The structural remodelling of CF-EHTs was slower at each SB concentration started at d1 of culture than in controls (a decrease in width from d1 to d8 of 16% vs 49% in 10 µM SB treated CF-EHTs vs controls, n≥4/group), whereas TGF-ß1 had no impact. Serum reduction negatively impacted on CF-EHT force, regardless whether initiated at d3 or d14 of culture. As force remained sufficient for contractility analysis, serum reduction was still carried out at d3 of culture in light of

the importance of fibroblast quiescence. Transcript abundance of the activation and proliferation markers collagen 1a1, connective tissue growth factor and periostin were each ≥5 times higher (or 0.5 times lower) in fibroblasts treated with TGF-β1 (or SB).

Conclusion: Several questions needed to be addressed in order to make CF-EHT feasible for the study of enhancer deletion. After defining the tolerance of the model to serum and TGF-ß1 manipulation, we have now commenced experiments with enhancer-deleted fibroblasts.

280

The Impact of SGLT-2 inhibitors on laboratory parameters

C. Morgovan[1], **D. G. Moisă**[1], C. M. Dobrea[1], A. M. Arseniu[1], A. Frum[1], A. M. Juncan[1], L. L. Rus[1], A. A. Chiș[1], F. G. Gligor[1], S. Ghibu[2]
[1]Lucian Blaga University of Sibiu, Sibiu, Romania
[2]"Iuliu Haţieganu" University of Medicine and Pharmacy, Cluj-Napoca, Romania

Questions: SGLT-2 inhibitors (iSGLT2) have been approved for the treatment of non-insulin-dependent diabetes (DM), and more recently heart failure (HF) [1, 2]. A positive impact on the patients` health status could be induced by modifying some laboratory parameters (LP), but at the same time, other modifications could alter the quality of life in these patients. The aim of the present study is to identifiy the influences of iSGLT2 on LP in order to warn, to monitor or to elaborate some restrictions regarding their use.

Methods: The current research of the literature was analysed employing the comparative and interpretation method.

Results: The use of iSGLT2 is determined by the increase of glycosuria, the reduction of glycemia and glycosylated hemoglobin. In patients with HF, the blood concentration of the type B natriuretic peptide (BNP) is increased. By stimulating natriuresis and reducing volume, iSGLT2 reduced NT-proBNP and BNP levels. On the other hand, iSGLT2 inhibits the Na+/H+ exchanger, responsible for the increase of Na+ in the myocard and subsequently the appearance of arrhythmias, cardiac hypertrophy and worsening of HF. iSGLT2 reduce plasma leptin levels and increase adiponectin levels. There was a reduction in albuminuria and in the risk of progression to macroalbuminuria, LP linked to worsening of renal failure and GFR. SGLT2 inhibition improves lipid profile and reduces glucose oxidation. On the other hand, they increase the oxidation of fats and augment the plasma concentrations of ketone bodies. iSGLT2 therapy is associated with a modest increase in hematocrit and reduce plasma uric acid levels. SGLT2 inhibition reduces circulating levels of IL-6, TNF, nuclear factor-κB and IL-6 in renal tissues [2-4].

Conclusions: Despite the positive impact on most laboratory parameters, the administration of iSGLT2 is conditioned first by the GFR and on the other hand, it may require certain warnings or additional monitoring, such as: glycosuria, plasma KB, hematocrit, and electrolytes in patients with volume depletion, etc.

References:

1. Morgovan, C. et al. Int. J. Environ. Res. Public Health 2020, 17, 4456. https://doi.org/10.3390/ijerph17124456
2. Nassif ME et al. Circulation. 2019 Oct 29;140(18):1463-1476. doi: 10.1161/CIRCULATIONAHA.119.042929.
3. Cowie, M.R., Fisher, M. Nat Rev Cardiol 17, 761–772 (2020). https://doi.org/10.1038/s41569-020-0406-8
4. Garvey TW et al. Metabolism. https://doi.org/10.1016/j.metabol.2018.02.002

Pharmacology – Immunopharmacology / inflammation / anti-infectives

33

B lymphocyte-Deficiency in mice promotes venous thrombosis -Role of Neutrophils

N. Xia[1], S. Hasselwander[1], S. Ascher[2], M. Mimmler[1], T. Knopp[2], G. Reifenberg[1], W. Ruf[2], C. Reinhardt[2], H. Li[1]
[1]Medical center Mainz, Department of Pharmacology, Mainz, Germany
[2]Medical center Mainz, , Mainz, Germany

Cells of the innate immune system, including monocytes and neutrophils, are key players in the process of venous thrombosis. T lymphocytes have recently been implicated in venous thrombus resolution but the role of B lymphocytes in thrombosis is unknown.

To address this question, a mouse model of partial ligation of the inferior vena cava was used. Although only a very low number of B cells was found in the venous thrombi of wild-type mice, B cell-deficient mice developed larger venous thrombi than the wild-type controls. Consistent with enhanced thrombogenesis, increased neutrophil counts were found in the circulating blood and in the thrombi of B cell-deficient mice. One of the mechanisms by which neutrophils contribute to venous thrombosis is the formation of neutrophil extracellular traps (NETs). In agreement, higher quantities of NETs were observed in the thrombi of B cell-deficient mice. In vitro assays showed no difference in the NETs building capability of the isolated neutrophils between B cell-deficient and wild-type mice, indicating that the enhanced NETs formation in the thrombi of B cell-deficient mice are attributable to the increased number of circulating neutrophils in these animals. Furthermore, increased concentration of the clot-stabilizing macromolecule fibrinogen was detected in the plasma of B cell-deficient mice.

In conclusion, B cell-deficiency in mice indirectly promotes venous thrombosis by increasing neutrophil numbers and elevating fibrinogen levels.

Key words: B lymphocytes, neutrophils, deep-vein thrombosis, venous thromboembolism

75

The microtubule-targeting agent pretubulysin impairs inflammatory key features in endothelial cells *in vitro* and *in vivo*

T. Primke[1], R. Ingelfinger[1], M. Fabritius[2], C. Reichel[2], A. Ullrich[3], U. Kazmaier[3], R. Fürst[1]
[1]Goethe University Frankfurt am Main, Pharmaceutical Biology, Frankfurt am Main, Germany
[2]University of Munich, Department of Otorhinolaryngology, Munich, Germany
[3]Saarland University, Institute of Organic Chemistry, Saarbrücken, Germany

Questions: Our immune system shields us against noxious factors. The exposure to such factors induces the infiltration of leukocytes into affected tissues. Failure to resolve this state give rise to pathological conditions, which are characterized by constant leukocyte infiltration. Microtubule-targeting agents (MTAs), primarily used as chemotherapeutic drugs, also have anti-inflammatory properties. Aim of this study was to investigate the anti-inflammatory properties of the novel MTA pretubulysin (PT) on leukocyte-endothelial cell interactions and to shed light on the cellular mechanisms responsible for the anti-inflammatory properties of MTAs.

Methods: Intravital microscopy, flow-cytometry, western blotting, RT-qPCR, immunocytochemistry/microscopy, dual-luciferase reporter assay.

Results: Intravital microscopy of the cremaster muscle in mice showed that treatment with PT decreases the TNF-induced leukocyte adhesion and transmigration through the vascular endothelium. Subsequent, flow-cytometric analysis of the cell adhesion molecules (CAMs) E-selectin, ICAM-1 and VCAM-1 revealed that treatment with PT, vincristine (VIN), and colchicine (COL), but not paclitaxel (PAC), decreased ICAM-1 and VCAM-1 cell surface levels. Western blot analysis and RT-qPCR of PT-, VIN- or COL-treated cells showed reduced total protein and mRNA levels for all investigated CAMs. Based on these findings, the nuclear levels of NFκB, AP-1 and IRF-1 in PT-treated cells were examined by immunocytochemistry/microscopy and western blot analysis of cell fractions. While the nuclear levels of NFκB and AP-1 were increased at short and decreased at long TNF-stimulation times, IRF-1 was excluded from the nucleus. A dual-luciferase reporter assay of cells treated with PT showed a reduced promoter activity for NFκB and AP-1. Phosphorylation-based western blot analysis of associated kinases JNK and p38 revealed that PT induces an upregulation of MAPK activity, while perturbing the cytoplasmic to nuclear shuttling of these kinases.

Conclusions: This study shows that the effects of PT on the expression of CAMs involved in leukocyte adhesion are likely to be caused by modulated kinase activity and shuttling processes upstream of the transcription factor-induced CAM-expression. However, further investigations into the interplay between PT-influenced kinases and transcription factor activities are required to elucidate the anti-inflammatory properties of PT and other MTAs.

79

The carbazole derivative C81 provides promising anti-inflammatory and pro-resolving effects in leukocytes

S. Ciurus[1], L. Berger[2], B. Strödke[3], S. Müller[2], S. Knapp[2], L. D. Burgers[1], I. Bischoff-Kont[1], F. Bracher[3], R. Fürst[1,4]
[1]Institute of Pharmaceutical Biology, Frankfurt am Main, Germany
[2]Institute of Pharmaceutical Chemistry, Frankfurt am Main, Germany
[3]Center for Drug Research, Pharmacy, München, Germany
[4]LOEWE Center for Translational Biodiversity Genomics, Frankfurt am Main, Germany

Question: Inflammation is a protective response of the organism to an injury or infection. After successful elimination of the inflammatory trigger, resolution of inflammation is initiated to restore homeostasis. Dysregulated resolution of inflammation, however, can cause chronic inflammatory diseases like rheumatoid arthritis. C81 is a carbazole analogue of the β-carboline alkaloid annomontine and has recently been reported by our group to reduce leukocyte-endothelial cell interactions *in vitro* and *in vivo,* impairing the NFκB-signaling in endothelial cells (ECs). Preliminary data further indicate an influence of C81 on primary leukocytes (PL). Therefore, we aimed to identify the influence of C81 on PL cell functions and to gain insight into the mode of action of C81 during inflammation and its resolution.

Methods: The effect of C81 on cell function was investigated by cell adhesion assays, scratch assays and Boyden Chamber assays. The levels of integrins were determined by flow cytometry (FC); expression of cytokines was quantified by qPCR; proteins of the NFκB signaling pathway were examined by western blotting (WB) and

immunocytochemistry/microscopy. Apoptosis of PMNLs was measured by FC, and related caspase-3 and p38 activation were quantified by WB.

Results: C81 reduced cell functions of PL, including adhesion, directed and undirected migration, at a concentration up to 10 µM without impairing cell viability. The cell surface expression of integrins (VLA-4, LFA-1) on PL and the production of pro-inflammatory cytokines (IL-1b, IL-6, IL-8) in PL were decreased upon C81 treatment. In contrast to ECs, in which C81 was shown to increase IκB recovery after TNFα treatment, C81 treatment delayed rather than induced IκB recovery after LPS treatment in PL. At the same time, no influence of C81 on the nuclear translocation of the NFκB subunit p65 was observed. The apoptosis of neutrophils, but not of other PL, was dramatically induced. We observed an C81-dependent activation of caspase-3 in neutrophils, which could result from an increased p38 phosphorylation.

Conclusion: C81 exerts promising anti-inflammatory actions on PL and pro-apoptotic effects on PMNLs. Interestingly, the underlying mode of action seems to differ from the anti-inflammatory mechanism in ECs, since the NFκB signaling is affected differentially. Taken together, C81 provides promising anti-inflammatory properties in PL that warrant further in-depth investigations.

103

Genome-scale sgRNA screen to identify human genes required for thapsigargin-mediated inhibition of human coronavirus replication

B. V. Albert[1], C. Mayr-Buro[1], S. Werner[1], M. S. Shaban[1], J. Meier-Soelch[1], H. Weiser[1], L. Schmitz[2], M. Kracht[1]
[1]Rudolf Buchheim Institute of Pharmacology, Justus Liebig University Giessen, Gießen, Germany
[2]Institute of Biochemistry, Gießen, Germany

Objectives: Human coronavirus 229E is a member of the genus *Alphacoronavirus* and known to cause seasonal, mild upper respiratory tract infections. Recently we showed that the ER-stress inducer thapsigargin (Tg) inhibits the replication of three human coronaviruses (HCoV-229E, SARS-CoV2, and MERS-CoV) in multiple cell types and enhances the cell viability upon infection (https://doi.org/10.1038/s41467-021-25551-1). Here, we have used an unbiased genome-scale CRISPR-Cas9 knockout screen to identify host factors, which may support the Tg-mediated antiviral effect.

Methods: HuH7 cells were stably transduced with lentiviruses containing the GECKO2.0 library which encodes 123,411 sgRNAs (six per human gene) to generate a pool of cells with genome-wide genetic knockouts. 80 million GECKO cells served as an unselected control population. 200 million GECKO cells were infected with HCoV-229E (at a MOI of 1) in the presence or absence of Tg. Genomic DNA from surviving cells was harvested directly (72h after selection) or after further expansion for about two to four weeks (96 h after selection). The PCR amplified sgRNA libraries from three independent experiments of control and selected populations were subjected to DNA sequencing. Normalized read counts were analyzed by MAGECK bioinformatics tools to identify statistically significant differences in the abundance of integrated sgRNAs in the selected compared to the control populations.

Results and Conclusion: Deep sequencing of all the PCR-amplified libraries resulted an average coverage of at least 55 million reads. MAGECK analysis confirmed that the control samples displayed an evenly distributed integration of almost all sgRNAs. In contrast, we observed a strong depletion of integrated sgRNAs and corresponding read counts in the infected and/or Tg treated cells as a result of strong selection pressure after the 96h treatment. Aminopeptidase N (*ANPEP*) depleting sgRNAs represented the most strongly enriched sgRNAs. As *ANPEP* encodes the HCoV-229E entry receptor, this result confirms that the screen has worked. Altogether, we identified around 1,000 putative host cells factors relevant for cell survival upon infection and Tg treatment based on a MAGECK score ≤ 0.005. This list of genes, obtained by unbiased large-scale genomic screen, reveals the complexity of the host response to both infection and Tg treatment. The top candidates will be tested for their specific roles in host survival and the coronavirus life cycle.

120

Mechanistic studies on the anti-inflammatory effect of lefamulin in the LPS-induced pulmonary neutrophilia mouse model

M. Hafner[1], S. Paukner[1], S. P. Gelone[2]
[1]Nabriva Therapeutics GmbH, Vienna, Austria
[2]Nabriva Therapeutics US, Inc., Fort Washington, United States

Lefamulin (LEF) is a pleuromutilin antibiotic approved to treat community-acquired bacterial pneumonia. As several other antibiotics demonstrate anti-inflammatory/immunomodulatory activities, LEF was tested in an LPS-induced lung neutrophilia model in mice and potential mechanisms were investigated.

BALB/c mice were treated subcutaneously with LEF 30 min before intranasal LPS challenge and neutrophil infiltration into BALF was analyzed 4h post challenge. Mechanistic studies included evaluation of pro-inflammatory cytokines (TNF-α, IL-6, IL-1β, and GM-CSF) and chemokines (CXCL1, CXCL2, IL-8, and CCL2) in lung homogenates and supernatants of LPS-stimulated J774.2 mouse macrophage or human PBMC cultures. The effect of LEF was investigated on cytokines and chemokines secretion of LPS-activated mouse Precision Cut Lung Slices (PCLS) and on neutrophilic chemotaxis.

Single subcutaneous LEF doses (10–140 mg/kg) resulted in dose-dependent reductions of BALF neutrophil cell counts up to 77%. Pharmacokinetic analyses confirmed exposure-equivalence of 30 mg/kg subcutaneous LEF to a single clinical dose.

Strong (TNF-α, IL-6, GM-CSF, and CCL2) and moderate (IL-1β, CXCL1 and CXCL2) reduction of pro-inflammatory cytokines and chemokines compared to vehicle control was observed in lung homogenates of LEF treated mice suggesting cytokine/chemokine-producing cells are target cells of LEF"s anti-inflammatory activity. Macrophages are well known to produce large amounts of cytokines/chemokines following LPS-stimulation, however, *in vitro* studies with LPS-stimulated J774.2 mouse macrophage or human PBMC haven"t demonstrated inhibition of cytokines or chemokines secretion to the supernatant when treated with LEF at therapeutically relevant concentrations.

The role of neutrophils was investigated in a mouse PCLS model. There is no blood supply in this model and therefore no neutrophil infiltration induced by LPS can take place. LEF pretreatment strongly inhibited TNF-α, GM-CSF, and CCL2 at higher concentration suggesting neutrophil independent LEF activity. LEF did not inhibit IL-8-induced chemotaxis of human neutrophils.

In summary, these results suggest that the potent inhibition of LPS-induced neutrophilic infiltration by LEF is mediated by the reduction of cytokine and chemokine levels in the lung rather than by a direct inhibition of neutrophilic chemotaxis. Further studies are warranted to identify the cells targeted by LEF and its mode-of-action.

138

Cell-free Protein Synthesis for the analysis of key proteins involved in zoonotic viral infections exemplified by Hepatitis E Virus proteins

H. A. Trinh[1], F. Ramm[1], R. Ulrich[2], S. Kubick[1]
[1]Fraunhofer Institute for Cell Therapy and Immunology, Branch Bioanalytics and Bioprocesses IZI-BB, Cell-free and Cell-based Bioproduction, Potsdam, Germany
[2]Friedrich-Loeffler-Institut, Bundesforschungsinstitut für Tiergesundheit, Institut für neue und neuartige Tierseuchenerreger (INNT), Greifswald, Germany

New emerging or reoccuring infectious diseases caused by viral agents pose an increasing public health risk. Amongst those viral agents is the Hepatitis E virus (HEV), which is considered the main cause for acute hepatitis, an inflammation of the liver tissue. Hepatitis E is endemic in many developing countries in Central- and East Asia, North- and West Africa and in Mexico due to unsanitary water supplies. In industrialized countries HEV causes sporadic outbreaks via foodborne transmission due to undercooked meat and more recently blood transfusions. This leads to more than 20 Mio infections, with 3 Mio symptomatic cases, as well as 56.000 HEV associated deaths annually.

The key proteins for virus pathogenesis are, inter alia, viral glycoproteins which are involved in progeny formation and infectivity. HEV"s ORF2 capsid protein displays three glycosylation sites. HEV is difficult to propagate in cell culture with long generation times of several weeks, hence information about its replicative life cycle is limited. Therefore, we established a platform for sufficient HEV protein synthesis, which allows for the investigation of molecular mechanisms of HEV replication and elucidating pathogenesis.

Cell-free protein synthesis enables the generation of a protein of interest using the translation machinery without the necessity of viable cells. HEV proteins were synthesized using eukaryotic cell lysates based on *Spodoptera frugiperda 21* cells. This translation system enables sufficient translocation into membranes and posttranslational modifications such as N-linked glycosylation.

168

Investigation of the impact of chemical inhibitors on different epithelial cells infected with the human coronavirus 229E

C. Mayr-Buro[1], A. S. Geradts[1], M. Kracht[1]
[1]Rudolf-Buchheim-Institut für Pharmakologie, Giessen, Germany

Introduction: The human coronavirus 229E (HCoV-229E) belongs to the family *coronaviridae*, which also includes the well-known pandemic SARS-CoV-2. Both viruses cause the infection of the respiratory tract, but the clinical manifestation of the diseases differs from mild or moderate common cold to the severe covid-19. The underlying mechanisms for strain-specific differences in human CoV-induced pathology remain poorly understood.

Objectives: Previous transcriptomic and proteomic experiments revealed an impact of the HCoV-229E infection on different signalling pathways. Amongst others an induction of several pro-inflammatory NF-κB response genes such as *IL6*, *IL8*, and *TNFAIP3*/*A20* as well as genes of the ER stress pathway, e.g. *ATF3*, *ANKRD1*, and *EIF2AK3,* were detected. This raised the question if specific chemical protein kinase inhibitors (GSK2606414, PHA-408) can be used to block these pathways in cells infected with HCoV-229E. By appropriate dose-response curves we aimed to identify the lowest concentrations of inhibitor combinations that effectively suppress the virus-mediated upregulation of ER-stress and NF-κB response genes as well as the virus titers.

Materials & methods: The modulation of the virus-induced gene response in host cells was investigated using RT-qPCR. In parallel, viral replication was assessed by titrating viral particles in supernatants of infected cells by plaque assays. The analyses were performed in different epithelial cell systems such as Huh7, A549 and primary alveolar cells. Furthermore, virus-induced gene expression was assessed at the single cell level in A549 lung carcinoma and primary alveolar cells using immunofluorescence (IFA) combined with RNA fluorescence *in situ* hybridisation (RNA-FISH).

Results and conclusion: The virus-induced gene expression was modulated in a dose-dependent but cell type-independent manner by both, inhibition of the ER-stress pathway with GSK2606414 and the NF-κB pathway with PHA-408. GSK2606414 was more effective in suppressing gene expression than PHA-408. Combinations of low doses of both inhibitors synergistically decreased gene expression and viral titers, suggesting that inhibiting both pathways is advantageous to limit coronavirus replication.

170

Autophagy- and ER stress-related processes contribute to the replication of human coronaviruses

M. S. Shaban[1], C. Müller[2], C. Mayr-Buro[1], H. Weiser[1], B. V. Albert[1], N. Karl[2], M. L. Schmitz[3,4], J. Ziebuhr[2], M. Kracht[1,4]
[1]University of Giessen, Rudolf Buchheim Institute of Pharmacology, Giessen, Germany
[2]Institute of Medical Virology, Gießen, Germany
[3]Institute of Biochemistry, Gießen, Germany
[4]German Center for Lung Research (DZL) and Universities of Giessen and Marburg Lung Center (UGMLC), Gießen, Germany

Objectives: Coronaviruses are RNA viruses with genome size approximating 30Kb. They infect a broad range of species, including humans. Four of the "common" human CoV (HCoV-229E, -NL63, -HKU1, -OC43) can result in mild symptomatic infection mostly restricted to the upper respiratory tract. On the other hand, severe acute respiratory syndrome (SARS) CoV 1 and 2 and Middle East respiratory syndrome CoV (MERS-CoV) are highly pathogenic CoVs and can cause significant disease burden and mortality. We found that CoVs strongly modulate the unfolded protein response associated with ER stress and autophagy induction through several cross talking signaling pathways including the protein kinase PERK that is well known to confer translational suppression. This prompted us to investigate the role of ER stress and autophagy induction in CoV replication. Our findings indicates an intimate involvement of these cellular processes in CoV life cycle that can be exploited to suppress CoV replication.

Methods: To investigate the role of these cellular processes in CoVs life cycle, we used several types of model systems, including Huh7, MRC-5 and Vero6 cell lines. The cells were infected with HCoV-229E, MERS-CoV or SARS-CoV-2 in the presence or absence of the ER stress trigger thapsigargin, PERK inhibitor GSK2656157 and/or lysosomal V-ATPase inhibitor bafilomycin A1. Expression of viral or host proteins or mRNAs were examined using cell lysates for immunoblotting, mass spectrometry or RT-qPCR. In parallel, the supernatants were used for ELISA assays and plaque assays. Immunofluorescence assays were utilized to visualize subcellular sites of viral replication.

Results: We found that thapsigargin efficiently inhibits replication of all three CoV in different cell types in the lower nM range. The inhibition of viral replication by GSK2656157 required higher doses of the inhibitor and resulted in lower drop of the investigated CoVs titers than thapsigargin. The extent of bafilomycin A1 mediated inhibition of CoV was largely dependent on the time of the treatment, implicating an early role of autophagy induction in CoV life cycle. Double treatment of HCoV-229E infected cells with GSK2656157 and bafilomycin A1 showed an uncoupling between the inhibition of viral replication and autophagy flux.

Conclusion: Our data show an important role of cellular processes such as autophagy and ER stress in CoV replication that can be virus specific depending on the CoV investigated. These processes might be further exploited to counter CoV replications on multiple levels and to understand the different disease outcomes associated with different coronaviruses.

220

Type-IV phosphodiesterase inhibition followed by ischemic postconditioning ameliorates ischemia reperfusion-induced acute kidney injury in rats

K. Gupta[1], S. Gupta[1], G. Singh[2]
[1]M M College of Pharmacy, MM (Deemed to be University), Mullana, M M College of Pharmacy, MM (Deemed to be University), Mullana, Ambala, India
[2]Chitkara University, Chitkara College of Pharmacy, Patiala, India

Background: Accumulating evidence suggests that renal ischemia-reperfusion injury triggers the subsequent generation of inflammatory cytokines and immune cell trafficking. Ischemic postconditioning (IPostC) is a promising strategy to prevent experimental ischemia (1). Of note, PDE-4 inhibition is an emerging therapeutic intervention that prevents the hydrolysis of cAMP that leads to downstream signaling of various inflammatory mediators (2). We have previously reported that the PDE-4 inhibitor roflumilast exerts beneficial effects by reducing hyper inflammation and leukocyte migration in septic kidneys of rats (3) but in renal I/R injury it remains unexplored. Therefore, this study was designed to evaluate the effects of PDE-4 inhibition followed by IPostC in I/R induced AKI.

Methods: Forty rats were randomly assigned in five separate groups comprising sham-operated group, I/R group (both renal pedicels clamped for 45 min followed by 24h of reperfusion), I/R + roflumilast (1.2mg/kg;*p.o*) initiated 7 days prior to I/R, I/R + IPostC (six cycles of 10s reperfusion and re-occlusion after I/R), I/R+roflumilast+IPostC combination. After 24hr of I/R injury, renal dysfunction, cAMP levels, antioxidant assays, membrane Na^+K^+ATPase activity, inflammatory biomarkers were determined using respective biochemical assays and ELISA kits. Histological studies and urinalysis were also performed.

Results: Development of AKI due to I/R injury was confirmed by elevated serum creatinine, blood urea nitrogen, 24-hr urinary proteins, oxidative and inflammatory stress, fibronectin and caspase activity, the decline in creatinine clearance, and membrane Na^+K^+ATPase activity compared to the sham group. Moreover, ischemic kidneys displayed various morphological alterations, upregulated MPO activity, and interstitial leukocyte infiltration in renal tissue as well as deposition in urinary sediments. Roflumilast pre-treatment either alone or with IpostC application significantly improved renal functions and histological impairments. Nonetheless, IpostC treatment alone partially prevented these AKI manifestations in I/R rats.

Conclusion: The present findings addressed the renoprotective effects of PDE-4 inhibitor roflumilast and IpostC concurrently by suppressing ROS, inflammatory cell infiltration, and improving renal functions in I/R induced AKI in rats.

Reference:
1. https://doi.org/10.1093/ndt/gfm779
2. 10.1111/j.1476-5381.2011.01218.x
3. https://doi.org/10.1111/fcp.12711

Fig. 1

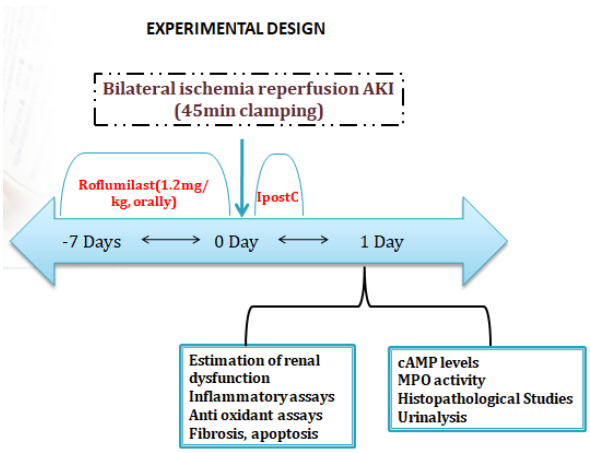

Fig. 2

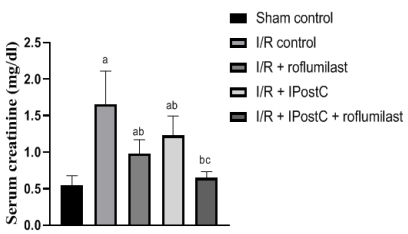

Figure.1: Effect of various treatments on **serum creatinine** levels. All values are represented as mean ± SD for each group. [a]$p < 0.05$ *vs* sham control; [b]$p < 0.05$ *vs* I/R control; [c]$p < 0.05$ *vs* I/R + IPostC group.

233

From inflammation to depression. Mechanisms of action of natural products

N. Mischer[1], C. Kolb[2], **O. Kelber**[1], K. Nieber[3]
[1]Steigerwald Arzneimittelwerk GmbH, R&D Phytomedicines, Phytomedicines Supply and Development Center, Bayer Consumer Health, Darmstadt, Germany
[2]Steigerwald Arzneimittelwerk GmbH, Scientific Affairs, Phytomedicines Supply and Development Center, Bayer Vital, Darmstadt, Germany
[3]University of Leipzig, Institute of Pharmacy, Leipzig, Germany

Introduction: Depressive disorder is a complex illness and it is likely that alterations in several interacting systems underlie its pathogenesis [1, 2]. The inflammatory hypothesis emphasises the role of neuroimmunological dysfunctions. An IFN-α-

induced raise of TNF-α and IL-6 can cause depressive symptoms, and even the microinflammation in the long COVID syndrome is often connected to depressive symptoms [3].

Therefore, it is necessary to re-evaluate the herbal treatment options for depression in terms of the mechanism of action. St. John's wort is very effective in depressive disorders and will therefore be evaluated for anti-inflammatory effects.

Methods: A broad and systematic literature review was conducted [Medline, EMBASE] and the evidence was assessed.

Results: St. John's wort extracts and a number of their constituents, especially flavonols and hyperforin, influence numerous inflammatory processes *in vitro* and *in vivo*, suggesting anti-inflammatory effects. This is also supported by recent data on the influence of phagocytic and migratory activity of microglial cells [5] or pituitary-derived AtT-20 cells in vitro [4].

Conclusions: The new data on potential mechanisms of action of St. John's wort extracts support its efficacy in depressive disorders, especially those with inflammatory etiology, and supports its use in these patients.

References: 1. Moisan MP et al. 2021, Transl Psychiatry 11:203; 2. Grundmann O et al. 2010, Neuropharmacology 58, 767; 3. Perlis RH et al. 2021, medRxiv preprint, doi: 10.1101/2021. 03. 26.21254425; 4. Dillenburger B et al. 2020, Nervenheilk 39: 565-571; 5. Bonaterra G et al. 2020, Frontiers in Pharmacol 11, doi: 10.3389 /fphar. 2020. 603575

236

On integrative Pharmaco-Physiology on Example of Viral Infections, e.g. SARS-CoV-2 (ACE-2-Virus-Complex)

M. C. Michailov[1], E. Neu[1], V. Foltin[1,2], T. Senn[1,3], J. Foltinova[1,4], D. G. Weiss[1,5]
[1]Inst. Umweltmedizin (IUM) c/o ICSD/IAS e.V., POB340316, 80100 M. (Int. Council Sci.Develop./Int.Acad.Sci. Berlin,Innsbruck,Paris,etc.), Muenchen, Germany
[2]St. Elisabeth Univ., of Health and Social Work, Bratislava, Slovakia
[3]IUM c/o ICSD-IAS-Section, Innsbruck, Austria, Innsbruck, Austria
[4]Comenius Univ., Med. Fac., Bratislava, Slovakia
[5]Univ., Fac. Biol., Inst. Cell Physiology (Dir.a.D.), Rostock, Germany

Introduction and objectives: In context of an integrative **Pharmaco-Physiology** will be given example for importance of mechano-sensitive (stretch ionic) channels (A), renin-angiotensin-aldosteron-system (RAAS) (B), ACE-2 virus complex of SARS-CoV-2C for pathogenesis-therapy-prophylaxis of this terrible infection.

Methods: Motor & electrical (intracellular-recording) activities of vascular & vesical preparations (see ref.).

Results: Recent observations reflect present conception.

A. MECHANO-SENSITIVE IONIC-CHANNELS (n=367,p<0.01)

Experiments about electrical spikes/S, bursts/B, burst-plateaus/BP of vesical detrusor/D myocytes (guinea-pig&human/surgical-tissue) described stretch channels (1989-1993). Contractions of D to neural (nCES: 10&100Hz,0.3ms,3-5V))&muscular electrostimulation (mCES: 10Hz,40ms,3-5V) are strongly increased after stretch (>100%). D generates spontaneous-phasic (SPC:4.0+0.7/min), trigone slow-tonic contractions (STC:0.28+0.15/min).

B. RENIN-ANGIOTENSIN-ALDOSTERON-SYSTEM (RAAS) (n=120,p<0.01)

Isolated human renal&uterine-vessels, rat-aorta generate SPC&STC. Angiotensin-2 (0.01-0.1ng/ml) induces contractions in human-renal-veins. Vasopressin (0.02-1 mU/ml) and prostaglandin F2alpha induces STC in human renal-arteries&rat-aorta.

C. On SARS-CoV-2 (ACE-2-virus-complex)

Angiotensin-converting-enzyme-2 (ACE-2)/metalcarboxypeptidase is essential factor for RAAS, also for SARS-CoV-2-receptor. Recently are discovered many kinds of mechano-sensitive ionic-channels. It is suggested that these channels could be responsible for interaction between ACE-2 and virus.

Conclusions: Interdisciplinary research incl. biophysics, physiology, pharmacology, pathology, etc. is necessary to clarify importance of ions (Na+,K+,Ca++,Mg++), hormonal receptors (nicotine, nACH alpha4_2, beta 2_3, alpha-/ß-adrenergic, VPR1a-1b, 5-HT1a-f, 5-HT2a-c, 5-HT7, etc.) as well as of dielectric, i.e. mesomorphic states (nematic-smectic-cholesteric) and ferro-pyezo-pyrroelectricity resp. electrical phenomena for genesis of ACE-2-virus complex & possible prevention.

An international project about corona pandemic conc. A-C will support UNO-Agenda21 for better health-education-ecology-economy on global level.

DEDICATION: Moral&scientific support by Nobel-Laureates: *see Michailov, Neu et al DGPT Congr 2022*

Ref see Neu & Michailov et al DGPT congress 2022

263

Analysis of *de novo* biosynthesis of RNAs and proteins by metabolic labeling & click-chemistry during interleukin-1 treatment or HCoV-229E infection

J. Meier-Sölch[1], L. Skrabanik[1], U. Linne[2], A. Weber[1], M. Kracht[1]
[1]Justus-Liebig-University Giessen, Rudolf-Buchheim-Institute of pharmacology, Giessen, Germany
[2]Phillips-University Marburg, Institute of chemistry, Marburg, Germany

Introduction: Coronaviruses (CoVs) or proinflammatory cytokines such as interleukin-1 (IL-1) rapidly and selectively regulate the *de novo* synthesis of RNAs and proteins.

Objectives: To precisely follow the dynamics of gene expression in IL-1-treated or HCoV-229E-infected human Huh7 cells, we leveraged the co-transcriptional or co-translational incorporation of uridine or tRNA analogues into living cells to measure the synthesis and degradation rates of nucleic acids or proteins.

Materials & Methods: We treated cells with the cell-permeable uridine analogue 5-ethynyluridine (5-EU) into newly synthesized RNA *in-vivo*. Subsequently, the 5-EU bases were covalently coupled to azide-containing biotin molecules *in vitro* by a copper-based click reaction and purified by streptavidin beads. Then, specific transcripts were analysed by RT-qPCR. Alternatively, 5-EU RNA was conjugated to fluorophore-azide to investigate global changes in RNA biosynthesis or decay rates by fluorescence microscopy. By the same principles, we used the puromycin alkyne analogue O-propargyl-puromycin (OPP), which is incorporated into nascent polypeptides in intact cells. After cell lysis, OPP was conjugated to biotin-azide allowing the purification of newly synthesized polypeptides with streptavidin beads and their (unbiased) identification by western blotting or LC-MS/MS.

Results: The mRNAs of the highly IL-1-regulated transcripts *IL8*, *NFKBIA*, and *TNFAIP3* were found to be mainly regulated by *de novo* biosynthesis. While the overall levels of these transcripts decreased over time, their synthesis remained above basal levels, showing that the stability of these transcripts is co-transcriptionally down-regulated by IL-1. Unlike IL-1, infection with HCoV-229E globally reduced RNA and protein biosynthesis within 24 h. Mass spectrometry and western blot results revealed an almost complete translational shutdown, while viral proteins and some selected host proteins were actively induced or repressed.

Conclusion: In combination with subsequent click chemistry the metabolic labeling of *de novo* synthesized RNAs or proteins offers multiple possibilities to detect, specify and quantify the biosynthesis and degradation rates of transcripts or proteins globally, at the single cell level, and for individual molecules. These methods are particularly useful to dissect levels of gene regulation in highly regulated conditions, such as inflammation or infection.

Pharmacology – Cancer pharmacology and treatment

17

BK_{Ca} promotes cancer cell malignancy by modulating intracellular Ca^{2+} homeostasis and stimulating the Warburg effect

H. Bischof[1], D. Gross[1,2], S. Maier[1,2], S. Burgstaller[1,3], K. Paulus[1], A. Vu[1], M. Schmidt[1], A. Kurzbach[4], A. L. Birkenfeld[4], L. Matt[1,2], R. Lukowski[1]
[1]Eberhard Karl University Tuebingen/ Institute of Pharmacy, Experimental Pharmacology, Tuebingen, Germany
[2]Eberhard Karl University Tuebingen/ Institute of Pharmacy, Department of Pharmacology, Toxicology and Clinical Pharmacy, Tuebingen, Germany
[3]NMI Natural and Medical Sciences Institute at the University of Tuebingen, Reutlingen, Germany
[4]University Hospital Tuebingen, Medical Clinic IV, Tuebingen, Germany

Introduction: Many cancer entities are associated with altered expression levels of ion channels, especially potassium ion (K^+) channels [1,2]. One of these, the voltage- and calcium- (Ca^{2+}) activated K^+ channel of large conductance, BK_{Ca}, was recently demonstrated in preclinical models to promote breast cancer development and to modulate endocrine treatment responses. It is therefore associated with increased cancer cell malignancy [3].

Questions: Based on these observations, we aimed to unravel the cellular mechanisms of BK-mediated enhanced rate of breast cancer development and -growth. Furthermore, we aimed to investigate, whether pharmacological modulation of BK_{Ca} could represent a novel treatment to delay or even block malignant cancer cell behaviours.

Methods: Whole-cell patch-clamp, high-resolution fluorescence live-cell imaging approaches, real-time measurements of glycolysis and oxidative phosphorylation as well as cell viability and -proliferation assays were applied to study the putative role of BK_{Ca} and its pharmacological modulation in promoting or reducing cancer cell

malignancy in diverse murine primary breast cancer cells and human (breast) cancer cell lines, either showing high- or low expression levels of BK_{Ca} [3].

Results: High expression levels of BK_{Ca} were associated with increased overall metabolic rates, increased cell proliferation and a glycolytic phenotype often referred to as "aerobic glycolysis" or Warburg setting. Additionally, cells lacking BK_{Ca} showed higher dependency on molecular oxygen for maintaining their energy homeostasis. These parameters were normalized by treating BK_{Ca} proficient cells either with paxilline or iberiotoxin, two frequently used inhibitors of BK_{Ca}, or by rescuing BK_{Ca} deficient cells with an RFP-tagged BK_{Ca} channel.

Conclusion: In summary, our results emphasize that modulation of intracellular Ca^{2+} homeostasis by BK_{Ca} channels promotes cancer cell malignancy by propelling the Warburg effect, the shifting of cellular metabolism towards "aerobic glycolysis". Furthermore, pharmacologic inhibition of BK_{Ca} reduces overall malignancy of BKCa positive cancer cells and might thus represent a future perspective for breast cancer treatment.

References:
[1] Pardo L.A., Stühmer W., Nat Rev Canc, 2014
[2] Kunzelmann K., J Membr Biol., 2005
[3] Mohr C.J., et al., BJP, 2020

55

Analysing the biological function of truncated variants of the RNA-binding protein ZFP36L1

A. Kasten[1], M. Kähler[1], I. Cascorbi[1], I. Nagel[2]
[1]Institute of Experimental and Clinical Pharmacology, Kiel, Germany
[2]Institute of Human Genetics, UKSH Campus Kiel, Kiel, Germany

Question: The zinc finger protein ZFP36L1 mediates mRNA-decay by binding to AU-rich elements in the 3" UTR of target genes and by this, posttranscriptionally downregulates gene expression. ZFP36L1 is composed of three domains: the mRNA-binding zinc finger domain (ZFD) and the N- and C- terminal domain recruiting degrading enzymes. In B-cell lymphoma, the recurrent deletion del(14)(q24q32) was described leading to two truncated *ZFP36L1* variants: one missing the first exon and one consisting of only the last 189 bp. However, it remains unclear if the observed truncated variants still remain functionally active and which parts of the protein are mandatory for protein function.

Methods: We analyzed the following ZFP36L1 variants: the two patient variants ("2nd exon variant" & "C-terminal variant"); the "ZFD-deficient variant" without zinc fingers; the "N-terminal variant" only consisting of the N-terminal domain and the "splice-variant" occurring by alternative splicing. Mutagenesis was performed using site-directed-mutagenesis. *ZFP36L1* variants were cloned into pSELECT-puro-mcs vector; the 3" UTR of *CDKN1A* and *CSF-1* were cloned into pmiRGlo luciferase vector. For transfection, HEK293-T cells were used, and luciferase reporter-gene assays were performed using Dual-Luciferase® Reporter Assays (Promega).

Results: ZFP36L1 variants were co-transfected with the well-known ZFP36L1 target *CDKN1A*. Besides wild-type ($p<0.001$) only the "2nd exon variant" ($p<0.001$) caused a significant decrease in luciferase activity, all other truncated variants showed no effects. Co-expression of the wild-type with the "2nd exon variant" decreased the luciferase activity by additional 33 % ($p<0.001$), whereas co-expression with the "ZFD-deficient variant" resulted in 51 % increase in the luciferase activity compared to wild-type ($p<0.001$). Co-expression of wild-type ZFP36L1 and *CSF-1* resulted in a significant decrease of luciferase activity ($p<0.001$), which was abrogated by mutation of three bases within the putative AU-rich element.

Conclusion: Our data showed the minimum requirement for ZFP36L1 function: The presence of two intact domains, one of them being the ZFD. While functional variants enhanced the effect of the wild-type, co-expression with the "ZFD-deficient variant" resulted in a dominant-negative effect. In addition, *CSF-1* was confirmed as a target of ZFP36L1. Overall, it is unlikely that the observed truncated patient variants influence B-cell lymphoma pathogenesis.

57

The extracellular matrix protein fibronectin 1 modulates tyrosine kinase inhibitor resistance in chronic myeloid leukemia

M. Kähler[1], L. S. Schmidt[1], M. Litterst[1], I. Nagel[2], I. Cascorbi[1]
[1]Institute of Experimental and Clinical Pharmacology, Kiel, Germany
[2]Institute of Human Genetics, UKSH Campus Kiel, Kiel, Germany

Question: Targeted therapy using tyrosine kinase inhibitors (TKIs), such as imatinib, led to tremendous success in the treatment of chronic myeloid leukemia (CML). The major cause of this hematopoietic neoplasm is formation of the BCR-ABL1 kinase resulting in malignant progression. Although BCR-ABL1-targeting using TKIs led to patient survival rates of 83 %, therapy resistances remain a clinical problem. Genome-wide gene expression studies of TKI-resistant CML cell lines revealed differential expression of genes associated with cell adhesion signaling, especially the cellular matrix protein fibronectin 1 (FN1). This raised the question on the role of FN1 in CML cells developing TKI-resistance.

Materials and Methods: Studies were performed using an CML in vitro-K-562-resistance model with biological replicate cell lines resistant to imatinib, nilotinib or both. mRNA and protein levels were analyzed by RT-qPCR and immunoblotting. Cell adhesion capacity was investigated using matrigel-coated plated and vybrant cell adhesion assay. Transfection was performed using FN1-encoding plasmids or siRNAs challenging the cells with 2 µM imatinib, 0.1 µM nilotinib or 0.01 µM dasatinib. TKI susceptibility was analyzed by total cell number, cell viability and proliferation assays.

Results: *FN1* mRNA and protein level were significantly decreased in all TKI-resistant sublines irrespective to the TKI compared to sensitive cells. SiRNA-mediated *FN1*-downregulation in K-562 cells led to reduction of cell adhesion ($p=0.02$), but a decrease in TKI susceptibility after 48 h imatinib (cell number: $p=0.04$; proliferation: $p=0.005$), nilotinib ($p=0.02$, $p=0.03$) or dasatinib treatment ($p=0.005$, $p=0.03$). Restoration of *FN1*-expression in biological replicates of imatinib resistant sublines increased cell adhesion to matrigel (0.5: $p=0.03$; $p=0.04$), decreased total cell number ($p=0.03$, $p=0.03$) and cell viability ($p=0.01$, $p=0.004$). These effects were likewise observed in nilotinib and combined resistances.

Conclusion: As FN1-reduction was associated with reduced TKI susceptibility in all tested sublines, our data suggest role for FN1 in TKI resistance, not only in the case of imatinib, but also second generation TKIs. Restoration of FN1 expression in all tested resistant cell lines led to improved TKI response potentially by modulation of cell adhesion signaling. While cell adhesion is widely associated with solid cancers, this finding indicates a target to overcome TKI resistance in CML.

102

CDK inhibitors differentially repress or induce mRNA expression and secretion of NF-κB target genes in ovarian cancer cells

J. Knauff[1], J. Dreute[2], M. L. Schmitz[2], M. Kracht[1]
[1]Rudolf Buchheim Institute of Pharmacology, Justus Liebig University Giessen, Gießen, Germany
[2]Institute for Biochemistry, Justus-Liebig University , Gießen, Germany

Introduction: The transcription factor NF-κB is activated by phosphorylation-dependent proteasomal degradation of inhibitor of NF-κB (IκB) proteins in response to inducers such as IL-1 or TNFα. IL-1 is a pro-inflammatory cytokine that also contributes to reprograming of the tumor microenvironment. Unpublished mass-spectrometry data of the phospho-proteome indicated that IL-1 (transiently) triggers the phosphorylation of several CDK family members in HeLa cells. CDKs represent a family of protein kinases involved in cell cycle regulation (e.g. CDK 4/6) and transcription (e.g. 7, 9, 12, 13), the latter through the phosphorylation of the C-terminal-domain (CTD) of RNA polymerase II. Genomic alterations of CDKs frequently occur in various human cancers. In high-grade serous ovarian cancer (HGSOC) CDK12 appeared among the ten most altered genes. In HGSOC the composition of the tumor microenvironment, which is highly influenced by NF-κB signaling, is critical for disease progression.

Objectives: We aim to characterize the role of the CDK-NF-κB crosstalk in the IL-1-driven gene expression and protein secretion in a model of human ovarian cancer.

Methods: Immortalized fallopian tube secretory epithelial cells (iFTSEC) were transformed into HGSOC cells by overexpression of MYC and the expression of a gain-of-function mutant of KRAS. Subsequently, control cells (iFTSECs or iFTSECs + empty vector) and iFTECS + mutKRAS/Myc were treated with the pan-CDK inhibitor flavopiridol or the selective CDK12/13 inhibitor THZ531. Gene expression and secretome analyses were performed to investigate the influence of CDK inhibition on IL-1-driven NF-κB gene expression.

Results: The inhibition of CDK12/13 has a differential and partially opposing effect on classical IL-1 target genes. This may result from a delayed (re-)synthesis of IκBα and A20, causing a prolonged activation of the NF-κB system. In contrast, the pan-CDK inhibitor flavopiridol profoundly suppresses the expression and secretion of tested NF-kB target genes.

Conclusion: These results demonstrate that CDK inhibitors have differential effects on the IL-1-driven tumor secretome. It will now be important to characterize the mechanisms by which CDK family members, in particular CDK12, affect the NF-κB driven *de novo* protein synthesis and the release of immunomodulatory mediators, to further assess a potential role of CDKs in shaping the NF-κB driven tumor microenvironment.

115

First preclinical insights into the anti-angiogenic actions of C81

T. Zech[1], I. Bischoff-Kont[1], G. M. Krishnathas[1], L. Berger[2], S. Rösser[3], B. Strödke[4], T. Schmid[3], S. Müller[2], S. Knapp[2], F. Bracher[4], R. Fürst[1]
[1]Goethe University Frankfurt am Main, Institute of Pharmaceutical Biology, Frankfurt am Main, Germany
[2]Goethe University Frankfurt am Main, Insitute of Pharmaceutical Chemistry, Frankfurt am Main, Germany
[3]Goethe University Frankfurt am Main, Institute of Biochemistry I, Frankfurt am Main, Germany
[4]Ludwigs-Maximilians-University München, Department of Pharmacy, Munich, Germany

Question: Angiogenesis, the formation of new blood-vessels from pre-existing ones, is a crucial physiological process. Dysregulated angiogenesis, however, is associated with poor prognosis for various pathologies, such as cancer. C81 is a carbazole analogue of the β-carboline alkaloid annomontine and has been shown to inhibit the kinases CLK1 and 4, DYRK2, and PIM3. Initial *in vitro* screenings indicated a reduction of endothelial cell functions without exerting cytotoxicity. In this project, we aimed to characterise the effect of C81 on angiogenic processes *in vitro* and to decipher the underlying mode of action.

Methods: The influence of C81 on angiogenesis-related cell functions of primary human umbilical vein endothelial cells (HUVECs) was measured with different assays, including spheroid sprouting, proliferation, scratch assays (undirected migration) as well as Boyden chamber and chemotaxis assays (directed migration) *via* live-cell imaging. On the molecular level, effects of C81 were assessed using western blotting, RT-qPCR, polysomal profiling, immunofluorescence microscopy, differential scanning fluorimetry, and nanoBRET analysis.

Results: C81 reduced the angiogenic cell activity in all models at a concentration of 3 or 10 µM. The action of C81 seemed to be selective on VEGF-induced processes over bFGF-induced ones, which might be due to a specific loss of VEGFR2 protein levels. This in turn might be explained by both a reduction of *de-novo* protein biosynthesis as well as of VEGFR2 mRNA expression. Using chemical probes for the identified target kinases of C81, we observed that neither PIM nor DYRK2 inhibition reduced VEGFR2 protein levels significantly. In contrast, CLK1/2/4 inhibition suppressed VEGFR2 protein expression in a concentration-dependent manner and mimicked C81s effects on EC spheroid sprouting and undirected migration.

Conclusion: We provide evidence that C81 acts as an inhibitor of angiogenetic processes, probably due to a strong interference with VEGFR2 expression both on the mRNA and protein level. Mechanistically, our findings suggest that CLK splicing kinases play a key role in the regulation of angiogenesis-related cell functions and the expression of VEGFR2. Further investigations regarding the mechanism of how CLK inhibition impacts angiogenesis-related cell functions as well as translational studies *ex vivo* and *in vivo* are planned to further evaluate C81 as a potential treatment option in anti-angiogenic therapy.

174

Molecular mechanisms involved in the modulation of the DNA damage response (DDR) by natural compounds (NC)

M. Sekeres[1], G. Fritz[1]
[1]Institute of Toxicology, Medical Faculty, Heinrich Heine University of Düsseldorf, Düsseldorf, Germany

Background and Aim: Recently, Secalonic acid F (SA), 5-epi-Nakijiquinone Q (NQ) and 5-epi-Ilimaquinone (IQ) were identified as the most promising NC that induce the DDR on their own or in combination with the conventional anticancer therapeutics (cAT) cisplatin and doxorubicin (doxo) in human pancreatic carcinoma cell lines. The aim of the present study is to elucidate in more detail the molecular mechanisms the aforementioned NC-based structures interfere with.

Methods: *In vitro* studies were performed employing the human pancreatic carcinoma cell line BxPC3. To characterize the influence of the NC on the mRNA expression of cisplatin-related resistance factors, qRT-PCR analyses were performed using a 96-well plate-based array. Based on the results, protein levels of selected target genes were determined by Western Blot analyses. To investigate if the NC affect the repair of doxo-induced double strand breaks (DSB), the cells were pulse-treated with doxo, followed by a post-incubation period with the NC. DNA repair of induced DSB was analyzed on the level of nuclear γH2AX foci.

Results: Mono-treatment with SA significantly reduced the expression of genes associated with DNA repair (e.g., *RAD51*, *BRCA1* and *BRCA2*). NQ significantly induced an upregulation of transporters and factors related to anti-oxidative stress response. Treatment with IQ altered the mRNA expression of the analyzed genes to a lesser extent. Western Blot analyses confirmed the downregulation of RAD51 on protein level after SA-treatment. Additionally, BCL-2 protein expression decreased upon treatment with SA. Both, SA and NQ were able to increase the number of residual γh2AX foci after pulse treatment with doxo.

Conclusion: Based on the obtained data we conclude that SA interferes with mechanisms of DNA repair by downregulating DSB repair proteins. Both, SA and NQ increased doxo-induced residual DNA damage, suggesting that both compounds inhibit DNA repair. In addition, SA stimulates apoptosis by reducing the expansion of the anti-apoptotic factor BCL-2. An objective of currently ongoing studies is to conduct RAD51-foci analyses in order to prove if their formation is affected in SA-treated cells. Additionally, further γH2AX-foci analyses are performed to analyze the impact of the NC on the repair of cisplatin- and IR-induced DSB. In summary, the results highlight SA for forthcoming pre-clinical studies to evaluate its anti-cancer efficacy *in vivo* and to determine its therapeutic window.

177

Cancer stem cell as potential diagnostic marker and new drug target in small cell lung cancer

E. Skurikhin [1], O. Pershina[1], A. Pakhomova[1], **M. Zhukova**[1], N. Ermakova[1], E. Pan[1], L. Kogai[1,2], V. Goldberg[3], E. Simolina[3], A. Kubatiev[4], S. Morozov[4], A. Dygai[1,4], A. Gabibov[5]
[1]Goldberg ED Research Institute of Pharmacology and Regenerative Medicine, Tomsk National Research Medical Centre of the Russian , Laboratory of Regenerative Pharmacology, Tomsk, Russian Federation
[2]Siberian State Medical University, Department of Pharmacology, Tomsk, Russian Federation
[3]Tomsk National Research Medical Centre of the Russian , Cancer Research Institute, Tomsk, Russian Federation
[4]Institute of General Pathology and Pathophysiology, Moscow, Russian Federation
[5]Shemyakin and Ovchinnikov Institute of Bioorganic Chemistry, Moscow, Russian Federation

Introduction: Small cell lung cancer (SCLC) is one of the most malignant tumors. Despite the fact that surgical treatment, radiation therapy, chemotherapy, and molecular targeted therapy have significantly improved the treatment of SCLC, the 5-year overall survival rate is low. The effectiveness of cancer treatment depends on a timely diagnosis, the choice of a therapeutic target, and the control of complications. Previously, we have shown a positive experience of using cancer stem cells (CSCs) for predicting complications and monitoring the effectiveness of chemotherapy in breast cancer. We suppose CSCs may be a potential therapeutic target. CSCs monitoring can be used to assess the effectiveness of treatment and to predict complications in SCLC.

Objectives: Investigate various populations of CSCs in patients with SCLC to search for effective therapeutic targets, diagnostic markers, and predictors of complications.

Patients and methods: The pilot study included healthy volunteers, patients with SCLC before treatment, and after treatment at the Cancer Research Institute of Tomsk NRMC (Tomsk, Russia). Informed consent was obtained from all individual participants included in the study. All procedures performed in the studies involving human participants were in accordance with the ethical standards. Blood samples were obtained from patients. We used the Lympholyte-H protocol for the elimination of erythrocytes and dead cells from human blood and receiving mononuclear cells. Using flow cytometry method, we studied the expression of ALDH, EGF, AXL, CD87, CD117, CD90, CD44, CD276, and CD279 on mononuclear. Intracellular markers Sox2 and Ki-67 were evaluated.

Results: Two groups of CSCs were identified: sensitive to chemotherapy and resistance of cytostatics. The study has some limitations. The study has a relatively small sample size. The results presented here need further validation using multi-center cohorts with large numbers of patients.

Conclusion: CSCs expressing ALDH, EGF, Axl, CD87, CD117, CD90, CD44, CD276, CD 279 can be both diagnostic markers and therapeutic targets in SCLC. Such cells like CD3-CD4-Axl+, CD117+CD90-CD87+, Axl+Sox2+, CD87+CD90+Sox2+, CD87+CD276+Sox2+, CD90+ CD87+CD276+CD44+Sox2+ we suggest using as markers of the effectiveness of treatment of SCLC. The predictors of chemotherapy complications are CSCs with the phenotype CD117+Axl+ EGF+CD44+, CD3-CD4-EGF+, CD117+CD90+CD87+, CD87+CD117+.

202

Functional characterization of BtkT316A, a variant either associated with germline immunodeficiency or somatic ibrutinib resistance in chronic lymphocytic leukemia

M. Wist[1], S. Endres[1], A. Schade[1], T. Monecke[1], C. Walliser[2], D. Niessing[1], P. Gierschik[2]
[1]Ulm University, Institute of Pharmaceutical Biotechnology, Ulm, Germany
[2]Ulm University, Institute of Pharmacology and Toxicology, Ulm, Germany

The approval of ibrutinib has revolutionized the treatment of chronic lymphocytic leukemia (CLL). By irreversibly binding to Cysteine 481 residue in the kinase domain of Bruton's tyrosine kinase (BTK), ibrutinib abrogates Btk kinase function and consequently inhibits B-cell receptor signaling, which is known to be crucial for the maintenance and the survival of both normal and malignant B-cells. Unfortunately, the development of acquired resistance to ibrutinib has become a major treatment obstacle. In most cases, mutations within Btk's kinase domain impairing the drug binding were found to be responsible for the acquired resistance. However, in 2016, the first and so far, only *BTK* mutation mediating ibrutinib resistance, but neither affecting the kinase domain nor drug binding was discovered. Interestingly, this SH2-domain mutation, BtkT316A, had already been reported to cause immunodeficiency, in particular X-linked agammaglobulinemia (XLA)-like symptoms. Here, we set out to determine the mechanism(s) by which BtkT316A causes immunodeficiency as a germline and mediate ibrutinib resistance as a somatic consequence and how it is able to cause ibrutinib resistance without affecting the drug binding to Btk. To this end,

we have established a reconstituted system in intact mammalian cells to analyze the functional interaction of wild-type and mutant BtkT316A with their effector protein phospholipase C-γ_2 (PLCγ_2). We show that the T316A mutation vastly enhances the ability of Btk to activate PLCγ_2 in terms of both PLCγ_2 phosphorylation and IP3 formation. Moreover, DT40 chicken B-cells, reconstituted with T316A mutant Btk showed increased levels of intracellular Ca^{2+} after B cell receptor activation, in comparison to cells expressing wild-type Btk. By examining pY-peptide-binding by fluorescence-polarization (FP), the T316A mutant had an about 10-fold higher binding affinity to the peptide, potentially indicating enhanced activation of BtkT316A by tyrosine-phosphorylated proteins endogenously present in B cells. This data suggests that the T316A mutation markedly increases Btk´s SH2 domain to activating pY ligands and, hence, its catalytic functions in intact cells. We propose that the enhanced residual BtkT316A activity at therapeutically achieved concentrations of Btk catalytic site inhibitors suffices to cause drug resistance in B cell malignancies.

208

Impact of subtype-selective histone deacetylase (HDAC) inhibitors on HER1 signaling in gastric cancer cells

R. Jenke[1,2], T. Zenz[1], L. Schäker-Hübner[3], F. Voigt[1], F. K. Hansen[3], A. Aigner[1], **T. Büch**[1]
[1]Leipzig University, Clinical Pharmacology - Rudolf-Boehm Institute of Pharmacology and Toxicology , Leipzig, Germany
[2]University Hospital Leipzig, University Cancer Center Leipzig (UCCL), Leipzig, Germany
[3]University of Bonn, Pharmaceutical Institute - Pharmaceutical and Cell Biological Chemistry, Bonn, Germany

Gastric adenocarcinoma represents one of the leading causes of cancer-related mortality worldwide. Although perioperative cytoreductive chemotherapy, targeted therapeutic approaches (e. g. HER2 inhibition), or immune checkpoint inhibitors may prolong survival, the overall outcome in patients with unresectable or metastatic gastric cancer ist still poor. Since epigenetic alterations significantly contribute to the pathogenesis of gastric cancer, epigenetic enzyme inhibitors like HDAC inhibitors represent a promising complement of the therapeutic armamentarium in this disease. Thus, we delineated the antitumor effects of HDAC inhibitors in a set of gastric cancer cells and characterized adaptive responses upon HDAC inhibition. Using HDAC inhibitors with different HDAC subtype selectivity, we found that inhibition of class I HDACs was necessary and sufficient for antiproliferative effects. Of note, class I-selective HDAC inhibitors showed potency comparable or even superior to antineoplastic unselective pan-HDAC inhibitors. With regard to adaptive responses, treatment of gastric cancer cells with pan-HDAC inhibitors or class-I-selective compounds led to an increased expression of the oncogenic receptor tyrosine kinase HER1 (EGFR) as well as HER1 ligands like amphiregulin, HB-EGF or EGF. This was seen in conventional cell culture experiments as well as in tissue slice cultures of tumor xenografts or primary patient tumor samples. Since these alterations may indicate potential resistance pathways, we further evaluated the effect of inhibiting HDAC plus the HER1 ligand amphiregulin or HER1 itself. In these experiments, inhibition of amphiregulin by siRNA-mediated knockdown did not impact the antitumor effect of HDAC inhibitors, possibly owing to the redundant functions of other upregulated HER1 ligands. In contrast, double inhibition of HDAC and HER1 led to improved antiproliferative effects indicating the usefulness of this combination strategy.

209

Antineoplastic effects of HDAC inhibitors in glioblastoma cells

A. Heinze[1], **T. Büch**[1], H. Kalwa[2], L. Schäker-Hübner[3], F. Voigt[1], R. Jenke[1,4], F. K. Hansen[3], H. Franke[2], A. Aigner[1]
[1]Leipzig University, Clinical Pharmacology - Rudolf-Boehm Institute of Pharmacology and Toxicology , Leipzig, Germany
[2]Leipzig University, Rudolf-Boehm Institute of Pharmacology and Toxicology, Leipzig, Germany
[3]University of Bonn, Pharmaceutical Institute - Pharmaceutical and Cell Biological Chemistry, Bonn, Germany
[4]University Hospital Leipzig, University Cancer Center Leipzig (UCCL), Leipzig, Germany

Glioblastoma is the most common type of malignant primary brain tumors. Since standard chemotherapy protocols show very limited efficacy in this tumor entity, there is an urgent need for novel therapeutic concepts. In the present investigation, we analyzed the antineoplastic effects of a panel of histone deacetylase (HDAC) inhibitors with different HDAC subtype selectivity in various glioblastoma cell lines in vitro as well as ex vivo. With respect to antiproliferative effects, the substance screen revealed that growth-impairment was dependent on the inhibition of class I HDACs. Specifically, the class I-selective inhibitors entinostat, VK1, and VK2 showed comparable or even superior antitumor effects as the pan HDAC inhibitor vorinostat. In contrast, agents without the propensity to inhibit class I HDACs (e.g., tubostatin, TMP-269, or PCI-34051) showed only poor antitumor activity. Since the marked infiltration of normal brain tissue by glioblastoma cells is the main obstacle for surgical intervention, we next tested antimigratory effects of HDAC inhibitors using in vitro wound healing and spheroid outgrowth assays as wells as tandem tissue slice culture systems ex vivo. Especially the latter model comprising glioblastoma xenograft tissue slices positioned on top of murine brain tissue slices allows for the evaluation of expansive growth (increase in tumor volume) and infiltrative tissue invasion. Of note, HDAC inhibition - even at cytotoxic concentrations - did not efficiently impair the motility of glioblastoma cells in vitro. More importantly, HDAC inhibition did not show substantial effects on the invasive potential of glioblastoma cells in tandem slice cultures. These findings suggest that HDAC inhibitors may not be sufficiently effective as single agents but should be combined with therapeutics targeting the invasive phenotype of glioblastoma cells. Moreover, these investigations illustrate that in anticancer drug screens holistic experimental models are required, covering a comprehensive picture of the malignant phenotype.

226

LPA-induced phosphorylation of Filamin A regulates association with Myocardin-related transcription factor A (MRTF-A) and cellular senescence

A. Konopa[1], M. A. Meier[1], S. Muehlich[1]
[1]Friedrich-Alexander University Erlangen-Nürnberg, Department of Chemistry and Pharmacy, Erlangen, Germany

Myocardin-related transcription factor A (MRTF-A) is a coactivator of the ubiquitously expressed transcription factor Serum Response Factor (SRF) which controls fundamental biological processes such as cell growth, migration, differentiation and plays an important role in hepatocellular carcinoma (HCC) formation. Lysophosphatidic acid (LPA) stimulation leads to translocation of MRTF-A from the cytoplasm to the nucleus resulting in SRF activation, association with the actin-binding protein Filamin A (FLNA) and MRTF/SRF target gene expression. We found that the G protein-coupled LPAR1 receptor promotes phosphorylation of Filamin A (FLNA) at serine 2152 via protein kinase C (PKC). By using the nonphosphorylatable FLNA S2152A mutant or LPAR1 depletion, we demonstrate that FLNA phosphorylation plays a crucial role for binding to MRTF-A, MRTF/SRF target gene expression and senescence induction in HCC cells. Since LPAR1 is overexpressed in human HCCs, LPAR1 represents a promising druggable therapeutic target for HCC therapy.

264

A LC-HRMS method for drug exposure measurement of 57 oral anticancer drugs in human plasma

N. Kehl[1], P. Dürr[1], K. Schlichtig[1], R. Maas[1], M. F. Fromm[1], A. Gessner[1], R. V. Taudte[1]
[1]Institute of Experimental and Clinical Pharmacology and Toxicology, FAU Erlangen-Nürnberg, Clinical Pharmacology and Clinical Toxicology, Erlangen, Germany

Introduction: The approval of multiple oral antitumor drugs has led to significant improvements in the treatment of several tumor entities. During therapy with oral anticancer drugs, highly variable plasma concentrations can be observed, resulting in risks for reduced therapeutic effects or increased rates of side effects. Therapeutic drug monitoring is a useful tool to detect increased or reduced patient plasma levels of oral anticancer drugs. However, current methods do not cover the broad range of oral antitumor drugs used in clinical routine. Therefore, there is a strong need for a method, which can simultaneously determine the plasma concentrations of a variety of oral anticancer drugs.

Objective: The aim of this work was to develop and validate a method for the simultaneous quantification of 57 oral antitumor drugs.

Material & Methods: Ultra-high performance liquid chromatography coupled to an Orbitrap mass spectrometer was used for quantification of these drugs. The method was fully validated according to the FDA guideline and constitutes a simple and robust way for exposure monitoring of a wide variety of oral anticancer drugs. Applicability to real world samples was demonstrated with 71 samples taken from 39 patients of the Comprehensive Cancer Center Erlangen-EMN.

Results: All oral anticancer drugs included in the method fulfilled the FDA recommendations for validation. Furthermore, in accordance with other studies, highly variable plasma concentrations were observed. This underlines the need for further clinical studies focusing on the correlation between plasma concentrations and clinical outcome in patients during therapy with oral anticancer drugs.

Conclusion: Our new multi-drug method allows simultaneous quantification of 57 oral antitumor drugs, which can be applied to exposure monitoring in clinical studies, taking into account the broad variety of oral antitumor drugs prescribed in clinical routine.

271

Medication review and therapy optimization in survivors of gynecological tumors as part of the study "Survivorship Clinic for long-term survivors with gynecological cancer"

E. Algharably[1], F. Meinert[1], R. Kreutz[1], J. Porst[2], S. Roll[3], M. Keller[4], T. Reinhold[5], P. Hühnchen[6], W. Böhmerle[6], M. Endres[6], K. Wittke[7], C. Scheibenbogen[7], A. Pirmorady[8], M. Rose[8], E. Steinhagen-thiessen[9], F. Edelmann[10], K. Mai[11], L. Maurer[11], V. Krell[2], C. Stoklossa[12], S. Boz[4], S. Willich[13], B. Wolfarth[2], J. Sehouli[14], H. Woopen[14]
[1]Charité – Universitätsmedizin Berlin, Institut für Klinische Pharmakologie und Toxikologie, Berlin, Germany
[2]Charité – Universitätsmedizin Berlin, Institut für Sportmedizin, Berlin, Germany
[3]Charité – Universitätsmedizin Berlin, Institut für Sozialmedizin, Epidemiologie und Gesundheitsökonomie, Berlin, Germany
[4]Nord-Ostdeutsche Gesellschaft für Gynäkologische Onkologie (NOGGO e.V.), Berlin, Germany
[5]Charité – Universitätsmedizin Berlin, Institut für Sozialmedizin, Epidemiologie und Gesundheitsökonomie, Berlin, Germany
[6]Charité – Universitätsmedizin Berlin, Klinik für Neurologie, Berlin, Germany
[7]Charité – Universitätsmedizin Berlin, Fatigue-Zentrum, Berlin, Germany

[8]Charité – Universitätsmedizin Berlin, Medizinische Klinik mit Schwerpunkt für Psychosomatik, Berlin, Germany
[9]Charité – Universitätsmedizin Berlin, Medizinische Klinik für Endokrinologie, und Stoffwechselmedizin, Berlin, Germany
[10]Charité – Universitätsmedizin Berlin, Klinik für Kardiologie, Berlin, Germany
[11]Charité – Universitätsmedizin Berlin, Medizinische Klinik für Endokrinologie, Diabetes und Stoffwechselmedizin, Berlin, Germany
[12]Charité – Universitätsmedizin Berlin, Sozialdienst, Berlin, Germany
[13]Charité – Universitätsmedizin Berlin, Institut für Sozialmedizin, Epidemiologie und Gesundheitsökonomie, Berlin, Germany
[14]Charité – Universitätsmedizin Berlin, Klinik für Gynäkologie mit Zentrum für onkologische Chirurgie, Berlin, Germany

Question: Improvement of quality of life (QoL) is an important goal in long-term survivors (LTS) of patients with cancer, which applies also to LTS of gynecological tumors. We aim to improve QoL by implementing a structured medication review and assessment in LTS of gynecological tumors in routine clinical practice. We evaluate the impact of clinical pharmacological assessment on medication safety, therapy optimization and QoL.

Methods: A total of 180 electronic patient records in the context of the ongoing *'Survivorship Clinic for long-term survivors with gynecological cancer'* study will be reviewed by clinical pharmacologists at baseline. Available data include disease and medication history for all prescribed, over the counter, dietary supplements, and complementary medications in conjunction with clinical parameters. Indications, contraindications, agreement with current guideline recommendations, identification of drug-related problems including inappropriate dosing, over-treatment, under-treatment, non-adherence, adverse effects and drug-drug interactions (DDI) using electronic drug information systems will be identified. Based on the review, recommendations for changes in therapy will be provided to the treating physician in routine care. As a follow-up, patient records will be reassessed at 6 and 12 months. Change in QoL score (SF-36) is the primary outcome for the overall intervention. Secondary outcomes of this project include evaluation of the number of contraindications, significant DDI, and inappropriate medications for patients older than 65 according to the Fit for the Aged (FORTA) criteria.

Results: Preliminary data for 35 patients (mean age 60.4±10.5 years) with ovarian (79.2%), cervical (17%) and endometrial (3.8%) cancer show, that in 32 patients (91.4%) proposals for specific disease-monitoring (mostly blood pressure and laboratory control) and/or medication adjustment were made. Polypharmacy was detected in 5.7%, clinically relevant DDI in 8.6%, inadequate medications in older patients in one patient. Dose adjustment was recommended in two patients due to underdosing.

Conclusions: Our current experience in this pilot project documents the feasibility of a structured medication review with clinical pharmacology assessment. Our preliminary data indicate that the frequency of patients exposed to polypharmacy and significant DDI is relatively low. Nevertheless, clinical pharmacology assessment may contribute significantly to the improvement in QoL of LTS of gynecological cancer.

274

Non genomic hypoxia sensing through TRPA1 enhances malignancy of glioblastoma

W. Haupt[1], N. Urban[1], B. Stattelmann[1], T. Büch[2], H. Franke[1], A. Aigner[2], U. Krügel[1], W. Nörenberg[1], F. Gaunitz[1], M. Schaefer[2], H. Kalwa[1]
[1]RBI Leipzig, Pharmakology, Leipzig, Germany
[2]RBI Leipzig, Leipzig, Germany

Background: Glioblastoma multiforme (GBM) is the most common and also deadliest type of primary malignant brain tumor. Resistance to chemo-therapeutics is a frequent occurrence in GBM patients, leading to subsequent tumor regrowth /relapse. The transient receptor potential channel A1 (TRPA1) is present in GBM and can be activated by either hypoxia or chemical stimuli. The MARCKS protein is altered in many cancers including GBM and is a constituent of directed cellular movement and development of chemoresistance. Furthermore, it occurs to be of importance in the TRPA1 pathway. We presume TRPA1 to be the sensor allowing GBM cells, via the activation of MARCKS, to evade chemotherapy and invade healthy brain tissue.

Results: We analyzed 20 primary samples of GBM cells as well as 5 established GBM cell lines for the functional expression of TRPA1. We found TRPA1 to be present in half of all samples and cell lines. Here in the individual tumor / line only a subset of cells expressed TRPA1. We divided the GBM cell line T98G (32% A1 positive cells) into TRPA1 expressing (A1+) and non expressing (A1-) subclones and validated their identity via genomic fingerprinting. A1+ cells showed TRPA1 presence on mRNA, protein and functional level. Upon activation of TRPA1 via the known activators Allyl isothiocyanate (AITC) and clopidogrel we could detect calcium influx that was abolished in the presence of known the TRPA1 blockers HC-030031 and ruthenium red. Activation of TRPA1 expelled MARCKS from the plasma membrane and led to its association with the actin cytoskelleton dependent on the presence of extracellular calcium. Gap closure assays showed a faster movement of A1+ cells in the presence of clopidogrel (500nM). Prolonged culture of the A1+ and A1- subclones (50 passages) led to the reestablishment of the expression ratio present in the T98G-WT cells. Analysis of tumor organoids composed of 1/3 optically traceable A1+ (+ H2B-RFP) and 2/3 A1- showed the accumulation of A1+ cells in the outer perimeter of the spheroid. The same phenomenon was observed in xenografts of T98G-WT cells where TRPA1 positive cells were notably more present in the outer areas of the tumor.

Conclusion: TRPA1 is expressed in GBM tumors allowing for the detection of adverse microenvironments and the initiation of evasive mechanisms. Therefore TRPA1 is an important factor for GBM progression and its inhibition could be a novel and powerfull therapeutic option.

285

Cardiac hERG channel blockers sensitize human glioblastoma cells towards the genotoxic effects of temozolomide

L. Knödler[1,2], **I. Roth**[1,3], M. Wos-Maganga[3], S. Weickhardt[1], M. Vogel[1], B. Haas[1]
[1]Federal Institute for Drugs and Medical Devices, Bonn, Germany
[2]University of Bonn, Institute of Biochemistry and Molecular Biology, Medical Faculty, Bonn, Germany
[3]Cologne University of Applied Sciences, Faculty of Applied Natural Sciences, Leverkusen, Germany

Question: Voltage-gated potassium channels transfer K+ ions from the cytosol to the exterior of the cell and inhibition can result in QT prolongation and arrhythmias[1]. Beside cardiac membrane repolarization, K+ channels play a crucial role in cell proliferation and growth and have been studied extensively in relation to cancer. Especially K+ channels of the ether-à-go-go (EAG) family are overexpressed in tumor tissue and inhibition of the channels has been shown to induce cell death in tumour cell lines of different origins[2]. Here, the role of EAG channels in glioblastoma multiforme (GBM) cells was determined in terms of chemosensitizing effects in combination with the standard treatment temozolomide (TMZ).

Methods: Expression of EAG channels hERG and EAG1 was visualized in three GBM cell lines and primary cells by immunocytochemistry and Western blotting. Cytotoxicity of two EAG channel inhibitors, astemizole (AST) and terfenadine (TERF) alone or in combination with TMZ was determined by MTT assays and Annexin V/PI FACS analyses. P53 phosphorylation status was investigated by Western blotting. Intracellular concentrations of AST and TERF were determined by LC-MS analytics.

Results: Both, hERG and EAG1 were expressed in GBM cell lines and primary cells. IC_{50} values of AST and TERF in MTT assays were nearly the same in three tested GBM cell lines (U87, U251 and U373, IC50: x, y, z, respectively) and in primary GBM cells. Combination treatment of TMZ and AST or TERF significantly reduced IC_{50} values in comparison to TMZ alone indicating a sensitization of the cells. This effect was strongest for U87 and BT74 cells while it was only borderline significant for U373 and U251 cells. In line with that, cells treated with both, EAG channel inhibitor and TMZ showed a higher number of apoptotic rates compared to mono TMZ treatments. This was also resembled in P53 Ser15 phosphorylation status. As AST and TERF are highly protein bound and theorized to attach to plastic materials, intracellular concentration was determined in U87 cells confirming this theory.

Conclusion: The results suggest that EAG channels play a crucial role in GBM cells and EAG inhibitors might be a promising approach to tackle GBM when applied alone or in combination with TMZ if problems of side effects like QT prolongation could be prevented by specific inhibitors.

1 Zünkler BJ. Human ether-a-go-go-related (HERG) gene and ATP-sensitive potassium channels as targets for adverse drug effects. Pharmacol Ther. 2006 Oct;112(1):12-37.

2 Wang X, et al. Eag1 Voltage-Dependent Potassium Channels: Structure, Electrophysiological Characteristics, and Function in Cancer. J Membr Biol. 2017 Apr;250(2):123-132.

Pharmacology – CNS / endocrine pharmacology and treatment

21

Patients with medical cannabis exhibited prolonged survival in Specialized Outpatient Palliative Care (SAPV)

K. Gastmeier[1], A. Gastmeier[2], **R. Böhm**[3], R. Bimberg[4], T. Herdegen[3]
[1]GP practice, Potsdam, Germany
[2]GP practice, Kleinmachnow, Germany
[3]University Hospital Schleswig-Holstein (UKSH), Institute of Experimental and Clinical Pharmacology, Kiel, Germany
[4]StatConsult IT-Service GmbH, Magdeburg, Germany

Question: Medical cannabinoids (MC such as THC/dronabinol) are relevant therapeutics in palliative care settings. Its progressing use is limited by insufficient data of efficacy, especially endpoints like mortality, quality of life, reduction of polypharmacy and associated side effects and morbidity.

Methods: In this retrospective, observational analysis, we compared survival of all patients in a GP"s practice who were in Specialized Outpatient Palliative Care (SAPV). A cohort of 800 patients was extracted using Pallidoc® and analysed using a Kaplan-Meier survival curve using R/survival&survminer. A Cox proportional hazard model was employed to further assess the influence of sex, age, dosage and disease coded in ICD-10.

Results: 800 SAPV patients were included in the analysis. 137 patients received MC (female: 45.3%; >75 years: 44.5%); 663 SAPV patients (female: 51.3%; > 75 years: 62.7%) served as control group.

MC therapy was associated with a significantly longer median survival time (65 vs. 44 days, p=0.0046) (Figure 1).

Subgroup analysis (provided evidence of the benefit for women (64 vs. 43 days, p=0.036), older patients (>75 years: 62 vs 37.5 days, p=0.022) and in particular women > 75-years (62.5 vs. 33 days , p=0.041). Men showed a trend towards longer median survival time under MC therapy (75 vs.47 days), but this prolongation of survival did not reach statistical significance.

The multivariable analysis confirmed the observed positive correlation of the MC therapy on the median survival time of SAPV patients (control / MC HR: 1.29; p = 0.008) taking into account the influencing factors age and gender.

Segmenting into low dose (<7.5 mg THC / day; median daily dose 3.2 ± 2.1 mg THC) and patients with a higher dose MC therapy (median daily dose 12.0 ± 8.4 mg THC) suggests that the higher-dose therapy is superior in terms of median survival time (104 days high dose vs. 57 days low dose).

Conclusions: Palliative patients with MC had a significant and clinically relevant prolonged median survival time in an outpatient setting, with a trend of stronger effects for women and elderly patients and higher dosages.

Since this analysis is not a pre-designed study, confounding factors leading to the difference of the endpoint cannot be excluded and any conclusions concerning the causality cannot be drawn.

Acknowledgement: The authors thank Dr. Nadine Mikuda for her assistance in analysing the data and preparing the tables and figures.

Fig. 1

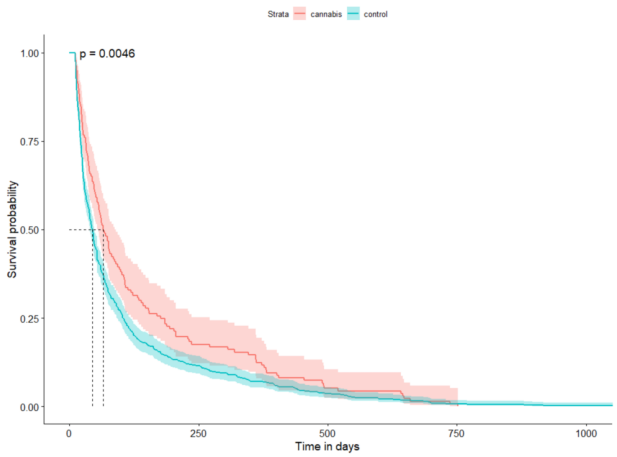

43

The extracellular signal-regulated kinases ERK1/2 are critical for the outcome of ischemic stroke

C. Schanbacher[1,2], M. Bieber[3], Y. Reinders[2], C. Mathejka[2], A. Sickmann[2], C. Kleinschnitz[4], F. Langhauser[4], K. Lorenz[1,2]
[1]Institute of Pharmacology and Toxicology, University of Würzburg, Würzburg, Germany
[2]Leibniz-Institut für Analytische Wissenschaften - ISAS - e.V., Dortmund, Germany
[3]University Hospital Würzburg, Department of Neurology, Würzburg, Germany
[4]University Hospital Essen, Department of Neurology, Essen, Germany

Objectives: Ischemic disorders are the leading cause of death worldwide. The extracellular signal-regulated kinases 1 and 2 (ERK1/2) are part of the Raf/MEK/ERK1/2 cascade and are thought to affect the outcome of ischemic stroke. However, it is under debate whether activation or inhibition of ERK1/2 is beneficial. Therefore, this study aimed to investigate the impact of ERK1/2 after cerebral ischemia using transgenic mice with ubiquitous overexpression of ERK2 or of the Raf kinase inhibitor protein (RKIP), an inhibitor of the ERK1/2 signaling cascade.

Methods: We generated mice with ubiquitous overexpression of $ERK2^{wt}$, $RKIP^{wt}$ or a mutant of RKIP ($RKIP^{S153A}$). Phosphorylation of serine 153 of RKIP was shown to release RKIP from Raf, thus, $RKIP^{S153A}$ acts mainly as a Raf/MEK/ERK1/2 inhibitor. Transgenic mice and wild-type (wt) littermates were subjected to transient occlusion of the middle cerebral artery (45min) to induce cerebral ischemia. 24h after reperfusion, infarct volume was analyzed by TTC-staining, the neurological phenotype by applying the Bederson Score and Grip-test, blood brain barrier (BBB) stability by Evans Blue extravasation and rt-PCR of endothelin-1, inflammation by rt-PCR and immunostaining of adhesion molecules, cytokines and neutrophils and apoptosis by TUNEL-staining.

Results: Overexpression of ERK2 led to a massive increase in infarct volume whereas $RKIP^{wt}$ and $RKIP^{S153A}$ expression significantly reduced the infarct size compared to wt controls. The extent of the infarct volume translated into respective neurological deficits, i.e. $ERK2^{wt}$ mice had a significantly worse motoric and neurological phenotype, while the one of RKIP-tg mice was significantly better compared to wt mice. Interestingly, BBB leakiness, inflammation and apoptotic neurons were significantly increased in $ERK2^{wt}$ compared to wt controls. The protective effects of RKIP overexpression correlated with anti-inflammatory signaling. However, RKIP expression had no impact on BBB disruption and neuronal apoptosis. Thus, in particular inhibition of inflammation might be an important mechanism to combat a worse outcome after ischemic stroke.

Conclusion: Our data suggest that a tight control of the Raf/MEK/ERK1/2 cascade is essential for a less detrimental outcome after ischemic stroke. Further studies need to analyze co-factors for the aggravation of a detrimental ERK "hyper"-activation in stroke and how RKIP can counterbalance the inflammatory responses to cerebral ischemia.

59

Serotonin plays a pivotal role in the regulation of glucose homeostasis during pregnancy in a prediabetic mouse model

M. Liebmann[1], M. Asuaje Pfeifer[1], S. Scherneck[1]
[1]Technische Universität Braunschweig, Institute of Pharmacology, Toxicology and Clinical Pharmacy, Braunschweig, Germany

Question: Gestational diabetes mellitus (GDM) is the most common disorder in pregnancy characterized by impaired glucose tolerance (IGT). New Zealand obese (NZO) mice are a prediabetic model, exhibiting IGT preconceptionally (pc.) and during pregnancy, pc. hyperinsulinemia associated with impaired glucose-stimulated insulin secretion and develop hyperlipidemia during gestation. Serotonin (5-HT) a neurotransmitter known for modulating complex neuronal functions like cognition and mood, is considered a modulator in metabolic processes outside the nervous system. Interestingly, after the second trimester at day 14.5 (d14.5) pancreatic 5-HT levels are markedly increased in NZO mice. The aim of this project was to elucidate the modulatory influence of 5-HT upon hepatic glucose metabolism of the prediabetic model during pregnancy.

Methods: Animals were sacrificed at 9-10 weeks of age, livers were harvested and primary hepatocytes (PH) were cultured with optional 5-HT incubation. Insulin-stimulated AKT activity and cAMP levels were determined by ELISA. Hepatic glucose production (HGP) was determined by fluorometric assay after overnight fasting with optional insulin stimulus. Glucose uptake was measured by 2-deoxyglucose (2-DG) uptake assay, after initial glucose deprivation. 5-HT receptor antagonists, ketanserin and SB206553, were used as controls.

Results: NZO PH showed decreased AKT activation compared to NMRI controls pc. and at d14.5. Combined, insulin and 5-HT caused a slight induced AKT activation as well as increased intracellular cAMP levels after 5-HT treatment. In 5-HT treated NMRI PH, insulin-mediated HGP was subdued. The treatment with antagonists led to a further reduction. In 5-HT treated NZO PH, insulin-mediated HGP was increased, indicating a diminished response to insulin. The HGP was reduced by antagonists, but the inadequate response remained. Contrary to NZO, NMRI PH responded to insulin with increased 2-DG uptake both, pc. and at d14.5. In both strains, 5-HT tended to reduce 2-DG uptake compared to the non-5-HT and insulin-only stimulated condition, which was reversed by SB206553.

Conclusion: 5-HT revealed several endocrine effects on metabolic signaling in PH. Thus, increased HGP and diminished 2-DG uptake foster a prediabetic phenotype by promoting altered glucose homeostasis. Pharmacological interaction with peripheral 5-HT synthesis and its hepatic signaling are potential targets for the treatment of prediabetes and GDM.

126

Increase of glutamate-induced HT22 cell death by BioDEP involves ferroptosis and Epac1

H. Yan[1], M. Veen[1], L. S. Gerber[1], Y. Zhang[1], F. Cassee[1], F. Lezoualc'h [1], A. Dolga[1], M. Schmidt[1]
[1]Faculty of Science and Engineering, Department of Molecular Pharmacology, Groningen, Netherlands

Question: Air pollution exposure is one of the important threats to human health. Diesel combustion produces diesel exhaust particles (DEP) which seem to contribute to the onset of different neurological diseases due to the induction of oxidative stress, inflammation and neuronal degeneration. Underlying molecular mechanisms are ill defined. Glutamate-induced neurotoxicity has been linked to oxidative stress and neuronal cell death including the newly identified iron-dependent form of cell death ferroptosis [1]. Cyclic adenosine monophosphate (cAMP) seems to be linked to ferroptosis type of cell death in processes involving Epac (exchange protein directly activated by cAMP) [2]. We investigated 1) a potential interaction between glutamate-

induced neurotoxicity and (Bio)DEP, and 2) underlying molecular mechanism using HT22 cells as a model system.

Methods: Hippocampal neuronal (HT22) cells were treated with DEP and BioDEP [3] at different concentrations (up to 600 µg/mL) for 24h alone or in combination with glutamate (3 mM, 18h) at the indicated concentrations. Cell viability was measured by MTT assay, and propidium iodide (PI) staining by fluorescence microscopy. To further determine the basis of BioDEP and glutamate mediated cell death, several inhibitors (QVD, 10 µM; ferrostatin-1, 5 µM; ESI-05, 30 µM; CE3F4, 30 µM) were used.

Results: HT22 cells were treated for the indicated time points and concentrations with DEP and BioDEP. Neither DEP nor BioDEP alone did not significantly change HT22 cell viability. Compared with glutamate treatment alone, combined glutamate and BioDEP (100 µg/mL) – but not DEP - treatment significantly reduced cell viability measured by MTT and PI staining. Neither pan-caspase inhibitor QVD nor Epac2 inhibitor ESI-05 restore cell viability after treatment of glutamate and BioDEP, but ferroptosis inhibitor ferrostatin-1 and Epac1 inhibitor CE3F4 did.

Conclusions: Our current work demonstrates that co-treatment of HT22 cells with glutamate and BioDEP – but not DEP - caused a significant increase in cell death. Accelerated cell death of HT22 cells by glutamate and BioDEP seems to involve ferroptosis (ferrostatin-1), in a process independent of caspase (QVD) but dependent on Epac1 (CE3F4). Currently, we study the mechanisms leading to the regulation of ferroptosis by Epac1.

References:
1. Wan et al. Trends Cell Biol. 26, 165-176
2. Fazal et al. Circ Res, 2017. 120, 645-657
3. Gerlofs-Nijland et al. Inhal. Tox. 31, 89-98

137

Influence of estradiol and serotonin on hyperglucagonemia in a pregnant mouse model with impaired glucose tolerance

M. Asuaje Pfeifer[1], M. Liebmann[1], K. Grupe[1], S. Scherneck[1]
[1]Technische Universität Braunschweig, Institute of Pharmacology, Toxicology and Clinical Pharmacy, Braunschweig, Germany

Question: Hyperglucagonemia plays a crucial role in the pathophysiology of type 2 diabetes and prediabetes. Recently published data from our group have shown that preconceptional (pc.) hyperglucagonemia improves during gestation in female New Zealand obese (NZO) mice, which show an impaired glucose tolerance but no overt diabetes. Pregnancy is characterized by hormonal changes, including elevated estradiol (E2) plasma levels and serotonin (5-hydroxytryptamine, 5-HT) content in pancreatic islets, which are able to secrete 5-HT in a glucose-dependent manner. An inhibitory effect on glucagon secretion has been described for both E2 and 5-HT. Therefore, the aim of this study was to investigate the role of 5-HT and E2 as compensatory modulators of pancreatic islet glucagon secretion during pregnancy under conditions of impaired glucose tolerance.

Methods: Female NZO mice and NMRI control mice were examined pc. and on day 14.5 of gestation. Islets were isolated by collagenase digestion technique. To determine 5-HT secretion, islets from pregnant mice were incubated in the presence of 5 or 20 mM glucose. Thereafter, islet 5-HT was extracted. For determination of glucagon secretion, islets from pc. mice were incubated in the presence of 5 or 20 mM glucose (control) and 20 mM glucose in combination with 5-HT or E2. Hormone concentrations in medium, islets and plasma were measured by ELISA.

Results: On day 14.5 of gestation, NZO mice exhibited both elevated plasma 5-HT and E2 levels as well as an increased islet 5-HT content compared to NMRI control mice. Furthermore, 5-HT secretion of isolated islets was significantly enhanced by 20 mM Glucose compared to 5 mM Glucose in NMRI mice on day 14.5 of gestation, while NZO mice showed no substantial response to 20 mM Glucose. Glucagon secretion from NMRI islets was not significantly affected by E2 and 5-HT, but in NZO mice, a concentration of 100 nM E2 led to an increase and 1,000 nM 5-HT led to an inhibition of glucagon secretion.

Conclusion: Although plasma E2 levels are elevated during pregnancy in NZO mice, E2 does not appear to improve plasma glucagon levels. Increased islet 5-HT content could contribute to improved hyperglucagonemia in NZO mice during gestation through a paracrine effect by secretion of 5-HT in a glucose-independent manner.

180

Renoprotective effects of Fenofibrate and Fosinopril combination in Alloxan induced diabetic nephropathy in rats

A. Jain[1], J. Chaudhary[1], N. Gahalain[1], K. Gupta[1]
[1]M M College of Pharmacy, MM (Deemed to be University), Mullana, Pharmaceutical Sciences, Ambala, India

Background: Diabetic nephropathy is a consequence of the interaction between hemodynamic and metabolic factors due to long-standing diabetes mellitus and poor glycemic control. Antihypertensive agents have been shown to delay the progression of diabetic complications. Also, several experimental studies have demonstrated the efficacy of PPARα agonists to ameliorate the progression of glomerulosclerosis and direct beneficial renal effect but its combination with fosinopril remains unexplored. Therefore the present study was aimed to investigate the protective role of fenofibrate and fosinopril either alone or in combination against diabetes nephropathy.

Methods: Diabetes was induced by intraperitoneal injection of 150 mg/kg Alloxan. Thirty male Wistar rats were randomly allocated into five groups comprising normal control, alloxan-diabetic control, fenofibrate (32 mg/kg *p.o.*) + diabetes, fosinopril (40 mg/kg *p.o.)* + diabetes, fenofibrate + fosinopril + diabetes respectively. Assessment of blood glucose levels, electrolyte imbalance, dyslipidemia, renal dysfunction, and oxidative stress were carried out by their respective biochemical assays and ELISA kits. All parameters were assessed at zero, 21st, and at the end of 6 weeks in normal and diabetic rats with or without drug treatments. Histopathological changes were evaluated by H&E staining at the end of the study.

Results: Alloxan administration resulted in significant bodyweight decline, increased blood glucose levels, and renal dysfunction which was manifested as an increase in serum creatinine, BUN, 24-hr proteinuria, reduced clearance, and severely imbalanced electrolyte levels. Additionally, triglycerides and cholesterol in diabetic rats were found to be remarkably elevated as compared to normal rats which were also evident in previous studies. Notably, post-treatment with fosinopril and fenofibrate combination initiated after three days of alloxan administration reduced the blood glucose levels, resolved renal dysfunction, improved lipid, and electrolyte imbalance. Moreover, diabetic kidneys displayed morphological alterations partially resolved in treatment groups and an increase in oxidative stress depicted by downregulated GSH and MDA levels which were ameliorated in all the treatments groups.

Conclusion: The present study revealed that fenofibrate and fosinopril exhibits synergistic effects against diabetes-induced nephropathy and renal oxidative damage in rats following two distinct pathways

Fig. 1

Table 1: Effect of Fenofibrate, Fosinopril and Feno-Fosino Combination on Glucose, Triglyceride, Cholesterol, GSH and MDA levels at 42nd day in Alloxan-Induced Diabetic Nephropathy in Rats.

Groups	Glucose (mg/dl)	Triglycerides (mg/dl)	Cholesterol (mg/dl)	GSH (nmol/mg protein)	MDA (nmol/mg protein)
Normal control	110.40±3.968	60.80±2.673	68.20±2.253	5.44±0.118	0.83±0.0462
Alloxan-Diabetic control	333.86±2.576 ^{a}	110.35±2.499 ^{a}	101.15±2.461 ^{a}	1.31±0.12 ^{a}	1.89±0.0822 ^{a}
Fenofibrate Treated Group (32 mg/kg)	220.75±3.956 ^{a,b}	83.37±3.674 ^{a,b,d}	71.40±4.145 ^{a,b}	3.53±0.138 ^{a,b}	1.54±0.0430
Fosinopril Treated Group (40 mg/kg)	281.00±5.268 ^{a,b,c}	88.64±2.620 ^{a,b,c}	89.20±3.035 ^{a,b,c}	3.29±0.154 ^{a,b}	1.38±0.0296
Feno-Fosino Treated Group	149.14±3.43 ^{b,c,d}	77.64±3.114 ^{a,b,c,d}	64.17±1.922 ^{b,d}	4.30±0.134 ^{a,b,c,d}	1.05±0.0445 ^{b}

All values are represented as mean ± SD for each group. $^{a}p < 0.05$ *vs* Normal Control; $^{b}p < 0.05$ *vs* Diabetic Control; $^{c}p < 0.05$ *vs* Fenofibrate treated group; $^{d}p < 0.05$ *vs* Fosinopril treated group;

Fig. 2

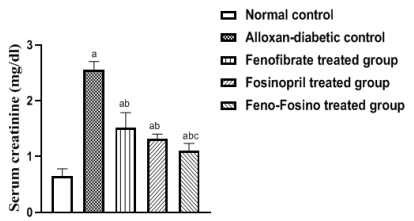

Figure 2: Effect of Fenofibrate, Fosinopril and Feno-Fosino Combination on Creatinine at 42nd day in Alloxan-Induced Diabetic Nephropathy in Rats. All values are represented as mean ± SD for each group. $^{a}p < 0.05$ *vs* Normal Control; $^{b}p < 0.05$ *vs* Diabetic Control; $^{c}p < 0.05$ *vs* Fenofibrate treated group; $^{d}p < 0.05$ *vs* Fosinopril treated group

282

Regulation of the c-fos gene promoter by dual leucine zipper kinase

K. Köster[1,2], J. Duque Escobar[2,3], E. Oetjen[1,2,4]
[1]University Medical Center Hamburg-Eppendorf, Institute for Clinical Pharmacology and Toxicology, Hamburg, Germany
[2]DZHK (German Center for Cardiovascular Research), Hamburg/Kiel/Lübeck, Germany
[3]University Medical Center Hamburg Eppendorf, UHZ, Hamburg, Germany
[4]University of Hamburg, Institute of Pharmacy, Hamburg, Germany

Introduction: The dual leucine zipper kinase (DLK, MAP3K12) is predominantly expressed in the neuronal system, and [KK1]in [EO2] beta-cells of the endocrine pancreas. Activation of DLK [EO3] has been shown to contribute to the pathogenesis of neurodegenerative diseases such as Alzheimer"s disease via phosphorylation of the transcription factor c-Fos.

Objectives: C-Fos as an immediate early gene is mainly regulated at a transcriptional level so our aim was to investigate the effect of DLK on the c-fos promoter activity and gene expression in the electrically excitable β-[EO4]cell line HIT-T15.

Materials & methods: [EO5]Transient transfections and luciferase reporter gene assays of 5" and 3" deletions and internal deletions of the human c-Fos gene promoter (-711-+48 bp). Mutation of the catalytical domain of the endogenous DLK by exchange of the Lysine 185 to Alanine (K185A) in HIT-T15 cells was mediated through CRISPR-Cas9 and homology directed repair. When indicated cells were treated with KCl [40mM] to induce calcium influx and/or the adenylate cyclase activator forskolin [10µM] for 6 hours. RNA was extracted by RNAzol B and reverse transcription was performed using the High-Capacity cDNA Reverse Transcription Kit (Applied Biosystems, Massachusetts, USA) following manufacturer"s instructions. Gene expression was measured with TaqMan and real time quantitative PCR.

Results: DLK increased c-fos promoter activity twofold. Using 5"-, 3"- promoter deletions, the promoter regions from -348 to - 339 base pairs (bp) and from a -284 to - 53 bp conferred basal activity, whereas the promoter region from -711 to - 348 bp and from -52 to +48 bp mediated DLK responsiveness. Mutation of the cAMP response element within the promoter prevented the stimulatory effect of DLK. Treatment of HIT cells with KCl and forskolin increased c-FOS promoter transcriptional activity 9-fold. Since the transcriptional activity of those promoter fragments activated by KCl and forskolin was decreased by DLK, DLK might interfere with KCl/ forskolin-induced signaling. In a newly generated, genome-edited HIT cell-line lacking catalytically active DLK, c-Fos mRNA levels were reduced by 80 % compared to the wild-type cell-line.

Conclusion: DLK increased c-Fos promoter activity but decreased stimulated transcriptional activity, suggesting that DLK fine-tunes c-Fos promoter dependent gene transcription. Moreover, at least in HIT cells, DLK is required for Fos mRNA expression.

Pharmacology – Pharmacogenomics and personalized medicine

8

Role of *FNTB* promoter polymorphisms for prognostic stratification in triple negative breast cancer

D. Jung[1], T. Link[2,3,4,5,6], A. Arnold[1], E. Kantelhardt[7,8], M. Vetter[7], C. Thomssen[7], P. Wimberger[2,3,4,5,6], J. D. Kuhlmann[2,3,4,5,6], H. S. Bachmann[1]
[1]Witten/Herdecke University, Institute of Pharmacology and Toxicology, Centre for Biomedical Education and Research (ZBAF), Witten, Germany
[2]Technische Universität Dresden, Department of Gynecology and Obstetrics, Medical Faculty and University Hospital Carl Gustav Carus, Dresden, Germany
[3]National Center for Tumor Diseases (NTC), Dresden, Germany
[4]German Cancer Research Center (DKFZ), Heidelberg, Germany
[5]Helmholtz-Zentrum Dresden-Rossendorf (HZDR), Dresden, Germany
[6]German Cancer Consortium (DKTK), Dresden, Germany
[7]Martin-Luther-University Halle-Wittenberg, Department of Gynecology, Halle, Germany
[8]Martin-Luther-University Halle-Wittenberg, Insitute of Medical Epidemiology, Bioinformatics and Statistics, Halle, Germany

Introduction: In breast cancer, a promising efficacy of farnesyltransferase (FTase) inhibitors (FTIs) in preclinical studies is in contrast to only limited effects in clinical phase II-III trials, pointing to a gap in our understanding of the transcriptional regulation of FTase.

Objectives: We aimed to explore the clinical relevance of three FTase β-subunit (*FNTB*) promoter polymorphisms (rs3215788, rs11623866 and rs192403314) in breast cancer patients and investigate how genetic variability of the *FNTB* promoter may affect binding of transcription factors (TFs).

Patients & methods: *FNTB* genotyping was performed by pyrosequencing in 797 patients from a representative cohort of non-metastasized breast cancer patients (51.7% pT1, 42.9% pT2, 4.6% pT3, 0.8% pT4; 76% luminal, 9.4% luminal-HER2, 4.5% HER2-positive, 10% triple negative breast cancer, TNBC), recruited in terms of the prospective multicenter observational PiA trial (NCT 01592825). Genotype-dependent survival analyses were performed with recurrence free interval (RFI), overall survival (OS) and breast cancer specific survival (BCSS) as outcome variables. Putative functional impact of selected *FNTB* promoter polymorphisms on TF binding was investigated by electrophoretic-mobility-shift assays and *in silico* analysis.

Results: In the total cohort, rs3215788 was an independent predictor for RFI (HR=0.568;95%CI=0.339–0.949,p=0.031), OS (HR=0.629; 95%CI=0.403–0.980,p=0.040) and BCSS (HR=0.433;95%CI=0.213–0.882;p=0.021), whereas rs11623866 was an independent predictor for RFI (HR=0.453;95%CI=0.226–0.910,p=0.026) and BCSS (HR=0.227;95%CI=0.075–0.687,p=0.009). Analysis according to intrinsic breast cancer subtypes revealed an independent prognostic relevance of rs3215788 in TNBC (RFI: HR=0.214;95%CI=0.049-0.925,p=0.039; OS: HR=0.031;95%CI:0.047-0.865,p=0.031) but not in luminal or HER2-positive intrinsic subtypes. Finally, we identified two TF candidates, preferentially binding to either the 5G or 6G allele in three different breast cancer cell lines, indicating that rs3215788 is likely to modulate *FNTB* transcriptional activity.

Conclusion: This is the first study on breast cancer suggesting that *FNTB* promoter polymorphisms i) are independent prognostic biomarkers, particularly in TNBC patients, and ii) could modulate *FNTB* transcriptional activity. Our results encourage further prospective evaluation of the role of *FNTB* promoter polymorphisms in predicting response to FTIs, preferentially in TNBC patients.

155

Proof of concept for 2D-printed orodispersible films with midazolam – a bioavailability and bioequivalence trial in healthy volunteers

M. H. Breithaupt[1], E. Krohmer[1], L. Taylor[2], E. Körner[2], T. Hoppe-Tichy[2], J. Burhenne[1], K. I. Foerster[1], M. Dachtler[3], R. Venkatesh[3], K. Eggenreich[4], D. Czock[1], G. Mikus[1], A. Blank[1], W. E. Haefeli[1]
[1]Universitätsklinikum Heidelberg, Klinische Pharmakologie und Pharmakoepidemiologie, Heidelberg, Germany
[2]Universitätsklinikum Heidelberg, Apotheke, Heidelberg, Germany
[3]Digital Health Systems GmbH, Schwäbisch Gmünd, Germany
[4]Gen-Plus GmbH & Co KG, München, Germany

Introduction: Common solid formulations for oral drug administration are tablets or capsules. Both present challenges for vulnerable patients, such as elderly with difficulty swallowing pills and children whose doses require significant adjustment. Two-dimensional (2D) drug printing technologies on orodispersible films (ODFs) could solve these challenges.

Objectives: We examined the absolute and relative bioavailability of two midazolam doses (0.03 mg and 3 mg) printed on ODFs swallowed immediately (ODF-IS) or delayed after 2min (ODF-DS) by comparing their pharmacokinetics with an intravenous and oral midazolam solution.

Patients & Methods: A single-center, open-label, fixed-sequence, GCP-compliant, phase I trial was conducted in 12 healthy volunteers (EudraCT 2020-003984-24). Volunteers received midazolam as i.v. solution, oral solution, ODF-IS, and ODF-DS, and midazolam plasma pharmacokinetics were analyzed using validated liquid chromatography tandem mass spectrometry assays. ODFs were manufactured with a 2D drug printer (Flexdose, DiHeSys, Schwäbisch Gmünd, Germany) in doses of 0.03 mg and 3 mg.

Results: Absolute bioavailability of ODF-IS 0.03 mg was 24.9 % (90 %-CI: 21.2-29.2) and for 3 mg 28.1 % (23.4-33.8). This was similar to the absolute bioavailability of oral solution: 0.03 mg: 24.4 % (22.0-27.1); 3 mg: 28.0 %, (25.0-31.2). Absolute bioavailability of midazolam ODF-DS was significantly higher than ODF-IS (0.03 mg: 61.4 %; 3 mg: 44.1 %; p<0.0001). Geometric mean ratio (GMR) of AUCo-inf and Cmax of ODF-IS/oral solution 0.03 mg was 109.9% (89.4-116.1) and 95.5 % (83.2-109.5) and for macro dose 100.5 % (86.8-116.2) and 106.1 % (88.0-127.9). Paired t-test of dose-normalized AUCo-inf ODF-IS 3 mg and 0.03 mg showed no significant differences (p>0.05).

Conclusion: This first-in-human trial demonstrates good tolerability and unchanged bioavailability of midazolam in a printed dosage form over a 100-fold dose range, thus proving the suitability of ODFs for dose individualization. Midazolam ODF-IS AUC0-inf in 0.03 mg and 3 mg was bioequivalent to oral solution. However, GMR of Cmax of the macro dose ODF-IS exceeded the upper limit of the 90 %-CI by a clinically not relevant amount. In addition, midazolam bioavailability increases with prolonged oral residence times and confirms the potential utility of such a formulation also in emergency situations or for premedication when rapid action or fasting administration is required.

169

A fast and reliable method for genotyping of oncologically relevant genetic variants in TPMT, NUDT15, and UGT1A1

M. J. Meyer[1], I. Arnhardt[1], L. Schwarz[1], M. V. Tzvetkov[1]
[1]University Medicine Greifswald, Institute of Pharmacology, C_DAT, Greifswald, Germany

In 1956, the first pharmacogenetic (PGx) marker glucose-6-phosphate dehydrogenase (G6PD) was identified and one year later the term pharmacogenetics was introduced. Currently, next to a number of somatic tumor genetic markers, also some germline variants in drug metabolizing enzymes may be used to guide pharmacological treatment. Among the best known of them are amino acid substitutions in thiopurine methyltransferase (TPMT) and varying numbers of short tandem repeats in UDP-glucuronosyltransferase 1-1 (UGT1A1). TPMT variants are known to affect the metabolism and thus the risk of toxicity of 6-mercaptopurine (6-MP) and UGT1A1 variants are known to affect pharmacokinetics and to increase risk of neutropenia of irinotecan treatment. Ca. 1 in 300 Germans has a complete loss of TPMT function and 7-10% are homozygous UGT1A1*28 carriers and thus at high risk of severe bone marrow suppression. Furthermore, genetic variants in nudix hydrolase 15 (NUDT15) were recently demonstrated to additionally affect 6-MP metabolism and were included in the recommendations of the Clinical Pharmacogenetics Implementation Consortium (CPIC) and the Dutch Pharmacogenetics Working Group (DPWG).

Here, we report an assay for simultaneous genotyping of TPMT and NUDT15 that can be combined with a fragment analysis assay for UGT1A1 genotyping. The assay is based on a multiplex single base primer extension reaction with florescence detection. It enables genotyping of TPMT*2A (rs1800462), *3A (rs1800460, rs1142345), *3B (rs1800460), *3C (rs1142345) and NUDT15*2 (rs116855232) in combined detection with the UGT1A1 promotor VNTR. To validate the assays, we analyzed 79 healthy individuals. The observed allele frequencies were in line with literature data. The

analyses successfully passed the following quality controls: independent repetition of 20% of the samples, accordance of genotyped and reported sex, and conformity to Hardy-Weinberg equilibrium. Furthermore, the key assay results were confirmed by Sanger sequencing and 24 controls preselected from 1000 Genomes Project were genotyped correctly.

In conclusion, we report a fast and reliable method for genotyping of common variants in TPMT, NUDT15, and UGT1A1 in a combined assay. This method enables genetic testing prior to thioguanine or irinotecan therapy and could easily be integrated into daily clinical practice. This is an inexpensive method, which could simplify the application of PGx marker for tumor treatment decisions in every clinic.

185

RBM20-mutations induce disturbed calcium handling and guide pharmacological treatment in different cardiomyopathies

S. Rebs[1,2], T. A. Buchwald[2], D. Hübscher[2], F. Sedaghat-Hamedani[3], E. Kayvanpour[3], G. Hasenfuss[2], B. Meder[3], **K. Streckfuß-Bömeke**[1,2]
[1]Institute of Pharmacology and Toxicology, University of Würzburg, Würzburg, Germany
[2]University of Göttingen, Cardiology and Pneumology, Göttingen, Germany
[3]University of Heidelberg, Cardiology, Heidelberg, Germany

Background/aim*:* Mutations in the splice factor RBM20 at position p.R634 in the RS-domain were found to cause dilative cardiomyopathy (DCM) (R634W) or left ventricular non-compaction cardiomyopathy (LVNC) (R634L), but the pathophysiological mechanisms responsible for thehetrogenous phenotype remain unknown. Here, we aimed to identify the molecular events caused by the distinct RBM20 mutations from DCM and LVNC patients using a patient-specific stem cell models and to test if the currently clinically used β-blockers are suitable for different RBM20-dependent cardiomyopathies *in vitro*.

Methods: We generated induced pluripotent stem cell-derived cardiomyocytes of 2 DCM- and 2 LVNC-patients harboring the RBM20-mutations R634W (DCM) or R634L (LVNC) as well as isogenic rescue lines by CRISPR/Cas9 and investigated alternative splicing activity, sarcomeric regularity, cAMP level, expression of Ca2+ players, and physiological cardiac functions on a patient-specific cardiomyocyte level. Different clinically approved drugs as Metoprolol and Verapamil were used to analyze the pharmacological improvement *in vitro*.

Results: We investigated the splicing pattern of the 2 RBM20 mutations and observed common mis-splicing in *TTN* and *RYR2*. The structural gene *LDB3* is mis-spliced in DCM-CM, whereas the Ca2+ handling gene *TRDN* is mis-spliced in LVNC-Cs. As a possible consequence, both DCM and LVNC-CM exhibited an irregular sarcomeric structure. *CAMK2δ* was predominantly mis-spliced in LVNC-CM. This may lead to shortened Ca2+ elimination time and weakened response to β-adrenergic stimulation. In line with the fastened basal Ca2+ kinetics in LVNC-iPSC-CM, we observed an increased cAMP level and a downregulated expression of phospholamban. By contrast, DCM-CM showed increased Ca2+ sparks and decreased systolic Ca2+ levels. All effects were rescued in the isogenic CRISPR/Cas9 lines underscoring the causative nature of the 2 mutations and their diverging effects. Ca2+ channel blockage with Verapamil showed a significant improvement of some of the LVNC Ca2+ disease characteristics compared to commonly clinically used β-blocker.

Conclusion: Taken together, these results suggest that the molecular aberrations in alternative splicing differ depending on the distinct missense mutation in RBM20 and lead to shared pathologies and different Ca2+ handling aberrations. This may guide the pharmacological treatment of RBM20-dependent cardiomyopathy phenotypes.

218

A fast and reliable method for genotyping of clinically relevant genetic variants in dihydropyrimidine dehydrogenase (DPYD)

M. J. Meyer[1], I. Arnhardt[1], F. Morof[1], M. V. Tzvetkov[1]
[1]University Medicine Greifswald, Institute of Pharmacology, C_DAT, Greifswald, Germany

Dihydropyrimidine dehydrogenase (DPD) is the rate-limiting enzyme for degradation of the cytostatics 5-fluorouracil (5-FU) and its prodrugs capecitabine, and tegafur. Genetic variants in DPYD, the gene encoding DPD, lead to a reduction or complete loss of DPD activity in 9-10% of Europeans, which is associated with an increased risk for severe adverse effects of 5-FU. The European Medicines Agency recommends DPD testing prior to treatment with 5-FU, capecitabine, and tegafur. Dose reduction for carriers of four common DPYD variants is recommended also in the oncological guidelines. Since October 2020, DPYD genotyping is covered by public health insurance in Germany.

Our aim was to establish a reliable assay for genotyping of DPYD variants that are included in the recommendations and a phenotyping assay for DPD activity.

We used single base primer extension with fluorescent detection to genotype DPYD*2A (rs3918290), c.2846A<T (rs67376798), HapB3 (rs75017182, rs56038477), and *13 (rs55886062) in a multiplex reaction. To validate the genotyping assay, we analyzed 114 healthy individuals. The observed allele frequencies were in line with literature data. The analyses successfully passed the following quality controls: independent repetition of 20% of the samples, accordance of genotyped and reported sex, and conformity to Hardy-Weinberg equilibrium. Furthermore, the key assay results were confirmed by Sanger sequencing and the DPYD genotypes of 24 controls preselected from the 1000 Genomes Project were correctly determined.

In addition, we established a DPD phenotyping assay based on LC-MS/MS quantification of uracil and dihydrouracil (DHU) in human plasma. To validate the phenotyping assay, we quantified uracil and DHU plasma levels in the same cohort of 114 healthy individuals. Mean levels were 7.8 ng/mL (2.7-19 ng/mL) for uracil and 130 ng/mL (49-339 ng/mL) for DHU. Based on correlation with DPYD genotypes, uracil levels were more suitable for phenotyping due to higher variance in DHU measurements. Analyzed genotypes explained only part of the variability in uracil plasma levels.

In conclusion, we report a fast and reliable genotyping method for common DPYD variants of clinical relevance. In addition, we established an LC-MS/MS-based method for DPD phenotyping. These methods could easily be integrated into daily clinical routine and represent one more step towards introducing personalized medicine into practice.

Pharmacology – Pharmacoepidemiology and drug safety

7

Lack of Evidence for Blood Pressure Effects of Caffeine Added to Ibuprofen

T. Weiser[1], R. Lange[2], **A. Lampert**[2]
[1]Sanofi Aventis Deutschland GmbH, Medical Affairs, Frankfurt am Main, Germany
[2]Sanofi Aventis Deutschland GmbH, Medical Affairs, Frankfurt am Main, Germany

Introduction: A caffeine dose of 100-130 mg enhances the efficacy of non-opioid analgesics (Derry et al., 2104). Although numerous investigations of higher doses of caffeine on cardiovascular effects are available, studies on cardiovascular effects of caffeine at co-analgesic doses are sparse.

Objectives: To explore cardiovascular effects of an ibuprofen 400 mg+caffeine 100 mg combination (IbuCaff) in comparison to ibuprofen alone.

Methods: Secondary analysis of a previously reported bioequivalence study of a single dose of IbuCaff (400/100 mg) vs. ibuprofen alone (randomized cross-over study in 36 healthy volunteers; NCT02629354, Weiser et al., 2019). Subjects were administered a single dose of IbuCaff or ibuprofen 400 mg (>= 6 d washout phase between administrations). Blood pressure and heart rate measurements were performed at the time points of blood sampling.

Results: Data from 10 subjects had to be excluded because of detectable pre-dosing caffeine levels in plasma samples. In the remaining 26 subjects, vital signs were comparable over a 24-h period in the absence and presence of caffeine (Figure 1).

Conclusion: Single doses of 400 mg ibuprofen, as well as 400 mg ibuprofen plus 100 mg caffeine, did not affect blood pressure and heart rate. Both treatments did not induce shifts in blood pressure and heart rate compared to baseline values. Thus, ibuprofen or IbuCaff can be expected not to pose relevant cardiovascular risks after intake of single doses.

References: Derry CJ et al. (2014) Cochrane Database of Systematic Reviews, Issue 12. Art. No.: CD009281. DOI: 10.1002/14651858.CD009281.pub3. Weiser T et al. (2019) Clinical Pharmacology in Drug Development, 8(6) 742–753

Funding: The study was funded by Sanofi-Aventis Deutschland GmbH.

Conflicts of Interest: The authors are employees of Sanofi-Aventis Deutschland GmbH

Fig. 1

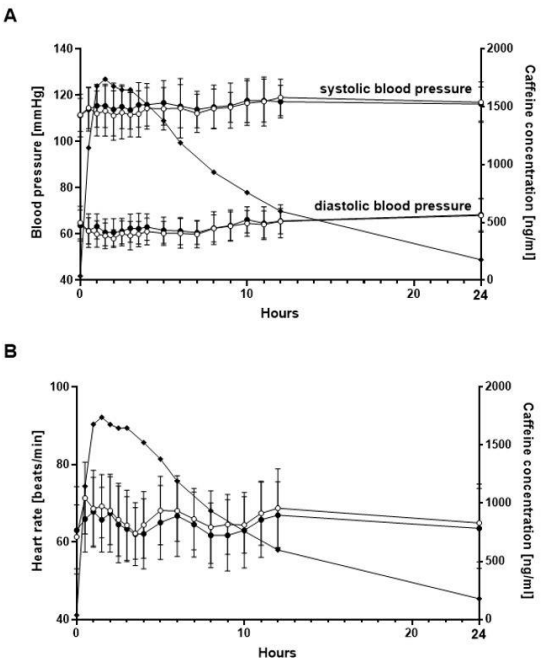

Figure 1: Time course of blood pressure (A) and heart rate (B) over 24 h after a single dose of ibuprofen 400 mg (open circles) and IbuCaff (closed circles). Data are means ± standard deviation of 26 subjects. Data on corresponding plasma concentrations of caffeine (closed diamonds as reported in Weiser et al. 2019) are overlaid.

27

Prescription of QT interval prolonging drugs in Germany and discrepancies between their Summary of Product Characteristics and the international CredibleMeds® database

M. I. Then[1], W. Andrikyan[1], R. Maas[1], M. F. Fromm[1]
[1]Friedrich-Alexander-Universität Erlangen-Nürnberg, Institute of Experimental and Clinical Pharmacology and Toxicology, Erlangen, Germany

Question: Warnings or contraindications regarding QT interval prolongation appear in many Summaries of Product Characteristics (SmPCs). The aim of this study was to assess differences between German SmPCs and the CredibleMeds® database as well as to quantify the amount of QT interval prolonging drugs prescribed in the German outpatient sector using the CredibleMeds® database as reference.

Methods: The German drug prescription report by the public health insurances from 2013 to 2019 was used to extract the number of prescriptions in the German outpatient sector, based on the number of defined daily doses (DDDs). In addition, the data was aggregated based on the official heading of the first four digits in the German ATC index. The CredibleMeds® database served as an international reference database for drugs with QT interval prolongation and/or torsade de pointes (TdP) risk. The German SmPCs of the German top 500 prescription drugs and 253 CredibleMeds® listed drugs were analysed for contraindications regarding QT prolongation.

Results: The DDD-based number of prescriptions of CredibleMeds® listed drugs in Germany increased 4.6fold from 4.6% to 20.9% among the top 3.000 prescribed medicines between 2013 and 2019. The 3,000 most prescribed medicines from 2019 can be aggregated in 193 groups on a four-digit ATC-level, of which 55 contained QT drugs of any category with an average share of 53.4% (SD= 38.9%). Amongst the top 500 prescription drugs, there were 17 drugs with known TdP risk, of which four drugs accounting for 78.6% of the DDDs (citalopram, escitalopram, amiodarone, donepezil). Regarding all categories of CredibleMeds® listed QT drugs, in total 61 of 185 (33.0%) of German SmPCs lacked adequate information regarding any risk for QT prolongation.

Conclusions: QT prolongation is linked to a significant number of prescribed DDDs in the German outpatient sector. There are major discrepancies between German SmPCs and the international CredibleMeds® database. To increase medication safety the pharmaceutical industry and regulatory authorities should develop a uniform and internationally harmonized strategy to eliminate outdated as well as inconsistent information in SmPCs regarding QT risk.

Reference: Then MI, Andrikyan W, Maas R, Fromm MF. The CredibleMeds® list: Usage of QT interval prolonging drugs in Germany and discordances with prescribing information. Br J Clin Pharmacol. 2021. Online ahead of print. https://doi.org/10.1111/bcp.14951

34

Comparing conventional spasmolytics with a phytotherapeutic drug in the treatment of crampy abdominal pain – Real-world evidence data from a pharmacy-based patient survey

H. Weigmann[1], L. Dorsch[1], M. Plomer[1], S. Landes[1]
[1]Sanofi, CHC, Frankfurt, Germany

Introduction: Spasmolytic drugs and phytotherapeutics are commonly used to treat abdominal cramps. However, there are little data on how patients perceive the effectiveness and tolerability of those interventions on their abdominal symptoms in a real-world setting.

Objective: A pharmacy-based patient survey was performed to compare Peppermint oil 182mg (PO), Hyoscine-N-butylbromide 10mg (HBB) as well as a fixed dose combination HBB+ (10mg HBB and 500mg paracetamol) in patients" perception.

Patients & methods: Patients purchasing either PO, HBB, or HBB+ were offered to participate in a survey to evaluate among others the perceived onset of action, effectiveness, and tolerability. Severity of complaints was assessed on a 10-point numeric rating scale, 0 representing *no pain/discomfort* and 10 representing very *severe pain/discomfort*.

Results: 1686 patients aged between 18 to 93 years (average 45 years) participated in the survey of whom 79% were females and 21% males. Notably, HBB (86%) and HBB+ (60%) were most frequently used for treatment of "abdominal cramps and pain in the gastrointestinal tract", PO (63%) most frequently due to "bloated/distended abdomen".

Almost 92% of PO users stated onset of action within 4 hours, while 94% of HBB and 93% of HBB+ users reported onset of action within 1 hour. On average, the severity of complaints improved by -3.5 for PO, 4 hours after the first dose, by -4.0 (HBB) and -4.3 (HBB+) 1 hour after the first dose.

The effectiveness of HBB/HBB+ was rated as either very satisfactory or satisfactory by 97%/96% of the users, this percentage was slightly lower for PO, at 86% (Fig. 1A) but generally leading to a high recommendation rate of the respective preparation to others (HBB/HBB+: 97%, PO: 87%).

Conclusion: Comparison of the spasmolytic HBB-containing preparations with the phytotherapeutic PO in the treatment of patients with different abdominal discomforts, revealed that users felt HBB to act faster and more efficient in comparison to PO in a real-world setting. This indicates that HBB could be useful in acute treatment of crampy abdominal pain, while PO might be more suitable in the treatment of persisting symptoms.

The study was sponsored by Sanofi

Fig. 1

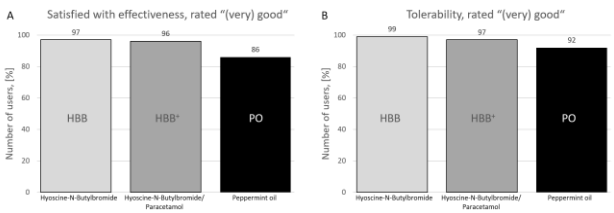

54

PRISCUS 2.0 – An update of the German PRISCUS list of potentially inappropriate medication for older patients

N. K. Mann[1], T. Mathes[2], A. Sönnichsen[3], D. Pieper[2], M. Moussa[3], P. A. Thürmann[1,4]
[1]Witten/Herdecke University, Department of Clinical Pharmacology, Witten, Germany
[2]Witten/Herdecke University, Institute for Research in Operative Medicine, Cologne, Germany
[3]Medical University of Vienna, Department of General Practice and Family Medicine, Vienna, Austria
[4]Helios University Hospital Wuppertal, Philipp Klee-Institute for Clinical Pharmacology, Wuppertal, Germany

Background: The German PRISCUS list contains medications, which are potentially inappropriate medications (PIM) for older patients. Since the first PIM list, the American Beers list, was published, PIM lists have become a popular tool to optimise geriatric pharmacotherapy. The PRISCUS list was created a decade ago explaining the necessity of an update.

Objective: The objective of this project was to update the PRISCUS list in a collaboration between researchers from Germany and Austria, taking changes in the national drug market and new evidence and data into account.

Methods: Experts in geriatric pharmacotherapy were recruited from clinical practice and research. Drugs were selected from the original PRISCUS list and international PIM lists considering their prescribing prevalence in Germany and Austria, respectively. During a 2 round Delphi survey, experts rated the appropriateness of the pre-selected drugs on a 5-point Likert scale. Experts were provided with an extensive body of literature, which included a set of systematic reviews (e.g. for PPI and DPP4-inhibitors) conducted for this project. Drugs that did not receive a definite rating as either PIM or not PIM in the first round of the survey were included in the second Delphi round. After the second Delphi round, a preliminary PIM list was temporarily hosted on the project website and public comments were invited.

Results: In the Delphi survey, 187 drugs were rated as PIM, 36 drugs as "not PIM" and 49 drugs did not receive a definite rating as either. In comparison to the original PRISCUS list, 1 drug was no longer rated as PIM, 6 drugs were removed (e.g. because they were no longer available) and 133 new drugs were added of which 27 are solely relevant for the German and 3 only for the Austrian drug market. Comments on potential alternative treatments, monitoring strategies if PIM use is not avoidable and concerns/discussion points regarding the classification as PIM were collected and included in the long version of the PRISCUS 2.0 list.

Conclusion: The PRISCUS list was updated using a Delphi survey resulting in the PRISCUS 2.0 list which can be used for teaching, optimising geriatric pharmacotherapy and for research projects such as claims data analyses.

Funding: BMBF 01KX1812

71

Melanoma reported as an adverse drug reaction

B. Sachs[1,2], D. Dubrall[1,3], K. Kraywinkel[4], M. Schulz[5], M. Schmid[3], J. Bäte[6], W. Fischer-Barth[7]
[1]Federal Institute for Drugs and Medical Devices, Research Department, Bonn, Germany
[2]University Hospital Aachen, Department for Dermatology and Allergy, Aachen, Germany
[3]University Hospital of Bonn, Institute for Medical Biometry, Informatics and Epidemiology, Bonn, Germany
[4]Robert Koch Institute, Berlin, Germany
[5]Central Research Institute of Ambulatory Health Care in Germany, Berlin, Germany
[6]Federal Institute for Drugs and Medical Devices, Clinical Trials, Bonn, Germany
[7]Federal Institute for Drugs and Medical Devices, Pharmacovigilance, Bonn, Germany

Introduction: Melanoma accounts for the majority of skin cancer deaths. Its main environmental risk factor is ultraviolet light radiation. Further downstream, the elimination of neoplastic melanocytes by the immune system is important. The occurrence of melanoma associated with drug therapy has been described in literature. However, there is no analysis of a substantial number of validated reports of drug-associated melanoma.

Objectives: The first objective of this study was to analyse a large number of validated spontaneous adverse drug reaction (ADR) reports of melanoma with regard to their suspected drugs and reported characteristics. The second objective was to compare these characteristics to those of melanomas occurring in the general population.

Materials and methods: For the first objective, we identified 1,101 ADR reports originating from Germany in a large ADR database (EudraVigilance, standardized MedDRA query level 2 "skin malignant tumours (narrow)", time period 01/1978-03/2019). After individual case assessment concerning causality and exclusion of non-melanoma skin cancer reports, 179 validated melanoma reports remained (first case from 1995). These were then analyzed with regard to the suspected drugs and reported characteristics. For the second objective, we compared the characteristics of the 179 validated melanoma reports with those of 314,415 melanoma cases from the German cancer registry (time period 1995-2018).

Results: The ten drugs most often suspected in the melanoma reports all target the immune system, seven being immunosuppressants. Likewise, more than 57.0% of the patients suffered from at least one autoimmune disorder. Over all reports, the median time to onset of melanoma diagnosis was 2.0 years. Both, the annual number of melanoma reports and the estimated crude incidence rates of melanoma cases from the registry increased since 1995, both curves showing similarities. The patients in the melanoma reports were 11 years younger (median) than melanoma patients of the cancer registry, the difference being stronger for females than for males.

Conclusion: Our results underline the importance of regular dermatological examinations of patients being treated with immunosuppressants. Physicians treating patients with immunosuppressants should be aware that in these patients melanoma may be detected at younger ages and within two years after initiating therapy.

92

A pharmacovigilance study of the adverse event photosensitivity reaction in children and adolescents

S. Steinbrecht[1], T. Herdegen[1], T. Ankermann[2], **R. Böhm**[1]
[1]University Hospital Schleswig-Holstein (UKSH), Institute of Experimental and Clinical Pharmacology, Kiel, Germany
[2]Städtisches Krankenhaus Kiel, Kiel, Germany

Question: Photosensitivity reactions are triggered by more than 100 chemicals, among them commonly prescribed drugs like tetracyclines, chinolones and common OTC drugs like St. John"s Wort.

Do children develop more likely photosensitivity reactions for certain drugs compared to adults? Drug safety analyses rarely focus on the pediatric population for this adverse drug reaction. We used pharmacovigilance data to address this question.

Method: In this observational, retrospective, pharmacovigilance study, we scanned for drugs, which were strongly associated with the adverse event "photosensitivity reaction" (MedDRA preferred term) in different age groups (0-5 years, 6-11 years, 12-17 years, 18-64 years, older than 64 years) using OpenVigil 2 in U.S. American pharmacovigilance data. The resulting respective most disproportionate signals were compared within different age groups by means of their Reporting Odds Ratio (ROR) and their 95%-confidence intervals. The signal concept was used to avoid the over-interpretation of spurious associations.

Results: Throughout the entire dataset 3975 age-coded AEs of photosensitivity reaction were identified. The most frequently reported drugs in context of photosensitivity were voriconazole (n =207), ciprofloxacin (n = 133), pirfenidone (n = 113), doxycycline (n = 104) and vemurafenib (n = 101).

Age range 0 to 5 years: Vemurafenib had the highest ROR of 656, eight of 31 drug administrations of vemurafenib (23%) induced a photosensitivity reaction. Voriconazole had a ROR of 190 (Fig. 1), pimecrolimus 20.2, methotrexate 12.3 and quetiapine 6.2.

Age range 6 to 11 years: The most disproportional signal with a ROR of 239 was found for the monoclonal antibody daclizumab. Voriconazole had a ROR of 188.

Age range 13 to 17: Vemurafenib had a ROR 95 and voriconazole 61.

Age-range 18 to 64 years: Prasterone had the highest ROR of 67, followed by levobupivacaine (ROR 52.65). Vemurafenib (ROR 29.1) and voriconazole (ROR 28.6) still showed a signal, albeit with less disproportionality than in the younger age groups.

Conclusion: We identified several drugs whose adverse events are much more common in a pediatric population. Voriconazole and vemurafenib showed a much higher disproportionality for experiencing a photosensitivity reaction in children than in older age groups.

Fig. 1

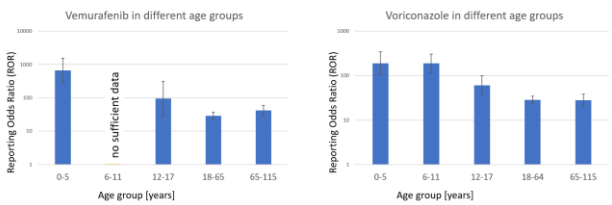

106

Public opinion and information may correlate with harmful adverse events: an OpenVigil pharmaovigilance study

F. Rottmann[1], T. Herdegen[1], I. Cascorbi[1], H. J. Klein[2], **R. Böhm**[1]
[1]University Hospital Schleswig-Holstein (UKSH), Institute of Experimental and Clinical Pharmacology, Kiel, Germany
[2]independend researcher, Kiel, Germany

Question: Prominent opinions, media coverage and guidelines may have an impact on drug usage and subsequent harmful adverse events (AE). The impact of the public attention to drugs by media coverage has been estimated for both prescriptions and purchases. Consequences on drug therapy safety are largely unknown.

Methods: We analysed U.S. American pharmacovigilance data using OpenVigil 2 to identify drugs used against coronavirus infections (coded as preferred terms of the Standardized MedDRA Query "COVID-19 (SMQ)") and their other indications and depicted them weekly aggregated.

EMA and FDA approvals and withdrawals, news headlines concerning these drugs and the publication date of scientific papers were annotated in order to explain the temporal change of spontaneous reporting.

Results: AE were most commonly reported for the drugs (in descending order): hydroxychloroquine (n=1873, 15.7%), remdesivir (14.2%), bamlanivimab (9.2%), azithromycin (8.2%), tocilizumab (6.2%), ritonavir/lopinavir (4.8%), dexamethasone (4%). Recently emerging trending drugs like ivermectin are yet a minority (0.38%).

For all off-label cases, the reported adverse events were mostly not a consequence of the disease but the inappropriate or excess use of the drug.

The extracted reports showed, that not only approvals/withdrawals, on- and off-label recommendations, clinical guidelines based on expert opinions and scientific articles, but also prominent lay opinions and rumors in social networks contribute to drug usage and thus subsequent adverse events.

E.g., for hydroxychloroquine, the coverage of a prominent opinion in lay media and a subsequent scientific article nine weeks later had the strongest impact on its off-label use against coronavirus infections (fig. 1). Commonly reported adverse events, ranked by their proportional reporting ratio (PRR) were: cardiac arrhythmias like prolonged QT time 27.6 and ventricular extrasystoles 5.8, type IV allergies like eosinophilia 23.2, AGEP 18.4 or DRESS 25.9, electrolyte disturbances like hypernatraemia 20.3. The mortality for the event prolonged QT time associated with hydroxychloroquine was 20.5% when used against COVID-19, as compared to only 11.1% for all other indications (Odds ratio 2.1, p<0.01).

Conclusion: Media coverage has an influence on drug usage and subsequent adverse events. A high mortality suggests a patient relevant impact. Lay opinions and social media may account for a loss of drug therapy safety.

Fig. 1

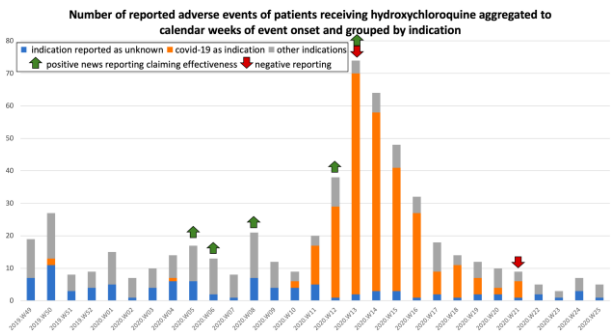

127

Identification of diagnosis-related contraindications based on the medication plan alone

W. Andrikyan[1], M. I. Then[1], K. G. Gaßmann[2,3], T. Tümena[3], P. Dürr[1,4], M. F. Fromm[1], R. Maas[1]
[1]Friedrich-Alexander-Universität Erlangen-Nürnberg, Institute of Experimental and Clinical Pharmacology and Toxicology, Erlangen, Germany
[2]Malteser Waldkrankenhaus St. Marien, Geriatrics Centre Erlangen, Erlangen, Germany
[3]Geriatrics in Bavaria-Database, Nürnberg, Germany
[4]Erlangen University Hospital, Pharmacy Department, Erlangen, Germany

Question: Automated routine checks for contraindications have become a widespread standard in medication safety. However, in clinical practice medication-related clinical decision support systems frequently only focus on drug-drug contraindications, leaving drug-disease contraindications undetected. Moreover, in many clinical settings only medication data are available. We hypothesized, that even if only medication data are available, some diagnoses related to contraindications can be identified based on the medication data alone.

Methods: In a proof of principle study we identified very common clinical diagnoses (gout, epilepsy, coronary artery disease, congestive heart failure, bronchial obstruction) that also constitute contraindications for commonly used drugs. We devised algorithms to identify these diagnoses based on highly specific drugs exclusively used for these conditions (such as allopurinol for gout or salbutamol for bronchial obstruction). Additionally, we developed expert-based and machine learning algorithms to identify diagnoses based on specific medication patterns. In a set of 3,506 anonymized discharge records of geriatric patients we applied these algorithms solely to the medication data to identify diagnoses and possible diagnosis-related contraindications and compared the performance to expert assessments based on medication data and documented diagnoses.

Results: Depending on the technical approach (simple drug list, expert-based algorithm or decision tree) and the desired focus (i.e. high sensitivity vs. high specificity) we could identify diagnoses with a specificity of 44.0% to 99.8% and a sensitivity of 3.8% to 83.1%. Using only medication data and the simple drug list we were able to identify 123 of 240 (51.3%) contraindications identified by experts with access to medication data and diagnoses.

Conclusions: The present study indicates that extrapolation of diagnoses from medication data can be applied to the detection of diagnosis-related contraindications. This may help to extend the range of datasets and clinical settings accessible for the evaluation of medication safety.

154

Effect of clarithromycin, a P-gp and strong CYP3A inhibitor, on the pharmacokinetics of oral factor Xa inhibitors in healthy volunteers: a microdose cocktail approach

A. Lenard[1], S. A. Hermann[1,2], F. Stoll[1], J. Burhenne[1], K. I. Foerster[1], D. Czock[1], G. Mikus[1], A. D. Meid[1], W. E. Haefeli[1], A. Blank[1]
[1]Universität Heidelberg, Klinische Pharmakologie und Pharmakoepidemiologie, Heidelberg, Germany
[2]University Hospital Würzburg, Department of Diagnostic and Interventional Radiology, Würzburg, Germany

Introduction: Oral factor Xa inhibitors (FXaI) are characterized by their effectiveness, easy dosing regimens, low monitoring requirements, and a favorable safety profile. Because different pathways with varying relative contribution are involved in the absorption, distribution, metabolism, and elimination of FXaI, drug-drug interactions (DDI) need evaluation for each compound, which can be done safe and efficiently by a microdosed FXaI cocktail.

Objectives: We assessed the differential effect of clarithromycin, a P-glycoprotein inhibitor and a strong cytochrome P450 (CYP) 3A4 inhibitor, on the pharmacokinetics (PK) of a regular dose of edoxaban and on a microdose cocktail of three FXaI. CYP3A activity was monitored by midazolam.

Patients & methods: In an open-label fixed-sequence trial in 12 healthy volunteers, we evaluated the PK of a microdosed FXaI cocktail (µ-FXaI, 25 µg apixaban, 50 µg edoxaban, and 25 µg rivaroxaban) and of 60 mg edoxaban before and during clarithromycin (2 x 500 mg/d) dosed to steady-state. Midazolam and FXaI plasma concentrations were measured using validated ultra-high performance liquid chromatography - tandem mass spectrometry assays.

Results: Clarithromycin significantly increased the exposure of a therapeutic 60-mg dose of edoxaban with a geometric mean ratio (GMR) of the area under the plasma concentration-time curve (AUC) of 1.53 (90%-CI: 1.37-1.70). Clarithromycin also increased the exposure of microdosed FXaI: apixaban to 1.38 (1.26-1.51), edoxaban to 2.03 (1.84-2.24), and rivaroxaban to 1.44 (1.27–1.63). AUC ratios observed for the therapeutic edoxaban dose were significantly smaller than those observed with the microdose ($p < 0.001$). AUC ratios for apixaban and rivaroxaban were comparable to the data reported in the literature.[1;2]

Conclusion: Clarithromycin increases exposure for all tested FXaI. However, the magnitude of DDI is not expected to be clinically relevant. For edoxaban, the magnitude of effect on its pharmacokinetics differs between the microdose and the therapeutic dose. This might be caused by a saturation of gut transporters at therapeutic edoxaban doses or due to a different relative contribution of pathways to the clearance in different dose situations.

[1] Garonzik S et al, Am J Cardiovasc Drugs

[2] Mueck W et al, Br J Clin Pharmacol

Figure 1 GMR (90% CI) of 60 mg edoxaban, 50 µg edoxaban, 25 µg apixaban, 25 µg rivaroxaban and published values for therapeutic doses of apixaban and rivaroxaban.

Fig. 1

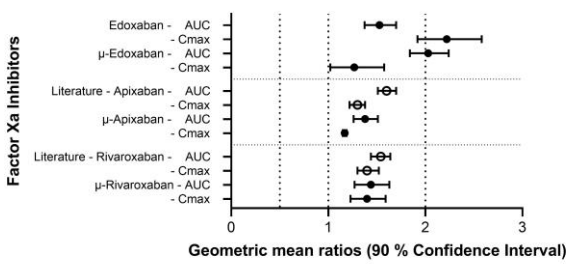

159

Developing of algorithms and assessment of potential implementation of four PIM lists within the POLAR study

L. Redeker[1], B. Mussawy[2], S. Härterich [2], F. Tröger[1], N. Lüneburg [2], P. Thürmann[1,3], S. Schmiedl[1,3]
[1]Witten/Herdecke University, Department of Clinical Pharmacology, School of Medicine, Faculty of Health, Witten, Germany
[2]University Medical Centre Hamburg-Eppendorf, Hospital pharmacy, Hamburg, Germany
[3]Helios University Hospital Wuppertal, Philipp Klee-Institute for Clinical Pharmacology, Wuppertal, Germany

Introduction: Due to the aging population, polypharmacy contributes to several medication related problems (e.g. potentially inappropriate medication (PIM)). Lists to avoid PIM prescriptions are important to improve medication safety in the elderly. While PRISCUS and EU(7)-PIM focus mostly on drugs, the FORTA list and the START/STOPP criteria additionally consider diagnoses, laboratory values, and further clinical data. The POLAR project of the Medical Informatics Initiative (https://www.medizininformatik-initiative.de/de/POLAR) is a use case analyzing electronic health record data of 13 university hospitals focusing on several polypharmacy related problems.

Objectives: For the four PIM lists (PRISCUS (1), EU(7)-PIM (2), FORTA (3), START/STOPP (4)) algorithms for automated computational analysis were developed. And the proportion of potentially implementable items were assessed considering available electronic health record data of the participating hospitals.

Materials & methods: Drugs were identified by their ATC codes, diagnoses by ICD-10 codes, laboratory and other clinical data by LOINC codes (logical observation identifiers names and codes). For defining algorithms previously published studies were considered.

Results: ATC-Codes were defined for all 83 drug-related items of the PRISCUS list, allowing a potential implementation of 100 %. For the EU(7)-PIM list, a lower potential implementation was shown (203 of 282 items; 72 %). Some items of the EU(7)-PIM list were omitted due to lacking approval for the German pharmaceutical market. While for the FORTA list a potential implementation of 80 % (231 of 296 items) was achieved, only 69 % of the most complex START/STOPP criteria (79 von 114 items) were assessed as potentially implementable.

Conclusion: In line with their complexity of the four different PIM lists, the proportion of potentially implementable items profert accordingly. The items which could not be implemented yet present a particular challenge for quantifying the potential misuse and overuse of drugs in elderly patients in electronic health records.

Acknowledgement: The POLAR study is funded by a grant from the German Federal Ministry of Education and Research (FKZ 01ZZ1910S).

[1] Holt S et al. (2010), Dtsch Arztebl Int. 107(31-32):543-51.

[2] Renom-Guiteras A et al. (2015), Eur J Clin Pharmacol. 71(7):861-75.

[3] Pazan F et al. (2019), Drugs Aging. 36(5):481-4.

[4] O'Mahony D et al. (2015), Age Ageing. 44(2):213-8.

221

Symptoms, comorbidities and their medication as risk factors for hospitalization after SARS-CoV-2 infection: a prospective observational study from the Northeast of Germany

E. Schäfer[1], C. Scheer[2], W. Hoffmann[2], S. Engeli [1], K. Hahnenkamp [2], M. V. Tzvetkov[1]
[1]C_DAT, University Medicine Greifswald, Pharmacology, Greifwald, Germany
[2]University Medicine Greifswald, Greifswald, Germany

Since the onset of the SARS-CoV-2 pandemic in 2020, daily medications used to treat existing comorbidities were assumed to influence the course of infection. While ACE inhibitors and PPIs were hypothesized to exacerbate infection, sustained use of corticosteroids or statins were reported to positively influence the course of the infection.

Here we present a prospective observational study of outpatients infected with SARS-CoV-2 in the district of Vorpommern-Greifswald. In this study, we asked more than 3800 SARS-CoV-2 PCR-positivly tested individuals from May 2020 to February 2021 to document comorbidities, the daily medications they used to treat them, and the course of infection symptoms in a paper based questionnaire. We related these parameters to the risk of hospitalization due to COVID-19. We additionally included COVID-19 patients directly recruited from the Greifswald University Hospital.

In total, we analyzed 838 infected individuals, of which 179 were hospitalized. The firstly reported symptoms of the infection were fatigue, myalgia/arthralgia, headache, and dry cough. In contrast, specific SARS CoV-2 symptoms, such as loss of smell (anosmia) and loss of taste (ageusia), appeared with a substantial delay. At day one, only 18% of the participants reported loss of smell or loss of taste, but up to 49% reported them between days 7 and 9. Not every participant, who suffered from loss of taste, suffered also from loss of smell. Participants with loss of taste but not loss of smell had the highest risk of hospitalization (OR 6.8, CI 95% 2.5-18.1).

Comorbidities and other factors leading to an increased risk of hospitalization were age above 60 years, neurological diseases, kidney disease, COPD, or diabetes. We found that participants taking ACE inhibitors or angiotensin receptor blockers (OR 2.23; p<0.001), statins (OR 4.2, p<0.001), PPI's (OR 3.2, p<0.001), or glucocorticoids (OR 4.4, p<0.001) were associated with a higher risk of hospitalization. When adjusting for confounders such as age and concomitant diseases, increased risk for hospitalization remained significant for statins and glucocorticoids.

In conclusion, in addition to the well-known risk factors such as age above 60 and comorbidities like COPD and history of stoke, this study points to loss-of-taste without loss-of-smell and the use of statins and glucocorticoids as additional predictors for hospitalization following SARS-CoV-2 infection. This data requires further validation.

230

Gender pharmacology in herbal medicinal products: Data from the PhytoVIS study, a pharmaco-epidemiological NIS in more than 20,000 patients

T. Al-Shehab[1], E. Raskopf[2,3], **O. Kelber**[1,4], K. Nieber[5,4]
[1]Steigerwald Arzneimittelwerk GmbH, R&D Phytomedicines, Phytomedicines Supply and Development Center, Bayer Consumer Health, Darmstadt, Germany
[2]ClinNovis GmbH, Köln, Germany
[3]Universitätsklinikum Köln, Institut für Medizinische Statistik und Bioinformatik, Köln, Germany
[4]Kooperation Phytopharmaka GbR, Bonn, Germany
[5]University of Leipzig, Institute of Pharmacy, Leipzig, Germany

Question: Gender differences in the safety and efficacy of medicinal products are increasingly attracting attention, also as they are a precondition for personalized medicine. However, for medicinal plants and herbal medicinal products, data are rare. To address this gap, data from the PhytoVIS study, presumably the world"s largest pharmacoepidemiological study on the use of herbal medicinal products [1], were assessed.

Methods: The PhytoVIS data set contains information on epidemiology of patients and therapeutic indications, efficacy and tolerability of herbal medicinal products used by them, which have been captured in pharmacies and in doctor´s practices in Germany, in compliance to the ENCePP Code of Conduct, and was evaluated regarding gender differences.

Results: Overall, 24,056 data sets were evaluated, thereof 16,443 were from women and 7,613 from men. The efficacy of the therapy in women/men was rated very good in 45.9/42.5%, good to moderate in 38.2/41.5%, minimal in 11.6/11.5% and unchanged to worsened in 4.2/4.6% of cases. The tolerability was good in 91.5% of the women and 90.6% of the men. Besides differences in medicines for menopausal/prostate complaints, the proportion of men taking herbal products for cough and cold and for joint pain was higher, while women were more likely to take herbal products for anxiety, sleep disturbances, and bladder dysfunction.

Conclusion: The data shed light to a field of gender pharmacology, in which up to now data have been rare, and give a picture of the use of herbal medicines in an unselected cohort of patients. Despite clear differences regarding the relevance of some therapeutic areas, safety and efficacy of herbal medicinal products were similar in men and women.

References: 1. Wegener T. et al., Pharmind 2021, 83: 416 – 423

276

Impact of Gas and Bloating in Patients Suffering from Episodic Constipation

S. Landes[1]
[1]Consumer Healthcare Sanofi Aventis, Medizin, Frankfurt am Main, Germany

Introduction: Constipation typically is defined as difficult, unsatisfactory, or infrequent defecation, but occurring symptoms can be more diverse. With the updated Rome IV criteria for functional constipation additional emphasis is given on abdominal complaints specifying that abdominal pain and/or bloating may be present (but not dominating).(1) Abdominal complaints such as gas and bloating have been shown to frequently occur in chronic constipation, with the latter being rated by affected as bothersome and impacting the quality of life (QoL).(2)

Aim & Methods: With this investigation we intended to gain insights into the properties and accompanying symptoms of episodic constipation in the general population. Therefore, a web-based survey was conducted in November 2021 in a panel of adults (supported by BILENDI).

Results: 1046 German adults (25-69 years of age; Figure 1) had been interviewed. Gastrointestinal (GI) disorders such as hard dry stools, irregularity, sluggish bowel, or constipation have been reported to occur "frequently"/"rather frequently" in the past 12 months by 23%, 33%, 25% and 22% of the respondents (categories: frequent, rather frequent, rarely, never). Defecation related complaints has been rated as "very" /"rather unpleasant" by 52-75% (Figure 2)). About 2 out of 3 (65%) reported the (rather) frequent cooccurrence of gas-related symptoms such as bloating or abdominal pressure. The related complaints were typically experienced as "very" or "rather unpleasant" by 65-83% (Figure 2). The majority confirmed to manage their GI disorders and accompanying bloating via life-style adjustments (diet (77%), increase in movement (75%)), followed by home remedies (67%) and pharmacy products (55%); only 37% stated to wait until symptoms improve by themselves (multiple mentions allowed).

Summary and Conclusion: Episodic constipation affected a relatively high proportion of the participants. Most respondents experienced multifaceted symptoms, oftentimes of unpleasant nature, suggesting a considerable effect on their QoL. Interestingly, in about two thirds of those suffering from constipation, gas-related symptoms were present and mostly associated with unpleasant complaints. Thus, when dealing with patients suffering from episodic constipation, it might be reasonable to also take gas and bloating into account.

References: (1) Lacy BE et al. Gastroenterol 2016; 150:1393ff; (2) Johanson JF, Kralstein J Aliment Pharmacol Ther 2007; 25:599ff

Fig. 1

Number of Respondents (N)	1046
Female; N (%)	695 (66%)
Age [years]; mean (SD)	47.3 (12.6)

Figure 1: Demographic data

Fig. 2

Defecation-related Complaints		Gas-related Complaints	
	Proportion rating as 'very' or 'rather unpleasant'		Proportion rating as 'very' or 'rather unpleasant'
Hard dry stools	70%	Abdominal swelling	83%
Irregularity	52%	Abdominal pressure	83%
Constipation	75%	Bloating	82%
Straining	74%	Bowel sounds	65%
Feeling of incomplete evacuation	67%	Pain	82%
		Uncomfortable / tight clothing	71%

Figure 2: Subjective perception of defecation- and gas-related complaints by respondents (n=1046). Respondents were asked to rate the degree to which their complaints were experienced as unpleasant using the following descriptors: very, rather, rather not and not at all unpleasant, as well as not applicable.

279

Thrombosis and death: serious coincidental events after COVID-19 vaccination

A. Frum[1], **D. G. Moisă**[1], A. M. Juncan[1], L. L. Rus[1], C. M. Dobrea[1], A. M. Arseniu[1], A. A. Chiș[1], A. Butuca[1], F. G. Gligor[1], C. Morgovan[1]
[1]Lucian Blaga University of Sibiu, Sibiu, Romania

Questions: Nowadays, humanity is confronted with a health crisis due to the COVID-19 pandemic [1]. To manage it, several vaccines were developed and administered worldwide. Four of the used vaccines were Comirnaty (Pfizer/BioNTech), Spikevax (Moderna), Vaxzevria (AstraZeneca) and Janssen (Johnson & Johnson) [2]. Thrombosis was one of the adverse reactions (ADRs) that caused serious concerns regarding the safety of the vaccines all over the world [3]. The aim of this study was to assess the safety of four of the most used vaccines in the European Economic Area (EEA) regarding severe ADRs, like thrombosis and death.

Methods: In this retrospective observational study, we analyzed the Individual Case Safety Report Forms (ICSRs) recorded in EudraVigilance (up to December 3, 2021) [4] for countries from the EEA by healthcare professionals regarding serious ADRs to COVID-19 vaccines (Comirnaty, Spikevax, Vaxzevria and Janssen). The keywords "thrombosis" and "death" were used to filter the results. The descriptive analysis was undertaken by using SPSS 23.

Results: From a total of 647,977,946 doses of COVID-19 vaccines administered in EU/EEA countries, 10.63% were Vaxzevria, 2.80% Janssen, 10.42% Spikevax and 74.38% Comirnaty. The percentages of individual cases of ADRs reported were at most 0.33% for Vaxzevria and at least 0.10% for Comirnaty. From these, the ones from the EEA reported by healthcare professionals regarding serious ADRs were 9.38% for Vaxzevria, 10.66% for Janssen, 7.50% for Spikevax and 12.38% for Comirnaty, summing a total of 509,986 reported cases. The ones that reported thrombosis and death for Vaxzevria were 0.78%, for Janssen 0.79%, for Spikevax 0.26% and for Comirnaty 0.20%.

Conclusions: It can be observed that the reported ADRs were less than 0.35% per type of administered vaccine and following the analyzed data, 0.04% of the reported ADRs were represented by thrombosis and death. Thus, regarding coincidental events like fatalities and thrombosis, the safety of the four studied vaccines could be considered high.

References:

1. Ghibu S. et al., The Particularities of Pharmaceutical Care in Improving Public Health Service during the COVID-19 Pandemic. Int. J. Environ. Res. Public Health. 2021, 18, 9776. doi:10.3390/ijerph18189776
2. who.int, accessed 12.03.2021
3. Gupta A. et al. Prog. Cardiovasc. Dis. 2021, 67, 105-107. doi:10.1016/j.pcad.2021.05.001
4. adrreports.eu, accessed 12.03.2021
5. vaccinetracker.ecdc.europa.eu, accessed 12.03.2021

Toxicology – Practice/Alternative Methods

18

Combining quantitative *in vitro* phenotypic screening using the E-Morph Assay with *in silico* predictions for identification of environmental estrogens

S. Klutzny[1], M. Kornhuber[1], A. Morger[2], G. Schönfelder[1,3], A. Volkamer[2], M. Oelgeschläger[1], E. von Coburg[1], **S. Dunst**[1]
[1]German Federal Institute for Risk Assessment (BfR), German Centre for the Protection of Laboratory Animals (Bf3R), Berlin, Germany
[2]Charité – Universitätsmedizin Berlin, corporate member of Freie Universität Berlin, Humboldt-Universität zu Berlin, and Berlin Institute of Health, Institute of Physiology, In silico Toxicology and Structural Bioinformatics, Berlin, Germany
[3]Charité – Universitätsmedizin Berlin, corporate member of Freie Universität Berlin, Humboldt-Universität zu Berlin, and Berlin Institute of Health, Institute of Clinical Pharmacology and Toxicology, Berlin, Germany

Exposure to environmental chemicals that affect normal estrogen hormone function can lead to adverse health effects in humans, including cancer. High-throughput screening (HTS) projects using human-relevant *in vitro* methods, such as the E-Morph Assay [1-4], support the identification of endocrine disrupting chemicals (EDC) with estrogenic activities.

In a recent study, we combined *in vitro* phenotypic screening with *in silico* methods to identify estrogenic substances from a comprehensive substance library comprising 430 chemicals [4]. The *in vitro* screening identified 24 "known" estrogenic substances with potencies correlating very well with the published U.S. EPA ToxCast ER Agonist Score (r = +0.95), and nine potential "novel" estrogenic substances. Assuming that structurally similar substances can interact with similar targets, we used the "novel" substances as input for an *in silico* similarity search and thus identified further potential estrogenic substances by follow up HTS. Based on the publicly available U.S. EPA ToxCast/Tox21 dataset, we further built seven *in silico* ER prediction models using the conformal prediction (CP) framework to evaluate the HTS results. CP is a special case of machine learning, which adds confidence estimation to *in silico* model predictions. The concordance of the E-Morph screening results with the ToxCast ER reference data and the generated CP ER models was 71% and 73%, respectively, with a high predictivity for ER active substances of up to 87%, which is particularly important to address regulatory needs.

Therefore, the combination of HTS and CP models in testing and assessment strategies can ultimately help to increase confidence in *in vitro* results for regulatory decisions making and thus make an important contribution towards a next generation risk assessment framework that does no longer depend on animal testing. We will further discuss our attempts to adapt the E-Morph Assay to defined, xeno-free cell culture conditions. Replacing fetal calf serum (FCS) addresses ethical concerns about the use of FCS but also facilitates standardization by eliminating one, highly variable component of common cell culture conditions that might affect the availability and, thus, activity of test chemicals.

[1] doi.org/10.1016/j.isci.2020.101683

[2] doi.org/10.1016/j.envint.2021.106411

[3] *European Patent Office / U.S. Patent & Trademark Office*. EP3517967, WO/2019/145517, US20210055311.

[4] doi.org/10.1016/j.envint.2021.106947

35

hiPSCs and hiPSCs-derived renal proximal tubular cells showed different response to nephrotoxic compounds

I. M. Mboni Johnston[1], G. Fritz[1], J. Adjaye[2], N. Schupp[1]
[1]Institute of Toxicology, Heinrich Heine University of Düsseldorf, Düsseldorf, Germany
[2]Institute for Stem Cell Research and Regeneration Medicine, Heinrich Heine University of Düsseldorf, Düsseldorf, Germany

Objectives: Given that many drug candidates fail in clinical trials due to nephrotoxicity, better models are needed to identify potential toxicity early in the developing process. Animal toxicity models remain the gold standard for estimating nephrotoxicity despite ethical concerns as to excessive animal usage. Human-Induced pluripotent stem cells (hiPSCs) differentiating into PTCs could provide a valid alternative 3R-conform model to test and identify potential nephrotoxicants. Therefore,

the present study investigates the sensitivity of proximal tubular epithelial cell (PTEC) - like cells generated from hiPSCs towards well-known nephrotoxins. In addition, the hiPSC-based model will also be used to investigate the vulnerability of the differentiation process and the functionality of the differentiated cells to toxins and oxidants.

Materials and Methods: hiPS (Foreskin)-4 cells were differentiated into PTEC-like cells by cultivating them in renal epithelial cell growth medium (REGM) supplemented with bone morphogenetic protein (BMP)2 and BMP7, human epidermal growth factor (hEGF), insulin, epinephrine, and transferrin for nine days as was previously reported by Kandasamy *et al.* (2015) to drive hiPSC to PTEC-like cells.

Results: Currently, we have shown that hiPS (Foreskin)-4 can differentiate into PTEC-like cells showing similar morphology as compared to the PTCs *in vivo*. Moreover, the cells exhibited increased expression of prototypical PTC markers and transporters, while stemness markers being downregulated. In addition, the PTEC-like cells showed megalin-dependent, cubilin-mediated endocytosis of fluorescently labeled albumin. When treated with known nephrotoxic drugs, hiPSCs were more sensitive to the compounds cisplatin and cyclosporine A than the differentiated PTEC-like cells. Similarly, undifferentiated hiPSCs were also more susceptible to oxidative stress induced by tert-butylhydroquinone than PTEC-like cells.

Conclusion: Due to the demonstrated function and the enhanced expression of relevant renal proximal tubular transporters, these hiPSC-derived *in vitro* kidney model is ready to be used in the next phase of this study to investigate the nephrotoxic potential of a number of selected compounds and the effects of these toxins on the regeneration process and functional competence of the differentiated PTEC-like derived cells.

52

Precision cut kidney slices for 3R-conform assessment of nephrotoxicity

N. Schupp[1], C. Spruck[1], G. Fritz[1]
[1]University of Düsseldorf, Institute of Toxicology, Medical Faculty, Düsseldorf, Germany

Introduction: For the investigation of organ toxicity under 3R principles cell culture, co-cultures or even organoids are not sufficient to seize the high complexity and architecture of the whole organ. A method which might be suitable to overcome the limitations of existing models is the *ex vivo* cultivation of precision cut tissue slices. These could act as a link between the classical *in vitro* and *in vivo* systems. They reflect the complex organ anatomy and the interplay of different cell types and allow extensive kinetic analyses while lowering the animal numbers. In addition, the stress for the animals associated with *in vivo* testings is avoided. The aim of the present project was to establish an *ex vivo* model of mouse precision cut kidney slices (PCKS) for use in substance-oriented biomedical research.

Materials & methods: For this goal, among other parameters, different slice thicknesses, two oxygen concentrations, medium and buffer gassed with carbogen (95 % O2, 5 % CO2), various medium supplements and culture duration of the PCKS were systematically modified to optimize the incubation conditions. Viability assays, histological evaluations and DNA damage (γ-H2AX staining) were performed to compare the effects of the different conditions.

Results: The optimized cultivation conditions were identified and include a slice thickness of 200 µm, medium freshly prepared on a daily basis and cultivation in a medium with a glucose concentration of 2 g/l. The viability of the kidney slices was ~50 % after an incubation time of 72 h. However, changes of the morphology of the tissue became already apparent after 24 h incubation. Apoptosis was increased significantly after 24 h and after 48 h a loss of cell nuclei was detected. The level of the kidney damage marker KIM-1, reflecting damage to the cells of the proximal tubuli, was raised after 72 h incubation. DNA damage detected with help of the phosphorylated histone 2AX (γ-H2AX) was significantly higher after 48 h. Treatment of the *ex vivo* cultured precision cut kidney slices with the pro-oxidant menadione showed a dose dependent decrease in viability and glutathione content after 4 and 24 h incubation, demonstrating the ability of the slices to respond to environmental stress.

Conclusion: In conclusion, PCKS can be used for meaningful toxicity studies within 24 to 48 h after preparation of the slices. Longer treatments probably cannot be evaluated due to the onset of cell death in the slices.

62

The hepatocyte export carrier inhibition assay improves the separation of hepatotoxic from non-hepatotoxic compounds

T. Brecklinghaus[1], W. Albrecht[1], F. Kappenberg[2], J. G. Hengstler[1], J. Rahnenführer[2], J. Duda[2], I. Gardner[3]
[1]Leibniz-Institut für Arbeitsforschung an der TU Dortmund, Toxicology, Dortmund, Germany
[2]TU Dortmund University, Statistics, Dortmund, Germany
[3]Certara, Sheffield, Germany

An in vitro/in silico method that determines the risk of human drug induced liver injury in relation to oral doses and blood concentrations of drugs was recently introduced. This method utilizes information on the maximal blood concentration (C_{max}) for a specific dose of a test compound, which can be estimated using physiologically-based pharmacokinetic modelling, and a cytotoxicity test in cultured human hepatocytes. In the present study, we analyzed if the addition of an assay that measures the inhibition of bile acid export carriers, like BSEP and/or MRP2, to the existing method improves the differentiation of hepatotoxic and non-hepatotoxic compounds. Therefore, an export assay for 5-chloromethylfluorescein diacetate (CMFDA) was established. We tested 36 compounds in a concentration-dependent manner for which the risk of hepatotoxicity for specific oral doses and the capacity to inhibit hepatocyte export carriers are known. Compared to the CTB cytotoxicity test, substantially lower EC_{10} values were obtained using the CMFDA assay for several known BSEP and/or MRP2 inhibitors. To quantify if the addition of the CMFDA assay to our test system improves the overall separation of hepatotoxic from non-hepatotoxic compounds, the toxicity separation index (TSI) was calculated. We obtained a better TSI using the lower alert concentration from either the CMFDA or the CTB test (TSI: 0.886) compared to considering the CTB test alone (TSI: 0.775). In conclusion, the data show that integration of the CMFDA assay with an in vitro test battery improves the differentiation of hepatotoxic and non-hepatotoxic compounds in a set of compounds that includes bile acid export carrier inhibitors.

Fig. 1

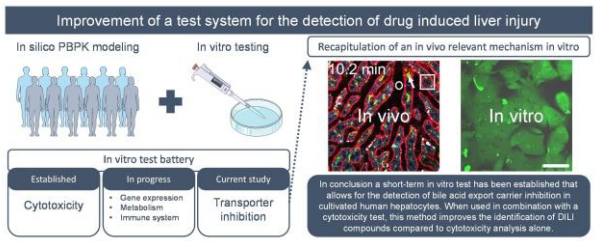

64

Virtual Control Groups in preclinical Studies

A. Gurjanov[1], J. Wichard[1], A. Kreuchwig[1], L. Vaas[1], T. Steger-Hartmann[1]
[1]Bayer, Investigational Toxicology, Berlin, Germany

There is a constant strive in preclinical toxicology to reduce the dependence on animals for safety decision making. One possible step towards the reduction of animals is the replacement of control animals by virtual control groups (VCGs), a method where data derived from control-groups of historical studies is re-used to analyze effects in newly performed studies.

Within the IMI eTransafe project the aim is to establish VCGs for preclinical studies and to test their performance to detect treatment-related effects with respect to the selected methods for generating them. We started with investigating as a first endpoint of an *in vivo* study the reproducibility of body weight results, after replacing the original control groups with the VCGs, generated by sampling from a previously collected VCG dataset comprised of 231 studies.

To determine the performance of the VCGs, a subset was taken from Bayer"s preclinical database with studies which are similar in their study design. Afterwards, body weight values of the control groups in a selected study were replaced by body weight values sampled from the VCG-body-weight dataset. The selection was performed by random sampling without replacement. After the replacement of the control-group values, the statistical significances between the original dose-group animals and the original control group were compared with the results obtained from using the VCGs instead.

Three selected studies were used as a reference. The body weight values of one study were distributed within the confidence interval of the VCG-body-weight dataset while the remaining two studies were distributed outside of the confidence interval (the body weight values were higher or lower respectively). In the prior study, 90 % of the original results were reproducible after replacing the original body weight values with VCG-body weights. The results latter two studies were reproducible by 34 % and 68 % respectively. However, by sampling solely initial VCG-body weight values which match the confidence interval of the reference study, the results of the two latter test sets were reproducible by 56 % and 89 %.

In conclusion, the performance of the sampling method for generating body weight values from virtual control groups is heavily dependent on the distribution of the body weights at start of the individual study.

70

Testing Chemicals for Skin Sensitisation in a New Single Assay with Enhanced T Cell Response Facilitated by Aryl Hydrocarbon Receptor (AhR) Knockout and Co-Inhibitory Molecule Blockade

A. Sonnenburg[1,2,3], R. Stahlmann[2], R. Kreutz[2], M. Peiser[1,3]
[1]Bundesinstitut für Risikobewertung, Berlin, Germany
[2]Charité-Universitätsmedizin Berlin, Institut für Klinische Pharmakologie und Toxikologie, Berlin, Germany
[3]Freie Universität Berlin, Institut für Chemie und Biochemie, Berlin, Germany

OECD validated methods are available for the first three key events (KE) of the adverse outcome pathway for skin sensitisation. Established *in vitro* assays for skin sensitisation testing partly suffer from only moderate sensitivity and specificity and thereby suboptimal predictivity. Moreover, the last and crucial KE – activation and clonal expansion of T cells – is not covered by a validated alternative method to date. One problem associated with the development of such tests is that the level of activation of dendritic cells *in vitro* is relatively low and thus presumably not strong enough to mediate subsequent activation of T cells.

Therefore, we aimed to suppress two inhibitory pathways in dendritic cells to investigate whether these alterations in receptor expression would lead to an enhanced T cell response to allergen activated dendritic cells *in vitro*.

We employed antibody blockade of Programmed Cell Death Ligand 1 (PD-L1) and CRISPR/Cas9-mediated knockout of AhR in the cell line THP-1 commonly used as surrogate for dendritic cells. These modified THP-1 were cocultivated with HaCaT keratinocytes and treated with allergens or an irritative substance. In a second coculture, activated THP-1 modifications were cocultivated with Jurkat T cells. Activation of T cells was determined by measuring cytokine release and CD3 expression of T cells by ELISA and flow cytometry.

We succeeded in integration of genome editing in a sensitisation assay evidenced by upregulation of specific inflammatory parameters under individual stimulation conditions. Anti-PD-L1 monoclonal antibody was demonstrated to efficiently block binding sites on THP-1 as evidenced by reduced expression in comparison to background levels. The expression of CD54 on THP-1 was enhanced in response to allergen stimulation after these modifications while irritant treatment downregulated this marker. Allergen treatment of AhR-k.o. cells with blocked PD-L1 induced CD3 expression on cocultivated Jurkat as compared to untreated controls. Cytokine secretion was altered in a test substance specific way with more pronounced responses in cocultures with modified THP-1 than in wild type control cultures.

In summary, PD-L1 blockade or AhR-knockout advanced subsequent Jurkat response by release of allergen-specific cytokines as well as expression of immunomarkers, thereby facilitating discrimination between irritant and sensitisers.

(Some of the experiments were part of BMBF funded project 031L0069.)

73

Characterization of substance induced mutations in the *in vitro* Transgenic Rodent (TGR) assay

A. Göpfert[1], C. Rülker[1], M. Eichenlaub[2], B. Tokovenko[3], R. Landsiedel[1], D. Funk-Weyer[1], N. Honarvar[1]
[1]BASF SE, Experimental Toxicology and Ecology, Ludwigshafen am Rhein, Germany
[2]BASF SE, White Biotechnology Research, Ludwigshafen am Rhein, Germany
[3]BASF SE, Digitalization of Research & Development, Ludwigshafen am Rhein, Germany

Mutagenicity is a critical endpoint in the hazard assessment of industrial chemicals, biocides and pesticides. The OECD test guideline (TG) no. 488[1] describes an *in vivo* assay that detects induced gene mutations in transgenic rodents that contain copies of chromosomally integrated reporter genes. The "*in vitro* TGR" is not yet an OECD TG but is developed to be an *in vitro* analogue of the OECD 488. The mutagenicity is assessed by isolating DNA from primary MutaMouse hepatocytes treated with the test substance. The reporter gene (*lacZ*) is then packaged into λ phages. Mutations of the *lacZ* gene are quantified by infection of *E. coli* C *lacZ-galE-* cultures and mutants selected via the LacZ enzyme activity.

To further characterize the gene mutations of the *lacZ* gene, a next-generation sequencing-based (NGS) method was implemented. *LacZ* gene mutations induced by five mutagens (N-ethyl-N-nitrosourea (ENU), Ethyl methanesulfonate (EMS), Mitomycin C (MMC), Benzo[*a*]pyrene (B[*a*]P) and Azathioprine (AZA)) were characterized and the induction of size changes in the excised target construct was additionally addressed.

The mutations identified matched the mutagenic mechanisms of the test substances described in literature. The alkylating agent ENU induced a greater proportion of A:T to T:A transversions than the second alkylating agent EMS, whereas EMS induced an increased proportion of smaller deletions (1-4 bp). G:C to T:A transversions accounted for the majority of mutations identified after MMC and B[*a*]P treatment, both of which are known to form monoadducts at the N2 position of guanine. AZA was found to mainly induce G:C to A:T transitions, a mutation caused by the structural analogy to guanine by one of its metabolites. An increased proportion of size changes (>300 bp) was only detected for the crosslinking mutagen MMC.

In conclusion, the "*in vitro* TGR" identifies mutagenic substances before conducting *in vivo* studies; additional mutation spectra analysis facilitates further evaluation of the induced mutations. However, further assessments using additional test substances including moderate and weak mutagens are required to corroborate the above data.

[1] OECD (2020), *Test No. 488: Transgenic Rodent Somatic and Germ Cell Gene Mutation Assays*, OECD Guidelines for the Testing of Chemicals, Section 4, OECD Publishing, Paris, https://doi.org/10.1787/9789264203907-en.

81

Identification of site-specific biomarkers of nephrotoxicity in larval zebrafish

B. Bauer[1,2], D. Liedtke[3], M. Kruse[2], J. Unsöld[2], E. Klopocki[3], A. Mally[2]
[1]Rheinische Friedrich-Wilhelms Universität Bonn, Institute of Nutritional and Food Sciences, Bonn, Germany
[2]Julius-Maximilians Universität Würzburg, Institute of Pharmacology and Toxicology, Würzburg, Germany
[3]Julius-Maximilians Universität Würzburg, Institute of Human Genetics, Würzburg, Germany

Legal restrictions for the use of animals and an increasing demand for toxicological testing have created a strong need for alternative approaches to assess systemic toxicity. Cell-based high-throughput *in vitro* assays cannot reflect the complexity of a whole organism, while traditional testing in rodents is time- and cost-expensive. Zebrafish larvae (*Danio rerio*) are increasingly recognized as a promising alternative, medium- to high-throughput amenable, whole-animal model that may be able to bridge the gap between cell-based *in vitro* screening and experiments in mammals. Although simple in terms of anatomical structure - composed of only two nephrons - the zebrafish larval kidney (pronephros) is highly homologous to kidneys of higher vertebrates like humans and rodents. Renal cell types and transporters are evolutionary conserved between zebrafish and humans. Glomerular filtration begins as early as 2 days post fertilization.

The aim of our current study was to further explore zebrafish larvae as an alternative model by investigating site-specific biomarkers of nephrotoxicity in larval individuals exposed to model nephrotoxins, including aristolochic acid, ochratoxin A, cadmium chloride and gentamicin for 48h starting at 3 days post fertilization. Transgenic zebrafish larvae, which exhibit *cdh17* marker gene associated fluorescence in the pronephros, showed morphologic alterations of the proximal tubule after nephrotoxin exposure, including dilation and reduction of *cdh17* gene expression. These effects were confirmed by immunostaining of α6F, a Na^+-K^+-ATPase that is located in the basolateral membrane of kidney cells. Gene expression analysis in pronephros cells, isolated by Fluorescence Activated Cell Sorting, showed upregulation of the kidney injury marker genes *clusterin* (*clu*), *tissue inhibitor of metalloproteinases 2* (*timp2*), *kidney injury molecule 1* (*kim-1*), *secreted phosphoprotein/osteopontin* (*spp1*) and *heme oxygenase 1* (*hmox1*). Further potential nephrotoxicity marker genes were identified by microarray gene expression analysis. Biomarker based approaches, including generation of transgenic zebrafish lines exhibiting upregulated fluorescence associated with kidney injury biomarker expression combined with automated high-throughput imaging, may provide a useful tool for future nephrotoxicity screening.

83

THP-1 cells as a suitable screening tool for NLRP3 inflammasome activation applied to micro- and nanoplastics

M. Busch[1], **G. Bredeck**[1], F. Waag[2], K. Rahimi[3], H. Ramachandran[1], T. Bessel[2], S. Barcikowski[2], A. Herrmann[3], A. Rossi[1], R. P. F. Schins[1]
[1]IUF - Leibniz Research Institute for Environmental Medicine, Düsseldorf, Germany
[2]University of Duisburg-Essen, Technical Chemistry I, Center for Nanointegration Duisburg-Essen (CENIDE), Essen, Germany
[3]RWTH Aachen University, DWI – Leibniz Institute for Interactive Materials and Institute of Technical and Macromolecular Chemistry, Aachen, Germany

Due to the ubiquity of environmental micro- and nanoplastics (MNP), inhalation and ingestion by humans is very likely, but human health effects remain largely unknown. The NLRP3 inflammasome is a key player of the innate immune system and is involved in responses towards foreign particulate matter and the development of chronic inflammatory diseases.

To investigate the potential of MNP to activate the NLRP3 inflammasome in a macrophage-like cell type, we generated a THP-1 *NLRP3-/-* cell line. By investigating cytokine release (IL-1β and IL-8) and cytotoxicity, THP-1 cells were validated against published data from murine bone marrow-derived macrophages and against murine *in vivo* data. The results from the validation process showed a strong correlation with previously published data, verifying that THP-1 cells are a suitable model to investigate NLRP3 inflammasome activation.

We investigated the proinflammatory potential of commercial model plastic particles (PS-NH2, PS, PVC, PE) and model particles generated by novel methods (PET, PES, PAN, PA6). Only PS-NH2 acted as a direct NLRP3 activator. However, PET particles induced a significant increase in IL-8 release. Our results suggest that most MNP are not direct activators of the NLRP3 inflammasome, but specific types might still possess pro-inflammatory potential via other pathways.

123

Assessing reproducibility, robustness and predictivity of an *in vitro* method to assess DIO1 inhibition in human liver microsomes

A. Weber[1], B. Birk[1], C. Herrmann[1], H. A. Huener[1], K. Renko[2], S. Coecke[3], S. Schneider[1], D. Funk-Weyer[1], R. Landsiedel[1]
[1]BASF SE, BASF SE, RB/TB, Ludwigshafen, Germany
[2]Bundesinstitut für Risikobewertung (BfR), German Centre for the Protection of Laboratory Animals (Bf3R), Berlin, Germany
[3]European Commission, Joint Research Centre (JRC), Ispra, Italy

Impairment of thyroid hormone homeostasis has been associated with several adverse effects. Regulatory requirements are increasing to identify different mode of actions (MoA) impacting thyroid hormone (TH) signaling pathways. The European Union Reference Laboratory for alternatives to animal testing (EURL ECVAM) is coordinating the validation of multiple *in vitro* methods focusing on different thyroid MoA by cooperating with a network of EU laboratories (EU-NETVAL).

Deiodinases (DIO) are important, local regulators of TH action by enzymatically activating or inactivating TH via deiodination. DIO1, one of the three isoforms and mainly expressed in thyroid, liver, and kidney tissue, serves as one main source for circulating T3 via deiodination of T4 and plays a role in recycling of iodide via deiodination of inactive TH metabolites.

A non-radioactive approach to determine DIO1 inhibition based on enzymatic activity in human liver microsomes was transferred to our laboratory [1] and further developed following the GIVIMP concept [2]. The released iodide was quantified via the Sandell-Kolthoff (SK) reaction. The reproducibility assessment (Part 1) testing of six known DIO1 inhibitors has been finalized and resulting acceptance criteria were used to test 40 blinded items (Part 2) assessing predictivity of the method. 22 test items were de-blinded by ECVAM and compared to available *in vitro* data. Additional testing strategies were implemented to show specificity of the observed DIO1 inhibition.

Reproducibility is given for all six test items with IC50 values in range of literature (e.g., IC_{50}: 6-Propyl-2-thiouracil: 3.8 µM in this study, compared to [3]: 5.4 µM). High concordance with *in vitro* data obtained in recombinant enzyme [3] is given for 22 unblinded substances. Silychristin, a natural substance from milk thistle and described thyroid hormone transport inhibitor, interfered with DIO1-SK assay and was not applicable.

The DIO1 inhibition assay using human liver microsomes is a robust and reproducible *in vitro* assay to assess potential DIO1 inhibition of chemicals with high concordance with known *in vitro* data. Additional tests on specificity improves the assessment of the data. Finally, integrative testing strategies considering other thyroid related MoA are needed to assess the biological relevance of the assay.

[1] https://doi.org/10.1210/en.2011-1863

[2] https://doi.org/10.1787/9789264304796-en

[3] https://doi.org/10.1093/toxsci/kfy302

125

Assessing substance-induced thyroid hormone displacement of serum proteins using a LC-MS based readout

A. Weber[1], L. H. Köppl[1], M. Weissenfeld[1], B. Birk[1], E. Fabian[1], S. Schneider[1], S. Melching-Kollmuss[2], D. Funk-Weyer[1], R. Landsiedel[1]
[1]BASF SE, BASF SE, RB/TB, Ludwigshafen, Germany
[2]BASF SE, Global Toxicology, Agriculture Solutions, Limburgerhof, Germany

Thyroid hormones (TH) play an important role in various physiological processes such as cell differentiation, endogenous metabolism, regulation of cell proliferation and fetal neurodevelopment. In the bloodstream, >99% of THs are bound to their respective carrier proteins; mainly thyroxine binding globulin, transthyretin (TTR), and serum albumin which consequently play a significant role in the distribution of TH to target tissues and in maintaining the extrathyroidal TH pool. Some chemicals might displace the thyroid hormone thyroxine (3,5,3′,5′-tetraiodothyronine, T4) from its transport proteins in serum, which indicates one potential mode of action of substance-induced disruption of thyroid hormone homeostasis.

Here, a method assessing the displacement of T4 at thyroid hormone binding proteins is presented, using the human TTR. This method requires an initial incubation step with TTR, T4, and the test substance to generate an affinity-based binding equilibrium. Protein-bound and unbound T4 are separated by size exclusion chromatography and the protein-bound T4 is dissociated from the proteins via ethanol extraction. The T4 concentration of the resulting solution is then quantified by LC-MS analysis.

T4-response curves as a function of protein and T4-concentrations were derived using human TTR as T4-binding protein. The method was characterized regarding maximum solvent (DMSO) concentration and storage stability of extracted samples. The dose-response curves, generated in the assay with several known T4-displacers (e.g., TBBPA, Pentachlorophenol), and negative test items with and without thyroid activity showed the expected results and the IC_{50} values were comparable to published literature. Further, Diclazuril, a described thyroid hormone receptor antagonist, was identified showing T4-displacing activity (IC_{50}: 0.63 µM).

This assay showed reliable and reproducible results for test-substance induced displacement of T4 from TTR. Testing of serum as a source for TH binding protein will further promote the significance of the method by integrating *in vivo* characteristics like plasma protein binding of T4 as well as of the test substances. This method allows to investigate the mode of action (MoA) of chemicals by using the respective proteins and to finally assess the biological relevance of this MoA by using rat/human serum.

128

Assessing substance-induced thyroid hormone receptor modulation *in vitro* using the TRβ CALUX - Optimization of reference control items and cell viability readout

A. Weber[1], S. Wingerter[1], B. Birk[1], S. Schneider[1], B. Ravenzwaay[1], D. Funk-Weyer[1], R. Landsiedel[1]
[1]BASF SE, BASF SE, RB/TB, Ludwigshafen, Germany

Thyroid hormones primarily influence metabolic rate and play a crucial role in growth and neurodevelopment. Their action is mediated by thyroid hormone receptors (THR), a receptor family consisting of different isoforms with tissue-specific expression. Substance-induced interference of thyroid hormone binding to the THR is one target for substance-induced thyroid disruption. An established cell based *in vitro* reporter gene assay (TRβ CALUX assay system, BDS, Netherlands) was used to screen for potential control items to monitor assay performance.

The TRβ CALUX assay uses human osteoblast (U2OS) cells transfected with a firefly luciferase gene that is under control of a thyroid hormone response element containing promotor. The THRβ is constitutively expressed, so the agonist activates luciferase expression via binding to the responsive element. The assay can be used to analyze agonistic or antagonistic (in the presence of the physiological agonist triiodothyronine, T3) potential of test items. The aim of this study was: 1) the evaluation of the reliability and specificity of reference items used in the assay and 2) optimization of the viability assay considering the effects of T3 on cell viability.

We identified several compounds as suitable control items based on activity and specificity of inhibition: Diclazuril, a veterinary drug, showed specific inhibition with an IC_{50} value of 0.24 µM. Deoxynivalenol, a mycotoxin, that was classified as a potential THRβ antagonist [1], was considered inappropriate based on nonspecific response in the assay. 6-Propyl-2-thiouracil, a known inhibitor of deiodinase 1 and thyroid peroxidase, was defined appropriate as a negative control for the assay system.

Moreover, the influence of T3 on different viability readouts was investigated. The Realtime-Glo assay (Promega) that was used to assess cell viability showed increasing signal in response to higher T3 concentrations. Whether this effect is caused by increased expression of metabolizing enzymes or induction of proliferation is subject of further analysis. The CellTiter-Glo (Promega) assay system which quantifies the ATP content in the cell as a readout for cell viability was unaffected by addition of T3.

Specific antagonistic control items and an appropriate cell viability assay were defined based on potency and specificity. These additions improve the quality of the assay and allow more robust assessment of the data.

[1] https://doi.org/10.1016/j.fct.2016.07.033

134

The mycotoxin beauvericin impairs development, fertility and life span in the nematode *Caenorhabditis elegans* accompanied by increased germ cell apoptosis and lipofuscin accumulation

C. Büchter[1], K. Koch[1], M. Freyer[1], S. Baier[1], C. Saier[1], S. Honnen[2], W. Wätjen[1]
[1]Martin-Luther-University Halle-Wittenberg, Institute of Agricultural and Nutritional Sciences, Halle (Saale), Germany
[2]Heinrich-Heine-University Düsseldorf, Institute of Toxicology, Düsseldorf, Germany

Introduction: Beauvericin is an ubiquitous mycotoxin produced mainly by *Fusarium* fungi under moist conditions with relevant occurrence in food and feed. It is a cyclic hexadepsipeptide belonging to the mycotoxin class of enniatins. *In vitro*, beauvericin was reported to disturb signalling pathways, to generate oxidative stress and to induce apoptosis as well as necrosis. It causes a high toxicity in several cell lines, but its general mechanism of action is not fully understood and only limited *in vivo* studies have been performed.

Objectives: We used the nematode *Caenorhabditis elegans* as a model organism to investigate toxic effects of beauvericin *in vivo* regarding physiologic parameters like development, fertility and life span as well as possible molecular mechanisms e.g., apoptosis and oxidative stress.

Materials & Methods: *C. elegans* strains N2 (wild type), CF1553 [*muIs84 (pAD76) (sod-3p::GFP+rol-6)*] and MD701 [*bcIs39 (lim-7p::ced-1::GFP+lin-15(+))*] were used.

Acute and chronic toxicity were tested (food clearance assay, body size, fertility, life span, locomotion). Thermal stress resistance (SYTOX® Green assay), ROS accumulation (H2DCF-DA assay), SOD-3::GFP expression, lipofuscin accumulation (oxidative stress marker) and germ cell apoptosis were investigated.

Results: The mycotoxin displays a moderate acute toxicity at 100 µM; at this concentration reproductive toxicity also occurred (reduction of total progeny by 32.1%), developmental toxicity was detectable at 250 µM. However, even lower concentrations were capable to reduce stress resistance and life span of the nematode: A significant reduction was detected at 10 µM beauvericin (decrease in mean survival time of 4.3% and reduction in life span of 12.9%). An increase in lipofuscin fluorescence was demonstrated starting at 10 µM suggesting oxidative stress as a mechanism of beauvericin toxicity. Beauvericin (100 µM) increases the number of apoptotic germ cells comparable to the positive control UV-C (400 J/m2).

Conclusion: We have investigated the acute and chronic toxicity of the mycotoxin beauvericin in *C. elegans*, demonstrating several toxic effects e.g., impaired reproduction, development and life span. Our study indicates a participation of oxidative stress and apoptosis in beauvericin-mediated adverse effects.

136

In vitro methods to assess metabolic effects of endocrine disrupting chemicals

K. Fritsche[1], J. Kueblbeck[2], J. Niskanen[2], S. Pitkänen[2], P. Honkakoski [2], A. Braeuning[1]
[1]BfR, Food Safety, Berlin, Germany
[2]University of Eastern Finland, A.I. Virtanen Institute for Molecular Sciences, Kuopio, Finland

Endocrine disruption can lead to metabolic effects that may be involved in the onset of diseases like obesity, diabetes, and fatty liver disease. However, we are still lacking validated test methods for the detection of endocrine disrupting chemicals. In this regard, the European Union is funding a cluster of eight projects on endocrine disruptors (EDs), including three projects on metabolic disruption, amongst them the EDCMET (Metabolic effects of endocrine disrupting chemicals: novel testing methods and adverse outcome pathways) project. Combining in silico, in vitro, in vivo approaches, and epidemiologic studies, we aim to identify novel ED mechanisms, to generate (pre)validated test methods and to predict adverse outcomes. In the vitro work package, we are specifically establishing in vitro and omics methods to determine ED-induced metabolic disruption. These methods include reporter gene assays to determine the activation of nuclear receptors involved in metabolism, and AdipoRed assays, which measure the accumulation of intracellular triglycerides upon ED treatment. Using a reference set of 17 known endocrine disruptors and HepG2 cells, we screened 19 nuclear receptors that are known to be involved in metabolism for their activation at a minimum and maximum concentration. Those compounds found positive were further analyzed in dose response reporter gene assays. Using HepaRG cells instead, we directly demined in a dose-response manner the accumulation of triglycerides upon treatment with the 17 reference compounds. We found that 15 of the receptors were activated by at least one compound and that their activation occurs in the micro molar range. Moreover, most compounds of the reference set did induce accumulation of triglycerides in HepaRG cells. Interestingly, we observed differences between chemicals and their metabolites, as well as differences between compounds of similar chemical classes, both, in activating nuclear receptors and inducing steatosis in vitro. Thus, we have successfully tested and established both methods with a well-selected reference set. Together with the other in vitro and omics methods, they will be validated as a test battery for endocrine metabolic disruption using chemicals with unknown endocrine properties.

147

***In vitro* skin models as a tool to assess sensitization of a gel-based pharmaceutical preparation containing a complex mixture of natural components**

I. Zilkowski[1], F. K. Groeber-Becker[2], A. Rossi[2], L. Kiesewetter[2], J. Züfle[3], N. Mörbt[3], C. Turek[1], F. C. Stintzing[1]
[1]WALA Heilmittel GmbH, Pharmacological and Clinical Research, Bad Boll/Eckwälden, Germany
[2]Fraunhofer Institute for Silicate Research ISC, Translational Center Regenerative Therapies TLC-RT - In vitro Test Systems, Würzburg, Germany
[3]WALA Heilmittel GmbH, Regulatory affairs, Bad Boll/Eckwälden, Germany

Evaluation of skin sensitization of pharmaceuticals is part of the required safety data assessing local-tolerance as described in the respective EMA Guideline (EMA/CHMP/SWP/2145/2000 Rev. 1, Corr. 1*, 22th Oct. 2015). To omit *in vivo* testing, 3R principles should be applied. An OECD test battery, meeting these requirements, for prediction of skin sensitization of chemicals, is available, based on *in chemico* as well as 2D cell culture methods (OECD Test No. 442C, D, E). However, these assays have limitations such as solubility of the test item as well as exclusion of metal ions. Therefore, they often cannot be applied to certain pharmaceutical preparations and natural products. The gel-based medicinal product examined in this study contains complex mixtures of various natural components. Due to limited solubility, it could only be assessed in one of the three standardized OECD tests. In particular, the KeratinoSens assay using a 2D keratinocyte cell culture was used, only addressing Key Event 2 of the adverse outcome pathway for sensitization. To overcome limitations of the OECD test battery and still evaluate skin sensitizing of this pharmaceutical product, a 3D cell culture was employed, where topical application is possible.

Methods: An anthroposophic medicinal product containing seven active natural substances was tested in a KeratinoSens assay according to OECD Test Guideline No. 442D and in full-thickness skin models, consisting of differentiated primary human epidermal keratinocytes and primary human dermal fibroblasts. The latter were used to study key events of sensitization by measuring cell viability via MTT-test, lactate dehydrogenase release indicating cellular damage, interleukin-8 and interleukin-18 as pro-inflammatory markers as well as by evaluating the tissue morphology using hematoxylin and eosin staining.

Results: The test item did not show activation of keratinocytes in the 2D KeratinoSens assay. Also, no negative effects of the test item were revealed with regard to the evaluated parameters of the 3D tissue models compared to the controls, thus not showing a potential for skin sensitization.

Conclusion: As part of preclinical safety assessment, the present data contribute to a better understanding of sensitization evaluation in 3D skin models applied to pharmaceutical products containing natural components. Especially the use of dermal-epidermal models might be a promising approach to assess various pathways in skin sensitization.

161

Contributions of 2D and 3D *in vitro* skin coculture systems to assess activation of dendritic cells by fragrance chemicals

N. Peter[1], U. Bock[1], B. Blömeke[1]
[1]Trier University, Environmental Toxicology, Trier, Germany

Skin contact to low molecular weight chemicals and especially fragrances is frequently causing skin sensitization. Here, immune and structural cells, particularly dendritic cells (DC) and keratinocytes, are receptive to signals from their environment and interact with each other. The coculture activation test (COCAT), composed of HaCaT keratinocytes and THP-1 cells as surrogate for DC, can be used to determine the skin sensitizing potential and potency of fragrance chemicals. In this study, 8 of 35 common fragrance chemicals posing a challenge to the 2D system COCAT were investigated in a more complex 3D system. Here, a 3D reconstructed human epidermis (RHE) model is combined with THP-1 cells. We placed THP-1 cells underneath the RHE and topically applied the chemicals. This way, testing of some chemicals with issues was achieved (5 of 8) but fragrance chemicals like α-hexylcinnamal still posed a challenge to the more complex 3D system. Testing a broad range of common fragrance chemicals with varying skin sensitizing properties was achievable in COCAT (27 of 35), but a limited number posed a challenge. Testing these chemicals in a 3D coculture model offered advantages (e.g. by topical application) for some chemicals. In conclusion, results from 3D RHE-THP-1 and 2D COCAT suggest that the combination of both assays allows testing of substances that prove difficult to test in aqueous *in vitro* systems.

179

The impact of butyrate on particle-induced toxicity in intestinal in vitro models

A. Kämpfer[1], J. Becht[1], H. Kohlleppel[1], R. Schins[1]
[1]IUF - Leibniz Research Institute for Environmental Medicine, Düsseldorf, Germany

Oral exposure to engineered nanomaterials (ENM) has been shown to alter intestinal microbiota composition in murine models [1]. Such alterations may also change intestinal levels of microbial metabolites, including short-chain fatty acids (SCFA). Butyrate, the best-studied SCFA, is involved in various mechanisms in the intestine, extra-intestinal organs, and the immune system and can exert cytoprotective effects *in vitro*.

The objective of this study was to investigate potential effects of butyrate at physiologically relevant levels on the toxicity of different types of particles in human intestinal *in vitro* models.

Undifferentiated Caco-2 cells were exposed to pristine or artificially digested silver [Ag-PVP], zinc oxide [ZnO], amine-modified polystyrene [PS-NH2], or food-grade titanium dioxide [E171], in presence of absence of butyrate. The cells were analysed for cytotoxicity and induction of pro-inflammatory cytokines. E171 was further investigated in a triple culture model of Caco-2, HT19-MTX and THP-1 cells to investigate the impact of cell differentiation and inflammation on ENM toxicity.

Butyrate affected the toxicity of some but not all tested materials. For Ag-PVP and E171, butyrate significantly reduced cytotoxicity, while little or no impact was seen for PS-NH2 and ZnO. This effect was induced by both co-incubation with butyrate and ENM as well as after pre-incubation with butyrate. Furthermore, butyrate enhanced the release of interleukin-8 after co-incubation with ZnO and E171. Toxicity was absent for E171 in the triple culture model.

The results demonstrate a cytoprotective effect of butyrate in proliferating Caco-2 monocultures for some ENM. For E171, these effects were absent in the advanced triple cultures. The underlying mechanisms remain to be elucidated. These results raise questions on the potential of butyrate and other SCFA to enhance the physiological relevance of simple intestinal *in vitro* systems.

Acknowledgement: This research has received funding from the European Union"s Horizon 2020 research and innovation program under grant agreement No.760813 (PATROLS).

[1] Bredeck, G.; Kämpfer, A.A.M; Sofranko, A.; et al. 2021, *Nanotoxicology*, DOI 10.1080/17435390.2021.1940339

195

Miniaturization of in vitro liver metabolomics– a screening approach to predict the mode of action of liver toxicants in HepG2 cells

S. Ramirez Hincapie[1], B. Birk[1], M. Herold[2], P. Ternes[2], V. Haake[2], V. Giri[1], F. Zickgraf[1], A. Verlohner[1], H. A. Hüner[1], H. Kamp[2], R. Landsiedel[1], E. Richling[3], D. Funk-Weyer[1], B. van Ravenzwaay[1]
[1]BASF SE, Experimental Toxicology and Ecology, Ludwigshafen, Germany
[2]BASF Metabolome Solutions GmbH, Berlin, Germany
[3]University Kaiserslautern, Kaiserlautern, Germany

in vitro Metabolomics (MIV) enables to predict the mode of action (MoA) of liver toxicants in HepG2 cells. The currently used method at BASF (LUMOX-MIV) is robust, reproducible, and predictive for different MoA [1] but is not yet applicable for a fast and low-cost screening approach. The aim of this study was to miniaturize the method on a 96-well plate (µMIV). 7 substances (aroclor, pendimethalin, b-naphthoflavone, WY-14643, acifluorfen, bezafibrate, and ketoconazole) known to cause liver toxicity through three different MoAs (Peroxisome proliferation (PP), liver enzyme induction (EIND) and liver enzyme inhibition (EINH)) were tested.

The analytical method, cell seeding number, passage number and cytotoxicity testing for dose selection were optimized. To establish IC values, the optimal cytotoxicity assay was defined as a multiplexing approach of ATP measurement and membrane integrity assessment. 15. 000 HepG2 cells/well were cultivated in a 96 well plate (TPP). After 24 hours of cell attachment, the substances were added in 5 concentrations (IC1, IC5, IC15 IC50 IC85). Then, 48 hours later, the assay was stopped by washing the wells with NaCl, quenching the cells with isopropanol 80% and freezing at -80°C. The plates were extracted and analyzed by LC-MS/MS for metabolic profiling.

243 unique metabolites were identified. PCA analysis showed a clear clustering by substance MoA. At the metabolite level, a common impact in the lipid metabolism was observed in the 3 MoAs (general liver toxicity). Sets of specific metabolite changes were identified to for each MoA: PP showed a downregulation of metabolites belonging to fatty acid oxidation (FAO), glycerolipids, sphingolipids and cofactors and an upregulation of phospholipids (PL) and triacylglycerol"s (TAGs). EINDs were characterized by an upregulation of redox carriers (RC), Lysoglycerophospholipids and TAGs and a downregulation FAO metabolite. EINHs exhibited a downregulation of amino acids and related metabolites, RC, acylglycerols, ceramides and cholesterol and an upregulation of sphingolipids and FAO metabolites. Importantly, a metabolomics dose response was observed for each of the treatments.

The µMIV method can distinguish between different MoAs of liver toxicity and provides mechanistic information about the disrupted pathways at lower costs and high throughput. µMIV is a promising in vitro tool for screening approaches in toxicology and pharmacology.

[1] Ramirez et al., Arch Tox, 2018

213

Predictive power of three alternative methods for prenatal developmental toxicity

B. Flick[1], P. Wilhelmi[1], I. Fort I Bru[1], B. Birk[1], R. Landsiedel[1], B. van Ravenzwaay[1], D. Funkt-Weyer[1]
[1]BASF SE, Experimental Toxicology and Ecology, Ludwigshafen, Germany

The predictive power of a single alternative method to animal experiments for prenatal developmental toxicity is limited. The combination of different assays offers the opportunities to include different species, combine different developmental stages as well as different complexities of target structures from the individual assays. This might improve the predictive power for their use in screening approaches of new chemicals and could enhance the confidence in the outcome to a level that is accepted by authorities for decision making in the future.

We investigated a set of 14 chemicals representing a balanced number of positive (n = 7) and negative (n = 7) prenatal developmental toxic substances in three alternative methods: First, a cell culture-based assay on non-differentiating human pluripotent stem cells using two metabolic biomarkers. Second, a murine embryonic stem cell test comprises fibroblasts and embryonic stem cells differentiating into cardiomyocytes. Third, a zebrafish embryotoxicity assay representing the most holistic and complex test system using morphological endpoints. The predictivities (accuracy) of the individual methods were 57%, 71% and 64%, respectively.

The test strategy was optimized in a stepwise approach. We started by exploiting the test systems in terms of different evaluation parameters and analytical statistics aiming to simplify the assays for screening purposes and to improve robustness and reproducibility of the individual assay. Afterwards, prediction models based on different decisions rules combining two and three in vitro embryotoxicity assays were assessed.

The first step improved the reproducibility but not the accuracy of the individual assays. However, the second step using the three assays in a test battery or a tiered test scheme could improve the accuracy to predict the *in vivo* prenatal developmental toxicity of the selected chemicals up to 86%. This was reached by the combination of two assays, the murine embryonic stem cell test and the zebrafish embryotoxicity assay. No *in vivo* positive substance was overlooked. The zebrafish model additionally provided hints for potential manifestation sites of teratogenicity in mammals.

224

The Botanical Safety Consortium´s strategy to enhance the botanical safety toolkit

C. A. Mitchell[1], M. R. Embry[1], S. Gafner[2], H. Johnson[3], D. S. Marsman[4], **O. Kelber**[5], H. A. Oketch-Rabah[6], C. V. Rider[7], E. Sudberg[8], C. Welch[9]
[1]Health and Environmental Sciences Institute, Washington DC, United States
[2]American Botanical Council, Austin, Texas, United States
[3]American Herbal Products Association, Silver Spring, Maryland, United States
[4]Procter & Gamble Health Care, Cincinnati, Ohio, United States
[5]Steigerwald Arzneimittelwerk GmbH, R&D Phytomedicines, Phytomedicines Supply and Development Center, Bayer Consumer Health, Darmstadt, Germany
[6]United States Pharmacopeia, Rockville, Maryland, United States
[7]National Institute of Environmental Health Sciences, Triangle Park, North Carolina, United States
[8]Alkemist Labs, Garden Grove, California, United States
[9]US Food and Drug Administration, Silver Spring, Maryland, United States

Introduction: Botanical substances have been widely used for centuries to preserve and enhance human health and well-being, as medicinal products and as botanical dietary or food supplements. However, evaluation of the safety of these supplements is often inadequate. Thus there is an urgent need for appropriate toxicity evaluations to support their safe use.

The Botanical Safety Consortium (BSC) is a public-private partnership aimed at enhancing the toolkit for the *in vitro* safety evaluation of botanicals. This partnership is the result of a Memorandum of Understanding between the US Food and Drug Administration (FDA), the National Institutes of Health"s National Institute of Environmental Health Sciences (NIEHS), and the Health and Environmental Sciences Institute (HESI). The BSC serves as a global forum for scientists from government, academia, consumer health groups, industry, and non-profit organizations to work collaboratively on developing and integrating *in silico* and *in vitro* methods into a framework.

Question: Can non-mammalian toxicological tools available for single chemicals be applied for botanicals as complex mixtures?

Methods: The BSC is identifying pragmatic, fit-for-purpose, *in vitro* and *in silico* assays to assess botanical safety, evaluate the usefulness of these tools via comparison to the currently available safety information, and integrate these tools and approaches into a framework that can facilitate a robust evaluation of botanical supplements.

Results: Initial endpoints of focus are genotoxicity, hepatotoxicity, absorption-distribution-metabolism-excretion (i.e. "ADME"), developmental and reproductive toxicity, cardiotoxicity, neurotoxicity, and systemic toxicity (Fig. 1). In addition there are supportive working groups, including chemical and data analyses, and pharmacognosy. A number of well-known botanicals has been identified to evaluate the assays.

Conclusions: With selection and prioritization of botanicals based on putative toxicological properties, and pilot work regarding the level of chemical characterization of these candidates, the basis for evaluating a set of screening level assays (*in vitro* and *in silico*) has been established. The ultimate aim is a robust, comprehensive predictive toxicology testing strategy that integrates existing published data with *in silico* and *in vitro* tools to provide actionable safety data for botanicals as complex mixtures, while minimizing the need for mammalian animal testing.

Fig. 1

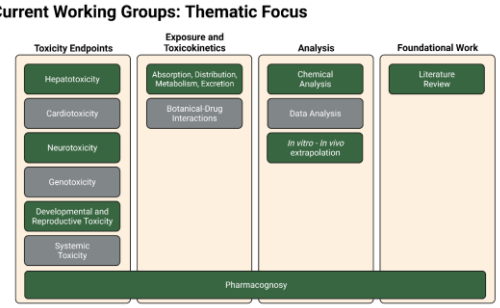

225

Laser ablation-ICP-MS as an alternative method to determine spatially resolved and quantitatively the organ burden directly in histological sections

S. B. Seiffert[1], I. Nordhorn[2], L. Ma-Hock[3], S. Gröters[3], O. Hachmöller[1], M. Wiemann[4], U. Karst[2], S. Kröger[1]
[1]BASF SE, Elemental Analysis, Ludwigshafen, Germany
[2]University of Münster, Institute of Inorganic and Analytical Chemistry, Münster, Germany
[3]BASF SE, Experimental Toxicology and Ecology, Ludwigshafen, Germany
[4]IBE R&D Institute for Lung Health gGmbH , Münster, Germany

Nowadays nanomaterials (NMs) are essential for a variety of applications and therefore their production volume along with their pollution into the environment is rapidly increasing. To access potential risks to organism, animal testings still remain a necessity in regulatory toxicology. However, the development of novel analytical tools and strategies can help to reduce the number of animals.

Whenever adverse reactions are found in the organs of NM-treated animals, additional animals are required to determine their organ burden. For this purpose, inductively coupled plasma-mass spectrometry (ICP-MS) or optical emission spectroscopy (OES) after digestion protocols are utilized. But these results are limited to the bulk concentration of NMs within the respective organ whereas spatially resolved information are lost. In contrast, laser ablation (LA)-ICP-MS provides spatially resolved and quantitative information of elements directly in histological sections without the need of additional animals.

In this study, we used LA-ICP-MS with matrix-matched gelatine standards to quantify various elemental distributions in different organs derived from animal testings on NMs. The developed method was validated by an interlaboratory comparison of the quantitative iron distribution in spleens from different aged rats, showing that it is independent of the sample thickness and sample preparation procedure. Furthermore, the quantitative NM distribution of samples after a short-term inhalation of ZnO NPs and samples after a long-term inhalation of CeO_2 are in good agreement to organ burden calculations by organ digestion of additional animals. Our data indicate that LA-ICP-MS is a promising method to quantify NMs in histological sections without the need of additional animals.

231

Inter-laboratory comparison of the assessment approaches for the zebrafish embryotoxicity assay

P. Wilhelmi[1], E. Teixidó[1], B. Birk[1], R. Landsiedel[1], B. van Ravenzwaay[1], D. Funkt-Weyer[1], **B. Flick**[1]
[1]BASF SE, Experimental Toxicology and Ecology, Ludwigshafen, Germany

The zebrafish embryotoxicity test is widely used. Since there is no harmonized protocol, the comparability of results between laboratories is limited. In this study we determined the impact of differences in the morphological scoring of the zebrafish, such as terminology, morphological features included, manual assessment and half-automated measurement (FishInspector) on effective concentrations, pattern of effects, and the prediction of prenatal developmental toxicity *in vivo*.

For this study five test substances, three with and two without a prenatal developmental toxic potential *in vivo,* were tested in two independent laboratories using their standard protocols. The photographs of exposed zebrafishes from one laboratory were transferred to another one for an assessment using the FishInspector.

Comparable morphological features could be determined under the dissection microscope for a culture duration of 96 and 120 hours. The advanced development of the zebrafish at 120 hours opened the opportunity for a grading of alterations, which could be used to distinguish between slight treatment related effects and adverse outcomes of concern. The morphological scoring system based on 15 instead of 38 features was limited to identify all test substance-related effects by more grouped features, less included organ anlagen and less locations of findings. However, the larger scoring system was also limited because 20% of the morphological features of the smaller scoring system were not included. With the FishInspector 10 features of length and area measurements from which only 8 could be linked to features of the morphological scores. The half-automated measurements had the advantage to detect more alterations in the size of organ anlagen but the disadvantage not detecting alterations of the shape and within the tissues of the organ anlagen. Thereby, the sensitivity of the assessment was only partially higher than the morphological scoring systems.

In conclusion, a higher number of endpoints lead to the determination of more specific test substance-related patterns of effects. However, the reproducibility of individual findings was lower even though the overall manifestation pattern was reproducible. The effective concentrations of the five test substances were in the same order of magnitude. All assessment approaches of the three laboratories had in common that the zebrafish embryotoxicity assay was over predictive resulting in two false positive predictions.

252

Physiological oxygen and human fibroblasts enhance human renal proximal tubule epithelial cell functionality

F. Piossek[1], **S. Beneke**[1], D. Dietrich[1]
[1]Universität Konstanz, Biologie / Human & Ökotoxikologie, Konstanz, Germany

Pharmacological testing of new drugs is time consuming and expensive, even before reaching the clinical phase I. One essential part is testing in animals, most often rodents, to predict safe usage in humans. Despite the fact that animals are the gold standard model system to test drug distribution, activity and metabolism in a complete organism, still a high number of drugs entering clinical trials have to be retracted due to adverse effects detected in humans, and some of them are related to impairment of kidney function. This is based on molecular and physiological differences between rodents and humans, i.e., enzyme sub-type usage and anatomy. Thus, changing current testing strategies is mandatory, not only because data from animal models have only a restricted predictability to drug activity and fate in humans, but also because of high cost associated with animal testing and ethical reasons, summarized in the 3R concept.

We therefore set out to develop an improved *in vitro*-test system, which recapitulates essential parts present in whole organisms, i.e., co-culturing of different cell types and physiological oxygen concentration. Most *in vitro* setups use ambient oxygen concentration, which exceeds O2-concentration in many tissues more than twofold. To mimic the human renal cortex environment, we co-cultured human renal proximal tubule cells (RPTEC) together with human fibroblasts, both immortalized by stable expression of human TERT1 protein, and measured a variety of different parameters, ranging from metabolic effects to protein expression and functional changes. In addition, we analyzed the impact of physiological (PhysOx) and ambient (AtmOx) oxygen concentration on the different co-culture setups.

Our results show that both, fibroblasts and PhysOx, significantly change RPTEC-associated parameters in regard of protein expression and functional properties, cumulating in facilitation of directional transport of organic anions, which was nearly undetectable in standard culture conditions.

253

PODO/TERT256 – a promising human immortalized podocyte cell line and its potential use for in vitro research at different oxygen tensions

N. Schlichenmaier[1], S. Beneke[1], D. Dietrich[1]
[1]Universität Konstanz, Biologie / Human & Ökotoxikologie, Konstanz, Germany

Podocytes are a critical part of the glomerular filtration barrier (GFB) responsible for size- and charge selective filtration of the blood in the renal glomeruli. Destruction of the GFB by nephrotoxins or disease results in proteinuria, glomerulosclerosis and end-stage renal disease. Consequently, a reliable and robust predictive *in vitro* model system is critical for better detection and characterization of glomerulotoxicity in humans. Three factors are key for a predictive *in vitro* system *i)* cell-cell interactions, *ii)* dimensionality and *iii)* O2 tension. Routine atmospheric O2 (21%), at which routine *in vitro* experiments are run, exceeds physiological O2 tensions (10% O2) encountered in the human renal cortex *in vivo*, by two-fold. Accordingly, the question was raised whether excessive O2 tensions leads to adaptive responses and thus to false negative and/or false positive results following exposure to glomerulotoxins. Therefore, the objective was to phenotypically, genotypically and functionally characterize a human podocyte cell line (PODO/TERT256) cultured under both atmospheric and physiological O2 conditions with the focus to determine its suitability as a predictive *in vitro* model. PODO/TERT256 were cultured at 10% (PhysOx) and 21% O2 (AtmOx) in transwells that would also support the polarity of the cells and facilitate the formation of a functional filtration barrier. Morphology, cell proliferation and expression levels of a panel of podocyte markers (both at the mRNA and the protein level) were assessed. To prove *in vivo* like functionality, size-dependent permeability of the cell layer and its response to the known glomerulotoxin doxorubicin was analyzed. PODO/TERT256 formed a contact inhibited layer of cells that expressed several podocyte specific markers and were kept in culture ≥ 30 days without apparent increased cell death when cultivated at 21% O2. Cells cultured at 10% O2 reacted comparably to cells at 21% O2 with regard to cell death levels and podocyte marker expression. Culturing cells at 10% O2 resulted in larger cells with a more rounded morphology and cytoplasmic protrusions (filipodia). The latter resembled the *in vivo* like phenotype in relation to their functional tasks. Under both 10% and 21% O2 PODO/TERT256 established a size-selective filtration barrier and reacted to the known glomerulotoxin doxorubicin with loss of barrier integrity and increased cell death.

254

Cultivation of RPTEC/TERT1 and PODO/TERT256 cells on silk fibroin wafers at atmospheric and low oxygen tension

G. Mucic[1], N. Schlichenmaier[1], S. Beneke[1], D. Dietrich[1]
[1]Universität Konstanz, Biologie / Human & Ökotoxikologie, Konstanz, Germany

Cell morphology in conjunction with proteome expression is an important denominator for cell function, and both can often not be properly recapitulated in standard 2D cell culture. Thus, adaption of the cellular environment to a more physiological setting is mandatory to achieve this. We explored the latter with two renal cell types (glomerular podocytes (PODO), renal proximal epithelial tubule cells (RPTEC), where structure is

an intrinsic part of their functionality. PODO are characterized by interdigitating foot processes that form together with endothelial vessel cells the glomerular filtration barrier, facilitating retention of large and charged molecules in the blood. RPTEC build a tight layer of cells forming an apical brush-border-membrane characterized by microvilli to excrete waste products and take up nutrients from the primary urine. The two factors we investigated were the application of physiological oxygen tension to cells of the respective tissue and the substitution of standard cell-culture plastic by introduction of a stable but biodegradable matrix the cells grow on. The latter is important in co-cultures, where cell interaction is a part of functionality. Therefore, PODO and RPTEC were cultured at both atmospheric and physiological (10%) oxygen tensions on wafers fabricated from silk fibroin (SF), including an additional coating for podocytes. Morphology was assessed using scanning electron microscopy (SEM) and transmission electron microscopy (TEM). Gene expression was assessed by qPCR.

257

Adaptation of human podocytes and renal proximal tubule epithelial cell lines to physiological oxygen conditions

N. Schlichenmaier[1], **A. Zielinski**[1], S. Beneke[2], D. Dietrich[1]
[1]Universität Konstanz, Biologie / Human & Ökotoxikologie, Konstanz, Germany
[2]Universität, Biologie / Human & Ökotoxikologie, Konstanz, Germany

The past decade of research demonstrated that conventional cultivation of cells cannot recapitulate their physiological environment, thereby altering the cellular phenotype. The latter limits the usefulness of *in vitro* approaches in e.g. drug testing for adverse or off target effects due to limited or lack of predictivity. To overcome this, research is focusing on providing cells with conditions that mimic their physiological environment, whereby one key factor that has to be considered is O2 tension. Routine atmospheric O2 (21 %), at which nearly all *in vitro* experiments are carried out, exceeds physiological O2 tensions (10% O2) encountered in the human renal cortex *in vivo*, by two-fold. Accordingly, the question was raised whether excessive O2 tension, by triggering oxidative stress dependent pathways, leads to adaptive responses that influence key cellular functions like metabolism thereby leading to misleading results in conjunction with the exposure to nephrotoxins. Consequently, characterization of the adaptation of renal proximal tubular epithelial cells (RPTEC) and podocytes (PODO) to physiological O2 conditions incl. any phenotypical changes was considered key prior to any further testing.

RPTEC/TERT1 and PODO/TERT256 were cultured at 10% (PhysOx) and 21% O2 (AtmOx). To study the adaptation processes both short and long term, cells were transferred into 10% O2 and analyzed either after 0.5, 1, 3, 6 & 24 h (short term) or 2, 7 & 14 days (long term). For comparison, cells that had been constantly cultivated at 10% O2 for at least 4 weeks were considered fully adapted. The adaptation process was analyzed using metabolic parameters (incl. glycolytic rate, oxygen consumption and ATP levels) and the expression levels of markers for hypoxia and oxidative stress as well as downstream effectors, at the mRNA and protein level.

In both RPTECs & PODOs, HIF1A expression/abundance was increased within 30 min at 10% O2, leading to a significant increase in its downstream effector GLUT1 in fully adapted cells. Both cell lines showed decreased oxygen consumption rates when fully adapted which, however, was not reflected in ATP levels that remained stable for PODOs and even increased for RPTECS. The latter suggests metabolic compensation via different pathways and indeed, fully adapted RPTECs show a higher glycolytic rate. The analysis of glutaminolysis and production of reactive oxygen species is ongoing.

284

Amino Reactivity of Schiff Base Forming Aldehydes – Nonanimal Assessment of Their Skin Sensitization Potency

A. Böhme[1], J. Moldrickx[1], G. Schüürmann[1,2]
[1]UFZ - Helmholtz Centre for Environmental Research, Ecological Chemistry, Leipzig, Germany
[2]Technical University Bergakademie Freiberg, Institute of Organic Chemistry, Freiberg, Germany

Allergic contact dermatitis (ACD) is a worldwide health disease. It is initiated by sensitizing the immune system through dermal contact to an elecrophile, which covalently binds to skin proteins.1 Possible sources of respective sensitizers include care products, cosmetics, and industrial products. For many years, the murine local lymph node assay (LLNA) has been used as gold standard to assess the skin sensitization potency. Driven by regulations, animal welfare, and high costs, several non-animal alternatives such as the direct peptide reactivity assay (DPRA) and a respective kinetic variant (kDPRA) have been developed in order to reduce the need for animal testing. Based on peptide reactivity (cystein-SH and lysine-NH2), the DPRA allows for predictively discrimminating sensitizing from non-sensitizing agents, while the kDPRA uses cystein-SH reactivity only to identify highly potent sensitizers (GHS class 1A). However, the applicability of both DPRA versions for aldehydes forming imines (Schiff bases) with amino groups of skin proteins is limited. Hence, within the BMBF-funded project "ProHapTox" a kinetic amino chemoassay has been developed which overcomes limitation of existing chemoassays for aldehydes forming imines (Schiff bases).2 This communication presents the newly developed amino chemoassay and demonstrates its appicability for profiling the reactivity of glutardialdeyhde and monoaldehydes. The results show that LLNA skin sensitization potency of aldehydes is driven by the thermodynamic stability of formed aldehyde-skin-protein adducts rather than by the rate of adduct formation. Moreover, analytically determined adduct patterns and the impact of α- and β-carbon substitution on aldehyde reactivity are presented.

The authors thank the BMBF-funded project ProHapTox (FKZ 031A422A and 031A422B) for financial support.

[1] OECD. 2012. The Adverse Outcome Pathway for Skin Sensitisation Initiated by Covalent Binding to Proteins Part 1: Scientific Evidence. In Series on Testing and Assessment No. 168 ENV/JM/MONO(2012)10/PART1.

[2] Böhme A, Moldrickx J, Schüürmann G 2021. Amino reactivity of glutardialdehyde and monoaldehydes — chemoassay profile vs skin sensitization potency. *Chem. Res. Toxicol.* 34: 2353–2365.

Toxicology – Regulatory toxicology

104

Safety of pesticides and biocides for pets and farm animals from a toxicological point of view

A. Schmitt[1], L. Niemann[1], S. Rotter[1], C. Kneuer[1], M. Hamann[2]
[1]Federal Institute for Risk Assessment, Department of Pesticides Safety, Berlin, Germany
[2]Justus-Liebig University, Institute for Pharmacology and Toxicology, Giessen, Germany

Objectives: The manufacturing and making available on the market of biocides should not result in harmful effects on human and animal health ((EU) No 528/2012). The same holds true for plant protection products ((EC) No 1107/2009). Whereas the risk assessment of pesticides for human health is well regulated through clear guidelines, no official evaluation concept for the risk assessment for farm animal and pets is currently available. In the recent study a systematic literature search on toxicological data for selected pesticides in various groups of animals was performed, which could serve as a starting point to establish an approach for the risk assessment for pets and farm animals. The aim was to answer the following questions:

1. Are the reference values derived for humans (ADI, ARfD) also applicable for animals?
2. If not, how should a separate risk assessment be performed for certain animal species?

Material and methods: A literature search was performed for a total of seven substances. Toxicological data for herbivores, carnivores, omnivores, poultry/birds, reptiles and fish were considered. The retrieved publications were assessed with regard to their reliability and relevance.

Results: The literature search revealed significant differences in the quality of the database for the specific substance groups. For the acaricides acequinocyl and fenpyroximate, only few published data are available. More is known about insecticides (carbofuran, fluralaner, fipronil) as some of them are used as veterinary drugs, resulting in a more comprehensive database. For substances with long-lasting use such as the molluscicide metaldehyde the toxicological database is extensive. In view of the rodenticide flocoumafene data are available for selected species, including many pets, but missing for ruminants, horses and reptiles. A detailed analysis will be provided.

Conclusion: The limited toxicity database available indicates that the human toxicological reference values may not always be protective for the various animal species. Toxicokinetic species differences may play a role. Further research is needed to collect more information in order to develop an approach for the risk assessment for pets and farm animals.

112

Okadaic acid modulates NF-κB activation and subsequent signaling in HepaRG cells

L. Würger[1], H. Sieg[1], A. Braeuning[1]
[1]German Federal Institute for Risk Assessment, Berlin, Germany

Introduction: The marine Biotoxin Okadaic acid is produced by dinoflagellates and enters the human food chain through marine organisms. As a lipophilic toxin, it accumulates in the fatty tissue of filter feeding shellfish. Okadaic acid causes the diarrheic shellfish poisoning (DSP) in humans, symptoms include severe gastrointestinal disorders, like diarrhea, stomach pain and vomiting. Okadaic acid leads to hepatic and mucosal damage and can also act as a tumor promotor. The molecular mechanisms of okadaic acid toxicity in the liver, however, are still not fully understood.

Objectives: In this study, we attempt to understand the molecular changes to the NF-κB signaling pathway in liver after exposure to Okadaic acid. As NF-κB activation leads to changes in protein expression and subsequent activation of JAK/STAT in hepatocytes, that pathway was our main objective.

Materials and Methods: NF-κB activation was visualized by confocal microscopy using an antibody against NF-κB. Expression of different interleukins, which are direct targets of NF-κB, was determined at the RNA level using qPCRs and at the protein level using the ProcartaPlex™ assay. Molecular inhibitors of NF-κB were used to determine whether interleukin activation was caused by NF-κB. SOCS3 expression was also determined, as SOCS3 is a direct target of the JAK/STAT signaling pathway in hepatocytes.

Results: Obtained data demonstrate activation of NF-κB in HepaRG hepatocarcinoma cells upon okadaic acid exposure. Interleukin 6 and 8 expression in HepaRG cells was upregulated on RNA and protein levels, and SOCS3 expression was induced in HepaRG cells after exposure to okadaic acid.

Conclusion: In conclusion, Okadaic acid activates NF-κB and thereby modulates interleukin expression in HepaRG cells. The regulation of the JAK/STAT target SOCS3 indicates that the interleukins subsequently activate JAK/STAT signaling.

178

Experiences with in vitro comparative Phase II Liver enzyme induction studies

S. Melching-Kollmuss[1], M. Kemeny[1], F. Stauber[1], S. Stinchcombe[1], C. Wiemann[2]
[1]BASF SE, Limburgerhof, Germany
[2]BASF Österreich GmbH, Wien, Austria

Question: European Regulation for pesticides and biocides requires an endocrine disruption assessment, also covering the thyroid pathway. A common mechanism for substances causing thyroid effects in the rat is liver enzyme induction and subsequent increased excretion of thyroid hormones. The methodology, experimental and assessment challenges and results from a novel non-standardized *in vitro* comparative liver enzyme induction assay in rat and human hepatocytes are presented; comprising data from reference compounds (beta-naphthoflavone, phenobarbital, rifampicin, pregnenolone-16alpha-carbonitrile, 3-methylcholantrene, dexamethasone and omeprazole) and four pesticides generated in two laboratories.

Methods: Liver enzyme induction studies were conducted in two different laboratories. Individual cryopreserved rat and human hepatocytes were seeded in 96-well plates in either adhesion or sandwich culture. After an attachment period, cells were exposed to either test substance or the reference compounds. Besides cytotoxicity examinations, Cytochrom P450 (Cyp) and UDP-glycosyltransferase (UGT) mRNA expression and Cyp and T4-UGT activity were measured at days 2 or 3 and at day 7 (for one laboratory).

Results: The reference compounds showed in most of the assays the expected inductions for Phase I and Phase II liver enzymes in rat and human hepatocytes (for mRNA expression and Cyp and T4-UGT activity). T4-UGT activity was much higher in rats compared to human hepatocytes, while the fold-inductions were between 2 and 5-fold for rat hepatocytes and usually below 2-fold in human hepatocytes for the reference compounds. The variance between the individual donors was relatively high, as well as variability of results when studies are compared. It was challenging to discriminate real effects from background noise. The test substances likewise showed much lower T4-UGT activities in human vs rat hepatocytes. Using the 2-fold induction as a threshold for treatment relationship, none of the test substances was able to induce T4-UGT activity in the two test systems.

Conclusion: There is a large difference in absolute T4-glucuronidation activity between rat and human hepatocytes, not necessarily reflected in fold induction alterations. Due to high interindividual donor and test assay variability, reference compound performance criteria are needed in future, as well as a better understanding on applicability and standardization of this test method.

188

Heavy metal contamination in recorded and unrecorded spirits in Hungary. Should we worry?

L. Pál[1], T. Muhollari[1], O. Bujdosó[1], E. Baranyai[2], A. Nagy[1], E. Árnyas[1], R. Ádány[1], J. Sándor[1], M. McKee[3], S. Szűcs[1]
[1]University of Debrecen, Faculty of Medicine, Department of Public Health and Epidemiology, Debrecen, Hungary
[2]University of Debrecen, Faculty of Science, Department of Inorganic and Analytical Chemistry, Debrecen, Hungary
[3]London School of Hygiene and Tropical Medicine, European Centre on Health of Societies in Transition, London, Hungary

Introduction: Heavy metals can release into alcoholic beverages including recorded and unrecorded spirits. Consequently, besides ethanol, their adverse effects should also be considered. Although the concentrations of heavy metals may be higher in unrecorded spirits, especially in those produced in the household and small-scale stills common in Central and Eastern Europe, differences between their levels in recorded and unrecorded spirits have not been investigated comprehensively.

Objectives: Therefore, the aim of our study was to ascertain whether there is any difference between the heavy metal content of recorded and unrecorded spirits and thereby in the related health risk.

Materials & methods: Recorded spirit samples (n=97) including Hungarian fruit spirits, whiskey, vodka, brandy, rum, artificially flavoured spirits, gin, tequila, and absinth were purchased from Hungarian supermarkets. Unrecorded spirits without tax stamps (n=100) were bought informally in Eastern-Hungary from people who ferment fruits at home and either distil the mash in their own stills or send it to small local distilleries. The levels of heavy metals were determined in recorded and unrecorded spirits by inductively coupled plasma optical emission spectrometric analysis. To estimate the health risk associated with the consumption of recorded and unrecorded spirits we used a probabilistic risk assessment approach in which the target hazard quotient method was combined with Monte Carlo simulations. Average, regular and chronic heavy drinker scenarios were considered when estimating the health risks.

Results: We found that the concentrations of Cu, Zn, and Sn were significantly higher in unrecorded spirits than those of in their recorded counterparts and recorded spirits contained significantly higher levels of Fe, Mn, and Ni than unrecorded spirits. Combined exposure to heavy metals posed a health risk only in chronic heavy drinkers consuming recorded spirits.

Conclusion: Considering only heavy metal contamination in recorded and unrecorded spirits, the increased risk for chronic heavy drinkers could be negligible when comparing with the overall health risk from drinking large volumes of ethanol. Therefore, we should not worry about the adverse health outcomes of heavy metal intake in recorded and unrecorded spirits.

196

Close to the border: on the uncertainty of skin sensitization new approach methodologies based on their ring trial data

S. Kolle[1], A. Natsch[2], M. Mathea[3], **R. Landsiedel**[4]
[1]BASF SE, Experimental Toxicology and Ecology, Ludwigshafen, Germany
[2]Givaudan Schweiz AG, Kemptthal, Switzerland
[3]BASF SE, Innovation Management & Strategic Controlling, Ludwigshafen, Germany
[4]BASF SE, Experimental Toxicology and Ecology, Ludwighshafen, Germany

In many (toxicological) assays, continuous data is translated into a binary classifications ("positive" or "negative") using cut-off values. Any test result is however subject to variation and these variations increase the uncertainty of a test result in particular close to a (classification) cut-off (in the borderline range). While the variability of the data is not considered in most assay, some OECD test guidelines, call for repetitions of the test when a result in a range close to the cut-off is obtained. Nevertheless, these ranges are typically based on the test method developer"s experience and not on a systematic analysis. In the present study, borderline ranges from multi-laboratory ring trial studies for five new approach methodologies addressing skin sensitization were determined: the direct peptide reactivity assay (DPRA, OECD TG 442C) and the kinetic direct peptide reactivity assay (kDPRA, OECD TG 442C), KeratinoSens® (OECD TG 442D) and LuSens (OECD TG 442D), and human cell line activation test (h-CLAT, OECD TG 442E). Using the data produced during the interlaboratory assessments of the individual methods, we have used a statistical approach based on the log median absolute deviation (MAD) to derive the borderline ranges for the individual methods. Meanwhile the determined borderline ranges have found regulatory implementation in OECD guideline 497on defined approaches to skin sensitization to assess the uncertainty of predictions in the "2 out of 3" defined approach for skin sensitization.

Fig. 1

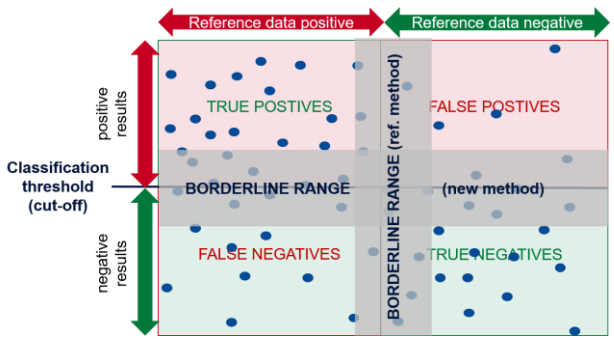

197

Thyroid disruption after exposure to mixtures of triazole fungicides *in vivo* and *in vitro*

A. Kadic[1], B. Fischer[2], T. Heise[2], V. Ritz[2], P. Marx-Stoelting[2], K. Renko[2,3], P. Oles[3], K. Feiertag[2], M. Marzo-Solano[2]
[1]BfR, Pesticides Safety, Berlin, Germany
[2]Bundesinstitut für Risikobewertung, Pesticides Safety, Berlin, Germany
[3]BfR, Experimental Toxicology, Berlin, Germany

Introduction: Mixture effects of chemical substances have been discussed also in the context of endocrine disruption. A key endocrine target organ of chemical substances in rodents is the thyroid with the repective effects being caused by a variety of mechanisms. The most prominent one following exposure to environmental chemicals

(ECs) is increased hepatic metabolism of T3 and T4 in conjunction with compensatory up-regulation of TSH.

Methods: A 28 day feeding study in rats examining the effects of treatment with the hepatotoxic fungicides cyproconazole, epoxiconazole and prochloraz as well as combinations thereof was performed as already described. Serum hormone concentrations were analysed by MagPix multiplex assays *post hoc*. Histopatholgy of the thyroid was analysed. Induction of hepatic metabolism was measured by qRT-PCR and hepatic T3/T4 clearance and UGT were measured by a microsomal enzyme activity assay. For cyproconazole additional assays were conducted *in vitro* including measurements of thyroidal I-uptake (NIS) and inhibition of thyroperoxidase (TPO) and iodothyronine deiodinases (D1-D3), respectively.

Results: Treatment with 1000 ppm cyproconazole, either as pure substance or in conjunction with azoles led to a decrease of T4 and increases of TSH. Also, expression and activity of UGT activity was increased as was metabolism of T3 and T4. Concomitantly animals treated showed clear signs of hepatocyte hypertrophy as well as thyroid follicular hypertrophy and hyperplasia.. Thus the effect on thyroid hormones and tissue may be secondary to hepatic enzyme induction. Preliminary results of *in vitro* assays interrogating for HPT axis-specific interference by cyproconazole are supporting this as no other targets seem to be affected.

Conclusion: Results of this study support the finding of UGT induction as the underlying MoA of cyproconazole and its mixtures. This results in marked decline of T4 and induction of TSH, with subsequent thyroid follicular hyperplasia and hypertrophy. The study also demonstrates the application of a battery of several assays *in vivo* and *in vitro* for characterizing potential endocrine disruptors that act by HPT primary and secondary mechanisms.

198

Investigation of toxicokinetic and toxikodynamic mixture effects of combinations of active substances in plant protection products *in vitro*

M. Karaca[1], D. Bloch[1], T. Willenbockel[1], T. Tralau[1], P. Marx-Stoelting[1]
[1]Bundesinstitut für Risikobewertung, Pesticides Safety, Berlin, Germany

Background: Currently, the authorisation process for plant protection products (PPPs) relies on the testing of acute and topological toxicity only. Contrastingly, the evaluation of active substances includes a more comprehensive set of toxicity studies. Nevertheless, mixture effects of different active ingredients and active ingredients and co-formulants may result in increased toxicity. This is especially true for potential toxikokinetic interactions, which often are at risk of being underestimated.

Methods: In a proof of concept study we therefore assessed toxikokinetic interactions of two PPPs: Product 1 was based on the active substances Tebuconazol (Teb) and Prothioconazol (Pro) and product 2 was based on Cypermethrin (Cyp) and Piperonylbutoxid (Pip). For both products we assessed cytotoxicity and triglyceride accumulation (AdipoRed Assay) in HepaRG cells for the individual substances as well as combinations of the active substances and products. Dose-response modelling of concentration-additivity was used to examine the observed mixture effects. Quantitative real-time RT-PCR was performed to examine and compare the relative expression of several CYP and steatosis-related genes (*CYP1A1*, *CYP1A2*, *CYP3A4*, *CYP2B6*, *CYP2D6*, *INSIG1*, *SLCO1B1*, *CD36*, *FASN*, *SREBF1*). HepaRG cells were treated with individual substances and the respective mixtures followed LC-MS/MS for pesticide quantification in order to identify toxikokinetic effects based on CYP interactions. Inhibition of CYP3A4 was investigated using membrane preparations containing recombinantly expressed protein.

Results: First results show that depending on the ratio of the active substances more than additive mixture effects are observed for the mixtures of Teb and Pro (cytotoxicity) and for the mixture of Cyp and Pip (triglyeride accumulation). Quantitative real-time RT-PCR showed effects on several CYP enzymes, with high induction rates for *CYP3A4* for almost all substances. All substances as well as some of the co-formulants inhibited CYP3A4 enzymatic activity, with Teb being the most potent inhibitor. Several steatosis-related genes are significantly affected by the mixtures and/or the products only, while the individual active substances showed no effect.

Conclusion: Altogether, these findings stress the importance of toxicokinetics when assessing potential effects of formulated products.

207

Heavy metals in recorded and unrecorded Albanian spirits: is there any health concern?

T. Muhollari[1], Z. Sajtos[1,2], E. Baranyai[1], S. Szűcs[1], J. Sándor[1], L. Pál[1]
[1]University of Debrecen, Faculty of medicine, Department of Public Health and Epidemiology, Debrecen, Hungary
[2]University of Debrecen, Doctoral school of chemistry, Debrecen, Hungary

Introduction: Heavy metals can be released into alcoholic beverages during distillation and storage. Previous studies have reported that unrecorded spirits can contain higher level of heavy metals than recorded spirits. Therefore, their consumption can be associated with increased health risks in countries, including Albania, where the share of unrecorded alcohol intake is high. However, there is no study on the concentration of heavy metals in recorded and unrecorded spirits and the health risk associated with their consumption in Albania.

Objectives: The aims of our research were to determine the concentration of heavy metals in recorded and unrecorded spirits in Albania and to estimate the health risks associated with their consumption.

Materials & methods: The levels of heavy metals were measured in recorded (n=17) and unrecorded (n=63) spirits by inductively coupled plasma optical emission spectrometric analysis. Concentration of heavy metals were used in Monte Carlo simulations combined with the margin of exposure (MOE) and target hazard quotient (THQ) methods. Different scenarios for average, regular and heavy drinkers were used to estimate the health risks associated with consumption of recorded and unrecorded spirits containing heavy metals. MOE values less than 100 and THQ values above 1 were considered as a potential health concern.

Results: Copper (Cu), manganese (Mn), lead (Pb) and zinc (Zn) were detected in 100.0%, 88.2%, 35.3% and 64.7% of recorded samples and in 100.0%, 76.2%, 79.4% and 65.1% of unrecorded spirits, respectively. The concentrations of Cu, Mn, Pb and Zn were significantly higher ($p<0.05$) in unrecorded spirits than in their recorded counterparts. The results of the population-based comparative health risk assessment showed that the distribution of MOE values for Pb reached below 100 in all scenarios when consuming recorded and unrecorded spirits. The distribution of combined THQ values for Cu, Mn, and Zn reached above 1 when consuming recorded spirits.

Conclusions: Heavy metals are present in a large share of spirits consumed in Albania. Our comparative risk assessment also confirmed that consumption of unrecorded spirits containing Pb poses a health risk for average, regular and heavy alcohol drinkers. These findings indicate the need for a public health monitoring system on the concentration of heavy metals, particularly Pb, in recorded and unrecorded spirits in Albania.

243

Characterization of unregulated psychoactive substances by means of LC-MS/MS and toxicological *in vitro* testing

B. Haas[1], **M. Vogel**[2], S. Weickhardt[2], N. Eckstein[2,3]
[1]BfArM, Genetic and Reproductive Toxicology, Bonn, Germany
[2]BfArM, Research, Bonn, Germany
[3]University of Applied Sciences Kaiserslautern, Campus Pirmasens, Applied Pharmacy, Pirmasens, Germany

Ouestion: In order to regulate designer drugs (research chemicals), the New Psychoactive Substances Act (NpSG) was implemented in Germany in 2016. Despite this, one internet distributer is still active and delivers the German market with psychotropics. None of these compounds is in the scope of the German Narcotic Drugs Act (BtMG) nor the NpSG. In addition, providers frequently check the legal status of the offered compounds and their non-classification as BtMG/NpSG molecules or prescription-only medicines. Neither any reliable data of the purity, identity and content is available nor toxicity profiles posing an incalculable risk for consumers. Our aim was to characterize different research chemicals from an internet distributor and analyse them for identity and purity by liquid chromatography – tandem mass spectrometry. MTT cytotoxicity assays were performed in SY-5Y cells in comparison to compounds of the same class.

Methods: 3 opioid-like (2-Methyl-AP 237, AP 238, Desmethylmoramide) and 3 stimulant-like (Troparil, RTI-111, Benocyclidin) agents were purchased and analysed for identity and purity by LC-MS analytics. Concentration-response curves were determined by MTT cytotoxicity assays in SY-5Y cells.

Results: For all compounds MS as well as MS/MS spectra were determined revealing low to medium levels of impurities. The designated compounds were confirmed in all samples, but varied in their contents, in particular RTI-111. For all molecules structure elucidations were performed. The opioid-like compounds were compared to oxycodone, morphine and methadone. While oxycodone and morphine were hardly cytotoxic at physiological concentrations (IC50: 2253 and 797 µM, respectively), methadone displayed more potent cell death inducing capacity (IC50: 73 µM). For comparison, IC50 values of 2-Methyl-AP 237, AP 238 and Desmethylmoramide were in the range of 200-400 µM. The stimulants Troparil and RTI-111 revealed IC50 values of 513 and 273 µM, while Benocyclidin was the most potent one (IC50: 69 µM).

Conclusion: Impurity levels for all confirmed substances were relatively low, but inorganic or polymeric contaminations are still conceivable. With respect to cell death induction in neuronal cells opioid-like compounds were more toxic then common opioids oxycodone and morphine. Benocyclidin was the most potent compound. However, as human pharmacokinetic data are not available and any kind of safety data is lacking no firm conclusion on consumer safety can be drawn.

244

The Use of Metabolomics to Support Read-Across and Category Justification for UVCB substances in REACH Utility of Metabolomics to Support Read-Across and Category Justification for UVCB substances in REACH

H. Kamp[1], N. Aygun Kocabas[2], M. Rooseboom[3], F. Faulhammer[4], N. Synhaeve[5], E. Rushton[6], B. Flick[7], V. Giri[7], S. Sperber[7], B. van Ravenzwaay[7], L. Higgins[8], M. Penman[8]
[1]BASF Metabolome Solutions GmbH, Berlin, Germany
[2]TotalEnergies Refining & Chemicals, Seneffe, Belgium
[3]Shell, Toxicology, The Hague, Netherlands
[4]BASF SE, Regulatory Toxicology, Ludwigshafen, Germany
[5]ExxonMobil Petroleum & Chemical BV, Machelen, Belgium
[6]LyondellBasell, Rotterdam, Netherlands
[7]BASF SE, Experimental Toxicology and Ecology, Ludwigshafen, Germany
[8]Penman Consulting, Bridlington, Germany

Hazard characterisation for categories of substances of Unknown or Variable Composition, complex reaction products or Biological materials (UVCBs) considers chemical (manufacturing processes, physicochemical properties, and compositions) and biological coherence (*in vivo* animal data, metabolomics) of representative category members. Once sufficient similarity among a category is established, systemic toxicity endpoints can be derived using read across from one category member to another. The approaches used to support read across by the Lower Olefins and aromatics EU REACH Consortium are outlined in an accompanying poster, "Approaches to Support Read Across for UVCB substances".

The current study hypothesized that metabolomics could demonstrate biological similarity within the resin oils and cyclic dienes steam cracker derived UVCB category, thereby supporting the category read across. Groups of rats were dosed orally for 14 days with all substances in the category. Other dose groups received mono constituent substances commonly found in the streams to act as markers. All animals were examined for classical toxicology endpoints: clinical examination, clinical pathology, and pathology including terminal plasma metabolome analysis. Moreover, a full compositional analysis was conducted for all substances in the category. Consistent with biological coherence, exposure to the UVCBs and markers resulted in a homogenous, treatment related systemic toxicity with liver, thyroid and hematopoietic system being the primary target organs.

Analysis revealed strong dose related effects on the plasma metabolome for most substances. Metabolome profile patterns observed with the UVCB substances were consistent with those observed for the marker substances tested. The metabolome patterns indicated primary effects to the liver (liver enzyme induction) with secondary thyroid and kidney effects. No metabolome patterns associated with direct thyroid toxicity were observed. Overall, the similarity of effects observed was high for all UVCB substances and the metabolomic profile was consistent with the observed classical toxicology endpoints. This supports metabolomics as a tool to assess biological coherence between UVCB streams and to strengthen read across justifications for UVCB substances.

245

Novel Approaches to Support Read-Across for UVCB substances

M. Rooseboom[1], **H. Kamp**[2], N. Aygun Kocabas[3], N. Synhaeve[4], F. Faulhammer[5], E. Rushton[6], B. van Ravenzwaay[7], M. Penman[8]
[1]Shell, Toxicology, The Hague, Netherlands
[2]BASF Metabolome Solutions GmbH, Berlin, Germany
[3]TotalEnergies Refining & Chemicals, Seneffe, Belgium
[4]ExxonMobil Petroleum & Chemical BV, Machelen, Belgium
[5]BASF SE, Regulatory Toxicology, Ludwigshafen, Germany
[6]LyondellBasell, Rotterdam, Netherlands
[7]BASF SE, Experimental Toxicology and Ecology, Ludwigshafen, Germany
[8]Penman Consulting, Bridlington, Germany

Read-across is a hazard characterization tool that uses endpoint information for one chemical to predict the same endpoint for another chemical. Utilization of read-across for complex and variable substances, known as "Unknown or Variable Composition, complex reaction products or Biological materials" (UVCBs) is challenging because the precise constituents and levels of each constituents vary from sample to sample. Steam cracker derived UVCB streams derived from similar manufacturing processes and described by similar physicochemical properties and compositions were hypothesized by the Lower Olefins and Aromatics (LOA) EU REACH Consortium to be categories of substances with similar hazard profiles for the purpose of fulfilling the EU REACH information requirements for repeat dose, developmental (2 species), and reproductive toxicity studies.

LOA developed test plans for these categories to generate higher tier data on representative category members and using that data to read-across to other streams in the category. Inherent in this process is a necessity to show the relevance of the data from one substance to another. Typically, this is shown by chemical coherence, but LOA has striven to include measures of biological coherence. These have included the use of OECD 422 screening studies and, for one category of resin oils and cyclic dienes, a pilot study using metabolomic analysis of blood sampled after 14-day oral dosing of all the substances within the category. Standard toxicological data were also collected and an accompanying metabolomic analysis was performed on terminal plasma. These data are being used to critically examine the utility of metabolomics as a new approach methodology to generate greater confidence in the read-across approach thus saving resources and animals when generating the data required by such regulatory initiatives as REACH. The availability of extensive data from OEED 422 screening studies enhance confidence that the individual UVCB substances in the categories described here are sufficiently chemically and biologically coherent to be considered within a category for the purposes of endpoint read-across. The data from the metabolomics study and some preliminary conclusions are given in the accompanying poster "Utility of Metabolomics to Support Read-Across and Category Justification for UVCB substances in REACH".

246

Ion-Pair LC-MS/MS Analysis of Mercapturic Acids of Heat-induced Food Contaminants in Urine Samples from Non-smokers, Smokers and Strict Raw Food Eater

N. Bergau[1], B. Datta[1], F. Gauch[1], K. Abraham[1], **B. Monien**[1]
[1]Bundesinstitut für Risikobewertung, Lebensmittelsicherheit, Berlin, Germany

Question: Mercapturic acids (MAs) are metabolites formed from glutathione conjugates. They are urinary short-term biomarkers for the exposure to toxic compounds taken up from foodstuffs. However, the MAs of heat-induced food contaminants, e.g. acrylamide, are not necessarily specific for the dietary uptake. In order to determine the ratio between dietary and non-dietary exposure of heat-induced contaminants in food, we compared the urinary excretion of various MAs in strict raw food eaters (non-smoking), who did not consume any food heated to higher temperatures than 42 °C for at least 4 months, with people following conventional dietary habits and smokers.

Methods: A suitable technique for the quantification of six MAs related to the exposure to acrylamide (AAMA and GAMA), acrolein (HPMA and CEMA), acrylonitrile (CYMA), and benzene (PMA) from human urine samples was developed. Extraction methods were selected after comparing SPE materials with a liquid-liquid-extraction and a dilute-and-shoot approach. The best combination of extraction and chromatography was optimized and validated. The MA concentrations were quantified in 24 h urine samples of strict raw food eaters (n = 16), and of non-smokers (n = 6) and smokers (n = 6) with a conventional diet.

Results: The SPE materials tested showed a very low analyte recovery regardless of the extraction parameters. Thus, a dilute-and-shoot method was chosen for the analysis of the polar MAs, while the hydrophobic MAs (CYMA and PMA) were analyzed following liquid-liquid extraction. Due to a superior performance, an ion-pair chromatography method was preferred over a conventional reversed-phase method. The validation showed satisfying LOD, LOQ, linearity and precision values. The analyses of the study samples demonstrated that raw food eaters have a lower excretion of AAMA and GAMA compared to non-smokers with normal dietary habits (Table). The median urinary excretion of all MAs was distinctly lower in non-smokers compared to that of smokers (Table).

Conclusions: In this study, a platform for the analysis of six MAs was established, which makes use of two different approaches of sample preparation depending on the polarity of the analytes. The data confirmed that smoking leads to higher exposure of the heat-induced contaminants. The excretion of AAMA and GAMA in strict raw food eaters suggest that non-dietary uptake or endogenous formation contribute significantly to the overall exposure to acrylamide.

Fig. 1

Table. Median excretion (µg/24 h) of different MAs determined in urine samples of strict raw food eaters, non-smokers and smokers.

Group	n	AAMA	GAMA	HPMA	CEMA	PMA	CYMA
Raw Food Eaters	16	18.8	5.5	201.0	46.5	0.7	1.4
Non-smokers	6	56.5	9.6	85.1	38.7	1.1	1.8
Smokers	6	90.1	13.9	667.6	108.7	10.4	167.4

260

Comparison of the CLP calculation method and *in vivo* animal studies for the assessment of acute toxicity and topological effects of plant protection products

J. F. Grottker[1], S. Seifert[1], S. Martin[1], D. Bloch[1]
[1]German Federal Institute for Risk Assessment (BfR), Pesticides Safety, Berlin, Germany

Background: Until recently, animal studies were the only approved method to assess the acute toxicity and topological effects of plant protection products (PPPs). However, since then animal welfare considerations have advanced the application of alternative methods. One of these is the calculation method according to CLP Regulation. However, results from this method can differ from those obtained *in vivo*. This project aims to investigate the extent of such deviations. A better predictability of acute toxicity by calculation would be valuable for an integrated test strategy, thereby improving animal-free acute toxicity assessment of PPPs.

Methods: A list of authorised PPPs in Germany has been generated. Only those candidates were chosen for further assessment, for which *in vivo* studies had been performed using the currently authorised formulation. *In vivo* studies with these PPPs were evaluated for acute oral, dermal, and inhalation toxicity as well as skin and eye irritation and skin sensitisation. In parallel, classification according to the CLP

Regulation calculation method and/or concentration limits, i.e. skin and eye irritation and skin sensitisation, was performed. Finally, CLP classification results from *in vivo* studies and from calculation/concentration limits were compared and categorised as true negatives (TN), true positives (TP), false negatives (FN), or false positives (FP).

Results: *In vivo* studies were conducted with the currently authorised formulation for about 450 out of 1392 authorised PPPs, about 300 of which being studies on inhalation toxicity. For acute dermal toxicity calculated and *in vivo* results agreed in the vast majority of cases (98 % TN, 0.40% TP, 1.3% FP and 0.20% FN). For acute oral and inhalation toxicity good conformity was observed (oral: 77% TN, 9.8% TP, 8.0% FP, and 5.2% FN; inhalation: 76% TN, 9.4% TP, 10% FP, 4.0% FN). However, acute local effects showed a slightly lower agreement between *in vivo* and calculation results. Conformity was highest for skin corrosion/irritation and lowest for eye corrosion/irritation (skin corrosion/irritation: 37% TN, 17% TP, 42% FP, and 4.4% FN; eye damage/irritation: 40% TN, 16% TP, 38% FP, and 6.2% FN). Skin sensitisation based on generic and specific concentration limits led to conformity of about 49% TN, 19% TP, 24% FP and 8.0% FN.

Conclusion: Our results demonstrate good conformity of *in vivo* and calculation-derived classification, especially for non-classified PPPs.

Toxicology – Inhalation toxicology/Respiratory toxicology

26

Toxicological evaluation of carbon fibre dusts after air-liquid interface exposure of lung cell cultures

A. Friesen[1], S. Fritsch-Decker[2], S. Mülhopt[3], C. Weiss[2], D. Stapf[3], A. Hartwig[1]
[1]Karlsruhe Institute of Technology, Institute of Applied Biosciences, Department of Food Chemistry and Toxicology, Karlsruhe, Germany
[2]Karlsruhe Institute of Technology, Institute of Biological and Chemical Systems - Biological Information Processing, Eggenstein-Leopoldshafen, Germany
[3]Karlsruhe Institute of Technology, Institute of Technical Chemistry, Eggenstein-Leopoldshafen, Germany

The role of carbon fibres (CF) as an advanced material is growing in various sectors of the industry, for example in the automotive, aerospace or wind power industries. However, there are only few studies addressing the release of CF dusts and their toxicological impact after inhalation. To fill this gap, within the CarbonFibreCycle project air-liquid interface (ALI) cultures composed of bronchial epithelial cells (BEAS-2B) and macrophage-like cells (THP-1) were established and exposed to a single dose of differently processed CFs via the Vitrocell® Automated Exposure Station. A high modulus CF was either milled in a ball mill or heated in a tube furnace at 800°C and then milled. The CF fragments were aerosolized and fed into the exposure station. The deposition within the exposure chamber and the resulting doses were measured by digital microscopy as well as by quartz crystal microbalance. After different post-incubation periods, the cultures were assessed with regard to viability (LDH, cell count), genotoxic effects (alkaline unwinding), gene expression (high-throughput RT-qPCR) and cytokine release (IL-8).

Exposure towards mechanically processed CFs did not generate any cytotoxic response in mono- (BEAS-2B) or cocultures (BEAS-2B/dTHP-1). In monocultures, gene expression profiles revealed a time dependent response in the inflammation and apoptosis clusters, which peaked at 1 hour of exposure and decreased with increasing post-incubation time. The initial increase in pro-inflammatory gene expression was mirrored in the IL-8 ELISA; however, cytokine release further increased with longer post-incubation times. While differences between mono- and cocultured cells were minor at the level of gene expression, IL-8 release was higher in cocultures.

Exposure towards thermally-mechanically processed CFs also did not induce cytotoxic effects as assessed with the LDH assay. However, this treatment resulted in a reduced cell count. The underlying mechanisms are still to be investigated.

In conclusion, we generated ALI cultures that are stable, easy to use and suitable for the assessment of fibre toxicity. Although the fibres were not highly toxic in the applied cultures, a specific response was detected on the gene expression and protein level, especially with respect to inflammation. The distinct responses induced by mechanically and thermally-mechanically processed fibres show that toxicological effects are highly dependent on fibre treatment and properties.

90

Oxidative and NLRP3 dependent inflammatory potential of Saharan dust compared to crystalline and amorphous silica particles

G. Bredeck[1], M. Busch[1], A. Rossi[1], B. Stahlmecke[2], K. W. Fomba[3], R. P. F. Schins[1]
[1]IUF - Leibniz Research Institute for Environmental Medicine, Düsseldorf, Germany
[2]Institute for Energy and Environmental Technology e.V. (IUTA), Duisburg, Germany
[3]Leibniz-Institute for Tropospheric Research (TROPOS), Leipzig, Germany

Environmental exposure to desert dust, of which about half worldwide is attributable to Saharan dust (SD), rises with climate change and has been associated to increased respiratory morbidity and mortality. SD contains high shares of crystalline silica, which is known to cause lung inflammation and fibrosis via oxidative stress and activation of the NLRP3 inflammasome. Our aims were to investigate the *in vitro* oxidative and pro-inflammatory potential of SD in relation to its physicochemical properties and to assess the involvement of the NLRP3 inflammasome in SD's inflammatory capacity.

Therefore, markers of inflammation and oxidative stress were studied in A549 human lung epithelial cells and NLRP3-deficient *versus* proficient THP-1 human macrophages upon exposure to SD, the crystalline silica dusts DQ12, Sikron F600 and Min-U-Sil or synthetic amorphous silica (SAS) nanoparticles.

The SD sample consisted mainly of silica and amongst multiple other ingredients contained about 4% of iron. The hydroxyl radical generating capacity of SD and DQ12 was comparable, whereas SD but not DQ12 contained endotoxin that could be inactivated by baking at 220°C. In A549 cells, exposure to pristine and baked SD increased the expression of *heme oxygenase (HMOX)-1*, while of the silica samples only baked DQ12 upregulated *HMOX-1*. All silica samples but not SD increased *IL-8* gene expression and IL-8 release. In THP-1 cells, pristine but not baked SD upregulated IL-1β release by about 9-fold. This effect was weaker and baking-independent after crystalline silica exposure and slightly stronger after SAS exposure. None of the particles induced IL-1β release from NLRP3-deficient cells. Preliminary data on more realistic co-cultures of A549 and THP-1 cells cultivated at the air liquid interface match the observed inflammatory effects of SD.

In conclusion, we found a higher oxidative potential of SD than of the crystalline and amorphous silicas as well as substantially differing inflammatory profiles. The iron content suggests an association of the oxidative potential to Fenton reactivity. Moreover, the induction of IL-1β by SD appears to depend on biological components such as endotoxin and to be NLRP3 inflammasome driven. Our findings support a substantial pulmonary toxicity of SD and warrant follow-up studies to further unravel the critical components of this ubiquitous dust.

This work was supported by the Leibniz Collaborative Excellence Programme project DUSTRISK.

96

Investigating the suitability of Co-cultures of human lung and endothelial cells for repeated exposure experiments with nano particle aerosols

D. Eckstein[1], F. Glahn[1], B. Schumann[1], L. Tomisch[1], H. Foth[1]
[1]MLU Halle-Wittenberg, Environmental Toxikology, Halle (Saale), Germany

These days it becomes more and more important to establish long-term in-vitro models for the respiratory system, as for nanoparticles (NP) the respiratory system is the main port of entrance. NP can be found in various products of the daily use, e.g. nano-functionalized plastics and textiles. They can be emitted at different stages of the product´s life-cycle from manufacturing to recycling. We established a novel cell-culture exposure system on inserts (MatriGrid = MG) shaped like alveoles with co-cultures of primary peripheral lung cells (PLC) and an endothelial cell line (EA.hy926) as a model for the blood lung barrier.

Viability of Co-cultures was determined by Resazurin-assay and Lactatdehydrogenase-assay, Glutathione (GSH) was determined by HPLC after derivatization with monobromobimane. The confluency of the cultures was detected by TEER-measurement (transepithelial/transendothelial electric resistance). The size-distribution of the particles in the aerosols was determined by SMPS and OPS.

First of all we exposed Co-cultures 2 times to $BaSO_4$- and TiO_2-NP aerosols (washing & additive exposure). In Resazurin-assay exposure of Co-cultures to aerosols of $BaSO_4$ with averagely 5 x 10^4 particles/cm^3 decreases viability to 40-60 % (depending on patient) when cultures were washed before exposure. Exposure of Co-cultures to averagely 1 x 10^5 particles/cm^3 of TiO_2 shows a clear decrease to 0-30 % (depending on patient) in the washed cultures, as well. For the GSH determination Co-cultures were incubated with $BaSO_4$- and TiO_2-aerosols for 1 h (postincubation 23 h and 71 h). The NP-aerosols show a reduction cellular GSH-levels for both NP when cultures were washed before exposure to the aerosols. Without washing (just additive aerosol exposure) there is a small increase in GSH. The particle size distributions of both aerosols were measured during every exposure. Based on the number size distribution most particles have a size below 100 nm. In the $BaSO_4$- and TiO_2-aerosols the median diameters were 57 and 76 nm, respectively.

The applied NP aerosols of $BaSO_4$ and TiO_2 cause more toxic effects in washed cultures than in just additively exposed cultures. These results show that Co-cultures (PLZ/EA.hy926) may build a barrier against the exposure stress. In the future we will also investigate the inflammatory response of this system after exposure to $BaSO_4$- and TiO_2-aerosols.

139

Impact of nano- and micro-sized chromium(III) particles on cytotoxicity and gene expression profiling related to genomic stability in alveolar epithelial cells

P. Schumacher[1], F. Fischer[1], J. Sann[2], D. Walter[3,4], A. Hartwig[1]
[1]Karlsruhe Institute of Technology, Food Chemistry and Toxicology, Karlsruhe, Germany
[2]Justus-Liebig-University, Institute of Physical Chemistry, Giessen, Germany
[3]Justus-Liebig-University, Institute of Occupational and Social Medicine, Giessen, Germany
[4]Justus-Liebig-University, Institute of Inorganic and Analytical Chemistry, Giessen, Germany

Chromium is a naturally occurring element with three stable forms, namely Cr(0), Cr(III), and Cr(VI). From a toxicological perspective, the distinction between Cr(VI) and Cr(III) is of major importance. Exposure to various Cr(VI) compounds has been consistently associated with genotoxicity and elevated incidences of respiratory cancers whereas Cr(III) is far less toxic, due to its poor cellular uptake. While respective water-soluble chromium compounds have been investigated thoroughly, controversial results have been published for particulate Cr_2O_3, raising the question of whether Cr(III) particles exert properties of Cr(VI), due to endocytic uptake and either intra- or extracellular chromium release.

Morphology and size distribution of three Cr_2O_3 particles, differing in size and manufacturer, was analyzed by TEM. The oxidation state of chromium was controlled by XPS measurements and the release of total chromium was determined via AAS. To differentiate between the release of Cr(VI) and Cr(III) a colorimetric assay was applied. Besides the determination of cytotoxicity via ATP content we applied a sensitive high throughput RT-qPCR approach to establish toxicological fingerprints of water-soluble Cr(VI) and Cr(III) and compared it to the Cr_2O_3 particles in human alveolar epithelial cells (A549).

Regarding the Cr_2O_3 particles, both toxicological endpoints indicated that the particles resemble water-soluble Cr(III), i.e., showing no or only mild effects. Therefore, Cr_2O_3 particles as such are neither cyto- nor genotoxic. However, this statement holds only for particles not releasing Cr(VI). If the latter is the case, as shown for one particle, observed effects resemble the toxicity of Cr(VI) and result in altered expression profiles of genes related to oxidative stress, DNA damage response as well as cell death pathways. The results of the present study show that gene expression analyses provide valuable toxicity profiles for different chromium compounds, reflecting the mode of action of chromium in different oxidation states, including the higher toxicity and genotoxicity of Cr(VI) vs. Cr(III). They further have an important impact on toxicological risk assessment of Cr_2O_3 particles either in the nano- or in the microsized range: Intracellular conversion to Cr(VI) with subsequent reduction and the induction of DNA damage appears to be negligible, provided that the Cr(III) particles are of high purity and Cr(VI) release is excluded.

186

Comparison of the genotoxic potential of different metal-based nanoparticles and nanowire with respect to DNA strand breaks and micronuclei

R. Neuberger[1], J. Wall[1], A. Grove[1], E. Weschenfelder[1], P. Schumacher[1], M. Hufnagel[1], A. Hartwig[1]
[1]Karlsruhe Institute of Technology, Department of Food Chemistry and Toxicology, Karlsruhe, Germany

Nano-sized metals and their compounds can cause oxidative stress, possibly resulting in genotoxicity. Here, both the chemical composition of these materials as well as their shape could further enhance these effects. As the application of fibrous nanomaterials (NM) increases, we evaluated the impact of different metal-based NM in a granular and a fibrous shape on human alveolar epithelial cells (A549) and bronchial epithelial cells (BEAS-2B), focussing on their genotoxic potential.

Six particulate and three fibrous NM, namely Ag, Cu, CuO, Ni, TiO_2, and CeO_2 nanoparticles (NP) and Ag, Cu, and Ni nanowire (NW) were assessed and compared regarding their genotoxic potential in A549 and BEAS-2B cells. Two different endpoints were applied: Alkaline Unwinding (AU) detecting DNA strand breaks in both cell lines, and the micronucleus test (MNT) using flow cytometry in A549 cells.

No genotoxic effect was observed for TiO_2 NP and CeO_2 NP. In contrast, Cu-based NM led to a slight increase of MN in A549 cells with CuO NP having the more distinct impact. However, Cu NW induced more DNA strand breaks compared to Cu NP and CuO NP. In case of Ni NM, a slight increase in MN was observed for both materials, while the induction of DNA strand breaks was restricted to Ni NP. Concerning Ag NP, a moderate genotoxicity was seen. In contrast, the Ag NW treatment led to no (A549) or low (BEAS-2B) induction of DNA strand breaks but a pronounced, dose-dependent increase of MN in A549 cells.

In most cases both DNA strand breaks and MN were observed. However, MNT appeared to be the more sensitive approach as genotoxic effects were observed at lower doses. In the case of some NM, variations between metal species could also be caused by differences in material-dependent intracellular metal ion release, which was shown to result in elevated intracellular metal ion concentrations, also in the nucleus. This can lead to direct or indirect genotoxicity. Of special interest are the results obtained in case of Ag NM. Ag NP and Ag NW were apparently insoluble in cell culture medium and artificial lysosomal fluid but exhibited high ion concentrations in the nucleus, indicating cellular dissolution. The distinct increase in MN by Ag NW with only little DNA strand break induction may possibly be due to an aneugenic mode of action which should be further investigated.

This research was funded by the German Federal Ministry of Education and Research (BMBF), grant number 03XP0211 (MetalSafety).

192

Particle deposition and effects in an air-liquid interface lung model: an international interlaboratory comparison study

H. Braakhuis[1], A. Bannuscher[2], B. Drasler[2], S. Doak[3], **B. Birk**[4], R. Landsiedel[4], M. Clift[3], B. Rothen-Rutishauser[2], R. Vandebriel[1]
[1]National Institute for Public Health and Environment, Bilthoven, Netherlands
[2]Adolphe Merkle Institute, Fribourg, Switzerland
[3]Swansea University Medical School, Swansea, United Kingdom
[4]BASF SE, Experimental Toxicology and Ecology, Ludwigshafen, Germany

For hazard testing of airborne engineered nanoparticles (NPs), air-liquid interface (ALI) exposure systems have been developed for *in vitro* tests with lung cell cultures to mimic realistic inhalation exposures. Within the EU-project PATROLS, we have further advanced an epithelial lung-cell model with the aim to produce standard operation protocols (SOPs) allowing to reproduce the experiments in different laboratories. The model consists of the human bronchial epithelial cell line, Calu-3. To further improve the physiological relevance of the model, we added human blood monocyte derived macrophages (MDM) or macrophages differentiated from human THP-1 monocytes (dTHP-1), to the Calu-3 cell layer. For exposure, we used a commercially available exposure device, i.e. the VITROCELL Cloud system.

As a first step to advance these models towards regulatory use we initiated interlaboratory comparison studies with seven PATROLS partners. First, we compared deposition upon aerosolization of quartz silica particles (DQ12), titanium dioxide (TiO2 NM-105) NPs and the chemical fluorescein. Results show comparable deposited doses for the different particles between the participating laboratories. Second, We compared effects of exposure to DQ12, TiO2 NM-105 and LPS (positive control) in the Calu-3 ALI system with and without MDM or dTHP-1. Barrier function (trans-epithelial electrical resistance[; TEER), cell viability (WST-1 and LDH), and cytokine release (e.g. IL-6, IL-8 and TNF-α) were measured. No exposure effects on TEER and cell viability were measured. A slight induction of cytokines by DQ12 and TiO2 were observed, while the positive control LPS increased cytokine release in both Calu-3 alone and in co-cultures with macrophages.

Despite the complexity of the study including air liquid application of nanomaterials on an in vitro co-culture model, the study showed adequate intra-laboratory reproducibility. A detailed SOPs will be provided to the scientific community soon. Further studies including several nanomaterials are needed to finally assess the predictivity of the in vitro system compared to in vivo inhalation studies.

This work is funded by EU-project PATROLS (Physiologically Anchored Tools for Realistic nanomaterial hazard asessment), No. 760813.

194

MetalSafety - Cytotoxic potential of higher concentrations of silver nanowires in primary human peritoneal mesothelial LP9 cells

S. M. Reamon-Buettner[1], S. Lamsat[1], M. C. Schoebel[1], T. Hansen[1], F. Schulz[1], C. Ziemann[1]
[1]Fraunhofer Institute for Toxicology and Experimental Medicine ITEM, Hannover, Germany

Silver nanowires (AgNW) are nanomaterials with promising technical properties (e.g. high transmission rates, low resistance) and versatile applications in advanced technologies. Owing to their fiber-like morphology and similar dimensions, there is concern about AgNW inducing carbon nanotube-like adverse effects such as cellular senescence or malignant mesothelioma. Using *in vitro* approaches with primary human peritoneal mesothelial LP9 cells, we analyzed different concentrations of a model AgNW (GM of WHO fibers: ø 45 nm, length 7.55 µm) to mediate cell death and effects on cytoskeleton and chromatin structure. Results were compared to $AgNO_3$ (ion effects), silver nanoparticles (AgNP; particle morphology; Z-average: ø 74 nm) and a long and straight multiwalled carbon nanotube (MWCNT3; positive control; GM of WHO fibers: ø 85 nm, length 8.57 µm), which has previously been shown to induce adverse effects in LP9 cells, notably cellular senescence. Essentially, LP9 cells (4.2 x 10^4) were grown on 18 mm coverslips and treated for 24 h with the silver materials (18, 50, and 100 µg/mL) or MWCNT3 (18 µg/mL). Due to steep, most likely ion-based cytotoxicity, effects on cytoskeleton and chromatin could not be analyzed for $AgNO_3$ and AgNP. Microscopic analysis of cell density pointed to a cytotoxicity ranking of $AgNO_3$ (no cells at 18-100 µg/mL) > AgNP (no cells at 50-100 µg/mL)>> Ag NW (still some viable cells at 100 µg/mL). Like for MWCNT3, Annexin V/propidium iodide probing showed necrosis rather than apoptosis accounting for AgNW-mediated cell death. By DAPI-staining of AgNW-treated cells (i.e. at 50-100 µg/mL) we found various chromatin abnormalities such as nuclei with DAPI foci, reminiscent of senescence-associated heterochromatin foci, a well-known marker for cellular senescence. Moreover, immunofluorescence of α-tubulin and γH2A.X showed cytoskeletal abnormalities and concentration-dependent γH2A.X nuclear panstaining. However, number of panstained nuclei was clearly higher for MWCNT3. Furthermore, PNA-FISH analysis pointed to AgNW-mediated induction of senescence-associated distended satellites. In conclusion, our results suggest that higher concentrations of AgNW can induce various abnormalities of both cytoskeleton and chromatin in mesothelial LP9 cells, eventually causing cell damage, cellular senescence and

necrotic cell death. This research was funded by the German Federal Ministry of Education and Research (BMBF), grant number 03XP0211 (MetalSafety).

211

An *ex vivo* perfused ventilated murine lung model suggests lack of acute pulmonary toxicity of the potential novel anticancer agent (-)-englerin A

C. Schremmer[1], D. Steinritz[2], T. Gudermann[1], D. J. Beech[3], A. Dietrich[1]
[1]Walter Straub Institute of Pharmacology and Toxicology, Munich, Germany
[2]Bundeswehr Institute for Pharmacology andToxicology, Munich, Germany
[3]University of Leeds, Leeds, United Kingdom

Objectives: (-)-Englerin A (EA), a novel potential anti-cancer drug, is a selective activator of classical transient receptor potential 4 and 5 (TRPC4, TRPC5) channels. As TRPC4 channels are expressed and functional in the lung endothelium, possible side effects like lung edema formation may arise during its administration. Well-established *in vivo* rodent models for toxicological testing however fail to identify possible side effects like lung edema formation due to rapid metabolic degradation to its inactive derivative englerin B. We hypothesized that an *ex vivo* isolated perfused and ventilated murine lung (IPVML) model, which is perfused blood-free outside the body, is well suited to evaluate acute lung toxicity of EA.

Methods: Lungs were prepared from C57BL/6 mice ventilated with room air and perfused with blood-free electrolyte solution. Lung weights and tidal volumes were continuously measured for 1h and wet-to-dry weight ratios were quantified after the experiment. To evaluate the sensitivity of the IPVML model, short time (10 min) pH drops from 7.4 down to 4.0 in the electrolyte solution were applied. Fluorescein isothiocyanate (FITC)-coupled dextran particles were added to the electrolyte solution to measure their permeation from the perfusate to the lung tissue in histological sections.

Results: The IPVML model was sensitive enough to detect short time pH drops from 7.4 to 4.0. Tidal volumes, lung weights and wet-to-dry weight ratios increased in a linear fashion. The same was true for the incorporation of FITC-coupled dextran particles in lung tissues. Concentrations of 50 to 100 nM EA (5 and 10 fold of the *in vitro* active concentration) continuously perfused through the IPVML model did not change tidal volumes and lung weights significantly compared to electrolyte solution only. Wet-to-dry weight ratios were only increased after perfusion of 100 nM EA, but permeation of FITC-coupled dextran particles from the perfusate to the lung tissues was not significantly different.

Conclusion: The IPVML model is suitable to evaluate acute pulmonary toxicity of drug candidates by quantification of lung edema formation independently of drug application and metabolism, while eliminating stress in living mice according to the 3R rules. In our experiments we detected no acute edema formation after application of EA (50 nM). Therefore, our data suggest that EA as a promising anti-cancer drug lacks acute pulmonary toxicity.

216

Comparison of metal-based nanoparticles and nanowire: Solubility, reactivity, bioavailability and cellular toxicity

J. Wall[1], D. Ag Seleci[2], R. Neuberger[1], M. Link[1], F. Schworm[1], P. Schumacher[1], M. Hufnagel[1], W. Wohlleben[2], A. Hartwig[1]
[1]Karlsruhe Institute of Technology, Karlsruhe, Germany
[2]BASF SE, Ludwigshafen, Germany

Inhalation followed by endocytosis is an important route of exposure of metal-based nanomaterials. However, while the toxicity of metal-based nanoparticles (NP) has been investigated in an increasing number of studies, only little is known about metal-based fibrous materials, so-called nanowire (NW). Within the present study, the physicochemical properties of particulate and fibrous nanomaterials based on Cu, CuO, Ni, and Ag as well as TiO_2 NP and CeO_2 NP were characterized and compared with respect to abiotic metal ion release in different physiologically relevant media as well as acellular reactivity. Subsequently, four different cell lines were applied to compare cytotoxicity and bioavailability, as well as intracellular metal ion release in the cytoplasm and nucleus.

While no relevant dissolution of nanomaterials was observed in artificial alveolar fluid (AAF; pH 7.4), Cu-, CuO- and Ni-based materials exerted distinct dissolution under acidic conditions, present in artificial lysosomal fluids (ALF and PSF; pH 4.5). In contrast, TiO_2 and CeO_2 materials showed no dissolution in either model fluid, and Ag only partial dissolution to ions, linked to transformation and passivation of the remaining NW and NP. Regarding cellular studies, both cytotoxicity and bioavailability reflected the acellular dissolution rates in physiological lysosomal media (pH 4.5); only Ag-based materials showed no or very low acellular solubility, but pronounced intracellular bioavailability and cytotoxicity, leading to particularly high concentrations in the nucleus. As with model fluids, no intracellular bioavailability was seen for TiO_2 NP and CeO_2 NP.

This study shows that particulate as well as fibrous Cu-, Ni- and Ag-based nanomaterials can be taken up via endocytosis followed by lysosomal dissolution, releasing potentially toxic metal ions. This leads to elevated levels of respective metal ions in the cytoplasm and also in the nucleus, mediating oxidative stress and inflammatory responses. However, in spite of some quantitative differences, the intracellular bioavailability as well as toxicity is mainly driven by the respective metal species and is less modulated by the shape of the respective NP or NW.

This research was funded by the German Federal Ministry of Education and Research (BMBF), grant number 03XP0211 (MetalSafety).

Toxicology – Carcinogenesis

19

How much DNA damage in the Comet Assay is too much for cells to survive?

E. E. Bankoglu[1], C. Schüle[1], **H. Stopper**[1]
[1]University of Wuerzburg, Institute of Pharmacology and Toxicology, Wuerzburg, Germany

The comet assay is widely used in basic research, genotoxicity testing and human biomonitoring. Often, percentages of DNA in the tail region (considered representative for the DNA damage) in the range of 20% and even 50% and more damaged DNA are reported. However, the further fate of such heavily damaged cells is not known. DNA damage is in principle repairable. Surviving cells with unrepaired or falsely repaired DNA damage are at risk to yield a mutated cell. If damage is too extensive, repair may be overwhelmed, and cells may die later on and not pose a mutagenic risk. Thus, interpretation of comet assay data might benefit from a better understanding of the future fate of a cell with DNA damage. For this, we compared the maximally induced DNA damage in TK6 cells with the survival of the cells. As test substances we selected hydrogen peroxide (H2O2; oxidizing agent), methyl methanesulfonate (MMS; alkylating agent) and etoposide (topoisomerase II inhibitor). Cell viability, cell proliferation, and apoptosis were analyzed one day after substance exposure and comet assay performance in the same cell culture.

A concentration dependent increase in DNA damage and in the percentage of non-vital and apoptotic cells was observed for each of the three test substances. More than 20-30% DNA in the tail region of the comets was related to the later death of more than 50% of the cells. However, in all cases cells were able to repair at least some of the DNA damage within a few hours after substance removal. In conclusion, for these three chemicals, the further fate of the cells was determined by DNA repair and survival as well as by the death of heavily damaged cells. For better interpretation of comet assay results it might be advisable to provide survival data such as a proliferation assessment on the day following the experiment for treated cells if the DNA damage is greater than about 20% DNA in tail.

113

p21-dependent CDK4 silencing and activation of the DREAM complex is sufficient to mediate B[a]P and IR-induced cellular senescence

A. Schmidt[1], S. Allmann[1], M. T. Tomicic[1], M. Christmann[1]
[1]Institut of Toxikology, Mainz, Germany

Introduction: Senescence is an important outcome of genotoxic stress. In our previous work, we showed that various DNA repair factors are repressed upon exposure to B[a]P or ionizing radiation via E2F1 degradation and p21/DREAM-mediated abrogation of the E2F1 signaling. Furthermore, we showed that the repression of theses repair pathways is associated with the induction of cellular senescence.

Objectives: Here we investigated the impact of the p21/DREAM axis on the induction of cellular senescence.

Materials & methods: Cell death, senescence, cell cycle progression and expression of cell cycle regulators were analyzed by flow cytometry, β-Gal assay, qPCR and immunodetection in MCF7 cells upon exposure to ionizing radiation or the CDK4/6 inhibitor Palbociclib. Furthermore, the impact of p21 knockdown on senescence, cell death and gene regulation were evaluated by flow cytometry, β-Gal assay and qPCR.

Results: Our data show that in p14/p16 deficient MCF7 cells, induction of senescence completely depends on p21. Co-immunoprecipitation experiments revealed that especially the inhibition of CDK4 by p21 is important for the activation of the DREAM complex. Transcriptional analysis further revealed that the DREAM complex silences the transcription of FOXM1, LIN1 and MYBL2 targets including HMGB2 and LMNB1, which have been shown to be important factors in mediating cellular senescence. Repression of these factors was abrogated by knockdown of p21. A similar gene regulation pattern was observed upon CDK4 inhibition, which also strongly induced the senescence phenotype.

Conclusion: Based on our data the DREAM complex was identified as the master regulator of genotoxic stress-induced senescence and revealed that p21/DREAM-dependent CDK4 inhibition is sufficient to induce the senescence phenotype.

117

Hemoglobin Adducts of Heat-induced Food Contaminants in Blood Samples of Non-smokers, Smokers and Strict Raw Food Eaters

B. Monien[1], F. Gauch[1], K. Abraham[1]
[1]Bundesinstitut für Risikobewertung, Lebensmittelsicherheit, Berlin, Germany

Question: Various genotoxic carcinogens are present in human diets. They or their reactive metabolites form adducts in DNA and proteins, which can be used as biomarkers of internal exposure. Recent biomarker studies indicate that there is substantial internal background exposure of some heat-induced contaminants (e.g. acrylamide) independent from the dietary intake. To clarify this objective, we compared hemoglobin (Hb) adduct levels of heat-induced food contaminants in strict raw food eaters, who did not consume any food heated to higher temperatures than 42 °C for at least 4 months, with those from people following conventional dietary habits.

Methods: Val adducts of various genotoxic substances in Hb were cleaved with fluorescein-5-isothiocyanate and the resulting analytes were quantified by isotope-dilution UHPLC-MS/MS. Four adducts were from the heat-induced food contaminants (abbreviations of adducts in parentheses) glycidol (DHP-Val), acrylamide (AA-Val), glycidamide (GA-Val), and furfuryl alcohol (FFA-Val). The adduct levels are determined in three groups of adult study participants: strict raw food eaters, as well as non-smokers and smokers following conventional diets (vegans or omnivores).

Results: As yet, adduct level data from all strict raw food eaters (n = 16, non-smokers) and in part from non-smokers (n = 6) and smokers (n = 6) were determined. The median levels of AA-Val (25.9 pmol/g Hb), GA-Val (12.2 pmol/g Hb) and DHP-Val (4.7 pmol/g Hb) in non-smokers were significantly lower compared to those of smokers (AA-Val, 69.0 pmol/g Hb; GA-Val, 44.2 pmol/g Hb; DHP-Val, 8.6 pmol/g Hb). Median FFA-Val were 11.5 pmol/g Hb in non-smokers and 10.5 pmol/g Hb in smokers. The median adduct levels in Hb samples from strict raw food eaters were comparably low: AA-Val (12.3 pmol/g Hb), GA-Val (5.2 pmol/g Hb), DHP-Val (1.3 pmol/g Hb) and FFA-Val (5.1 pmol/g Hb).

Conclusion: The median levels of AA-Val, GA-Val, DHP-Val and FFA-Val in non-smokers with conventional dietary habits were in the same range compared to previous studies. Smoking led to higher levels of AA-Val, GA-Val and DHP-Val which also confirms previous data. The adduct levels in Hb samples of strict raw food eaters suggest that non-dietary uptake or endogenous formation contribute significantly to the overall exposure to acrylamide, glycidol and furfuryl alcohol.

132

Denervation as an independent cancer risk factor – lessons from urinary bladder cancer in people with long-term spinal cord injury

R. Böthig[1], O. Balzer[1], C. Tiburtius[1], K. Fiebag[1], B. Kowald[1], R. Thietje[1], W. Schöps[2], M. Zellner[3], T. Kadhum[4], **K. Golka**[5]
[1]BG Klinikum Hamburg, Hamburg, Germany
[2]Urological Practice, Sankt Augustin, Germany
[3]Johannesbad Fachklinik, Bad Füssing, Germany
[4]Mittelrheinklinik, Boppard-Bad Salzig, Germany
[5]Leibniz Reseach Centre for Working Environment and Human Factors (IfADo), Dortmund, Germany

Background: Bladder cancer in spinal cord injury (SCI) patients, associated with a dramatically worse prognosis, is thought to be due to adverse effects of chronic indwelling catheters like chronic local irritation and urinary tract infections. We challenged this commonly accepted explanation by investigating two large study groups of traumatic spinal cord injury patients managed without chronic indwelling catheters.

Methods: We investigated all 40 bladder cancer cases of 7396 long-term traumatic SCI patients, 4 bladder cancer cases diagnosed at the initial urological workup on the occasion of the acute spinal cord injury, all in- and out-patients of our Hamburg centre observed from 01.01.1998 to 12.31.2019, and 135 SCI bladder cancer cases from a multicentre study in 28 centres in the German speaking area, managed by different types of bladder management, except chronic indwelling catheters. The urinary bladder cancer data of the German population were obtained from the German Centre for Cancer Registry Data at Robert Koch Institute in Berlin.

Results: T category and grading of the 40 Hamburg cases were significantly poorer, compared to bladder cancer cases from the general population (p lower to 0.0001, each) and the 4 incidental cases at initial urological workup, resulting in a median survival of 12.0 months. However, these findings are comparable to those in SCI patients managed with chronic indwelling catheters. In the multicentre study, the mean latency time between the onset of SCI and bladder cancer diagnosis was significantly longer in patients with catheter-free emptying methods, compared to patients with intermittent catheterization.

Conclusion: The described findings in SCI bladder cancer patients managed with and without chronic indwelling catheter point to the disturbance of the innervation of the urinary bladder as an independent bladder cancer risk factor.

References:

Böthig R et al. (2020) Traumatic spinal cord injury confers bladder cancer risk to patients managed without permanent urinary catheterization: lessons from a comparison of clinical data with the national database. World J. Urol. 38:2827-2834

Böthig R et al. (2020) Incidental bladder cancer at initial urological workup of spinal cord injury patients. Spinal Cord Ser. Cases 6:55

Böthig R et al. (2021) Bladder management, severity of injury and period of latency: descriptive study on 135 patients with spinal cord injury and bladder cancer. Spinal Cord 59:971-977

142

A systematic analysis of the NAD booster, nicotinamide riboside, in genotoxic stress response towards sulfur and nitrogen mustard derivatives.

J. Ruszkiewicz[1], Y. Papatheodorou[1], J. Melzig[1], L. Kehrt[1], M. Thomann[1], A. Schmidt[2], S. Rothmiller[2], A. Bürkle[1], A. Mangerich[1]
[1]University of Konstanz, Biology, Konstanz, Germany
[2]Bundeswehr Institute of Pharmacology and Toxicology, Munich, Germany

Introduction: Nicotinamide adenine dinucleotide (NAD+) has multiple cellular roles, as a cofactor in energy production, redox regulation, and cell survival pathways. NAD+ is also a substrate for DNA repair factors, such as ARTDs (aka PARPs) and SIRTs, thus is considered essential for genome maintenance. Decreased cellular NAD+ levels, e.g., as a consequence of NAD+-consuming activity of ARTDs synthesizing poly(ADP-ribose) (PAR), has been observed in pathomechanisms of DNA alkylating agents such as sulfur mustard. These results suggest the supplementation of NAD+ boosting molecules as a plausible strategy to mitigate mustard-induced toxicity.

Objectives: In this systematic study, the effects of the NAD+ booster, nicotinamide riboside (NR), on the genotoxic stress response towards the sulfur mustard derivatives, i.e., the crosslinking agent mechlorethamine (HN2) and the monofunctional agent 2-chloroethyl-ethyl sulfide (CEES) have been investigated.

Materials & methods: Immortalized human keratinocytes (HaCaT) and human peripheral blood mononuclear cells (PBMCs) were exposed to NR in order to boost NAD+ levels before a 30-min exposure to CEES or HN2. Subsequently, the cellular NAD+ levels, ATP levels, PAR levels, and cell death were assayed. Moreover, the clonogenic survival assay and DNA damage analysis *via* automated fluorometric analysis of DNA unwinding (FADU) were performed.

Results: NR supplementation effectively raised basal levels of NAD+ in a dose-dependent manner over several hours. Furthermore, NR supplementation mitigated NAD+ loss and boosted PAR formation upon genotoxic treatment. Yet, at the conditions tested so far, NR supplementation did not attenuate cytotoxic and genotoxic effects of CEES and HN2. Thus, the effects of CEES and HN2 on ATP levels, cell death, as well as DNA damage and repair were not affected by NR in either cell type. In addition, no NR effect was observed in HaCaT colony formation assay upon genotoxic treatment.

Conclusion: Our present results suggest that despite its positive effects on NAD+ and PAR levels, NR is not effective in counteracting (geno-)toxicity of the alkylating agents CEES and HN2 in the model systems and conditions tested. These results suggest that at the conditions tested NAD+ metabolism already works at an optimum. Alternative conditions and endpoints will be analyzed to test this hypothesis.

Supported by the German Ministry of Defense (grant number E/U2AD/ID015/IF561).

162

TMZ-induced senescence is independent of DREAM signaling but associated with H3K9 dimethylation

C. Schwarzenbach[1], J. Rinke[1], M. Tomicic[1], M. Christmann[1]
[1]University Medical Center Mainz, Toxicology, Mainz, Germany

Introduction: Cellular senescence is a major outcome of cancer treatment based on alkylating drugs. In our previous work, we showed that following exposure to the alkylating agent temozolomide (TMZ) most glioma cells evade apoptosis, entering a senescent state and thereby are protected against anticancer therapy.

Objectives: We investigated the impact of the p21/DREAM axis and histone methylation on the induction of cellular senescence upon exposure to TMZ in glioblastoma cells.

Materials & methods: Cell death, senescence, cell cycle progression and expression of cell cycle regulators were analyzed by flow cytometry, β-Gal assay, qPCR and immunodetection in LN229 cells upon exposure to TMZ. Furthermore, the impact of histone methylation on senescence and cell death was evaluated by flow cytometry and β-Gal assay.

Results: Our data show that in LN229 cells induction of senescence depends on p21. Co-immunoprecipitation experiments revealed that especially the p21-mediated inhibition of CDK1/2 but not of CDK4 is causative for senescence activation. In line with this, activation of the DREAM complex was not observed and transcriptional analysis showed no reduction in the expression of FOXM1, LIN1 and MYBL2 targets including LMNB1. Opposingly, we observed an enhanced expression of H3K9me2, H3K9me3 and H3K27me3 upon TMZ treatment. Of note, prohibiting dimethylation of H3K9 through inhibition of the methyltransferases GLP and G9a reduced the induction of senescence significantly.

Conclusion: The DREAM complex is not involved in the induction of senescence upon treatment with the alkylating agent TMZ in glioma cells. In contrast, histone methylation is enhanced upon TMZ treatment. This indicates that particularly H3K9 dimethylation plays a crucial role in the induction of the senescence phenotype.

183

The Role of Replication Stress in Ochratoxin A Genotoxicity

C. Klotz[1], J. Borchers[1], J. Brode[1], A. Mally[1]
[1]University of Würzburg, Department of Toxicology, Würzburg, Germany

The mycotoxin and food contaminant Ochratoxin A is one of the most potent renal carcinogens known to date, but its mechanism of carcinogenicity still needs to be resolved to improve science-based assessment of human health risks associated with dietary exposure to OTA. While *in vitro* and *in vivo* studies suggest that disruption of mitosis coupled with compensatory stimulation of cell proliferation may promote genomic instability and tumorigenesis in rat kidneys *in vivo*, the causal chain of events preceding perturbation of mitosis by OTA remains to be established. As mitotic aberrations may result from replicative stress, the present work aimed to investigate if OTA interferes with DNA replication using the DNA fiber assay. This technique relies on the sequential pulse labeling of cells with thymidine analogs such as 5-iodo-2'-deoxyuridine (IdU) and 5-chloro-2'-deoxyuridine (CldU) and subsequent visualization of thymidine analogues incorporated into replicating DNA using indirect immunofluorescence. Analysis of replication forks dynamics revealed a significant reduction in replication fork velocity in human renal epithelial cells (HK-2) exposed to OTA at concentrations ≥10 µM for 1 hour. Analysis of individual track lengths indicated global slowing of fork progression in response to OTA rather than shortening of individual tracks as seen in cells exposed to the alkylating agent cisplatin. In support of the mild but significant effects of OTA on replication fork velocity, analysis by Western blot and/or immunofluorescence demonstrated a significant, concentration-related increase in γH2AX and pChk1 (S317) in cells treated with OTA. Importantly, costaining with CldU revealed γH2AX foci exclusively in cells with newly replicated DNA, thus supporting a mechanistic link between DNA replication and induction of γH2AX foci by OTA. Moreover, visualization of γH2AX in the extended chromatin fiber assay revealed a concentration-dependent increase in γH2AX along replicative chromatin fibers. Taken together, these data provide first experimental evidence for perturbation of the S-phase replisome machinery by OTA and suggest replication stress as an early key event in OTA genotoxicity.

Pharmacology – G-protein coupled receptors

12

Faster G protein interaction kinetics associated with lower agonist sensitivity of p115-RhoGEF compared to other RH-Rho-GEFs can be attributed to enhanced GAP activity in intact cells

F. Redlin[1], M. Bünemann[1]
[1]Phillipps University of Marburg, Pharmacology, Marburg, Germany

RH-RhoGEFs (guanine nucleotide exchange factors) display the link between subunits of the Gα12/13-family and the RhoA signaling cascade. While it is known that all three RH-RhoGEFs (p115-RhoGEF, LARG and PDZ-RhoGEF) possess GAP-activity towards Gα12/13 in vitro, previous studies in our group found that LARG slows down Gbg and Gα13 reassembly incompatible with relevant GAP-activity in intact cells.

Here we studied dynamics of interactions of Gα13 with the three RH-Rho-GEFs and also various truncated versions and chimeras by means of Foerster resonance energy transfer (FRET) in single intact cells.

We could show that the Gα13-p115 interaction displays significantly faster off kinetics than LARG and PDZ, which translates into a significantly shorter interaction time. Several truncated versions and chimeras of the various RhoGEFs were created to narrow down the structural origins and to attempt to speed up the interaction between Gα13 and LARG. We were able to locate the source of p115s faster kinetics to a motif just N-Terminal of the RH-Domain, which is the principle binding site of Gα13. A single amino acid mutation (E32G) in that motif eliminated this effect. With this mutation (p115-E32G) we not only found comparable G protein interaction kinetics to LARG, but also higher agonist sensitivity, proving a causative connection between the RhoGEF-G protein dissociation kinetics and the sensitivity towards receptor-induced activation. Furthermore, disturbing the interaction of this motif of p115 with Gα13 by mutating the corresponding interaction site in the alpha-helical domain of Gα13 impaired the shorter interaction with p115 but had no effect on LARG Gα13 interaction.

While the rgRGS domains of all RH-RhoGEFs showed GAP activity towards Gα13 in vitro, the results of our intact cell approach, suggests that only p115RhoGEF, exhibits a functionally relevant GAP activity towards Gα13 in intact cells.

20

Mutation of lysine residues in arrestin alters intracellular trafficking but not receptor affinity

N. Mösslein[1], M. Bünemann[2], **C. Krasel**[2]
[1]Philipps-Universität Marburg, FB Pharmazie, Institut für Pharmakologie und Klinische Pharmazie, Marburg, Germany
[2]Philipps-Universität Marburg, Institut für Pharmakologie und Klinische Pharmazie, Marburg, Germany

Question: One of many different ways of classifying G protein-coupled receptors (GPCRs) is their behaviour towards arrestins. Upon agonist stimulation, class A GPCRs interact with arrestins only transiently and internalize in endosomes while the arrestins remain at the plasma membrane. In contrast, class B GPCRs show a more stable interaction with arrestins and co-internalize with arrestins into endosomes. It has been proposed that the endosomal co-trafficking of receptor-arrestin complexes requires stable arrestin ubiquitination. We mutated several published ubiquitination sites of arrestin to investigate the effect of ubiquitination on the functionality of arrestin. We also treated cells with the ubiquitin-activating enzyme (E1) inhibitor TAK-243 to inhibit ubiquitinylation.

Methods: Lysine residues in bovine arrestin3 were mutated to arginines to prevent their ubiquitination. We deleted each site individually in arrestin single mutants and also combined different mutations in several multiple mutants. The affinity of the arrestin mutants to GPCRs was analyzed in FRET and dual-colour FRAP measurements. Furthermore, co-internalization of receptors and arrestins was visualized by confocal imaging. TAK-243 was used at 1 µM concentration for 4 hours.

Results: Two lysine residues were identified in bovine arrestin3 that, when simultaneously mutated to arginine, impaired co-internalization of arrestin3 with various Class B GPCRs. However, dual-colour FRAP measurements revealed that the affinity of this arrestin mutant to GPCRs was indistinguishable from wild-type arrestin. Treatment with TAK-243 reduced whole-cell and arrestin3 ubiquitinylation but did not alter co-internalization of arrestin3 with class B GPCRs. mdm2 is an E3 ubiquitin ligase that has been proposed to ubiquitinylate arrestins, but GFP-tagged mdm2 was localized exclusively to the nucleus of HEK293T cells, and various catalytically inactive mdm2 mutants did not visibly reduce arrestin3 co-internalization with class B receptors.

Conclusion: We conclude that the endosomal co-trafficking of arrestin with Class B GPCRs depends on the presence of certain lysine residues in arrestin. The role that is served by these lysine residues remains unclear since general inhibition of ubiquitinylation did not alter endosomal co-trafficking of arrestin.

47

Differential recognition of opioid analgesics by µ opioid receptors: Predicted interaction patterns correlate with ligand-specific voltage sensitivity

S. B. Kirchhofer[1], V. J. Y. Lim[2], J. G. Ruland[1], P. Kolb[2], M. Bünemann[1]
[1]Philipps-Universität Marburg, Institut für Pharmakologie & Klinische Pharmazie, Marburg, Germany
[2]Philipps-Universität Marburg, Institut für Pharmazeutische Chemie, Marburg, Germany

Question: The MOR is the key target for analgesia, but the application of opioids is accompanied by several issues. There is a wide range of opioid analgesics, differing in their chemical structure and their properties in receptor activation and subsequent effects. A better understanding of ligand-receptor interactions and resulting effects is important. A ligand-induced modulation of activity due to changes in membrane potential was described for the MOR. With a combined *in silico* and *in vitro* approach, we defined discriminating interaction patterns for this ligand-specific voltage sensitivity. With this, we present new insights for interactions likely in ligand recognition and their specific effects on activation of the MOR.

Methods: We evaluated the binding modes of several opioid ligands by molecular docking and analyzed the ligand-receptor interactions by a fingerprint analysis. We further examined the ligands for their voltage sensitivity by analyzing the extend and direction of the effect of depolarization, evaluated by FRET-based assays under the control of the membrane potential. In order to alter the binding modes of the ligands we applied site-directed mutagenesis and evaluated the influence of these on agonist-specific voltage sensitivity.

Results: We identified different predicted interactions for morphinan ligands versus methadone and fentanyl. These differential interaction patterns were connected to ligand-specific voltage sensitivity of the MOR, resulting in a comparable group-arrangement with one displaying a strong increase in efficacy upon depolarization and one displaying a decrease in activation. Furthermore, we were able to identify important regions in the receptor which we correlated with the voltage effect on the MOR.

Conclusion: These results suggest that ligand-specific voltage sensitivity of MOR activation is mechanistically based on the interaction patterns between ligands and the receptor. Our approach, strongly involving the opportunities enabled by *in silico* methods, allows the screening of a large number of predicted interactions and allows a subsequent *in vitro* analysis in a systematic and rational way. The MOR, with its diverse voltage pharmacology, was a good model system to illustrate the potential of this approach. With this we aim to get a better understanding of the ligand-specific signaling of the MOR and of the voltage modulated signaling of GPCRs in general.

48

Kappa Opioid Receptor (KOR) exhibits high basal activity and voltage sensitivity

C. Kurz[1], S. B. Kirchhofer[1], M. Bünemann[1]
[1]Institut für Pharmakologie und klinische Pharmazie, Marburg, Germany

Several GPCRs are already classified as voltage sensitive. By modulating the membrane potential, the agonist effect could be modulated in a ligand specific manner.

A very interesting type of voltage sensitive G protein coupled receptors (GPCR) are the opioid receptors**.** Due to their neuronal expression, they are exposed to large changes in membrane potential. There are different types of the opioid receptors: μ, κ, δ and the Nociceptin receptor. We recently investigated the μ Opioid receptor and found a ligand specific voltage sensitivity, which had a considerable effect on the ability of opioid analgesics to activate μ opioid receptors (Ruland *et al.*, 2020).

In this study we investigated the kappa opioid receptor (KOR) in terms of voltage dependence with a combination of Förster resonance energy transfer (FRET) and patch clamp in transfected single human embryonic kidney (HEK) cells. Additionally, we performed FRET measurements of multiple cells at a plate reader.

We started our measurements in an established FRET-based G-Protein activation assay. We found a high level of constitutional activity of KOR towards G Protein activation, which could be reversed by the antagonist naloxone. Using FRET sensors including those to measure KOR conformation, we confirmed the observation of a high basal activity of KOR. Surprisingly, we not only observed a voltage dependence of the KOR – induced G protein activation in presence of the endogenous agonist Dynorphin A, but also in the absence of any ligand. These findings could be confirmed in the receptor arrestin interaction assay. To our knowledge this is the first observation of a functional activation of a natural GPCR by voltage in the absence of any ligand.

In conclusion, KOR showed activation upon depolarization in presence and absence of agonist. KOR showed basal activity, which could be detected in different assays, including directly at the level of receptor conformation, which might potentially be linked to our observation of the voltage dependence in absence of agonist.

Ruland, J. G., Kirchhofer, S. B., Klindert, S., Bailey, C. P., & Bünemann, M. (2020). Voltage modulates the effect of μ-receptor activation in a ligand-dependent manner. *British Journal of Pharmacology*, *177*(15), 3489–3504. https://doi.org/10.1111/bph.15070

50

FRET-based prostaglandin E2 subtype 4 receptor conformation sensor to measure *in situ* prostaglandin concentration in real time

M. Kurz[1], M. Ulrich[1], M. M. Scharf[2], J. Shao[3], N. Wettschureck[3], P. Kolb[2], M. Bünemann[1]
[1]Philipps Universität, Institut für Pharmakologie und klinische Pharmazie, Marburg, Germany
[2]Philipps Universität, Institut für pharmazeutische Chemie, Marburg, Germany
[3]Max Planck Institut für Herz- und Lungenforschung, Pharmakologie, Bad Nauheim, Germany

Prostaglandins (PGs) are important lipid mediators with a variety of crucial functions and almost ubiquitous occurrence in the human body. They are formed inside the cell and act autocrine as well as paracrine mainly via plasma membrane localized prostaglandin receptors, which belong to the G-protein coupled receptor (GPCRs) class. Prostaglandins are released from many different cell types and are short lived, likely leading to local unequal concentrations of PGs in tissues or organs. According to our latest knowledge, there is overall no suitable methodology available to measure the concentration of any extracellular ligand, such as prostaglandins, with temporal and spatial resolution. Antibody-based measuring procedures are often used which only provide a snapshot of the concentration of a particular prostanoid without spatial or temporal resolution and sometimes with no distinction between active and inactive metabolites.

To step in this gap, we generated and optimized a FRET conformation sensor based on the PGE-receptor subtype 4 (EP4 receptor) which seems suitable to act as a biological reporter especially for endogenous PGE1 and 2. Single living HEK cells stably expressing the EP4 receptor sensor were investigated by means of FRET at an inverted fluorescent microscope. Furthermore, FRET measurements of multiple cells with HEK cells alone or in co culture with either MDCK cells or macrophages, were performed at either a microscope or a plate reader.

Our sensor was sensitive to PGE2 in a nanomolar range and the activity could be blocked with the specific antagonist L-161,982. We measured the real-time release of paracrine PGE2, using a co culture based approach, not only of cell lines but also of primary cells. Moreover using this sensor, we were able to display artificially generated PGE2 gradients spatially and temporally resolved.

In conclusion, we could show that our optimized new EP4 based FRET sensor can be used for concentration measurements of prostaglandins like PGE2 with temporal and spatial resolution. A successful implementation of our presented method of FRET-based measurements of the concentration of extracellular GPCR ligands will not only widen the possibility of studying prostanoids, but might potentially also pave the way to measure the spatial and temporal concentration of further hormones, neurotransmitters and mediators in the human body.

135

Impact of sphingosine-1-phosphate (S1P) and its receptors on thrombin formation

C. Tolksdorf[1,2,3], C. Heise[2], C. Joseph[2], B. H. Rauch[1,3]
[1]Carl von Ossietzky University of Oldenburg, Department of Human Medicine, Section of Pharmacology and Toxicology, Oldenburg, Germany
[2]University Medicine Greifswald, Department of General Pharmacology, Greifswald, Germany
[3]DZHK (German Centre for Cardiovascular Research), Partner site Greifswald , Greifswald, Germany

Background: Thrombocytes and leukocytes play a key role in inflammatory processes and in the development of arteriosclerotic lesions. In earlier studies, we have identified sphingosine-1-phosphate (S1P) as a mediator between inflammation and blood coagulation processes. S1P elevates Tissue Factor (TF) and thrombin receptor expression in immune cells. The signaling lipid exerts its effects via five G-coupled receptors (S1PRs 1-5). While thrombin stimulates platelet-derived S1P secretion, it's unknown whether S1P in return also regulates local thrombin formation, i.e., by upregulating TF expression in monocytes. Therefore, the aim of this study was to determine the expression of S1PRs and the impact of S1P and S1PR-agonists on thrombin formation in macrophages.

Methods: Human leukemia monocytic cells (THP1-cells) were differentiated using PMA into macrophage-like cells (dTHP1). mRNA expression levels of S1PRs 1-5 were determined. Adherent dTHP1-cells were stimulated with various S1P and S1PR-agonist concentrations for 1-24 h. Cells were harvested and lysed for incubation with human plasma samples to initiate thrombin formation. Endogenous thrombin generation was quantified by calibrated automated thrombography (CAT).

Results: In dTHP1 cells, S1PR2 mRNA was markedly upregulated compared to THP1 cells. The mRNA levels of other S1PRs were not significantly altered, the mean S1PR4 and -5 mRNA expression was reduced. Incubation of dTHP1 cells with S1P over time (0-24 h) resulted in a differential modulation of thrombin generation. At 1 µM, S1P only marginally accelerated thrombin formation (at 1-6 h). Only the S1PR5 agonist A971432 (1 µM) shortened the lag time significantly. At 3 µM, S1P significantly shortened both lag time and time to peak and increased the velocity of thrombin formation. S1PR2, -3 and -5 agonists had only minor and transient effects on thrombin generation. At 10 µM, S1P did not markedly modify thrombin formation. In comparison, S1PR1, -3 and -4 agonists (10 µM, respectively) did elevate the lag time of thrombin formation.

Conclusions: S1P concentrations of 1-3 µM can modulate thrombin formation at dTHP1-cells *in vitro*. Accelerated thrombin formation may be mediated via S1PR2 and -5, while agonists for S1PR3 and -4 delayed the onset of thrombin generation. This observation points towards a differential role of S1P and its receptors in regulating the thrombogenicity of tissues during inflammatory processes such as cardiovascular diseases.

149

RAMP gets a new role: modulation of GPCR activation

K. Nemec[1], H. Schihada[2], G. Kleinau[3], U. Zabel[4], E. O. Grushevskyi[1], P. Scheerer[3], M. Lohse[1,4,5], I. Maiellaro[6]
[1]Max Delbrück Centre for Molecular Medicine, Berlin, Germany
[2]Karolinska institutet, Section of Receptor Biology & Signaling, Stockholm, Sweden
[3]Charité - Universitätsmedizin Berlin, corporate member of Freie Universität Berlin, and Humboldt-Universität zu Berlin, Institute of Medical Physics and Biophysics, Group Protein X-ray Crystallography and Signal Transduction, Berlin, Germany
[4]University of Würzburg, Institute of Pharmacology, Würzburg, Germany
[5]ISAR Bioscience, München, Germany
[6]University of Nottingham, School of Life Sciences, Queen's Medical Centre, Nottingham, United Kingdom

Introduction: Receptor-activity-modifying proteins (RAMPs) are ubiquitously expressed membrane proteins that associate with different G protein-coupled receptors (GPCRs)[1] including the parathyroid hormone 1 receptor (PTH1R), a class B GPCR, and an important modulator of mineral ion homeostasis and bone metabolism[2].

Objectives: However, it is unknown whether and how RAMP proteins may affect PTH1R function.

Materials & methods: Using a set of revised optical biosensors[3-5], we measure the activation of PTH1R and its downstream signaling. In addition, we employ structural homology modeling to describe the mechanistic details responsible for altered PTH1R functionality.

Results: We describe that RAMP2 acts as a specific allosteric modulator of PTH1R, shifting PTH1R to a unique pre-activated state that permits faster activation in a ligand-specific manner. Moreover, RAMP2 modulates PTH1R downstream signaling in an agonist-dependent manner, most notably increasing the PTH-mediated Gi3 signaling sensitivity. Additionally, RAMP2 increases both PTH- and PTHrP-triggered β-arrestin2 recruitment to PTH1R. Finally, we present a structural homology model to describe the molecular mechanism underlying our functional findings.

Conclusion: These data uncover a critical role of RAMPs in the activation and signaling of a GPCR. That may provide a new venue for highly specific modulation of GPCR function and advanced drug design.

1. Serafin, D. S., Harris, N. R., Nielsen, N. R., Mackie, D. I., & Caron, K. M. (2020). Dawn of a new RAMPage. *Trends in pharmacological sciences*, **41**(4), 249-265.
2. Cheloha, R. W., Gellman, S. H., Vilardaga, J. P., & Gardella, T. J. (2015) PTH receptor-1 signalling—mechanistic insights and therapeutic prospects. *Nature Reviews Endocrinology*, **11**(12), 712.
3. Vilardaga, J. P., Bünemann, M., Krasel, C., Castro, M., & Lohse, M. J. (2003) Measurement of the millisecond activation switch of G protein–coupled receptors in living cells. *Nature biotechnology*, **21** (7), 807-812.
4. Patriarchi, T., Cho, J. R., Merten, K., Howe, M. W., Marley, A., Xiong, W. H., ... & Zhong, H. (2018) Ultrafast neuronal imaging of dopamine dynamics with designed genetically encoded sensors. *Science*, ***360*** (6396).
5. Schihada, H., Vandenabeele, S., Zabel, U., Frank, M., Lohse, M. J., & Maiellaro, I. (2018) A universal bioluminescence resonance energy transfer sensor design enables high-sensitivity screening of GPCR activation dynamics. *Communications biology*, **1**(1), 1-8.

Fig. 1

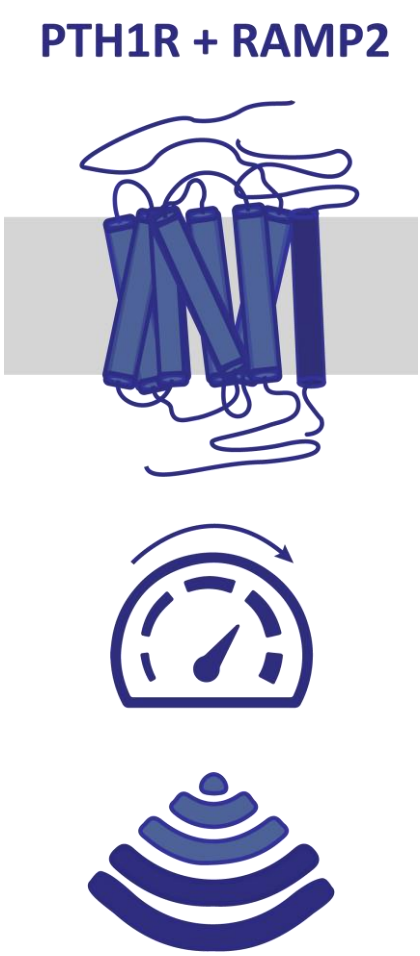

164

Heterodimerization of AT_1R and β_2AR increases AT_1R signaling leading to enhanced aldosterone synthesis

J. Fender[1], V. Boivin-Jahns[1], K. Lorenz[1,2]
[1]Universität Würzburg, Institut für Pharmakologie und Toxikologie, Würzburg, Germany
[2]Leibniz-Institut für Analytische Wissenschaften—ISAS e.V., Dortmund, Germany

Background: G-protein-coupled receptor (GPCR) signaling is of significant relevance for cardiac performance and homeostasis. Angiotensin II type 1 receptors (AT_1R) and β-adrenergic receptors (βAR) are activated under neurohumoral stress conditions and they are common drug targets in e.g. hypertension, acute and chronic heart failure or asthma therapy.

Objective: Since their functional interconnection may be of (patho)physiological relevance and a crosstalk between these receptors has been suggested, we aimed to investigate a potential crosstalk between these two GPCRs and its physiological consequences.

Methods and Results: A Bioluminescence resonance energy transfer (BRET)-based donor saturation assay suggests an hetero-dimerization between AT_1R and β_2AR under baseline conditions, while AT_1R stimulation led to a decreased BRET signal indicating a reorganization of the receptors. Moreover, coactivation of both receptors significantly potentiated the recruitment of βarrestin-1 and 2 to the AT_1R compared to AT_1R stimulation alone, indicating that βarrestin binding to the AT_1R is regulated by β_2AR coactivation. An increased recruitment of βarr to the β_2AR after coactivation was not observed. To investigate the physiological consequences of this crosstalk we used human adrenocortical cells capable of aldosterone synthesis and evaluated the mRNA levels of genes involved in the angiotensin II-dependent aldosterone synthesis. Indeed, expression levels of steroidogenic acute regulatory (StAR) protein and aldosterone synthase (CYP11B2) mRNA were potentiated by co-stimulation of βAR and AT_1R.

Conclusion: Our results strongly indicate a crosstalk between the AT_1R and β_2AR resulting from an hetero-dimerization. Coactivation of both GPCRs increased the AT_1R signaling in terms of βarrestin recruitment, which could be the key modulator leading to an enhanced secretion of aldosterone, a well-known cardiotoxic hormone. This could be particularly detrimental in chronic heart failure as circulating concentrations of both catecholamines and angiotensin II are highly increased.

172

GRK4 regulates cilia and kidney function independent of its kinase activity

J. Gerhards[1], L. Maerz[2], E. Matthees[3], C. Donow[2], B. Moepps[2], R. Premont[4,5], C. Hoffmann[3], M. Burkhalter[1], **M. Philipp**[1]
[1]University Hospital of Tübingen, Pharmacogenomics, Tübingen, Germany
[2]Ulm University, Ulm, Germany
[3]University Hospital Jena, Institute for Molecular Cell Biology, Jena, Germany
[4]Duke University Medical Center, Department of Medicine, Durham, United States
[5]University Hospitals Cleveland Medical Center, Harrington Discovery Institute, Cleveland, United States

Introduction: G protein-coupled receptor kinase 4 (GRK4) regulates sodium reabsorption and subsequent water retention in the kidney. In the presence of certain genetic variants of GRK4 sodium is excreted to a lesser extent causing a rise in blood pressure. Biochemical evaluation of these variants revealed elevated kinase activity towards G protein-coupled receptors.

Objectives: We aimed to investigate the function of GRK4 and its genetic variants in greater detail.

Materials & methods: We established loss-of-function models of GRK4 in zebrafish and in human cells and performed rescue experiments using mutated versions of GRK4.

Results: Loss of GRK4 produces kidney dysfunction in zebrafish embryos. Glomerular filtration is impaired, water retention is increased and patterning of the pronephric tubules is disturbed. Cilia within the developing kidney are more abundant and elongated and kidney cysts develop. Human fibroblasts depleted of GRK4 extend similarly longer, dysfunctional cilia. Interestingly, while hypertension-associated variants of GRK4 were unable to rescue the zebrafish and cilia phenotypes, kinase-dead GRK4 was capable of restoring normal cilium length. Treatment with the mTOR inhibitor rapamycin, however, partially rescued the phenotypes. Knockout of GRK4 in HEK cells revealed higher mTOR pathway activity. Co-IP experiments suggest that GRK4 modulates mTOR signaling by direct interaction with mTOR.

Conclusion: We provide evidence that GRK4 regulates kidney development and function independent of its kinase activity.

176

Effects of the FXa-Receptor PAR2 (Protease Activated Receptor 2) on the progression of colorectal cancer

U. Meyer[1], S. Polster[2], S. Grammbauer[3], C. Ritter[4], F. Dombrowski[3], B. H. Rauch[1]
[1]Carl von Ossietzky Universität Oldenburg , Pharmakologie, Oldenburg, Germany
[2]Universität Greifswald, allgemeine Pharmakologie, Greifswald, Germany
[3]Universität Greifswald, Pathologie, Greifswald, Germany
[4]Universität Greifswald, klinische Pharmazie, Greifswald, Germany

Question: Every year an average of 31.500 new cases of colorectal cancer are diagnosed in Germany. The absolute 5-year-survival rate is 52%.A known complication of cancer is the occurrence of venous and thromboembolic vascular occlusions triggered by increased coagulation activity. In addition to thrombin, an important factor in the coagulation cascade is the activated FX (FXa) whose cellular functions are mediated via PAR2. The aim of the present study was therefore to investigate the influence of the protease activated receptor 2 (PAR2) on the progression of colon cancer in vitro and in vivo.

Method: The effects of FXa and PAR2 on different colon cancer cell lines were investigated in vitro. Then Wild type C57bl/6 mice and PAR2 knockout (PAR2-ko) mice of the same background were s.c. injected with murine colorectal carcinoma cells and tumor growth was observed for 21 days. In addition, the influence of a direct FXa inhibitor Apixaban on the progression of colorectal cancer was investigated. At the end of the study, tumor and organs were removed and analyzed histologically and molecularly.All animal experiments were approved by the responsible animal welfare committee.

Results: FXa directly affects migration and proliferation of human and murine colorectal cancer cells (CRC cells) in vitro. The interaction of FXa and PAR2 could be mimicked by using PAR2 activating peptide. Western blot analysis showed increased activity of p44 /42, p38 and AKT signaling in these cells.

In vivo PAR2 knockout not only resulted in a lower tumor volume in the mice but also significantly reduced tumor weight compared to WT mice. The occurrence of various complications also occurred less frequently in PAR2 mice during the experiment. No differences could be determined histologically. Interestingly, spleen size was larger in relation to body weight in PAR2-ko mice compared to WT mice. The use of Apixaban has no effect on the progression of colorectal cancer in this study.

Conclusion: FXa directly influences migration and proliferation of various CRC cells. A connection with the activation of PAR2 could be shown in vitro. This cannot be demonstrated in vivo when using the direct FXa inhibitor Apixaban. Whether insufficient drug dose or bioavailability could be the cause has yet to be finally clarified. However, the knockout of PAR2 shows positive effects on the progression of colon cancer and represents a possible new therapeutic starting point in the future.

199

Differential signalling of endothelial B2 receptors in small blood vessels and aorta

S. Metry*[1,2], M. Krybus[1], O. Kocgirli[1], T. Suvorava*[1], G. Kojda[1]
[1]Institute of Pharmacology and Clinical Pharmacology, Heinrich-Heine-University, Düsseldorf, Germany
[2]Clinical pharmacy department, Faculty of Pharmacy, Ain Shams University, Cairo, Egypt

Introduction: The kallikrein-kinin system has been explored over many years with a special focus on the cardiovascular effects of B_2 receptors. However, still a lot about B_2-receptor related signalling pathways remains unknown. To study the role of endothelial B_2-receptor signalling in cardiovascular system, a new transgenic mouse model characterized by overexpression of the B_2 receptor (B_2^{tg}) in vascular endothelium was generated. In these mice, overexpression of endothelial B_2 reversed the vasoconstrictor effect of bradykinin to B_2-mediated, endothelium- and NO-synthase-dependent aortic relaxation suggesting the changes of vascular BK-signalling cascade to the favour of NO.

Objectives: The aim of the study was to evaluate the effect of endothelial overexpression of B_2 on aortic reactivity to acetylcholine, phenylephrine and the NO-donor diethylamine NONOate (DEA/NO) and the endothelial NO-synthase (eNOS) protein expression in aorta and skeletal muscle.

Materials & Methods: eNOS protein levels were assessed in aortic and skeletal muscle lysates by western blot. Thoracic aortic rings were used for vascular reactivity studies. In some experiments, N^{ω}-nitro-L-arginine methyl ester (L-NAME, 100µM) was applied to inhibit the activity of NOS. Statistical analysis of western blot data was done by unpaired t-test and vascular reactivity studies data was done by two-way ANOVA.

Results: B_2^{tg} showed no increase of eNOS expression in the resistance arteries as shown in skeletal muscle of B_2^{tg} (98.2±24.5%) and their transgene-negative littermates (B_2^{n}, 100.0±16.2%, n=6, n.s.). In contrast, there was a significant decrease of eNOS protein level in aorta of B_2^{tg} (62.3±13.4%) as compared to B_2^{n} (100.0±11.0%, n=8, P=0.046). Endothelial overexpression of B_2 had no effect on the acetylcholine-induced relaxation (87.0±3.0% vs 84.7±2.3% in B_2^{tg} and B_2^{n} respectively, n=8, n.s.) and NO-dependent aortic dilation in B_2^{tg} (pEC_{50}=6.9±0.1) and B_2^{n} (7.0±0.1, n=3, n.s.). Likewise, neither pEC_{50} values for phenylephrine in B_2^{tg} (6.7±0.2) and B_2^{n} (6.6±0.1), nor the maximally inducible vasoconstrictions were different (76.3±11.2 and 73.4±8.2, n=4, n.s.). Inhibition of NOS by L-NAME completely abolished relaxation to acetylcholine in B_2^{tg} (2.4±5.3%) and to the same extent in B_2^{n} (-6.3±2.8, n=5, n.s.).

Conclusion: The endothelial overexpression of B_2 receptors does not affect the endothelium- and NO-dependent relaxation and phenylephrine constriction in murine aorta.

217

Tuning GPCR allostery by directed evolution

C. Klenk[1], A. Niederer[1], M. Scrivens[2], E. Smith[2], M. Zauderer[2], A. Plückthun[1]
[1]University of Zurich, Department of Biochemistry, Zurich, Switzerland
[2]Vaccinex Inc., Rochester, United States

GPCRs represent the largest family of membrane proteins that receive external stimuli and allosterically transduce these stimuli across the membrane to initiate intracellular signaling pathways. Signal transduction involves a few highly conserved allosteric sites that undergo structural changes triggering receptor activation. How these conserved microswitches are physically connected throughout the receptor structure and define the allosteric pathways that control selective signal transductions remains poorly understood, thus hampering the understanding of receptor function and the development of new drugs.

Here we present a novel approach to evolve GPCRs in mammalian cells. Using a rational DNA library design in combination with a highly efficient viral transduction system in a mammalian cell surface display system, we were able to evolve parathyroid hormone 1 receptor with two distinct ligands. By maintaining the physiological cellular signaling environment, our approach fully functional receptor variants that exhibit increased ligand affinity and coupling efficacy to G proteins, suggesting a shift of the conformational equilibrium towards the active state. Sequence analysis of these receptor variants revealed a number of different mutation hotspots which may represent important allosteric coupling sites for long-distance communication required for efficient signal transduction.

247

Determination of Differential GRK Isoform Protein Levels by Simple Tag-Guided Analysis of Relative Protein Abundance (STARPA)

M. Reichel[1], V. Weitzel[1], L. Klement[1], C. Hoffmann[1], J. Drube[1]
[1]University Clinic Jena, Molecular Cell Biology, Jena, Germany

Introduction: Activated G protein-coupled receptors (GPCRs) are phosphorylated by GPCR kinases (GRKs) at intracellular domains. This phosphorylation leads to the recruitment of arrestins and mediates desensitization and internalization of GPCRs. Increasing evidence suggests differential roles of the GRK isoforms on GPCR signaling. As GRK expression is altered in many pathological conditions, determination of the different GRK isoform levels is the key to understand their role in aberrant cellular signaling. MRNA expression does not necessarily coincide with resulting protein levels. However, analysis of protein levels via western blot, faces issues regarding the comparison of different proteins detected by different antibodies.

Objectives: Establishing a cost-effective method to determine gene expression at the protein level and investigate differential protein abundance of GRK isoforms in commonly used cell lines.

Material & Methods:

STARPA implementation (Fig. 1): HEK293 GRK2/3/5/6 knockout cells (Drube *et al.* 2021, https://doi.org/g763) were transfected with HA-tagged GRK expression plasmids. Lysates were diluted using 1X sample buffer to achieve equimolar amounts of the respective HA-tagged GRK isoforms and confirmed via western blot analysis.

STARPA application (Fig. 1): HA-GRK protein standards together with cell lysates of HEK293, HeLa, HepG2, Jurkat, K562, MCF-7, Molm13, U20S and U-251 cells were analyzed with GRK specific antibodies as well as anti HA-antibody. The cell line signals obtained from incubation with GRK specific antibodies were divided by the signal with the GRK specific antibody of the respective standard, resulting in the relative GRK expression pattern of the analyzed cell lines.

Results: STARPA was established to determine GRK isoform protein levels. The relative expression levels of GRK2/3/5/6 were further analyzed in nine commonly used cell lines. While GRK2 was the most abundant isoform in all cell lines, protein levels of GRK3, 5, and 6 demonstrated high variation. Detected GRK protein levels did not match mRNA expression levels.

Conclusion: STARPA is a cost-effective method to determine and compare the relative expression levels of different proteins. Analysis of nine commonly used cell lines demonstrates differential expression of GRK isoforms. The deviation between mRNA and protein expression of the GRK isoforms highlights the importance of protein level determination.

Fig. 1

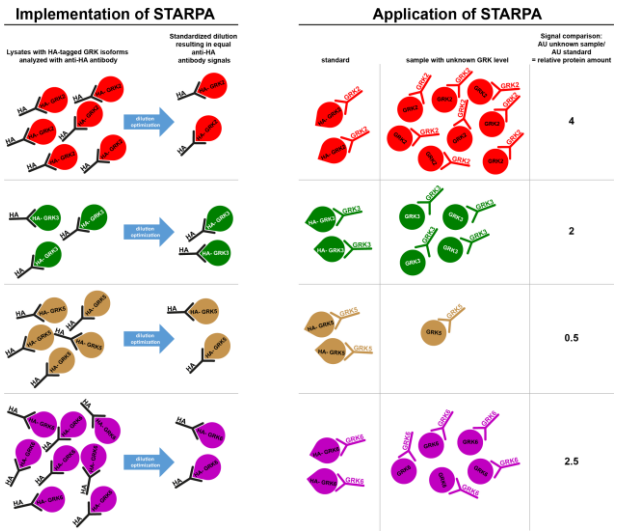

248

The C-terminus is not enough — Deciphering GRK-mediated β-arrestin interaction with the β2-adrenoceptor, the vasopressin V2R, and their chimeras β2V2 and V2β2

E. Matthees[1], R. Haider[1], L. Klement[1], V. Weitzel[1], E. Miess-Tanneberg[2], S. Schulz[2], J. Drube[1], C. Hoffmann[1]
[1]University Clinic Jena, Molecular Cell Biology, Jena, Germany
[2]University Clinic Jena, Pharmacology & Toxicology, Jena, Germany

Introduction: G protein-coupled receptors (GPCRs) form the largest group of human transmembrane receptors and are pharmacologically targeted to treat a multitude of pathophysiological conditions. β-arrestins are prominent GPCR binding proteins and have been shown to modify receptor signaling, internalization and trafficking. GPCR—β-arrestin complexes are formed by β-arrestins associating with the phosphorylated receptor C-terminus and possibly also the receptor core. The resulting complex configurations might lead to different signaling outcomes. However, the importance of specific receptor domains and the roles of individual GPCR kinases (GRKs) in this process remain elusive.

Objectives: Here, we investigate the role of the GPCR transmembrane helix bundle and C-terminus in GRK-specific β-arrestin interaction and differential signaling outcomes by comparing the β2-adrenoceptor (β2AR), the Vasopressin V2R, and their chimeras β2V2 and V2β2, consisting of the β2AR core and the V2R C-terminus and vice versa.

Materials & methods: Utilizing our generated quadruple knockout HEK293 cell line lacking GRK2, 3, 5, and 6, we designed NanoBRET-based *in cellulo* β-arrestin recruitment and conformational change assays to assess the GRK-specific functionality of GPCRs without endogenous background. We investigated GRK-specific internalization of the two GPCRs and their chimeras in living cells by using confocal microscopy.

Results: Our data show that the β2AR is targeted by all ubiquitously expressed GRKs, leading to comparable recruitment of β-arrestin2. In contrast to these findings, for the V2R we observed a pre-coupled complex with arrestin in the absence of agonist, mediated by the overexpression of each GRK. Interestingly, no pre-coupling was observed for either of the receptor chimeras. A schematic overview of GRK-specific recruitment is shown in Figure 1. We additionally correlate these findings with GRK-specific conformational change fingerprints of β-arrestins coupling to these receptors and measurements of receptor internalization.

Conclusion: The GPCR core and C-terminus differentially contribute to the interaction with and specificity for distinct GRK isoforms. This becomes evident, as the comparison of β-arrestin2 recruitment revealed clear differences between the parental receptors and their chimeras. Hence, the C-terminus alone is not sufficient to determine specificity in β-arrestin interaction and downstream receptor signaling.

Fig. 1

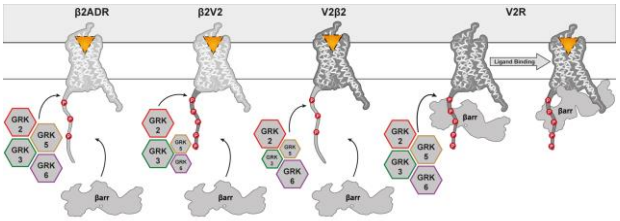

251

β-arrestin1 and 2 exhibit distinct phosphorylation-dependent conformations when coupling to the same GPCR

R. S. Haider[1], E. S. F. Matthees[1], J. Drube[1], M. Reichel[1], A. Inoue[2], C. Krasel[3], C. Hoffmann[1]
[1]Universitätsklinikum Jena, Molecular Cell Biology, Jena, Germany
[2]Tohoku University, Pharmaceutical Sciences, Sendai, Japan
[3]Philipps-Universität Marburg, Institut für Pharmakologie und Klinische Pharmazie, Marburg, Germany

Introduction: β-arrestin1 and 2 are hypothesised to mediate targeted processes for more than 800 different G protein-coupled receptors (GPCRs). They have been shown to act as important regulators of GPCR signaling, internalization, and trafficking. To facilitate this, the Individual β-arrestin isoforms have been shown to adopt different active conformations resulting from the geometry of the specific GPCR–β-arrestin complex.

Objectives: Whether β-arrestin1 and 2 respond differently upon binding to the same GPCR is still unknown. The aim of the study was to compare the complex configurations of β-arrestin1 and 2 for binding to the parathyroid hormone 1 receptor (PTH1R), including the assessment of β-arrestin conformational changes and their initial downstream functionality.

Materials & methods: With advanced NanoLuc/FlAsH-based β-arrestin1 and 2 biosensors we reveal the comprehensive signature of conformational changes for both isoforms when bound to the PTH1R. Further, we repeated these measurements in the absence of GPCR kinases (GRKs) and with two distinct phosphorylation-deficient variants of the receptor. Additionally, we use live-cell confocal micrsocopy and various knockout cell lines to characterize formed complexes.

Results: We provide evidence that β-arrestin1 prefers the formation of "hanging" GPCR complexes, in contrast to β-arrestin2, which makes extensive use of the "core" binding interface. Resulting from this, we found differences in conformational changes between β-arrestin1 and 2 in multiple positions, especially within their phosphorylation-sensing N-domains. After the assessment of two phosphorylation-deficient PTH1R variants and β-arrestin conformational changes induced in the absence of GRKs, it becomes evident that β-arrestin2 is less dependent on C-terminal GPCR phosphorylation to adopt active-like conformations, in contrast to β-arrestin1. Interestingly, proximal receptor phosphorylation has a lower impact on β-arrestin1 conformational changes, as these interaction sites mostly stabilize the less preferred "core" complex. In line with this, we show that exclusively β-arrestin1 is able to drive receptor internalization in a "hanging" configuration.

Conclusion: With this study we demonstrate that the GPCR phosphorylation state not only regulates differences in affinity between β-arrestin1 and 2 but also translates into specific conformational rearrangements that determine the functional diversity between the two isoforms.

Fig. 1

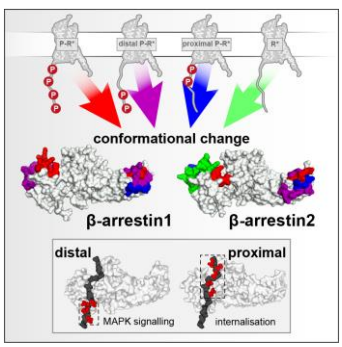

269

GRK2/3/5/6 knockout cells: New tools to investigate impact of individual GRKs on arrestin binding and GPCR regulation

J. Drube[1], R. S. Haider[1], E. S. F. Matthees[1], M. Reichel[1], C. Hoffmann[1]
[1]Universitätsklinikum Jena, Friedrich-Schiller-Universität Jena, Institut für Molekulare Zellbiologie, Jena, Germany

Introduction: G protein-coupled receptors (GPCRs) constitute the largest family of membrane receptors and are established targets for pharmacological intervention. The seven GPCR kinases (GRKs) GRK1-7 are differentially expressed in the human body, with GRK 2, 3, 5, and 6 being described as ubiquitously expressed in the non-visual system. They phosphorylate the GPCRs on their intracellular compartments and facilitate the binding of arrestins. The dysregulation of GRK expression or activity was reported in different pathological conditions e.g. cancer, influenza infection, malaria, and metabolic disease.

Objectives:

1. Establishment of GRK knockout (KO) HEK293 cell clones

2. Study the impact of GRKs on β-arrestin recruitment to GPCRs

3. Set up a GRK inhibitor screening assay

Methods: A panel of combinatorial GRK 2, 3, 5, and 6 HEK293 knockout cell clones was established using the CRISPR/Cas9 technology. We created all single KOs (ΔGRK2, ΔGRK3, ΔGRK5, ΔGRK6), all possible combinations of double KOs (ΔGRK2/3, ΔGRK5/6, ΔGRK2/5, ΔGRK2/6, ΔGRK3/5, ΔGRK3/6), triple GRK KOs (ΔGRK3/5/6, ΔGRK2/5/6, ΔGRK2/3/6, ΔGRK2/3/5), and a quadruple KO of GRK2, 3, 5, and 6 (ΔQ-GRK). We investigated the β-arrestin recruitment to selected GPCRs using these cell clones with or without overexpression of GRKs. To do so, we used a plate-reader based bioluminescence resonance energy transfer (BRET) assay to measure the recruitment and carry out the GRK inhibitor screening.

Results: We successfully established and characterized the GRK KO cell clones. Measurements with selected GPCRs revealed that β-arrestin recruitment can be facilitated for some GPCRs by overexpression of any tested GRK or by overexpression of GRK2 or 3 only. We did not identify GPCRs for which the β-arrestin interaction is mediated exclusively by GRK5 or 6.

Moreover, a GRK inhibitor screening assay was set up using ΔQ-GRK. We validated our platform by testing the selectivity of cmpd101. We observed a recruitment reduction in presence of GRK2 and 3, but not in case of GRK5 or 6. This confirmed the GRK2/3 selectivity of cmpd101.

Conclusion: Our GRK KO cell clones allow the analysis of GRK specific processes without the interference of residual GRK expression. The cells can be used to reintroduce wild type or mutant GRKs to study their behavior.

The established GRK inhibitor screening platform can be used for high-throughput screening of GRK2, 3, 5, 6 selectivity in living cells.

273

New insights into the role of Gi-proteins, GRKs and beta-arrestins on adenosine A1 receptor internalization

A. Godbole[1], P. A. Handreg[1], J. Drube[1], C. Hoffmann[1]
[1]University Hospital Jena, Institute for Molecular Cell Biology, Jena, Germany

Question: The Gi-coupled adenosine A1 receptor is ubiquitously expressed in the human body, and together with its natural agonist adenosine, has been implemented in inflammation and ischemic attacks. Adenosine can produce autocrine and paracrine effects, and the level of adenosine in interstitial tissue space is often a warning sign for inflammation.

Regulation of this adenosine-dependent Gi-dependent signaling is brought about by degradation or transport of extracellular adenosine. However, mechanisms of regulating the receptor itself by GRK-mediated phosphorylation and arrestin recruitment followed by receptor internalization have been poorly investigated due to lack of appropriate cell models.

Results: As a first step to characterizing internalization, we show that adenosine A1 receptors stably expressed in wild-type HEK293 cells undergo significant caveolae-dependent and dynamin-dependent internalization into early endosomes marked by Rab5 under 30 minutes. Surprisingly, we found significant internalization of the receptor in cells lacking Gi-alpha subunit (cells provided by Asuka Inoue) over wild-type HEK293 cells, suggesting that Gi-protein activation may not be a pre-requisite for receptor internalization.

Next, we investigated interaction between NanoLuc-tagged receptor and Halo-tagged beta-arrestins mediated by specific GRKs in GRK KO HEK293 cells (created in-house by Julia Drube) rescued by individual GRK overexpression. Firstly, our data suggests arrestin cannot interact with the receptor in the absence of GRKs. Secondly, no individual GRK overexpression can enhance arrestin recruitment to the receptor over its endogenous level and GRK2 showed the most reliable concentration-response curve.

Downstream of arrestin interaction, our data suggests that receptor internalization is beta-arrestin2- and GRK- dependent and the receptor does not co-internalize with beta-arrestin2. Rather, we found arrestin clusters on plasma membrane and could not detect presence of receptors in these clusters.

Outlook: Currently, we are investigating the role of serine in the third intracellular loop of the receptor on arrestin interaction (using alanine mutants), role of GRK4 (since both GRK4 and adenosine A1 are exclusively co-expressed in the testis), mechanism of arrestin interaction with adenosine A1 (using arrestin finger-loop deletion mutant), and finally arrestin clustering on the plasma membrane (by using bystander BRET between arrestin and CAAX domain).

Pharmacology – Receptor tyrosine kinases

30

Role of Bruton's tyrosine kinase in imatinib resistant chronic myeloid leukemia cells

L. Schmidlechner[1], S. Sebens[2], I. Vater[3], I. Nagel[1,3], I. Cascorbi[1], M. Kaehler[1]
[1]Institute of Experimental and Clinical Pharmacology, USKH Kiel, Kiel, Germany
[2]Institute of Experimental Cancer Research, UKSH, Kiel, Germany
[3]Institute of Human Genetics, UKSH, Kiel, Germany

Question: Targeting the Bruton's tyrosine kinase (BTK) by the tyrosine kinase inhibitor (TKI) ibrutinib is known as a promising target for B-cell malignancies. However, the role of BTK in other hematopoietic diseases remains unclear. Chronic myeloid leukemia (CML) can be successfully treated with TKIs, such as imatinib. Nevertheless, therapeutic resistances remain a clinical problem. Analysis of a imatinib-resistant K562 cell line, an in vitro CML model, revealed two de novo-*BTK* mutations namely c.G1699A and c.A1700G, potentially resulting in a double mutation. Additionally, there was a downregulation of *BTK* mRNA expression. Thus, the role of *BTK* and its mutations in imatinib-resistance were analyzed.

Material and Methods: *BTK* expression was analyzed via RT-qPCR and immunoblotting. BTK-downregulation was examined using stealth siRNAs; plasmid transfection by nucleofection. Cellular fitness was analyzed on the level of total cell number by trypan blue stain and colony forming assays, proliferation via Ki67 expression and cell cycle analyses, cell viability using WST-1 and apoptosis via Poly ADP-ribose Polymerase (PARP) immunoblotting. The effect of 25-1000 nM ibrutinib was analyzed by WST-1 assay on sensitive and imatinib-resistant cells.

Results: *BTK* mRNA expression was 5-fold downregulated in 2 µM imatinib-resistant cells compared to TKI-naïve ones ($p<0.001$). Inhibition of *BTK* through ibrutinib led to an abrogated impact of imatinib on native cells. SiRNA-mediated *BTK*-downregulation promoted imatinib-resistance (cell viability $p=0.003$; total cell number $p<0.001$; proliferation $p<0.001$). Restoration of *BTK* expression in imatinib-resistant cells reinstated susceptibility to this TKI (cell viability $p=0.003$; total cell number $p=0.02$; proliferation $p=0.006$). Regarding the mutations on the impact on imatinib susceptibility, c.G1699A showed the highest increase in cell viability ($p<0.001$) and proliferation ($p=0.004$) compared to *BTK* wild-type. In the case of double-mutations, similar results for c.G1699A were observed, whereas the impact of c.A1700G on *BTK* function seems minor.

Conclusion: We showed that *BTK* expression in imatinib-resistant cell lines led to restoration of TKI susceptibility, while loss of *BTK* promotes imatinib-resistance. The single mutation c.G1699A has the same abrogating impact on imatinib sensitivity as the double mutation. These findings might offer a potential perspective of considering ibrutinib usage in CML-treatment.

156

Resistance mechanisms circumventing the inhibition of IGF signaling in neuroblastoma cells

N. S. Pommert[1], I. Cascorbi[1], **V. Waetzig**[1]
[1]University Medical Center Schleswig-Holstein, Institute of Experimental and Clinical Pharmacology, Kiel, Germany

Question: The insulin-like growth factor (IGF) pathway has been implicated in many aspects of tumorigenesis and metastasis of multiple malignancies including neuroblastoma. The heterogeneous biological background of neuroblastoma cells has prevented the implementation of a specific oncological therapy, which also applies to selective inhibition of IGF-mediated signaling.

Material and methods: To understand how resistance is formed and may be prevented, we compared two neuroblastoma cell lines (SH-SY5Y and Kelly), which substantially differed in autocrine IGF2 production and its signaling. The cells were treated with linsitinib, an inhibitor of the IGF receptor 1 (IGFR1) and the insulin

receptor (IR), for up to 10 days, either under normal growth conditions or serum-deprived. We determined viability, proliferation and apoptosis. Additionally, IGF2-mediated survival signaling as well as IGFR1 regulation and IGF2 release were characterized.

Results: Application of linsitinib significantly ($p<0.001$), but only transiently reduced proliferation, so that both cell lines were able to adapt and sustain a pool of resistant cells. Under normal growth conditions, linsitinib treatment increased IGFR1 protein expression, but did not alter endogenous IGF2 levels. In contrast, serum deprivation of the IGF2-driven Kelly cells reduced the amount of IGFR1 protein, while IGF2 production remained stable. In this setting with reduced IGFR1 levels and without additional serum growth factors, the application of linsitinib significantly ($p<0.001$) and permanently reduced survival. In SH-SY5Y cells, which feature low autocrine IGF2 levels, serum deprivation reduced the amount of IGFR1 protein and further attenuated IGF2 production ($p<0.001$). Nevertheless, SH-SY5Y cells, which were resistant against linistinib exposure, developed under these conditions. In order to prevent the formation of resistant cells in both cell lines and under any growth condition, it was necessary to apply an inhibitor with higher affinity to IGFR1 and IR like BMS-754807 or inhibit more than one growth factor pathway.

Conclusion: As even neuroblastoma cell lines could easily and rapidly induce mechanisms to overcome selective IGFR1 inhibition regardless of their autocrine IGF2 production, it is not an option for monotherapy. Still, blocking IGF signaling might be helpful as a sensitizing effect, especially using inhibitors with higher affinity to IGFR1 or a wider target range of growth factor receptors.

Pharmacology – Signal transduction and second messengers

37

Cardiac-specific overexpression of PP2A-PR72 results in reduced force of contraction but enhanced β-adrenergic response

J. R. Herting[1,2], U. Kirchhefer[1,2]
[1]Münster University Hospital (UKM), Pharmacology and Toxicology, Münster, Germany
[2]University of Münster (WWU), Pharmacology and Toxicology, Münster, Germany

Question: PP2A-PR72 is a cytosolic, Ca^{2+}-binding protein, mainly expressed in myocardium. As a regulatory subunit of protein phosphatase 2A (PP2A), PR72 forms a heterotrimeric enzyme together with a catalytic C and structural A subunit. It has been suggested that PR72 regulates activity and targeting of PP2A. But only few is known about cardiac function of PR72-PP2A.

Methods: For this purpose, we overexpressed PP2A-PR72 in transgenic mouse hearts under control of the αMHC promoter (TG). We examined protein expression levels by Western blotting and measured contractile parameters of isolated atria under basal conditions and increasing doses of isoprenaline (ISO). Left atria were electrically stimulated at 1 Hz, right atria remained unstimulated.

Results: The total protein content of PP2A-PR72 was elevated by about 3-fold in homogenates of TG hearts and the catalytic PP2A subunit by 1.2-fold, while reference protein calsequestrin remained unchanged. Under basal conditions, isolated left atria of TG vs. wild type (WT) mice exhibited reduced force of contraction (amplitude: 1.7 ± 0.3 mN vs. 3.6 ± 0.5 mN, respectively, n = 7-8, $P<0.01$) and diminished contraction speed (maximum rise slope: 0.11 ± 0.02 mN/ms vs. 0.24 ± 0.03 mN/ms, respectively, n = 7-8, $P<0.01$). In addition, relaxation time (t_{90}: 34.9 ± 1.2 ms vs. 39.7 ± 1.3 ms, respectively, n = 7-8, $P<0.05$) and relaxation velocity (maximum decay slope: -0.08 ± 0.01 mN/ms vs. -0.15 ± 0.02 mN/ms, respectively, n = 7-8, $P<0.01$) were reduced in TG vs. WT atria. Basal heart rate of isolated right atria was unchanged between groups. Under β-adrenergic stimulation, isolated left atria of TG and WT mice showed a comparable maximum response (10^{-5} M ISO) regarding force of contraction, contraction velocity and relaxation velocity. In contrast, relaxation time remained lower in TG vs. WT atria (t_{90}: 24.7 ± 0.4 ms vs. 30.0 ± 1.2 ms, respectively, n = 7-8, $P<0.001$). Moreover, ISO dose response curve was leftward shifted regarding force of contraction by 29 % in TG vs. WT atria, suggesting a sensitization for β-adrenergic stimulation. Ventricle to body weight ratios were increased by 7.9 % in TG vs. WT mice (n = 6-7, $P<0.05$).

Conclusion: In the present study, heart-directed overexpression of PP2A-PR72 reduces cardiac contractility. This effect is compensated under maximum β-adrenergic stimulation. Thus, PP2A-PR72 may play a key role in the regulation of the catecholamine-mediated contractile function of the myocardium.

42

The proline-rich region of the farnesyltransferase α-subunit – impact on functional enzyme properties and inhibitability?

A. Hagemann[1], S. Tasillo[1], A. Aydin[1], M. C. Kehrenberg[1], H. S. Bachmann[1]
[1]Universität Witten/Herdecke, Pharmakologie und Toxikologie, Witten, Germany

Objectives: The farnesyltransferase (FTase) possesses a post-translational modification necessary for the function of many proteins including e.g. Ras. Inhibitors against FTase (FTIs) are under investigation for the treatment of diverse diseases (e.g. cancer, progeria, hepatitis D). The FTase is a heterodimer composed of an α-(FTα) and a β-subunit (FTβ). FTβ harbors the catalytic center, but FTα is strictly necessary for activity. A new role for truncated rat (FTαΔN29) and full-length yeast FTα by homo-dimerization has been suggested. However, full-length FTα of human and rat were not able to homodimerize. The N-terminus of human and rat FTα harbours a substantial number of prolines but not the truncated rat and full-length yeast FTα. So our aim was to elucidate, if this region has an impact on enzyme properties and inhibitability by FTIs.

Methods: We did *in silico* analyses of the truncated region (ΔN29) due to the differing dimerization behaviour. *In vitro*, we studied the influence of the proline-rich region (PRR) on FTα homo- and heterodimerization, as well as on activity with FTβ and the other physiological partner geranylgeranyltransferase (GGTase) β-subunit (GGTβ). Pulldown assays, yeast two-hybrid and cell-free as well as in-cell crosslinking but also continuous fluorescent enzyme assays were used to test for interaction and inhibitability of the truncated enzyme by known FTIs (lonafarnib and tipifarnib).

Results: Our *in-silico* analyses show that the PRR is absent in almost all taxa, but highly conserved in mammals except for marsupials. Marsupials have an alanine-rich region instead. Unexpectedly, not only the full-length but also the truncated FTαs showed no homodimerization. The experiments revealed that the PRR is not necessary for heterodimerization of rat and human FTα with FTβ and GGTβ. The enzymes are fully active showing no significant differences in Km values. Inhibition of truncated FTase by FTIs was not altered. Thus, the N-terminal PRR of FTα is highly conserved in mammals but has no impact on enzyme function of FTase and GGTase, respectively.

Conclusion: Our results suggest that the previously discussed FTα homodimerization and its new role as a homodimer are improbable. On the other hand, we suggest a crucial role for this region apart from dimerization with itself or β-subunits. These very important findings may lead to better understanding of FTase regulation and function as well as consequences of FTI treatment.

118

The CREM isoform ICER interacts with E3-ubiquitin protein ligase XIAP

D. Koppenhöfer[1], S. König[2], M. Düfer[3], U. Kirchhefer[1], F. U. Müller[1], M. Seidl[1]
[1]University of Münster, Institute of Pharmacology and Toxicology, Münster, Germany
[2]University of Münster, IZKF CU Proteomics, Münster, Germany
[3]University of Münster, Institute of Pharmaceutical and Medicinal Chemistry, Münster, Germany

Question: The inducible cAMP early repressor (ICER) is a short, cAMP dependent, inhibitory transcription factor isoform of the cAMP-responsive element modulator (CREM), known to be involved in the regulation of insulin secretion in pancreatic beta cells. We showed that ICER interacts specifically with the X-linked inhibitor of apoptosis (XIAP). XIAP is an E3-ubiquitin protein ligase, inhibiting apoptosis by binding and degrading caspases in various tissues including the endocrine pancreas. Moreover it participates in the ubiquitin-proteasome pathway and has the ability to undergo auto-ubiquitination. Here, we characterize the binding between ICER and XIAP in more detail and investigate the impact of this interaction on ubiquitination and proteasomal protein degradation.

Methods: For binding site identification, co-immunoprecipitations (Co-IPs) were conducted in HEK293 cells transfected with several deletion constructs of HA-tagged ICER and different c-myc-tagged domains of XIAP. The functional effect of the ICER-XIAP interaction was investigated by Co-IPs and western blotting in cells transfected with different combinations of ICER- and XIAP-constructs, treated with the proteasome inhibitor MG-132.

Results: Co-IP followed by mass spectrometry of HA-tagged ICER revealed XIAP as an interaction partner. One deletion construct of ICER (ICERmut), lacking 6 amino acids was not able to bind XIAP in Co-IPs. Vice versa, deletion of the BIR1 and BIR2 domain of XIAP impeded the binding of ICER to XIAP. In overexpression experiments we observed a decreased amount of full length XIAP in the presence of ICER. The ICERmut construct did not reduce protein levels of XIAP, showing that the binding of ICER to XIAP leads to XIAP degradation. Furthermore, treatment with the proteasome inhibitor MG-132 restored XIAP levels reduced by full length ICER, indicating that ICER regulates the degradation of XIAP possibly by (auto-)ubiquitination.

Conclusion: Here, we demonstrated for the first time that ICER, beyond its transcriptional activity, specifically interacts with the BIR1 and BIR2 domains of XIAP. This interaction leads to proteasomal degradation of XIAP, probably induced by autoubiquitination of this ligase. This direct interaction of ICER with XIAP broadens the regulatory relevance of ICER for cell survival and generates novel insights in, for example, the regulation of insulin secretion in pancreatic beta cells. (Supported by the IMF SE 212107)

133

CNP-induced stimulation of phosphodiesterase 2 affects arrhythmogenic calcium release in atrial cardiomyocyte

M. Günscht[1], M. Schubert[1], M. Hasse[1], M. Fahmi[1], A. El-Armouche[1], S. Kämmerer[1]
[1]Centre of Pharmacology, Pharmacology and Toxicology, Dresden, Germany

Questions: Atrial fibrillation (AF) represent the most common human cardiac arrhythmia affecting more than 30 million patients worldwide. AF is associated with

abnormal intracellular Ca2+ handling contributing to both the induction and maintenance of AF. Arrhythmogenic calcium release from the SR occurs via ryanodine receptors (RyR) due to increased phosphorylation from cAMP-dependent kinases. Phosphodiesterases (PDEs) are hydrolysing enzymes that degrade cAMP and cGMP. PDE2 is unique to be stimulated by cGMP while hydrolyzing cAMP. The natriuretic peptide type-C (CNP) was shown to promote beneficial effects via activated cGMP-signaling. Here, we aim to investigate the impact of CNP-induced PDE2 stimulation on arrhythmogenic calcium release in atrial cardiomyocytes.

Methods: PDE2 expression was evaluated in atrial biopsies from patients with AF and SR. Ca2+ imaging and Ca2+ spark (CaSp) measurements were performed in isolated atrial cardiomyocytes (mACM) from cardiac-specific PDE2 knockout (KO) mice and human iPS–derived atrial cardiomyocytes (hiACM). Arrhythmia susceptibility of KO mice were assessed via ECG telemetry under basal conditions.

Results: In AF patients, PDE2 expression was significantly upregulated compared to controls. In mouse and hiACM, β-adrenergic stimulation with isoproterenol (ISO) significantly increased the number of CaSp via RyR. The simultaneous application of CNP clearly reduced the ISO-induced increase of CaSp frequency in both WT mACM and hiACM. Interestingly, genetic deletion of PDE2 and specific PDE2 inhibition with BAY 60-7550 prevented the CNP effect in KO mACM or hiACM. Furthermore, intracellular Ca2+ transient amplitudes were similar in mACM from KO and WT. Upon β-adrenergic stimulation, ISO increased the occurrence of spontaneous arrhythmogenic SR Ca2+ waves (SCW) in mACM. In WT, the CNP-induced PDE2 stimulation reduced the number of SCW, whereas CNP did not affect ISO-mediated SCW in atrial cells from KO. The fractional Ca2+ release did not vary between WT and KO. Finally, ECG-telemetry revealed an increased number of irregular RR-intervals in cardiac-specific PDE2 KO compared to WT mice.

Conclusion: Our data indicate that CNP-induced PDE2 stimulation might attenuate abnormal cardiac Ca2+ cycling in AF and protect from arrhythmogenic Ca2+ leak due to excessive RyR2 activation. Thus, pharmacologically stimulation of cardiac PDE2 activity may represent a novel cardioprotective strategy in AF.

157

Dissecting pleiotropic effects of ketoconazole to identify specific targets in neuroblastoma

R. Sami Issa[1], N. S. Pommert[1], M. Kaehler[1], I. Cascorbi[1], **V. Waetzig**[1]
[1]University Medical Center Schleswig-Holstein, Institute of Experimental and Clinical Pharmacology, Kiel, Germany

Question: Ketoconazole, an antifungal agent, inhibits several cytochrome P450 enzymes, which can affect cancer-specific metabolic pathways as well as steroid hormone synthesis. In neuroblastoma, a hormone-related tumor with a heterogeneous biological basis, this particular range of intracellular targets might be helpful to limit growth. Due to its many side effects and drug-drug interactions, ketoconazole is not a desirable therapeutic option, but understanding its intracellular mechanisms appeared promising to identify more specific drug targets.

Material and methods: For the experiments, SH-SY5Y cells were used, which are a widely accepted model system for neuroblastoma. They were treated with ketoconazole alone (10 µM) or in combination with other substances, either known (fenretinide, 5 µM; retinoic acid, 5 µM) or new in anticancer approaches for neuroblastoma (tepotinib, 5 µM) before determining cell viability and proliferation as well as analyzing survival signaling and growth factor secretion.

Results: Ketoconazole significantly ($p<0.001$) reduced the number of viable cells, mostly due to decreased proliferation. To understand which of the manifold intracellular actions of ketoconazole were crucial for the observed growth reduction, we examined the contribution of single mediators like CYP26, CYP3A5, CYP51A1, PXR and growth factor-mediated signaling to the overall effect by using specific inhibitors. Blocking the activity of one or even two ketoconazole targets only led to a weak and transient decrease of viable cells. To analyze if a chemosensitizing effect could be observed, we applied ketoconazole in combination with further anticancer drugs. Thereby, the growth-limiting effect of fenretinide was not significantly enhanced, while the retinoic acid resistance of SH-SY5Y cells was attenuated ($p<0.001$). When ketoconazole and the c-Met inhibitor tepotinib were applied simultaneously, cell survival was significantly decreased ($p<0.001$) compared to single substance treatment.

Conclusion: Generally, not even the concurrent inhibition of at least two ketoconazole target proteins could mimic its pleiotropic effects, which is neither effective for long-term treatment nor an improvement in tolerability. The most promising chemosensitization target was detected in hepatocyte growth factor (HGF) signaling, so that the inhibition of exosome formation might be an important aspect of ketoconazole actions which warrants further investigations.

173

Establishing the analysis of *IL8* and *NFKBIA* mRNA expression in co-cultivated macrophages and A549 cells at the single-cell level using RNA-FISH

D. Heylmann[1], H. Peppler[1], M. Kracht[1]
[1]Rudolf Buchheim Institute of Pharmacology, Biomedical Research Center Seltersberg, Justus Liebig University, Gießen, Germany

The communication of cancer and immune cells in the tumor microenvironment is dependent on cytokines regulated by the NF-kB pathway. Here we aimed to investigate, how LPS and IL1 stimulation of co-cultured macrophages (Mph) and A549 lung carcinoma cells modulates mRNA expression of *IL8* and the inhibitor of NF-kB protein *NFKBIA* at single cell resolution by RNA-FISH (fluorescence *in situ* hybridization).

Monocytes were isolated from PBMCs (peripheral blood mononuclear cells) from buffy coat and differentiated into Mph within 9 days in cell imaging chambers (ibidi labware). A549 lung carcinoma cells were added to the Mph and the co-cultivated cells were stimulated with IL1 and LPS for various time points. After fixation with 4% paraformaldehyde, FISH was performed by using mRNA probe sets against *IL8* and *NFKBIA* mRNA as well as pre-amplifier, amplifier and labelled probes (*IL8*, AF 647; *NFKBIA*, AF 546) from the ViewRNA ISH Cell Assay Kit (Invitrogen). Images were acquired with the DMi8 Fluorescence microscope (Leica). mRNA spots were detected and quantified in each individual cells using the ICY bio image analysis software. Data distribution was visualized as violin plots using GraphPad PRISM.

We differentiated Mph and co-cultivated them with A549 cells in ibidi cell imaging chambers and measured *IL8* and *NFKBIA* mRNA spots at the single-cell level. There was a time dependent increase of *IL8* and *NFKBIA* mRNAs in Mph and A549 cell within 3 days. LPS and IL1 stimulation highly upregulated *IL8* and *NFKBIA* mRNA levels with no obvious differences between both cell types. Furthermore, we separately assessed mRNA signals in multi-nucleated, fused Mph (multi-nucleated giant cells), which developed under these culturing conditions. Overall, double-nucleated Mph produced twice the numbers of mRNA transcripts compared to non-fused cells, suggesting that both nuclei remain transcriptionally active in fused Mph.

These data reveal that it is possible to measure mRNA signals in Mph and cancer cells simultaneously with RNA-FISH as a high resolution read out for cell-cell communication. Future experiments will focus on the comparison of cells which are in direct contact compared to spatially separated cells and on gene-specific transcriptional activities of double-nucleated Mph. Furthermore, longitudinal studies of long-term co-cultures of Mph with tumor cells will be performed to reveal single cell differences of mRNA expression upon the development of trained immunity.

223

Pathological remodeling promotes proteosomal loading of cardiac-derived exosomes

F. Bleckwedel[1,2], E. Schoger[1,3,2], T. Weber[1,2], M. Samak[2,4], G. Germena[2,4], C. Rocha[2,4], P. Tucholla[1,2], M. Sitter[5], B. Guobin[1,2], W. Moebius[6], C. Lenz[7], R. Hinkel[2,4], G. Salinas[5], J. C. Gross[8], L. C. Zelarayán[1,3,2]
[1]Universitätmedizin Göttingen, Institute of Pharmacology and Toxicology, Göttingen, Germany
[2]DZHK (German Center for Cardiovascular Research), Goettingen, Germany
[3]Cluster of Excellence "Multiscale Bioimaging: from Molecular Machines to Networks of Excitable Cells" , Goettingen, Germany
[4]Deutsche Primat Zentrum (DPZ), Goettingen, Germany
[5]NGS Integrative Genomics Core Unit (NIG), Goettingen, Germany
[6]Max-Planck-Institute for Experimental Medicine, Goettingen, Germany
[7]Core Facility Proteomics University Medical Center Goettingen , Goettingen, Germany
[8]Health and Medical University, Postdam, Germany

After reporting that mice with inducible CM-specific Wnt activation (β-catΔex3) mimic pathological remodelling condition and heart failure (HF), we further explored the cardiac-derived extracellular vesicles (EVs). Though EVs analysis *in vivo* are challenging, our genetic model proved advantageous by focusing only on the relative changes between control (CT) and β-catΔex3 in the extracellular compartment *in vivo*. With an improved protocol we isolated EVs from CT and β-catΔex3 hearts by differential ultracentrifugation (n=3/condition). The fraction centrifuged at 100.000g containing small EVs was confirmed by electron microscopy and nanoparticle-tracking-analysis (mean size of 160±69nm). Western blot showed expression of EVs marker CD81 and absence of Calnexin (endoplasmic reticulum) and GM130 (Golgi) markers. Mass spectrometry (MS) analysis revealed that 47% of the proteins were included in Exocarta Top100 candidate with a major exosome (Exo) representation. Also, 391 significantly differentially enriched proteins in β-catΔex3 hearts were identified. The vast majority taking part of cardiac muscle tissue development, muscle contraction, hypertrophic and dilated cardiomyopathy. The cardiac origin of EVs and the HF phenotype in β-catΔex3 hearts was also corroborated by proteosome analysis. β-catΔex3-cardiac Exo were significantly loaded with all seven α and β chains of the constitute 20S proteasome, molecular chaperones and co-chaperones as well as proteasome associated proteins previously described in Exo (HSPA70, HSP90AB1, CRYAB, PKACA and BAG2). CRYAB, a chaperone protein that triages misfolded proteins for proteasomal degradation or repair found mainly in heart, was confirmed to co-localize with labelled Exo *in vitro*. We performed single whole cell transcriptome with an optimized protocol, followed by pairwise comparison of DEGs and their functional enrichment between β-catΔex3 and CT-CM populations. This revealed that a subpopulation of β-catΔex3 CM were active in EVs secretion and proteosomal activity.

Our results indicate an Exo-mediated maintenance of CM proteostasis. Upon stress, CRYAB and co-chaperones increase binding to damaged-sarcomeric-proteins heading towards degradation, overloading the proteasome capacity, which may activate EV-mediated cellular extrusion of misfolded proteins as a mechanism of cellular protection. Cardiac extracellular proteosome may serve as read-out of disease progression and for monitoring cellular remodeling *in vivo*.

261

NO-induced cGMP formed in cardiac fibroblasts elevates cAMP in cardiomyocytes via PDE3

L. Menges[1], J. Giesen[1], K. Yilmaz[1], D. Koesling[1], M. Russwurm[1]
[1]Ruhr-Universität Bochum, Pharmakologie und Toxikologie, Bochum, Germany

Introduction: The cyclic nucleotide cGMP is an important signaling molecule transmitting the signals of nitric oxide (NO) and of natriuretic peptides. NO-induced cGMP is formed by NO-sensitive guanylyl cyclases (NO-GCs) which are also activated by novel activators and stimulators developed e.g. for treatment of pulmonary hypertension and heart failure.

Objectives: Recently, we demonstrated in a co-culture model that NO-induced cGMP is formed in cardiac fibroblasts and enters cardiac myocytes via gap junctions. However, it remained unclear if the gap junction-mediated transfer of cGMP occurs in native tissue. And it is a matter of debate whether NO-induced cGMP has direct effects on the heart muscle.

Methods: To be able to specifically detect cGMP signals in cardiac myocytes, we generated a mouse line which expresses the indicator cGi-500 only in cardiac myocytes.

Results: By fluorescence real time measurements, we show that NO-induced cGMP signals are detectable in myocytes of acute cardiac slices. Inhibition of these signals by the gap junction inhibitor carbenoxolone demonstrates the origin of NO-induced myocyte cGMP in other cell types, presumably fibroblasts. As these NO-induced cGMP-signals are under control of the 'cAMP-degrading, cGMP-inhibited' PDE3, we wondered if NO-induced cGMP has an effect on cAMP levels in cardiomyocytes. Using cAMP radioimmunoassays for cAMP, we show that isoprenaline-induced cAMP was elevated by the NO-GC stimulator BAY41-2272 demonstrating that NO-GC-generated cGMP affects cAMP levels in acute cardiac slices. As this effect was abolished by carbenoxolone the cross talk between NO-induced cGMP and isoprenaline-induced cAMP depends heterocellular communication.

Conclusion: In sum, we propose that NO-induced cGMP formed in fibroblasts enters cardiomyocytes via gap junctions and elevates beta-receptor-induced cAMP via PDE3. Thus, it is tempting to speculate that NO-induced cGMP formed in fibroblasts elicits positive inotropic and lusitropic effects in the heart.

275

New insights into the non-canonical desensitization of Gq-signaling by GRK2/3 expression levels

N. Jaiswal[1], A. Godbole[1], M. Kauk[1], C. Große[1], J. Filor[1], J. Drube[1], C. Hoffmann[1]
[1]Universitätsklinikum Jena, Institute of Molecular Cell Biology, Jena, Germany

G_q-coupled receptors, upon agonist-driven activation, stimulate PLCβ to produce DAG and release Ca^{2+} stores. Desensitization of these agonist-bound receptors mediated by GRK2/3 involves sequestration of G_q to these GRKs for membrane anchoring (Penela et al 2003). Specifically; it has been shown that GRK2 interacts with the $G\alpha_q$ subunit and the βγ dimer by inserting itself between them (Tesmer et al 2005). Increased GRK expression has been reported in clinical samples of heart failure, cardiac hypertrophy, hypertension, colon cancer and several other pathophysiological conditions (Murga et al 2019, Jiang et al 2017, Obrenovich et al 2009). Influence of GRK2/3 overexpression on G_q-signaling as well as the underlying mechanism is poorly understood. Here, we address the effect of GRK overexpression on G_q-PLCβ interaction and the following impact on downstream signaling.

We used a Split Luciferase Complementation (SLC) system (Littmann et al 2018) and the model G_q-coupled M1AChR in GRK KO HEK293 cells (Drube et al 2021), to investigate influence of individual GRK overexpression on G_q-PLCβ interaction. GRK2 and GRK3 overexpression reduced G_q-PLCβ interaction whereas GRK5 and 6 overexpression did not (Figure 1a,b). We measured GRK2 function on G_q-PLCβ interaction in an expression dependent manner and observed a concentration dependent decrease in interaction with increasing GRK2 expression (Figure 1c).

Treatment with compound 101 (a GRK2/3 kinase activity inhibitor) was ineffective in preventing GRK2 from inhibiting G_q-PLCβ interaction (Figure 1d,e). Kinase dead mutants of GRK2/3 showed reduction in G_q-PLCβ interaction to the same extent as GRK2/3 (Figure 1f). This suggested that GRK2/3 mediated G_q sequestration is independent of GRK2/3 kinase activity. G_q-PLCβ interaction was rescued by using GRK mutants with reduced binding affinity to the $G\alpha_q$ subunit (GRK2/3(D110A) (Sterne-Marr et al 2003) or to the βγ dimer (GRK2/3(R587Q) (Carman et al 2000) (Figure 2a,b).

Furthermore, overexpressed GRK2/3 as well as kinase-dead GRK2 reduced DAG production and Ca^{2+} release as compared to GRK2/3 KO confirming that GRK2/3 overexpression can negatively affect G_q-initiated signaling (Figure 2c, d).

In conclusion, our findings suggest that PLCβ stimulation by the G_q activation is inhibited by the spatial presence of GRK2/3 and is independent of their kinase activities. This mode of desensitization by GRK2/3 appears to have immediate effects on downstream G_q signaling.

Fig. 1

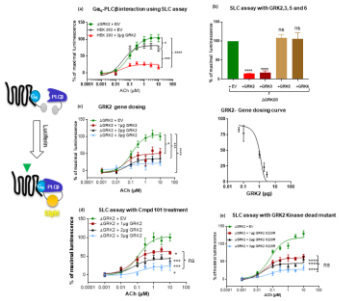

Fig. 2

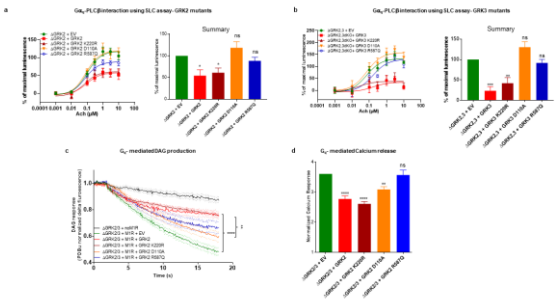

Pharmacology – Nuclear receptors, enzymes and other targets

49

Enzyme kinetics and pharmacological characterization of transcript and splice variants of the human farnesyltransferase

M. C. Kehrenberg[1], A. Hagemann[1], S. Hinz[2], H. S. Bachmann[1]
[1]Witten/Herdecke University, Institute of Pharmacology and Toxicology, Centre for Biomedical Education and Research, Department of Medicine, Witten, Germany
[2]Rheinische Friedrich-Wilhelms-Universität Bonn, PharmaCenter Bonn, Pharmaceutical Institute, Pharmaceutical & Medicinal Chemistry, Bonn, Germany

Introduction: The farnesyltransferase (FTase) is a heterodimeric enzyme consisting of an α- (FTα) and β-subunit (FTβ). FTase catalyzes the attachment of a farnesyl moiety to its substrate proteins leading to their membrane association. FTβ harbours the catalytic center. More than 200 proteins are farnesylated, e.g. the small G protein Ras, a key oncogene. Inhibitors of the FTase (FTIs) were initially of intense interest in cancer research and are meanwhile tested in various indications e.g. hepatitis D, malaria or progeria. Despite the predicted potential in cancer, results of most oncological studies are unconvincing so far. We identified two transcript and two splice variants of FTβ that are expressed in a tissue- and patient-specific manner. They all share at least the last eight C-terminal exons and differ in the N-terminal part.

Objectives: Our aim was to determine kinetic properties of all FTβ variants and to characterize them pharmacologically in order to unravel their relevance in current FTI administration and future drug design.

Materials & methods: The FTβ variants were cloned and co-expressed in *Escherichia coli* (α- and β-subunit). After purification by immobilized metal ion affinity chromatography, we analyzed their enzyme activity using a continuous fluorescence assay. We determined the Michaelis constant (K_M) and the inhibition constants (K_i) of four FTIs (tipifarnib, lonafarnib, α-hydroxyfarnesylphosphonic acid (α-HFP), and B581).

Results: Three of the four identified variants of FTase show enzyme activity. Our results demonstrate that they differ up to 15-fold in K_M. FTIs are potent inhibitors with respect to the commonly and in literature described FTase. Their K_i values are in a

nanomolar range. The newly identified variants, on the contrary, are only inhibited to a relevant extent in the micromolar range by α-HFP and B581.

Conclusion: Higher K_M values of FTase variants imply lower substrate affinity suggesting different catalytic functions in cells. This thesis is supported by the fact that the variants are tissue-specific and patient-specific expressed. Considering the significant differences of K_i's, our results provide new starting points for the study of FTIs. They underline the relevance of FTβ variants for the development of putative new FTIs and new therapeutic approaches.

141

Characterization of a novel small molecule inhibitor of murine and human ferroptosis suppressor protein-1

S. Höhlein[1], M. Fischer[1], E. Sfakianaki[1], K. Hadamek[1], A. Keller[1], S. Bothe[2], H. Schindelin[2], E. Jeanclos[1,3], J. P. Friedmann Angeli[2], A. Gohla[1]
[1]Institute for Pharmacology and Toxicology, University of Würzburg, Würzburg, Germany
[2]Rudolf Virchow Center for Integrative and Translational Biomedicine, University of Würzburg, Würzburg, Germany
[3]Leibniz Institute for Analytical Sciences/ISAS, Dortmund, Germany

Introduction: Ferroptosis is a recently discovered kind of cell death that is genetically, morphologically and biochemically different from other forms of cell death. The hallmark of ferroptosis is iron-dependent, lethal phospholipid peroxidation. Interestingly, drug tolerant cancer cells, especially those in the metastasis-prone state, are highly sensitive to ferroptosis. Pharmacological ferroptosis induction may therefore represent a novel antitumor strategy. Ferroptosis is under the perpetual control of various cell-intrinsic ferroptosis suppressing pathways. These include the essential glutathione peroxidase-4 (GPX4) axis, and the GPX4-independent ferroptosis suppressor protein (FSP1)-ubiquinone axis. Despite several described GPX4 inhibitors, only one inhibitor of human FSP1 (iFSP1) has been discovered. We have discovered a small molecule, termed CP1, that sensitizes human and mouse tumor cells to ferroptotic cell death triggered by GPX4 inhibition. However, the molecular target of CP1 was unknown.

Objective: Identification of the cellular CP1 target.

Methods: Cell viability in various (CRISPR/Cas9-engineered) tumor cell lines was assessed upon incubation with a panel of cytotoxic drugs compared to pharmacological ferroptosis inducers or -inhibitors. *In vitro* activity assays were performed with recombinant, purified FSP1, and ligand binding kinetics were determined in biolayer interferometry measurements.

Results: We found that HT1080 fibrosarcoma cells deficient in GPX4 died in a CP1 concentration-dependent manner, and that the ferroptosis inhibitor liproxstatin-1 or GPX4 add-back prevented CP1-induced cell death. CP1 sensitized HT1080 cells to ferroptosis to the same extent as FSP1 knockout did, and CP1 addition to FSP1 knockout cells did not cause any further loss of cell viability. CP1 did not sensitize tumor cells to apoptotic cell death induced by nine different cytotoxic drugs. Finally, CP1, but not iFSP1, sensitized a panel of murine or rat tumor cells to ferroptotic cell death induced by GPX4-inhibition. *In vitro* FSP1 activity and biolayer interferometry assays showed that CP1 directly inhibited both human and murine FSP1 with a potency and binding affinity in the low micromolar range.

Conclusion: Our findings establish CP1 as a novel small molecule FSP1 inhibitor. Future work will focus on improving the potency and selectivity of this compound, and on testing its suitability for *in vivo* studies in murine cancer models.

144

Pharmacological characterization and phosphorylation of human farnesyltransferase α-subunit wildtype and mutants

S. Hinz[1,2], M. C. Kehrenberg[2], A. Hagemann[2], D. Jung[2], H. S. Bachmann[2]
[1]University of Bonn, Pharmaceutical Institute, Bonn, Germany
[2]Witten/Herdecke University, Pharmacology and Toxicology, Witten, Germany

Introduction: Human farnesyltransferase (FTase) is a ubiquitous enzyme consisting of an α- and a β-subunit that catalyzes the post-translational modification of many proteins for example the protooncogene Ras. Farnesylation of Ras is required for its subsequent activation and signal transduction. The β-subunit of the enzyme harbors the catalytic center whereas the α-subunit is suggested to be the regulatory subunit and stabilizes the β-subunit. Phosphorylation of the α-subunit at defined serine residues was shown to lead to an increase of FTase activity and therefore of farnesylated Ras [1].

Objectives: In the present study, we pharmacologically characterized FTase α-subunit (FTα) wildtype (wt) and serine to alanine mutants. In addition, we explored their insulin-stimulated expression and phosphorylation in the human breast cancer cell line MDA-MB-231.

Methods: FTα wt and serine to alanine mutants as well as the β-subunit were heterologous co-expressed in *E. coli*. Recombinant enzymes were purified by immobilized metal affinity chromatography. Enzyme kinetics and pharmacological characterization of the wt and the mutant enzymes were determined by employing a continuous fluorescence enzyme assay. Insulin-stimulated FTα expression and phosphorylation in transient transfected MDA-MB-231 breast cancer cells were analyzed by immunoblots.

Results: The FTα mutants S60A, S62A, S60A/S62A, as well as the mutant with 11 serine residues substituted to alanine (11S>A) showed similar *KM*-values for the peptide substrate dansyl-GCVLS and the isoprenoid substrate farnesyl pyrophosphate (FPP) compared to the wt enzyme. Moreover, the determined *Ki*-values at the serine to alanine mutants for the potent, selective, and competitive FTase inhibitor tipifarnib (versus *N*-dansyl-GCVLS 2 µM) showed no significant differences compared to the wt enzyme. Furthermore, insulin (1 µM) was able to increase the expression of FTα wt in MDA-MB-231 cells but did not influence the phosphorylation of serine 62.

Conclusions: Our studies revealed, that the FTα mutants S60A, S62A, S60A/S62A and 11S>A did not influence the affinity of the peptide substrate dansyl-GCVLS, the isoprenoid substrate FPP and the competitive inhibitor tipifarnib. Further studies are necessary to investigate the insulin-stimulated phosphorylation of different serine residues in FTα and their role in enzyme activity.

[1]Solomon, C. S. et al. *Biochem Biophys Res Commun.* **2001**, 285, 161-166.

148

Interference with nuclear Ca2+-Calmodulin signalling in cardiomyocytes blocks catecholamine evoked protein translation and hypertrophy

A. Riedel[1,2], R. Medert[1,2], S. Monaco[3], E. Gjerga[4], X. Tolksdorf[1], C. Richter[1], M. Schrader[2,5], V. Kuryshev[1,3], M. Busch[2,5], A. Jungmann[2,5], A. Wirth[1,2], V. Benes[6], P. Most[2,5], C. Dieterich[3], M. Völkers[2], H. Bading[3], **M. Freichel**[1,2]
[1]Pharmakologisches Institut, Universität Heidelberg, Heidelberg, Germany
[2]DZHK (German Centre for Cardiovascular Research), Partner Site Heidelberg/Mannheim, Heidelberg, Germany
[3]Interdisciplinary Center for Neurosciences, Department of Neurobiology Heidelberg University, Heidelberg, Germany
[4]Klaus Tschira Institute for Computational Cardiology, Innere Medizin III, Bioinformatik und Systemkardiologie, Universität Heidelberg, Heidelberg, Germany
[5]Division of Molecular and Translational Cardiology, Department of Internal Medicine III University Hospital Heidelberg, Heidelberg, Germany
[6]EMBL, Heidelberg, Germany

During the development of cardiac hypertrophy, enhanced diastolic Ca^{2+} transients have been observed in the nucleus of cardiomyocytes. It has been established that nuclear signaling pathways during hypertrophic stimulation depend on nuclear calcium. It has not yet been conclusively determined whether nuclear Ca^{2+} signals act causally on the development of cardiac hypertrophy or represent a consequence of progressive calcium dysregulation.

Methods: We established a protocol for inducing a hypertrophic response upon phenylephrine (PE, 100µM) stimulation in cultured neonatal rat cardiac myocytes (NRVCM). Using HPLC-purified scAAV6-vectors, we introduced the nuclear calcium-calmodulin (CaM) inhibitor CaMBP4. We studied the impact of CaMBP4 on the hypertophic response by measuring cell area changes. Furthermore, RNAseq was performed on FACS-sorted NRVCMs. Translational activity was shown via a puromycin assay. Transcription factor activity was assessed using the RNAseq data and a regulatory build of the mouse genome.

Results: CaMBP4-transduced NRVCM were protected from PE-evoked cardiac hypertrophy, compared to the mCherry-transduced and untransduced controls, respectively. However, we found that $CaMBP4^+$ cells expressed high levels of hypertrophic markers and Mef2 target genes (eg ANF, BNP), unveiling an uncoupling of phenotype and gene expression. Gene set enrichment analysis revealed a cluster of genes involved in the regulation of translation (eg Eif3d, Eif2s1), whose PE-evoked upregulation was prevented by CaMBP4 transduction. We confirmed that the PE-evoked upregulation of translational activity was blunted by expression of CaMBP4. Analysis of transcription factor activity revealed a number of hypertrophy regulating CaM responsive transcription factors including Atf3, Klf2 and Klf4 (downregulated in PE-stimulated $CaMBP4^+$ cells) and several others, which are upregulated in PE-stimulated $CaMBP4^+$ cells, including Mef2a.

Conclusion: We identified nuclear CaM dependent signaling to play a pivotal role in cardiomyocyte hypertrophy evoked by catecholamine stimulation. Whereas classical MEF2 target genes are still upregulated in CaMBP4 expressing cells, we found that CaM signaling interference with the increase in protein translation. Future studies are needed to identify a Calcium responsive nuclear signaling Element (CaRNE) that integrates CaM dependent regulation of transcription, protein translation and development of cardiomyocyte hypertrophy.

Fig. 1

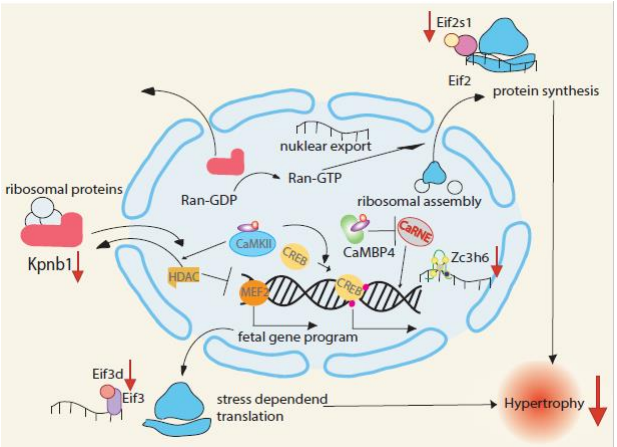

Pharmacology – Ion channels and membrane transporters

2

A novel role for TPC2 in hepatocellular carcinoma cell proliferation and tumor growth

M. Müller[1], S. Gerndt[2], Y. K. Chao[3], P. Nguyen[1], A. Gerwien[4], N. Urban[5], C. Müller[2], F. A. Gegenfurtner[1], F. Geisslinger[1], C. Ortler[1], C. C. Chen[6], S. Zahler[1], M. Biel[7], M. Schaefer[3], C. Grimm[3], F. Bracher[2], A. M. Vollmar[1], **K. Bartel**[1]
[1]Ludwig-Maximilians-University Munich, Pharmacy, Pharmaceutical Biology, Munich, Germany
[2]Ludwig-Maximilians-University Munich, Pharmacy, Center for Drug Research, Munich, Germany
[3]Ludwig-Maximilians-University Munich, Walter-Straub-Institute for Pharmacology and Toxicology, Munich, Germany
[4]Ludwig-Maximilians-University Munich, Pharmacy, CIPSM, Munich, Germany
[5]Leipzig University, Rudolf-Boehm-Institute of Pharmacology and Toxicology, Leipzig, Germany
[6]National Taiwan University, Department of Clinical Laboratory Sciences and Medical Biotechnology, College of Medicine, Taipai, Germany
[7]Ludwig-Maximilians-University Munich, Department of Pharmacy, Pharmacology, Munich, Germany

Introduction: Two-pore channels (TPCs) are important endolysosomal cation channels in controlling intracellular trafficking and transport, known to affect, migration, invasion, and autophagy. The TPC2 isoform, which is predominantly localized on endolysosomal membranes, was recently connected with poor survival1, neoangiogenesis2 and migration3. Despite understanding of the role of TPCs in cancer biology is increasing, its role in cancer development is still unclear and a major obstacle in using TPC2 as target in cancer therapy is the lack of highly potent and selective inhibitors

Objectives: We facilitated a multidisciplinary approach to unravel the role of TPC2 in cancer development by means of gene editing and pharmacological inhibition. Further, we created and screened a library of tetrandrine analogues to generate novel, synthetically accessible, potent TPC2 inhibitors

Materials & methods: Tetrandrine analogues were generated by chemical synthesis. Ion channel activity was analyzed by whole-endolysosomal patch clamp and calcium imaging. The CRISPR/Cas9 system was used to Knock-out TPC2. Cellular metabolism was analyzed using a SeahorseTM and a FRET biosensor. For mouse models, C57BL/6-Tyr mice were inoculated with luciferase expressing cancer cells i.v. or s.c. Luminescence was detected using the IVIS Lumina system.

Results: Genetic TPC2 knockout reduces proliferation of cancer cells in vitro, shifts energy metabolism towards oxidative phosphorylation, and effectively abrogates tumor growth in vivo. Additionally, we have developed simplified analogs of the known TPC2 inhibitor tetrandrine, by screening a library of synthesized benzyltetrahydroisoquinoline derivatives. Removal of dispensable substructures of the lead molecule tetrandrine revealed an increase in antiproliferative efficacy against cancer cells and impairs proangiogenic signaling of endothelial cells to a greater extent than the lead structure. Furthermore, simplifications reduced toxicity in healthy cells, allowing in vivo administration.

Conclusion: Our study reveals TPC2 as interesting target for cancer therapy and provides easily accessible tetrandrine analogues as a promising option for effective pharmacological interference4.

Refernece:

1. Li et al. Clin. Transl Oncol (2019) 21, 1067–1075.
2. Favia et al. Proc. Natl. Acad. Sci (2014). U S A 111, E4706–E4715
3. Nguyen et al. Cancer Res (2017). 77, 1427–1438.
4. Müller et al. Cell Chemical Biology (2021) 28, 1–13

3

Manipulating lysosomal function to improve chemotherapy response - Targeting lysosomal Two-Pore Channel 2 as novel strategy

F. Geisslinger[1], M. Müller[1], B. Vick[2], Y. K. Chao[3], F. Bracher[4], C. Grimm[3], I. Jeremias[2], A. Vollmar[1], K. Bartel[1]
[1]Ludwig-Maximilians University, Pharmaceutical Biology, Munich, Germany
[2]Helmholtz Center, Research Unit Apoptosis in Hematopoietic Stem Cells, Munich, Germany
[3]Ludwig-Maximilians University, Walther-Straub-Institute of Pharmacology and Toxicology, Munich, Germany
[4]Ludwig-Maximilians University, Pharmaceutical Chemistry, Munich, Germany

Introduction: Despite invention of many targeted cancer therapy strategies, classic cytostatics such as vincristine and doxorubicin are still an indispensable part of common chemotherapy regimens. However, development of resistance against these cytostatics leads to poor response to renewed chemotherapy. Lately, the lysosome has gained interest in cancer research influencing chemoresistance. This is mediated by lysosomal drug sequestration, the accumulation of drugs within the organelle by which they are prevented from reaching their intracellular targets. Additionally, lysosomal membrane damage can initiate lysosomal cell death by release of lysosomal proteases into the cytosol.

Objectives: Our aim is to employ ion channels as targets to manipulate lysosomal function and subsequently improve chemotherapy response in cancer. This study focusses on Two-Pore Channel 2 (TPC2), a lysosomal cation channel important for lysosomal and cellular function. We posed the hypothesis that targeting TPC2 could restore chemosensitivity in leukemia cells.

Materials and methods: TPC2 knock out (ko) cells were generated using CRISPR/Cas9. Cell survival and signalling pathways were analyzed by cell biological methods, including qPCR, immunoblotting, flow cytometry, confocal microscopy and CellTiter-Blue.

Results: Our data reveal for the first time that loss of TPC2 function sensitizes drug-resistant VCR-R CEM (acute lymphoblastic leukemia, ALL) cells to various cytostatics, including vincristine, doxorubicin and topotecan. This effect could be confirmed by employing the pharmacological TPC2 inhibitors naringenin and tetrandrine, showing beneficial effects in several leukemic cell lines or patient derived xenograft ALL cells when combined with vincristine. Mechanistically, chemo sensitization is achieved by impaired lysosomal drug sequestration and increased susceptibility to lysosomal damage in TPC2 ko cells as result of altered lysosomal morphology. Hence, altered drug distribution with higher abundance at the target site and release of cathepsin B into the cytosol through leaky lysosomal membranes triggers increased cell death by a dual mode of action.

Conclusion: The work presented here establishes TPC2 as promising target for combination therapy approaches in ALL cells to overcome chemoresistance. Mechanistically, beneficial effects of targeting TPC2 are mediated by impaired lysosomal functionality.

6

Slack potassium channels modulate TRPA1-induced pain in mice

F. Zhou[1], K. Metzner[1], P. Engel[1], P. Ruth[2], R. Lukowski[2], A. Schmidtko[1], R. Lu[1]
[1]Goethe University, Institute of Pharmacology and Clinical Pharmacy, Frankfurt am Main, Germany
[2]University of Tübingen, Department of Pharmacology, Toxicology and Clinical Pharmacy, Tübingen, Germany

Question: The transient receptor potential (TRP) ankyrin type 1 (TRPA1) channel is highly expressed in a subset of sensory neurons in dorsal root ganglia (DRG), and is well documented as an essential detector of painful stimuli. Recent single-cell RNA sequencing technologies suggest a co-expression of TRPA1 with the sodium-activated potassium channel Slack (also termed KNa1.1, Kcnt1, or Slo2.2) in sensory neurons. However, to which extent TRPA1 and Slack functionally interact remains elusive.

Methods: The cellular distribution of TRPA1 and Slack in DRG was investigated by *in situ* hybridization and immunostaining. The functional interaction of TRPA1 and Slack was assessed by characterizing the behavior of mice lacking Slack globally or conditionally in sensory neurons, by conducting calcium imaging experiments in sensory neurons, and by performing patch clamp recordings in HEK cells expressing TRPA1 and Slack.

Results: Our results show that TRPA1, but not TRP vanilloid type 1 (TRPV1), is substantially co-expressed with Slack in a subset of sensory neurons. Mice lacking

Slack demonstrated altered pain behavior after TRPA1 stimulation. *In vitro* patch clamp experiments support a functional coupling of TRPA1 and Slack.

Conclusion: Taken together, our findings suggest that TRPA1-mediated pain signaling is modulated by Slack.

14

Superadditive TRPV2 activation by cannabidiol and probenecid induces mast cell degranulation

R. Raudszus[1], M. Schaefer[1], K. Hill[1]
[1]Rudolf Boehm Institute for Pharmacology and Toxicology, Leipzig, Germany

Transient receptor potential vanilloid 2 (TRPV2) is a Ca2+-permeable cation channel that is highly expressed in different cells of the immune system, such as T-cells, macrophages, granulocytes and, particularly in mast cells. Considering rapidly rising prevalence of allergic diseases worldwide, a better understanding of allergic reactions and mast cell degranulation is highly desirable. As a TRPV2-mediated Ca2+ entry in mast cells might trigger degranulation, we aim at investigating whether pharmacological targeting of TRPV2 may regulate mediator release. By performing a two-dimensional serial dilution screening of the TRPV2 activators cannabidiol (CBD) and probenecid (Pro), we identified agonist concentrations that activate rat and human TRPV2 in a superadditive manner when applied simultaneously. The superadditive effect was confirmed by fluorometric Ca2+ influx assays and electrophysiological patch clamp recordings, which also revealed the applicability of the recently identified TRPV2-selective inhibitor X10056. Assessed by quantitative PCR and fluorometric Ca2+ influx assays, we confirmed TRPV2 mRNA and functional expression in RBL-2H3 mast cell-like cells and in primary bone marrow-derived mast cells isolated from mice (BMMC). Due to the superadditive effect of the CBD/Pro combination, we were able to activate TRPV2 channels without cytotoxic effects of the agonists. In RBL-2H3 cells or BMMC, β-hexosaminidase release was significantly promoted when TRPV2 was activated by CBD/Pro and inhibited in the presence of TRPV2 channel blockers X10056 or valdecoxib. Furthermore, TRPV2-mediated degranulation of BMMC was confirmed by performing histamine ELISA. The combination of CBD/Pro induced histamine release, which was attenuated in the presence of X10056. The TRPV2-mediated effects on mast cells were additive to the classical IgE-mediated mast cell degranulation, using anti-DNP-IgE and DNP-human serum albumin, indicating two independent pathways. Taken together, we present CBD and Pro as a potent and non-toxic agonist combination to activate murine and human TRPV2 channels. Moreover, we provide evidence that activation of TRPV2 contributes to mast cell degranulation independent of the classical IgE-induced mediator release.

41

Isolation of TRPA1 Channel from HEK293 Cells as a Target for Alkylating Agents

K. Müller-Dott[1], T. Gudermann[2], H. Thiermann[1], H. John[1], D. Steinritz[3]
[1]Bundeswehr Institute of Pharmacology and Toxicology, München, Germany
[2]Walther-Straub-Institute, München, Germany
[3]Medical Service Academy, CBRN Medical Defense, München, Germany

Introduction: Transient potential receptor (TRP) channels play an important role in the detection of pain, heat and various noxious stimuli. In the skin and the lung, TRPA1 channels are expressed in non-neuronal tissue. TRP channels, especially TRPA1 channels, can be activated by electrophilic toxic compounds supposedly via covalent modification of cysteine residues. The chemical warfare agent sulfur mustard (SM) is a blistering agent first used during World War I. It mainly affects the skin but also the respiratory system. TRPA1 channel activation caused by SM has already been described, however, the exact mechanism remains unclear (Stenger et al., Arch Toxicol, 2014).

Objectives: The aim of this study is the isolation and purification of human TRPA1 channels from overexpressing HEK293 cells for subsequent identification of TRP-channel modifications (alkylation) via LC-MS/MS measurements.

Methods: HEK293 cells were used as an overexpressing system. A plasmid containing a His-tagged TRPA1 channel was used. The TRPA1 channel was isolated using 1 % digitonin and was further purified by immunomagnetic separation (IMS) using TRPA1 specific antibodies. High-resolution LC-MS/MS measurements were performed to determine specific amino acid modifications.

Results: Different TRPA1 antibodies were tested. Their specificity was poor and only one antibody detected the TRPA1 channel in Western blot experiments. A typical double band at 125 kDa corresponding to the TRPA1 channel was found. Subsequently, IMS was elaborated using either an anti-His-tag antibody or the anti-TRPA1 antibody. LC-MS/MS analyses indicated a high recovery for both antibodies. Sequence coverage of TRPA1 after proteolysis with trypsin was higher than 35 %. These results were obtained with different TRPA1 lysates showing the same peptide pattern after proteolysis. In addition, TRPA1 channel modifications after SM exposure were detected.

Conclusion: TRPA1 represents a potential target for alkylating agents which possibly modulate the channel via cysteine modifications. Here, the establishment of an isolation protocol with successful purification of human TRPA1 channel from HEK293 cells was demonstrated. This was confirmed by Western blot and LC-MS/MS analyses.

58

Alteration of EF-hand phosphorylation site affects $Ca_V1.3$ calcium channel whole-cell currents

S. Salamon[1], C. Fried[1], P. Despang[1], E. Kuzmenkina[1], J. Matthes[1]
[1]University of Cologne, Department of Pharmacology, Cologne, Germany

Introduction: Activity of $Ca_V1.3$ L-type voltage-gated calcium channels is regulated by calcium dependent inactivation (CDI), alternative splicing and phosphorylation.

Objectives: We investigate how these regulatory mechanisms are integrated to modulate $Ca_V1.3$ channels. In particular, we are interested in the role of the C-terminal EF-hand phosphorylation site S1475 under conditions of induced or prevented CDI.

Materials & methods: We performed whole-cell patch-clamp recordings of wildtype (WT) and mutated human $Ca_V1.3_{42}$ channel variants that either prevent (S1475A) or imitate (S1475D) phosphorylation of serine 1475. Recordings were obtained from HEK-293 cells transiently transfected with the respective $Ca_V1.3_{42}$ variant together with human auxiliary $\alpha_2\delta$-1 and β_{1b} subunits. To examine the effect of CDI, Ca^{2+} currents were recorded with and without co-transfected calmodulin (CaM). Ba^{2+} currents were recorded to exclude the influence of CDI. For current-voltage relationships, 500ms depolarizing pulses from -80mV to +50mV were applied from a holding potential of -100mV.

Results: Mutants mimicking phosphorylation or dephosphorylation had opposing effects on whole-cell current density. The phosphorylation imitating mutant S1475D had decreased Ba^{2+} (mean ± SD: -16.3 ± 8.9pA/pF; p=0.02) and Ca^{2+} (-8.1 ± 2.7pA/pF; p<0.01) current density in comparison to the WT (Ba^{2+}: -31.9 ± 9.7pA/pF and Ca^{2+}: -20.8 ± 4.1pA/pF). In contrast, the phosphorylation resistant mutant S1475A had similar Ba^{2+} (-35.93 ± 8.9pA/pF; p=0.61), but increased Ca^{2+} (-31 ± 5.6pA/pF; p<0.01) current density compared to the WT. Co-transfecting CaM increased the current density for both WT (-33.85 ± 10.2pA/pF; p<0.01) and S1475A (-43.8 ± 28pA/pF; p=0.21), while the inactivation was unchanged. Co-transfecting CaM together with S1475D, however, reduced Ca^{2+} currents (-5.1 ± 1.2pA/pF; p=0.02) and decreased inactivation (remaining current at 0mV: 15.8 ± 9% without and 50.7 ± 10% with co-transfected CaM; p<0.01).

Conclusion: The results indicate the functional relevance of S1475 in $Ca_V1.3_{42}$. CDI was affected by the S1475 phosphorylation state and the expression level of CaM. Single-channel recordings and binding studies may help to reveal underlying molecular mechanisms. Together with the ongoing experiments with the short isoform $Ca_V1.3_{42A}$ the results will shed light on how distinct regulatory mechanisms interact to differentially modulate $Ca_V1.3$ channel activity.

63

The role of Ca^{2+} activated potassium channels of intermediate conductance in breast cancer autophagy

D. Groß[1,2], H. Bischof[2], P. Ruth[1], T. Proikas-Cezanne[3], R. Lukowski[2]
[1]Institute of Pharmacy, University of Tuebingen, Pharmacology, Toxicology and Clinical Pharmacy, Tuebingen, Germany
[2]Institute of Pharmacy, University of Tuebingen, Department of Experimental Pharmacology, Tuebingen, Germany
[3]Interfaculty Institute of Cell Biology, University of Tuebingen, Department of Molecular Biology, Tuebingen, Germany

Introduction: Breast cancer (BC) is the most common malignancy and leading cause of cancer related death in women [1]. Ion channels regulate the cellular membrane potential and aberrant expression of potassium (K^+) channels has been shown to affect malignant cell behaviours in many tumour entities [2]. Despite promoting cancer cell growth, migration and spread it was suggested that K^+ channels modulate calcium (Ca^{2+}) signals, which are implicated in autophagic signalling pathways, in BC cells [3,5]. The interplay of autophagy and K^+ channels of intermediate conductance (IK) could represent a potential new target in the development and therapy of BC [4,5].

Objectives: To investigate how IK K^+ channels contribute to catabolic processes such as autophagy in BC cells.

Materials & methods: BC cells obtained from murine MMTV-PyMT control and IK knockout (KO) mice [5] were exposed to normal and nutrient-limiting conditions to study autophagic flux and autophagy-related markers such as LC3, p62, and ULK1. FRET-based live cell imaging was employed to further study the role of IK on intracellular Ca^{2+}, K^+, and ATP dynamics as well as AMPK and mTOR activity.

Results: Our experiments indicate an involvement of IK in modulating autophagic activity, as IK deficient BC cells showed increased rates of autophagy. This effect was majorly mediated by an altered mitochondrial energy homeostasis, as cells lacking IK showed decreased levels of oxidative phosphorylation, potentially caused by an altered subcellular Ca^{2+} homeostasis. Subsequently, we observed an increased activity of AMPK, a central intracellular energy sensing kinase, thereby promoting autophagy initiation and flux.

Conclusion: Our results emphasize that IK activity is impacting on the subcellular Ca^{2+} homeostasis and the mitochondrial metabolic activity, causing a compensatory

upregulation of autophagic rates. These results highlight, that targeting IK channels in BC might represent suitable to decelerate cancer cell metabolism.

[1] Siegel et al. 2016 (CA Cancer J Clin)

[2] Huang and Jan 2014 (J Cell Biol)

[3] Kondratskyi et al. 2018 (Autophagy)

[4] Zhang et al. 2021 (Autophagy)

[5] Steudel et al. 2017 (Molecular Oncology)

65

IRAG2 interacts with IP_3-receptor types 1, 2 and 3 and regulates intracellular Ca^{2+}

S. Prüschenk[1], M. Majer[1], R. Schreiber[2], J. Schlossmann[1]
[1]University of Regensburg, Pharmacology and Toxicology, Regensburg, Germany
[2]University of Regensburg, Physiology, Regensburg, Germany

Background: The inositol 1,4,5-triphosphate receptor-associated 2 (IRAG2), also known as lymphoid-restricted membrane protein (LRMP) or Jaw1, is a type II membrane protein that is localized to the cytoplasmic face of the endoplasmic reticulum (ER) and shares a homology of 44% with the inositol 1,4,5-triphosphate receptor-associated cGMP kinase substrate 1 (IRAG1), especially in its coiled coil domain. As IRAG1 interacts with inositol trisphosphate receptors (IP_3R) via its coiled coil domain and modulates Ca^{2+} release from intracellular stores, we investigated if IRAG2 has similar interaction partners like IRAG1. Since we detected IRAG2 expression in pancreatic acinar cells (PACs), we analyzed if IRAG2 modulates intracellular Ca^{2+} release in these cells and if IRAG2 impacts exocrine pancreatic function like amylase secretion.

Methods: Expression and localization of IRAG2 in the pancreas was investigated via X-Gal-staining using IRAG2-KO mice, that express β-galactosidase as a reporter for IRAG2. Via coimmunoprecipitation interaction of IRAG2 with different IP_3R subtypes in the pancreas was analyzed. Ca^{2+} signaling in WT and IRAG2-KO PACs was examined by Fura-2-AM ratiometry. Furthermore, we performed an amylase secretion assay in isolated PACs and determined total amylase content in pancreata from WT and IRAG2-KO mice via immunohistochemistry.

Results: X-Gal-staining showed localization of IRAG2 in PACs and coimmunoprecipitation revealed interaction of IRAG2 with IP_3R subtypes 1, 2 and 3 in the pancreas. IRAG2-KO cells revealed lower basal, unstimulated intracellular Ca^{2+} levels than WT cells, though carbachol induced Ca^{2+} release normalized to basal release is higher in IRAG2-KO cells. Basal amylase secretion was lower in IRAG2-KO cells and maximum amount of secreted amylase upon stimulation with carbachol was also lower in IRAG2-KO. However, amylase secretion upon stimulation normalized to basal amylase secretion was higher in IRAG2-KO. Immunohistochemical analysis of pancreata showed that a higher amount of amylase remained in the PACs from IRAG2-KO compared to WT.

Conclusion: Our data suggest that IRAG2 modulates intracellular Ca^{2+} signaling and increases basal Ca^{2+} release in PACs. Furthermore, amylase secretion is affected due to modulation of Ca^{2+} release in the PACs. As loss of IRAG2 leads to an accumulation of amylase in the pancreas, it is possible that IRAG2 might play a role in prevention of severe pancreatic diseases like pancreatitis.

72

Various roles of two-pore channel 1 for endocytosis and regulation of growth factor receptor expression

S. Großmann[1], R. T. Mallmann[1], N. Klugbauer[1]
[1]Albert-Ludwigs-Universität Freiburg, Institut für Experimentelle und Klinische Pharmakologie und Toxikologie, Freiburg im Breisgau, Germany

Introduction: Two-pore channels (TPCs) are a small family of ion channels located in the membranes of intracellular organelles such as endosomes and lysosomes. There are only two representatives expressed in rodents and humans, TPC1 and TPC2.

They were shown to provide spatiotemporally restricted Ca2+-currents, likely responsible for fusion and/or fission events of endolysosomal membranes and thereby for intracellular vesicle trafficking.

Objectives: We recently investigated the effects of TPC1 loss on gene expression via RNA sequencing of wildtype and TCP1 knockout MEF cells. We observed an altered expression of plenty of different genes - not only in the endolysosomal context but also growth factor receptors and genes related to different signaling pathways as well. To gain further insights into how TPCs regulate expression of various genes, we took a closer look onto mechanisms of intracellular trafficking and receptor internalization and processing.

Material and Methods: A global RNA sequencing of three independent samples of WT and TPC1-KO MEF cells was performed. Computational analysis and evaluation of the data was made using tools integrated in the Galaxy platform and ClueGO software. Western blot of whole cell lysates of MEF cells were performed and probed for Caveolin 1. We carried out live cell imaging using wildtype and TPC knockout MEF cells expressing fluorescently labelled EGF-receptor and organellar markers.

Results: We observed a massive change in gene expression patterns in TPC1 knockout vs. wildtype cells with regard to proteins involved in endocytosis. One striking finding was the massive downregulation of key players of caveolae, Caveolin 1 and 2. We confirmed the decrease of Caveolin 1 protein levels in TPC knockout cells by Western analysis. We investigated individual steps of EGF-receptor trafficking, from endocytosis to intracellular transportation, using live cell imaging approaches.

Conclusion: RNA-seq data uncovered numerous aspects on the role of TPC1 for regulation of growth factor receptor gene expression. Delayed intracellular trafficking of endocytosed growth factor receptors leads to altered downstream signaling, associated with different feedback loops causing differential gene expression of other receptors and signaling proteins. Our results show that TPC1 affects endocytic players such as caveolins and thereby regulate membrane expression and response of various receptors.

80

An inhibitory Function of TRPA1 Channels in TGF-β1-driven Fibroblast to Myofibroblast Differentiation

F. Geiger[1], C. Staab-Weijnitz[2], A. Breit[1], T. Gudermann[1], A. Dietrich[1]
[1]Walther Straub Institute of Pharmacology and Toxicology, Member of the German Center for Lung Research (DZL), LMU-Munich Germany, München, Germany
[2]Comprehensive Pneumology Center, Member of the German Center for Lung Research (DZL), Helmholtz-Zentrum München, Munich, Germany, München, Germany

Question: Transient receptor potential anykrin 1 (TRPA1), a non-selective cation channel, is activated by exposure to several chemicals including allyl isothiocyanate (AITC) and evokes Ca2+ influx into the cells. This protein was originally identified in human pulmonary fibroblasts (HPFs), which form myofibroblasts after application of transforming growth factor β1 (TGF-β1) as a key event in the development of lung fibrosis. We aimed to elucidate its role in HPFs and TGF-β-driven fibroblast differentiation.

Methods: Expression and function of TRPA1 in TGF-β1-mediated fibroblasts to myofibroblast differentiation was analyzed in primary human pulmonary fibroblasts from five donors (diversity in age, sex and race). TRPA1 specific siRNAs were established to evaluate the impact of TRPA1 knockdown. HPFs were analyzed using transcriptome sequencing, qRT-PCR, immunoblotting, luciferase reporter assays and immunofluorescence. Functional analysis included electrical cell-substrate impedance sensing (ECIS), Ca2+ imaging as well as cell viability and apoptosis assays.

Results: TRPA1 mRNA expression was significantly reduced after adding TGF-β1 to primary HPFs, while expression of fibrosis markers (e.g. alpha smooth muscle actin (αSMA), plasminogen activator inhibitor (PAI), fibronectin (FN1) and collagen (Col1a1)) was increased. Down-regulation of TRPA1-mRNA by siRNA targeting in HPFs results in a similar increase in pro-fibrotic marker proteins. Moreover, AITC-induced Ca2+ entry was decreased after TGF-β1 treatment and by application of TRPA1 siRNAs, while AITC-treatment alone did not reduce cell viability or enhanced apoptosis. Cell barrier function increased after addition of TRPA1 siRNAs or TGF-β1 treatment. Moreover, AITC-induced TRPA1 activation augmented ERK phosphorylation, which might be responsible for inhibition of TGF-β-signaling.

Conclusion: Our results suggest an inhibitory function of TRPA1 channels in TGF-β1-driven fibroblast to myofibroblast differentiation by ERK-mediated inhibition of TGF-β-signaling. Therefore, activation of TRPA1 channels might be protective during the development of pulmonary fibrosis in patients.

85

Distinct functions of HCN3 channels in sensory neurons

K. Metzner[1], T. Hussein[1], S. Fenske[2], M. Biel[2], A. Schmidtko[1]
[1]Goethe University Frankfurt, Institute of Pharmacology and Clinical Pharmacy, Frankfurt am Main, Germany
[2]Ludwig-Maximilians-Universität München, Center for Integrated Protein Science (CIPS-M) and Center for Drug Research, Department of Pharmacy, Munich, Germany

Hyperpolarization-activated, cyclic nucleotide-gated (HCN) channels are a family of ion channels that are primarily activated by hyperpolarization and carry a mixed Na^+ and K^+ current. In mammals, the HCN family consists of four isoforms (HCN1-4), which are widely distributed throughout the body in a tissue-specific manner. HCN channels are involved in various physiological and pathophysiological processes, the most important being the generation of spontaneous electrical activity in the heart and the control of neuronal excitability. Previous studies detected HCN3 expression in sensory neurons. However, unlike HCN1, HCN2 and HCN4, the functions of HCN3 in sensory neurons are poorly understood.

In order to elucidate the distribution of HCN3 in sensory neurons we performed fluorescent *in situ* hybridization experiments of HCN3 together with established cellular markers in dorsal root ganglia (DRG) of mice. To assess a possible function of HCN3 in somatosensory processing, we performed behavioral tests in HCN3-deficient and wild-type (WT) mice and patch-clamp experiments in primary cell culture of dissociated DRG neurons.

We found HCN3 mRNA to be highly expressed in subpopulations of sensory neurons that detect and process information about pain, itch, temperature, and touch. We observed a decreased hyperpolarization-activated K^+ current (I_h) in subpopulations of sensory neurons of HCN3$^{-/-}$ mice as compared to WT mice.

Together, these results show that HCN3 channels exert specific functions in sensory neurons and might present a novel target for therapeutic approaches.

95

The contribution of NMDA receptors to pancreatic islet cell communication involves the co-activator glycine

A. Gresch[1], M. Düfer[1]
[1]Institut für Pharmazeutische und Medizinische Chemie, Pharmakologie, Münster, Germany

Question: Coordinated electrical activity is essential for adequate insulin secretion. To study intercellular coupling within an islet of Langerhans, so-called slow potentials (SPs) can be identified using microelectrode arrays (MEAs). SPs reflect the propagation of extracellular current flow between coupled cells. Recently, it has been shown that NMDA receptors (NMDARs), which are a potential target for the treatment of type 2 diabetes, are involved in the functional coupling of beta cells and therefore stimulation of NMDARs should affect SPs. To investigate SPs by activating the NMDAR requires the simultaneous binding of glutamate and a co-activator, such as glycine or serine. Given that glycine and serine (in combination with NMDA) exerted different effects on the membrane potential of individual β-cells, both co-agonists were investigated separately for their effects with respect to SPs.

Methods: Islets were isolated from C57Bl/6N mice. The electrical activity of whole islets was determined with MEAs.

Results: Islets cultured on MEAs were acutely stimulated with a glucose concentration of 8 mM to elicit a typical oscillatory pattern in the form of bursts and electrically silent interburst intervals. The FOPP (time with bursting activity related to the entire time interval) did not alter after the addition of NMDA/glycine (500/10 µM; control: 12±6 % *vs*. NMDA/glycine: 12±6 %, n=14, p=0.95). An identical series of MEA experiments using D-serine (100 µM) instead of glycine also showed no change in the FOPP (control: 26±8 % *vs*. NMDA/D-serine: 28±13 %, n=15, p=0.52). Evaluation of the frequency of the extracellular voltage waves within the bursts using a 20 Hz low-pass filter revealed no differences between the control and NMDA/glycine (control: 1.3±0.8 Hz *vs*. NMDA/glycine: 1.5±0.8 Hz, n=13, p=0.40). SPs were analyzed with a 2 Hz low-pass filter. Remarkably, the SPs exhibited a significant increase in frequency in response to NMDA/glycine (control: 0.5±0.2 Hz *vs*. NMDA/glycine: 0.6±0.2 Hz, n=13, p=0.012). This was not the case in the series of experiments with NMDA/D-serine (control: 0.9±0.3 Hz *vs*. NMDA/D-serine: 0.9±0.3 Hz, n=15, p=0.56).

Conclusions: Activation of NMDARs by NMDA/glycine influences cell communication within the islet of Langerhans. The different effects of NMDA/glycine and NMDA/D-serine on the frequency of slow potentials hint that the activator combination of NMDA/glycine might target a different collective of NMDAR subtypes.

119

Distinct functions of Slick potassium channels in the processing of pain and itch

P. Engel[1], C. Flauaus[1], F. Zhou[1], J. Petersen[1], P. Ruth[2], R. Lukowski[2], A. Schmidtko[1], R. Lu[1]
[1]Goethe Universität Frankfurt/Main, Institut für Pharmakologie und klinische Pharmazie, Frankfurt, Germany
[2]University, Institut für Pharmazie, Pharmakologie, Toxikologie und Klinische Pharmazie, Tübingen, Germany

Question: The sodium-dependent potassium channel Slick (also termed KNa1.2, Kcnt2, or Slo2.1) is expressed in dorsal root ganglia (DRG) and the spinal cord. However, the detailed distribution of Slick in these tissues and its functional role in somatosensory processing remains poorly understood.

Methods: The tissue distribution of Slick was investigated using immunohistochemistry, *in* situ hybridization, western blot and RT-qPCR. The behavior of mice lacking Slick globally and conditionally in the spinal cord was assessed in different models of pain and itch.

Results: We found that Slick is localized to subpopulations of sensory neurons and dorsal horn interneurons. Slick-deficient mice showed increased responses to noxious heat and intraplantar injection of algogens. Unexpectedly, Slick-deficient mice displayed reduced scratching behavior after administration of pruritogens.

Conclusions: Our findings indicate that Slick exerts distinct functions in the processing of pain and itch.

158

NMDA receptors influence mouse pancreatic beta cells by activation of KCa3.1 channels

H. Noguera Hurtado[1], R. Wiggers[1], B. Wünsch[2], M. Düfer[1]
[1]Pharmaceutical and Medicinal Chemistry, Department of Pharmacology, Münster, Germany
[2]Pharmaceutical and Medicinal Chemistry, Münster, Germany

Question: The use of NMDA receptor (NMDAR) antagonists is studied as a new option for therapy of type 2 diabetes. There is evidence that selective inhibition of NMDARs exerts a protective effect on pancreatic beta cells.

This study investigates the mechanism mediated by NMDARs and the possible involvement of KCa3.1 channels. For this purpose, NMDAR antagonists specific to the GluN2B subunit (WMS-1410 and Ro 25-6981), and the KCa3.1 antagonist senicapoc were used.

Methods: Islets or beta cells were isolated from C57Bl6/N mice. Glucose-stimulated insulin secretion was measured by radioimmunoassay and K^+current by the patch-clamp technique. Apoptotic cells were determined by TUNEL assay.

Results: Glucose-induced insulin secretion of mouse islets was decreased after treatment with 500 µM NMDA for 24 h. WMS-1410 (1 µM) prevented this effect. (G15: 3 ± 1; G15 + NMDA: 2.1 ± 0.9; G15 + NMDA + WMS-1410: 3 ± 1 ng/(islet*h), n=7; p< 0.05 *vs.* NMDA). To assess whether insulin depletion by NMDA was driven by an interaction of NMDAR with K^+ channels, K^+ currents of beta cells were analyzed. K^+ currents were increased by NMDA/Gly (500/10 µM) (Control: 111 ± 44, n=30; NMDA/Gly: 156 ± 35, n=26; p<0.001). In the presence of WMS-1410 K^+ currents were not altered by NMDA/Gly any more (NMDA/Gly + WMS-1410: 124 ± 40 pA/pF, n=24; n. s. *vs.* control). The K_{ATP} channel was not involved as the NMDA- and WMS-1410-mediated changes also occurred in beta cells of SUR1-knockout mice. The involvement of GluN2B was confirmed by experiments with Ro 25-6981. To test whether the increase in K^+ current was carried out by KCa3.1 channels, senicapoc (1 µM) was used. Similar to GluN2B inhibition, blocking KCa3.1 channels with senicapoc prevented the effect of NMDA/Gly. (Control: 106 ± 31, n=35; NMDA/Gly: 168 ± 36, n=31; NMDA/Gly + senicapoc: 122 ± 37 pA/pF, n =29; p<0.001). The inhibition of KCa3.1 was found to be involved in the protective effect of WMS-1410 from glucolipotoxicity-induced cell death.

Conclusions: Our data reveal an interaction between NMDAR and KCa3.1 channels in beta cells. This might trigger a hyperpolarized state and consequently a decrease in insulin secretion. NMDAR antagonists targeting the GluN2B subunit restore insulin secretion by disrupting the interplay between NMDAR and KCa3.1. Furthermore, reduced KCa3.1 activity seems to be involved in the protective effect of WMS-1410 on islet cell survival.

203

Influence of *Petasites hybridus* extract on intestinal handling of histamine – involvement of the organic cation transporter 3

K. Brecht Brüngger[1], L. Mettler[1], V. Butterweck[2], H. Meyer zu Schwabedissen[1]
[1]Universität Basel, Departement Pharmazeutische Wissenschaften, Biopharmazie, Basel, Switzerland
[2]Max Zeller und Söhne AG, Romanshorn, Switzerland

Histamine intolerance (HIT) or food-derived histaminosis is a common diagnosis in Western population with an estimated prevalence of 1% in a population. In patients with HIT exposure to exogenous histamine is linked to various symptoms such as rhinal congestion, dizziness, headache, tachycardia, hypotension, diarrhea, nausea, and flush. The uptake of food-derived histamine is assumed to be modulated by specific mechanisms in the intestine. Here, the diamine oxidase (DAO) and the histamine-N-methyltransferase (HNMT) metabolize histamine, while transport proteins are believed to contribute to the transcellular flux of histamine.

In previous studies it has been shown, that the *Petasites hybridus* CO2-leaf extract Ze 339 (Tesalin®) decreased histamine levels in nasal laryngeal fluids. The aim of the current study was to investigate the influence of Ze 339 on the intestinal mechanisms involved in the handling of histamine.

We used differentiated Caco-2 cells validated for the presence of DAO, HNMT and organic cation transporter 3 (OCT3; SLC22A3) to investigate the effect of Ze 339 on their mRNA and protein expression by real-time PCR and Western Blot analysis. Even though Ze 339 reduced the mRNA levels of HNMT and DAO, there was no influence on their protein levels. We further tested the effect of Ze 339 on DAO release from Caco-2 cells polarized on permeable supports (Transwell®) and DAO enzymatic activity. Here we found that Ze 339 neither affected the basal release of DAO from Caco-2 cells, nor changed DAO activity. However, applying Caco-2 Transwell® transport studies to assess the influence of the herbal extract on the transcellular histamine flux we observed a significant increase in the basal to apical flux (Papp b to a) in presence of high concentrations of Ze 339. This effect was limited to the early phase of the experiment. Since the luminal monoamine transporter OCT3 is one transporter possibly contributing to this finding we examined the influence of Ze 339

on the OCT3-mediated histamine uptake in MDCKII cells stably overexpressing OCT3. We revealed a dose-dependent inhibition with an estimated IC50 of 26.9 mg/mL for the extract.

In conclusion, we report an effect of Ze 339 on the transcellular transport of histamine resulting in a high efflux ratio, where inhibition of the luminal uptake transporter OCT3 may contribu

219

N^6-methyladenosine activates Ca^{2+}-influx through CRAC channels and facilitates antigen-evoked degranulation in primary mast cell

F. C. Haffelder[1], C. Grimm[2], C. E. Müller[3], M. Freichel[1], **V. Tsvilovskyy**[1]
[1]Heidelberg University , Institute of Pharmacology, Heidelberg, Germany
[2]Ludwig-Maximilians-University Munich, Walther-Straub-Institute of Pharmacology and Toxicology, Muenchen, Germany
[3]University of Bonn, Pharmaceutical Institute, Pharmaceutical & Medicinal Chemistry, Bonn, Germany

Mast cells are immune cells that play an essential pathophysiological role in allergy and inflammatory processes. A key feature of mast cell activation triggered by extracellular messengers, such as adenosine, is the increase of cytosolic Ca^{2+} concentration caused by the release of intracellularly stored Ca^{2+} and the influx of extracellular Ca^{2+} (1). N^6-methyladenosine (m6A) is the most abundant chemical modification of the messenger RNA and represents a widely recognized epigenetic mark in RNA. Following RNA breakdown, modified nucleosides are excreted as metabolic end products, and, N^6-methyladenosine was recently reported to be an activator of rat basophilic leukemia cells with a high affinity and activation potency to purinergic A3 adenosine receptors (2). In this study, we examined the effect of m6A on Ca^{2+} signaling in murine peritoneal mast cells (PMCs), a mature connective tissue-type mast cell model. We observed a potent m6A-evoked release of intracellularly stored Ca^{2+} and extracellular Ca^{2+} entry over a broad concentration range (0.1 nM to 30 µM). Our pharmacological analysis revealed that GSK-7975A (10 µM), a specific inhibitor of calcium release activated channels (CRAC) (3), abolished m6A-evoked Ca^{2+} entry. This suggests a prominent role of ORAI protein formed calcium channels in m6A-evoked PMC activation. The Gq-protein mediated PLC activation could be important for the depletion of intracellular calcium stores and subsequent CRAC activation. Our experiments revealed a high sensibility of the Ca^{2+} release from intracellular stores to Gq inhibition using YM-254890 (1 µM). The PLC blocker U73122 effectively suppressed m6A-evoked Ca^{2+} release whereas its non-active analogue U73343 did not. Using the ß-hexosaminidase release assay we showed that m6A significantly potentiates antigen-induced degranulation of PMCs. In sum, our study demonstrates a new role of m6A as a signaling molecule in primary connective type mast cells by operating as a potent facilitator of mast cell activation.

(1) Huber et al., J Allergy Clin Immunol 144(4S): S31-S45 (2019).

(2) Ogawa et al., Molecular Cell 81: 659-674 (2021s).

(3) Tsvilovskyy et al., Cell Calcium 71: 24-33 (2018).

222

Stereoselectivity in the Monoamine Transport by Human Monoamine Transporters and Organic Cation Transporters 1, 2 and 3

L. Gebauer[1], M. Rafehi[1], J. Brockmöller[1]
[1]Institute of Clinical Pharmacology, University Medical Center Göttingen, Göttingen, Germany

Introduction: Stereoselectivity in drug membrane transport has only scarcely been investigated in contrast to the prominent role of stereoselectivity in receptor binding and drug metabolism. Synaptic levels of monoamine neurotransmitters are controlled by transporter-mediated uptake. In addition to the high-affinity monoamine transporters (MATs), also polyspecific organic cation transporters (OCTs) contribute to monoamine clearance in the central nervous system and in peripheral organs. Although the endogenous neurotransmitters norepinephrine and epinephrine are always the *(R)*-enantiomers in humans, several structural analogues can be found as racemic mixtures for instance in dietary supplements.

Objectives: In this study, we investigated the stereoselective transport of racemic epinephrine and norepinephrine as well as 10 structural analogues of these neurotransmitters by the human norepinephrine (NET), dopamine (DAT) and serotonin transporter (SERT) as well as by the organic cation transporters 1, 2 and 3.

Materials and methods: Transport was studied by cellular uptake assays of racemic substrates using HEK293 cells stably overexpressing the transporters. Differences in the ratio of taken up enantiomers were assessed by chiral chromatography and quantified by mass spectrometry.

Results: MATs showed uptake of the investigated compounds with varying degree of stereoselectivity. Observed differences in the transport of both enantiomers ranged from none up to a two-fold higher transport capacity as for instance for the *(R)*-enantiomer of epinephrine over its respective counterpart by NET. In the direct comparison, stereoselectivity of NET and DAT transport was higher for substrates with a single *N*-methylation. Interestingly, SERT showed the opposite enantiopreference with some substances compared to NET and DAT. Although known for their polyspecificity, also the OCTs showed stereoselective uptake of many tested substrates as well.

Conclusions: Stereoselectivity was observed in the transport of many monoamines by different transporters. An interesting finding was that stereoselectivity was not always uniform for related transporters. Data on stereoselective transport may provide important insights into substrate binding and transport in the comparative analysis of high and low affinity organic cation transporters.

242

Amino acids cysteine$_{36}$ and phenylalanine$_{32}$ confer substrate selectivity of fenoterol and trospium uptake: lessons from comparing human and mouse OCT1 orthologs

M. J. Meyer[1], P. Schreier[1], M. Basaran[2], T. Seitz[3], J. Brockmöller[3], B. Zdrazil[2], M. V. Tzvetkov[1]
[1]University Medicine Greifswald, Institute of Pharmacology, C_DAT, Greifswald, Germany
[2]University of Vienna, Department of Pharmaceutical Chemistry, Wien, Austria
[3]University Medical Center Göttingen, Institute of Clinical Pharmacology, Göttingen, Germany

Organic cation transporter OCT1 (SLC22A1) is an uptake transporter that may be a limiting step in hepatic metabolism and excretion of cationic and weakly basic drugs. OCT1 transports structurally highly diverse substrates, but the mechanisms conferring this polyspecificity are unknown. Here, we comparatively characterized the transport kinetics of human and mouse OCT1 orthologs to identify amino acids contributing to the polyspecificity of OCT1 transport.

Comparing the uptake kinetics in HEK293 cells stably overexpressing human and mouse OCT1, we observed significant differences in the uptake of 13 out of 24 analyzed drugs, model substances, and endogenous compounds. The most extreme species differences in uptake were observed for fenoterol and trospium. Fenoterol was transported with 8-fold higher affinity but 9-fold lower capacity (v_{max}) by human OCT1, whereas trospium was transported with 11-fold higher affinity but 9-fold lower capacity by mouse OCT1.

Using human-mouse chimeric OCT1 and site-directed mutagenesis, we identified single amino acids in transmembrane helix 1 as causative for the species-specific differences of fenoterol and trospium transport. Substitution of cysteine$_{36}$-to-tyrosine$_{36}$ resulted in the reversal of affinity and capacity of fenoterol uptake and substitution of phenylalanine$_{32}$-to-leucine$_{32}$ in the reversal of affinity and capacity of trospium uptake from mouse to human and human to mouse phenotype, respectively. Comparing the uptake kinetics of structurally similar β2-adrenergics points to the second phenol ring as essential for the higher affinity conferred by cysteine$_{36}$ in human OCT1. These results were supported by structure-based computational modeling.

This is the first study reporting single amino acids as determinants of OCT1 polyspecificity and suggests that structure-to-function data about OCT1 may not be directly transferrable between substrates nor between species.

Pharmacology – Drug transport/delivery and metabolism

5

Expression of hepatic drug-metabolizing enzymes is significantly affected by different forms of liver diseases and correlated with the liver functional state.

M. Drozdzik[1], J. Lapczuk-Romanska[1], **C. Wenzel**[2], S. Szelag-Pieniek[1]; Post[3], Ł. Skalski[1], M. Kurzawski[1], S. Oswald[4]
[1]Pomeranian Medical University, Department of Experimental and Clinical Pharmacology, Szczecin, Poland
[2]University Medicine Greifswald, Institute of Pharmacology, Center of Drug Absorption and Transport, Greifswald, Germany
[3]County Hospital, Department of General and Transplantation Surgery, Szczecin, Poland
[4]Rostock University Medical Center, Institute of Pharmacology, Rostock, Germany

Due to the high abundance of drug metabolizing enzymes (DME) in the liver, it is one of the main organs where drug metabolism takes place. Thus, liver pathologies that affect expression and function of DME are expected to influence phase I and II metabolism of drugs and in turn drug efficacy and safety in a significant manner. We therefore investigated the expression of clinically relevant DMEs in samples of liver tissues (N=87) from patients suffering from various liver diseases (hepatitis C, alcoholic liver disease, autoimmune hepatitis, primary biliary cholangitis and primary sclerosing cholangitis) on mRNA- and protein level via real-time RT-PCR and targeted proteomics, respectively. The results were correlated with the liver functional state, expressed by the Child-Pugh score. Our results clearly show that the Child-Pugh class is associated with changes in the transcriptional expression and protein levels of several CYP and UGT enzymes. For example, deterioration of liver function is associated with a significant decrease in protein abundance of CYP1A2, CYP2C8, CYP2C9, CYP2E1, CYP3A4 and UGT2B7 in Child-Pugh score C compared to control samples. Moreover, it was found that some enzymes are more vulnerable to pathological changes than others: CYP2E1 is already downregulated in class A livers, while CYP2C8, CYP3A4, CYP1A2 and CYP2C9 are only significantly affected in class C. In addition, our study provides data on the abundance of DMEs in different forms of liver disease. Here, CYP1A1 abundance was found to be markedly reduced in

cholestatic pathologies, while hepatitis C is characterized by a decrease in CYP2E1 and UGT2B7 abundance. Alcoholic liver disease is associated with significant reduction of various enzymes (CYP1A2, CYP2C8, CYP2D6, CYP2E1, CYP3A4 and UGT2B7), unlike autoimmune hepatitis which lead to no significant changes in our study. Our results clearly show that liver diseases have major impact on the abundances of clinically relevant DMEs which are expected to translate to compromised drug metabolism. Data on disease-related changes in the abundance of DMEs may be useful for physiologically-based pharmacokinetic modeling and the prediction of appropriate dose adjustments, which is expected to improve the efficacy and safety of drugs.

45

Is Manumycin A really a potent Farnesyltransferase inhibitor?

P. K. Altrogge[1], A. Hagemann[1], M. C. Kehrenberg[1], D. Diehl [1], L. Weber[1], H. S. Bachmann[1]
[1]Witten Herdecke University, Pharmacology and Toxicology, Centre for Biomedical Education and Research, Witten, Germany

Objective: Farnesyltransferase (FTase) is an enzyme, which belongs to the prenyltransferases and attaches a C-15-moiety to a specific motif (-CAAX) of around 200 human proteins, like e.g. Ras. Only farnesylated proteins can fulfil their physiological role. Furthermore, farnesylation is a crucial step in different diseases like cancer, progeria or hepatitis D. Therefore, the inhibition of FTase might be an important step in fighting these diseases. In 1993 it was postulated, that the antibiotic Manumycin A (Manu-A) is a specific FTase inhibitor (FTI) against yeast FTase. Since then, almost all publications concerning Manu-A refer to these results. Most of the collected data analysing the inhibitory effect of FTase are from cell culture experiments and *in-vivo* experiments with *Caenorhabditis elegans*. Until now, there are no information about the kinetic parameters of *C. elegans* FTase or the IC_{50} for Manu-A inhibiting purified human FTase.

Material & Methods: We heterologously expressed and purified *C. elegans* and human FTases and investigated the thermal optimum as well as K_M and IC_{50} by continuous enzyme activity assays. Furthermore, we examined the effect of Manu-A on LnCaP cell line by cell culture and MTT-assays. Additionally, a literature search was performed for likely alternative Manu-A targets.

Results: Manu-A does not inhibit cell free FTase in physiologically or pharmacologically relevant concentrations. The IC_{50} of the human FTase is 32 µM and the one for *C. elegans* is 45 µM. Moreover, the cytotoxic effect of Manu-A on LnCaP cells started at much lower concentrations (15 µM). Our literature search indicates that Manu-A is also an inhibitor or inducer of several other enzymes. For example, Manu A inhibits thioredoxin reductase 1 with an IC_{50} of 272 nM. In addition, Manu-A induces the proapoptotic enzymes caspase 9 and caspase 3.

Conclusion: Different studies indicate that Manu-A has an influence on a variety of different proteins, which are all related to apoptosis. Having a closer look at these proteins, they also seem to interlock. Therefore, we suspect that the inhibitory effect of Manu-A on FTase is neglectable but that it rather promotes apoptosis through other pathways. Our results give a new perspective on the role of Manu-A and a possible starting point for the investigation of innovative applications for this drug aside from FTase inhibiton.

66

Comparison of two St. Johns wort formulations for their impact on Pregnane X receptor regulated CYP3A - hyperforin content matters

A. Schäfer[1], M. Rysz[1], J. Schädeli[1], M. Fehr[1], I. Seibert[1], J. Bouitbir[1], H. Meyer zu Schwabedissen[1]
[1]University of Basel, Pharmaceutical Sciences, Basel, Switzerland

St. John's wort is a popular herbal remedy often used to treat mild to moderate depressive symptoms. One constituent of St. John"s wort is hyperforin, whose concentration is highly variable across different commercially available St. John"s wort formulations. Importantly, hyperforin is known to be responsible for fatal drug-herb interactions observed in patients. The mechanism underlying these interactions is the hyperforin-mediated activation of PXR, which induces expression of genes involved in drug metabolism such as CYP3A4 and ABCB1. The involvement of hyperforin is supported by findings in a clinical study where the low hyperforin content formulation Rebalance® did not exert an impact on the pharmacokinetics of probe drugs of drug metabolism.

In this study, we intend to further investigate and compare the interaction potential of two St. John's wort formulations namely Hyperiplant® (3-6 mg/ 100 mg extract of hyperforin content) and Rebalance® (<0.2 mg/ 100 mg extract of hyperforin content). Applying a cell based reporter gene assay and mRNA expression analysis in rat and human liver cell lines, we were able to show a much lower impact of hyperforin on the rat compared to the human PXR regulated CYP3A isoforms. Surprisingly, Hyperiplant® and Rebalance® induced expression of the rat PXR target genes Cyp3a1/ Cyp3a2 whereas in the human system we observed induction only after Hyperiplant® treatment and no such effect in cells treated with Rebalance®. In the next step, we conducted an *in vivo* rat study, where the impact of a 10-day treatment with Hyperiplant® (400 mg/ kg) or Rebalance® (400 mg/ kg) was assessed. In animals treated with Hyperiplant®, expression of Cyp3a1 in the liver was significantly induced on mRNA and protein level. No such effect was observed for Rebalance®. Furthermore, testing Cyp3a-activity in rat liver microsomes revealed that Hyperiplant® but not Rebalance® treatment increased the formation 6-β-OH-testosterone. Further studies are warranted to elucidate the species-differences in response to hyperforin especially considering the herein observed *in vitro-in vivo* discrepancies.

87

Role of the ABC transporter ABCB1 in therapy of Glioblastoma multiforme with Temozolomide, Carmustine and Lomustine

L. Radtke[1], A. Majchrzak-Célinska[2], C. Awortwe[1], I. Vater[3], I. Nagel[3], I. Cascorbi[1], M. Kähler[1]
[1]Institute of Experimental and Clinical Pharmacology, Kiel, Germany
[2]Department of Pharmaceutical Biochemistry, Poznan University of Medical Science, Poznan, Poland
[3]Institute of Human Genetics, Kiel, Germany

Question: With a five-year survival rate of only 6.8%, glioblastoma multiforme (GBM) is one of the most common malignant tumors of the human brain. Alkylating agents being able to cross the blood-brain-barrier are a pillar of therapy, among them temozolomide and nitrosoureas, such as lomustine and carmustine. However, success is limited by primary and acquired therapy resistances. While ABC transporters are known to limit the transport through the blood-brain barrier, their role in drug resistance of GBM cells remains controversial. Here, we investigated the role of ABCB1 and ABCG2 in the development of resistances against temozolomide, carmustine and lomustine in GBM cells.

Methods: The GBM cell lines A-172, U-138MG and T98G were analyzed with inhibition assays using cyclosporin A. mRNA expression was measured using RT-qPCR. An *ABCB1* knockout model was established using CRISPR/Cas9-genome editing of T98G cells. Rescue of *ABCB1* expression as well as an overexpression model were obtained using *ABCB1*-coding plasmid transfection. Drug transport was investigated via indirect transport assays using rhodamine 123. Drug susceptibility was analyzed by performing a series of experiments including WST assay, colony formation assay, scratch assay and Ki-67 assay.

Results: *ABCB1* and *ABCG2* expression was detected in T98G, but bearly in A-172 and U-138MG cells. Cotreatment with temozolomide and the ABCB1-inhibitor cyclosporin led to a 2-fold reduction in cell viability of T98G cells in tested concentrations (0.2 mM: $p<0.002$; 1 mM: $p<0.001$). ABCB1-mediated rhodamine 123 transport was reduced by temozolomide (1.6-fold, $p<0.001$) indicating competition to almost the same extent as cyclosporine A (1.5-fold, $p<0.002$). Using CRISPR/Cas9, four homozygous *ABCB1* knockout T98G cell lines were established and validated by sequencing. The *ABCB1* knockouts were confirmed by lower ABCB1-mediated efflux than the wildtype or the wildtype with cyclosporin A. Cell fitness of ABCB1 wildtype and knockout cells was dose-dependently altered in the presence of temozolomide and carmustine, but not lomustine.

Conclusions: Our data indicates that ABCB1 contributes to a diminution of treatment response in GBM in vitro, while ABCG2 seems to be of minor relevance. There was indirect evidence on competition of temozolomide as well as carmustine but not lomustine with ABCB1 transport, indicating that transporter mediated efflux might play a role as a possible chemoresistance mechanism of GBM.

88

Inhibition of human carbonyl-reducing enzymes by plant anthrone and anthraquinone derivatives

A. G. Adomako-Bonsu[1], M. Westermann[1], S. Thiele[1], S. S. Çiçek[2], H. J. Martin[1], E. Maser[1]
[1]Universität Klinikum Schleiswig Holstein, Institut für Toxikologie und Pharmakologie für Naturwissenschaftler, Kiel, Germany
[2]Kiel University, Institute of Pharmacy, Kiel, Germany

Question: Aldo-keto reductases (AKR) and short-chain dehydrogenases/reductases (SDR), which catalyse NAD(P)H-linked oxido-reductions of various substrates, such as carbohydrates, reactive lipid aldehydes and steroids, are also essential in Phase I metabolism of xenobiotics. In humans, dysregulation of carbonyl reductases has been linked to the development of cancers, diabetes, and other metabolic disorders. Moreover, inactivation of chemotherapeutic agents cisplatin and oracin, and carbonyl reduction of doxo- and daunorubicin (by human AKR1C3 and CBR1) to their cardiotoxic alcohols (dauno- and doxorubinol) leads to drug resistance, side effects, and poor therapeutic outcomes. Hence, modulators of enzyme activity, particularly from medicinal plants, have gained considerable research interest as valuable tools in pharmacotherapy, or as adjuncts. The current study investigated the inhibitory potential of pharmaceutically-relevant plant anthrone (aloin - AL) and anthraquinone derivatives (frangula emodin - FE, frangula A - FA, frangula B - FB, and aloe emodin - AE) on six human carbonyl-reducing enzymes (AKR1B1, -1B10, -1C3, -1B1, -7A2 and -7A3, and CBR1).

Methods: Recombinant His-tagged proteins were prepared using an *E. coli* expression system and purified by FPLC on 1.5 ml Nickel-containing agarose columns. Enzyme activity and inhibition were then assessed with a microplate reader or HPLC. Isoxanthohumol (IX) was used as a positive control.

Results: FE, FA, FB, and AE inhibited all the enzymes except AKR7A2 and -7A3 (inhibited by only FE, IC50: 19.4 ± 5.1). The strongest inhibition was observed with CBR1 (Ki: 0.16 – 1.3 µM). IC50 values for AKR1B10 were in the low micromolar range (3.5 – 16.6 µM). AKR1B1 and -1C3 were poorly inhibited (IC50 >50 µM) by all

compounds. Results indicate non-/uncompetitive inhibition mechanisms by the anthrone and anthraquinone derivatives.

Conclusion: Weak inhibition by AL indicates that the quinone structure and the absence of a bulky substituent at C10 are fundamental to the structure of a putative inhibitor. Furthermore, the absence of a hydrogen bond in AE, predicted for the docking of FE (strongest inhibitor) in AKR1B10, could explain its lower inhibition. Inhibitors with significantly low Ki values (low micromolar range) may be applied in co-medication, and could advance the design of more potent and specific synthetic inhibitors to ameliorate the outcome of carbonyl group containing drugs upon chemotherapy.

238

Rifampicin induces *CYP3A4* and *ABCB1* more efficiently than rifabutin despite lower cell uptake and potency to activate pregnane x receptor in vitro.

J. Nilles[1], J. Weiss[1], W. E. Haefeli[1], T. Ebner[2], S. Ruez[2], D. Theile[1]
[1]Heidelberg University Hospital, Clinical Pharmacology and Pharmacoepidemiology, Heidelberg, Germany
[2]Boehringer Ingelheim Pharma GmbH & Co. KG, Biberach, Germany

Question: Rifampicin and rifabutin are standard drugs against mycobacteria. Rifampicin is considered the stronger inducer of cytochrome P450 isozyme 3A4 (*CYP3A4*) and P-glycoprotein (encoded by *ABCB1*). However, a comprehensive pharmacological comparison has never been performed. Moreover, it is unknown whether differences in the extent of induction are caused by different cellular availability or by different induction potency.

Methods: Using pregnane x receptor (PXR) reporter gene assays, quantitative real time-polymerase chain reaction, and ultra-performance liquid chromatography coupled to tandem mass spectrometry, drug uptake (after 24 h) and the concentration-dependent and exposure time-dependent dynamics of PXR activation (6 h to 72 h) and mRNA expression enhancements (after 24 h) was evaluated in LS180 cells, an induction model representing intestinal tissue.

Results: Initially, maximum PXR activation (Emax) was 30-50 % higher with rifampicin. But at 72 h, both compounds had reached the same maximum PXR activation (4-fold compared to untreated cells). However, PXR activation potency (EC50) of rifampicin sharply decreased from 7.3 ± 3.3 µM at 6 h to 0.3 ± 0.04 µM at 72 h. In contrast, the potency of rifabutin dropped from only 2.9 ± 0.8 µM at 6 h to 0.5 ± 0.1 µM at 16 h, without relevant changes thereafter, suggesting efficient drug uptake. Indeed, intracellular concentrations after 24 h exposure to 0.1, 1, or 10 µM were 3-5-fold higher for rifabutin ($P = 0.0084$, $P = 0.0123$, and $P = 0.0211$, respectively). At the mRNA level, rifampicin induced *CYP3A4* with 6.3-fold lower potency than rifabutin after 24 h exposure ($P = 0.0002$), but with 66 % higher efficacy ($P < 0.0001$). Similarly, rifampicin induced *ABCB1* with 7.8-fold lower potency ($P < 0.0001$) but with 85 % higher efficacy ($P < 0.0001$).

Conclusions: Together, this data suggests that rifampicin is poorly taken up into LS180 cells compared to rifabutin. Its maximum PXR activation seems comparable to rifabutin. However, rifampicin likely induces both *CYP3A4* and *ABCB1* more efficiently albeit with lower potency than rifabutin.

Pharmacology – Disease models, drug development

22

Engineering of a human sympathetically innervated cardiac muscle model

L. V. Schneider[1,2,3], G. Bao[1,2], N. Liaw[1,2], O. Jensen[4], K. A. Schmoll[1], J. Brockmöller[4], W. H. Zimmermann[1,2,3], M. P. Zafeiriou[1,2,3]
[1]University Medical Center Göttingen, Institute of Pharmacology and Toxicology, Göttingen, Germany
[2]German Center for Cardiovascular Research (DZHK), Göttingen, Germany
[3]Multi-Scale Bioimaging Excellence Cluster (MBExC), Göttingen, Germany
[4]University Medical Center Göttingen, Institute of Clinical Pharmacology, Göttingen, Germany

Cardiac homeostasis is controlled by an intricate interplay of the two branches of the autonomous nervous system. In the diseased state, sympathetic hyperactivity becomes a driver of heart failure. Currently, the interaction between sympathetic neurons (SN) and the remodelled myocardium is not well understood and we are lacking human models to gain further insights. To emulate the complex neurocardiac interface *in vitro*, we fused sympathetic neuronal organoids (SNO) with engineered human myocardium (EHM) to construct sympathetically innervated EHM (iEHM). SNO were generated from a genetically modified optogenetic iPSC line and were comprised of 55±1% $PHOX2B^{pos}$ autonomic neuron progenitors (n=9 tissues, N=3 independent differentiations). They presented robust expression of SN-marker dopamine-beta-hydroxylase and tyrosine hydroxylase (*DBH* 7123±981-fold and *TH* 3.86±0.52-fold to iPSC) on protein and transcript level, while showing low abundance of other peripheral or cortical marker genes (*MNX1* and *PAX6*, respectively). SN-identity was further confirmed by liquid chromatography-mass spectrometry that showed high norepinephrine (60.4±6.2 pmol/mg) and low cholinergic neurotransmitter acetylcholine (18.4±4.9 pmol/mg) concentrations. After four weeks of co-culture, wholemount immunofluorescence of iEHM revealed axons extending from the SNO towards cardiomyocytes. Under the same culture conditions, iEHM developed 2-fold higher maximum force of contraction compared to control-EHM (0.46±0.04 mN, n=20, N=1 and 0.26±0.04 mN, n=6, N=1, respectively), suggesting a positive inotropic effect of the SN in iEHM. Light stimulation of optogenetic iEHM evoked a clear positive chronotropic response of 24±4% in iEHM (n=40, N=3), which could not be detected in EHM (1±3% increase in beating rate, n=16, N=3). Notably, in the presence of muscarinic receptor blocker atropine (1 nM), addition of autonomic neuron stimulant nicotinic acid (30 µM) resulted in a statistically significant increase in beating rate in 19 out of 27 iEHM (38±13% to baseline, n=19, N=5). This positive chronotropic response was blunted (-13±11% to baseline, n=19, N=5) by beta adrenoreceptor-blockage (10 µM propranolol), suggesting a SN-specific effect on the muscle. In conclusion, we developed a sympathetically innervated human myocardium model *in vitro* that proves as a promising tool for future applications in disease modelling and drug screening.

25

Endothelial function is impaired in atherosclerosis as induced by AAV-PCSK9^{DY} injection and Western diet

W. Raasch[1], L. Achner[1], T. Klersy[1], C. Schmidt[2], O. Müller[3], Z. Aherrahrou[4], K. Kusche-Vihrog[5]
[1]University of Lübeck, Institute of Experimental and Clinical Pharmacology and Toxicology, Lübeck, Germany
[2]University of Lübeck, Institute of Neurobiology, Lübeck, Germany
[3]University Hospital Schleswig-Holstein, Campus Kiel, Clinic for Internal Medicine III, Kiel, Germany
[4]University of Lübeck, Institute for Cardiogenetics, Lübeck, Germany
[5]University of Lübeck, Institute for Physiology, Lübeck, Germany

Questions: It is established to investigate atherosclerosis in mice by using transgenic models such as ApoE-KO, LDL receptor-KO or ApoE/LDL-R dKO mice. We here aimed to investigate the aortic stiffness in an alternative atherosclerosis model, namely the adeno associated virus (AAV)-mediated mice overexpressing Pro-protein convertase subtilisin/kexintype 9 (PCSK9) by the Atomic Force Microscopy (AFM) technique, which is the hallmark technique for investigating endothelial dysfunction.

Methods: Male C57BL/6N mice were injected with AAV-PCSK9 (0.5, 1 or 5×10^{11} VG in 100 µl), or 100 µl saline via tail vein at an age of 10 weeks. Afterwards, mice were fed for 3 months with a 1.25% cholesterol containing Western diet. Cholesterol and triglycerids plasma levels were measured after 6 and 12 weeks. Aortas (from the aortic root to the iliac bifurcation) were used for AFM measurements or were fixed in 4% paraformaldehyde solution for histological analysis.

Results: Body weight was almost doubled in response to the 12-weeks lasting WD-feeding regime. Gain in body weight was 35% lower in the group treated with $5x10^{11}$ VG compared to controls. In accordance, mass distribution was also diminished by increasing virus loads, where in particular the lean mass remained stable while the fat mass was decreased in the 1x and $5x10^{11}$ VG groups. Compared to controls, cholesterol increased by factor 3 in mice treated with $0.5x10^{11}$ VG and by factor 5 in mice receiving 1x or $5x10^{11}$ VG. Oil Red O staining from aortic rings indicate atherosclerotic lesions in all groups of mice receiving PCSK9. Compared to controls, plaques and fat content clearly increased particularly by using the higher doses of 1x or $5x10^{11}$ VG. Cortical stiffness increased by appr. 10% in response to virus load. Moreover, we found a positive correlation between cortical stiffness and the aortic plaque content.

Conclusions: Our data clearly show that our used AAV-PCSK9-based atherosclerosis model is a good alternative to the established transgenic mouse models because it develops vascular dysfunction in parallel with the typical histological impairments. Further studies should be performed with at least $2x10^{11}$ VG. Compared with the ApoE-KO, LDL receptor-KO, or ApoE/LDL-R dKO models, the AAV-PCSK9-based model has the clear advantage of a simpler approach when using other transgenic mouse lines simultaneously, because time-consuming generation of double knockouts can be avoided.

51

Calcium sensing receptor antagonist NPS-2143 antagonist attenuates acute kidney injury in ceacal ligation puncture induced sepsis model

G. Singh[1], A. Dahiya[2], A. Singh[2]
[1]Chitkara College of Pharmacy, Chitkara University, Rajpura, Punjab, Pharmacology, Rajpura, India
[2]ISF College of Pharmacy, Moga, Punjab, Pharmacology, Moga, India

Question: Various studies have demonstrated that the elevated extracellular calcium levels is known to activate calcium sensing receptors which could produce renal injury by causing release of reactive oxygen species (ROS) and inflammatory mediators (Hu et al., 2018). Thus present study was designed to investigate the effects of calcium sensing receptor (CaSR) modulation on development of sepsis induced acute kidney injury (AKI) in rats.

Method: Sepsis was produced by ceacal ligation puncture (CLP), CaSR agonist cinacalcet (10 mg/kg, *p.o*) and antagonist NPS-2143 (4.5 mg/kg, *i.p*) was administered separately 2 days before CLP. Renal functional parameters including serum creatinine, creatinine clearance, proteinuria, electrolyte levels, oxidative parameters: catalase and superoxide dismutase activity, reduced glutathione, lipid peroxidation levels and inflammatory biomarkers (myeloperoxidase activity, tumour necrosis factor-α, interleukin-1β and IL-17 levels), and caspase-3, Na+K+ATPase activity, renal calcium content were determined after 24 hours. Renal CaSR, nuclear factor kappa-B (NFKB) and podocyte marker protein nephrin expression was

determined by immunohistochemistry procedure. Moreover, H & E staining of renal tissues were performed to evaluate the glomerular and tubular injury.

Results: AKI was evident 24 hour after sepsis as revealed by elevated serum creatinine (figure 1), BUN levels, and reduced clearance due to elevated renal oxidative and inflammatory biomarkers levels. Moreover, septic rats displayed increased vascular permeability and caspase-3 and declined membrane Na+-K+-ATPase activity, increased calcium renal content, histological damage as well as increased immunopositive reaction for CaSR, NFKB and reduced nephrin expression. Notably pre-treatment with CaSR activator aggravated these pathological manifestations in septic rats, which were prevented in septic rats group pre-treated with CaSR antagonist.

Conclusion: CaSR anatgonist NPS-2143 pre-treatment diminished sepsis induced AKI in rats.

Figure 1: *p vs Sham, vehicle and Cina *per se* groups, @p vs CLP group, #p vs CLP+Cina group p

Reference: Hu B, Tong F, Xu L, *et al* 2018 Role of calcium sensing receptor in streptozotocin-induced diabetic rats exposed to renal ischemia reperfusion injury. Kidney Blood Press. 43(1): 276-86.

Fig. 1

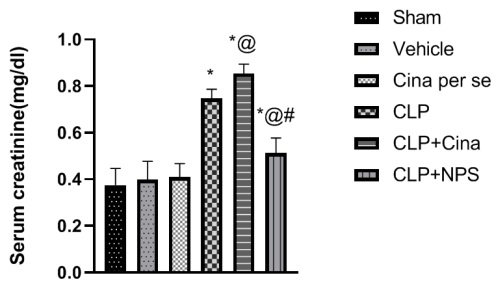

97

A Comprehensive Lipidomics and Metabolomics Profile of Ischemic Stroke

J. Folberth[1,2], Z. A. Shaheryar[1], A. Othman[2], S. Rhein[1], O. Jöhren[2], O. Herrmann[3], G. Royl[4], M. Schwaninger[1]
[1]University of Lübeck, Institute of Experimental and Clinical Pharmacology and Toxicology, Lübeck, Germany
[2]University of Lübeck, Bioanalytic Core facility, Center of Brain, Behavior and Metabolism (CBBM), Lübeck, Germany
[3]University of Heidelberg, Department of Neurology, Heidelberg, Germany
[4]University of Lübeck, Department of Neurology, Lübeck, Germany

Introduction: Ischemic stroke is one of the leading causes of mortality and adult disability worldwide. Although there has been great progress, the underlying metabolic alterations related to stroke are not yet fully understood and treatment options are still limited. Therefore, we performed untargeted metabolomics and lipidomics analysis using liquid chromatography coupled to tandem mass spectrometry (LC-MS/MS) to determine metabolic changes in ischemic stroke patients and mice with distal middle cerebral artery occlusion (MCAO).

Methods: Serum samples from 112 stroke patients and 140 healthy controls were analyzed with two different approaches using a high-resolution accurate mass (HRAM) platform. Reversed-phase (RP-) LC and hydrophilic interaction LC (HILIC) was conducted for lipidomics and metabolomics, respectively. Data-dependent data acquisition was performed using a hybrid quadrupole-Orbitrap mass spectrometer (Q-Exactive). Plasma, liver and brain tissue of mice were obtained 2 hours, 24 hours and 7 days after MCAO and analyzed with both lipidomics and metabolomics.

Results: In human serum, we were able to detect and confirm 174 lipid species out of 11 lipid classes as well as 94 metabolites related to several metabolic pathways. Particularly noteworthy are the statistical differences observed in relation to the phospholipid metabolism, including alterations in numerous phosphatidylcholines (PCs), lysophosphatidylcholines (LPCs), phosphatidylethanolamines (PEs) and ethanolamides (EAs). Several lipids were correlated to the outcome of patients, based on the modified Rankin Scale after 90 days (mRS90). In the mouse brain, metabolic changes were observed on the ipsilateral side compared to the contralateral side. Several metabolites and lipids in plasma, liver and brain tissue were correlated to infarct size or neurological impairment at different time points.

Conclusion: Our data not only provides insights into acute effects following ischemic stroke but also into early prediction of post-stroke impairment. The mouse model provides additional information, especially for metabolic changes in the brain, and is able to exclude confounding clinical parameters. Our findings contribute to a better understanding of ischemic stroke and could lead to new hypotheses and potentially new treatment options.

99

Therapeutic potential of activators of Slack potassium channels

A. Balzulat[1], F. Zhu[2], C. Flauaus[1], V. Olmos[2], J. Heering[3], R. Lu[1], H. Stark [4], D. Steinhilber[2], E. Proschak[2], A. Schmidtko [1]
[1]Institut für Pharmakologie und Klinische Pharmazie, Goethe-Universität, Frankfurt am Main, Germany
[2]Institut für Pharmazeutische Chemie, Goethe-Universität, Frankfurt am Main, Germany
[3]Fraunhofer Institut für Translationale Medizin und Pharmakologie (ITMP), Frankfurt am Main, Germany
[4]Institut für Pharmazeutische und Medizinische Chemie, Heinrich Heine Universität, Düsseldorf, Germany

Introduction: The sodium-activated potassium channel Slack (also termed $K_{Na}1.1$, Kcnt1, or Slo2.2) is highly expressed in a subpopulation of primary afferent neurons, where it controls neuronal firing and excitability. Previous studies in Slack-deficient mice revealed that Slack contributes to the processing of pain and itch, suggesting that Slack activation might be a potential therapeutic strategy. Here we developed novel compounds that activate Slack and characterized their efficacy *in vitro* and *in vivo*.

Methods: Novel compounds were screened in HEK293 cells expressing Slack using the FluxOR potassium ion channel assay and whole-cell patch-clamp recordings. Antinociceptive and antipruritic effects of novel compounds were investigated in behavioral models in mice.

Results: In the present study, several compounds were identified that activate Slack and increase Slack-dependent KNa currents *in vitro*. Furthermore, Slack activators seem to affect pain and itch behavior *in vivo* without inducing motor function impairments.

Conclusion: These results suggest that activation of Slack potassium channels might serve as a novel therapeutic strategy.

100

Formation of the reactive compound dimethylglyoxal from glucose

R. Costalunga[1,2], J. Folberth[1,2], Z. A. Shaheryar[1], S. Rhein[1], M. Schwaninger[1]
[1]University of Lübeck, Institute of Experimental and Clinical Pharmacology and Toxicology, Lübeck, Germany
[2]University of Lübeck, Bioanalytic Core facility, Center of Brain, Behavior and Metabolism (CBBM), Lübeck, Germany

Introduction: Reactive glucose metabolites are involved in complications of diabetes by generating advanced glycation end products (AGEs). In addition, high levels of blood glucose worsen the outcome of ischemic stroke. So far, only glyoxal, methylglyoxal and 3-deoxyglucosone have been recognized as reactive glucose metabolites.

Objective: Here, we have investigated the generation of dimethylglyoxal (DMG) from glucose. The role of *ILVBL*, a gene encoding the enzyme acetolactate synthase-like (ALS), in DMG formation was analysed.

Materials & methods: We used bEnd.3 mouse brain endothelial cells to evaluate the DMG generation from 13C-labeled glucose or pyruvate under normoxic and hypoxic conditions. The role of *ILVBL* was investigated *in vitro* by a siRNA knock-down in bEnd.3 cells and *in vivo* in knockout mice. Diabetic conditions were induced by streptozotocin (STZ) administration. Ischemia was generated by permanent occlusion of the distal middle cerebral artery (MCAO). Dicarbonyls were analysed by liquid chromatography coupled to tandem mass spectrometry (LC-MS/MS).

Results: Studies in bEnd.3 cells showed that DMG is generated from 13C-labeled glucose via two pyruvate molecules. We observed higher 13C-labeled DMG concentration under hypoxic conditions than under normoxia. Under hypoxic conditions, the *Ilvbl* knockdown reduced DMG formation from glucose. After inducing diabetes in mice by injecting STZ, we observed elevated DMG levels in the plasma. Concentrations of DMG correlated with the blood glucose levels, but *Ilvbl* knockout did not influence DMG generation. Moreover, hypoxic conditions generated by MCAO increased DMG levels on the ipsilateral side of the brain compared to the contralateral side. On both sides, we observed a higher concentration of 13C-labeled DMG in the control than in the ILVBL knockout mice.

Conclusion: Our data highlight the importance of DMG as reactive glucose metabolite. Levels are elevated in plasma under diabetic conditions and on the ipsilateral side of the brain after MCAO. Under hypoxic conditions, DMG generation seems to depend on ILVBL. DMG and ILVBL could be pharmacological targets in diabetes and hyperglycemic stroke.

108

The role of CRISPR/Cas9-mediated Drp1 knockout in ferroptosis

S. Tang[1], A. Fuß[1], S. Zika[1], C. Culmsee[1]
[1]Institute of Pharmacology and Clinical Pharmacy, Marburg, Germany

Mitochondria are highly dynamic organelles, undergoing constant fission and fusion in order to maintain mitochondrial integrity and function. Neurodegenerative diseases have been attributed to impaired mitochondrial dynamics, showing excessive mitochondrial fragmentation mediated by the GTPase Dynamin-related Protein 1. Pharmacological inhibition of Drp1 preserved mitochondrial morphology and function, leading to enhanced cellular resilience against oxidative stress [1]. Recent studies indicate an emerging role of mitochondria in ferroptosis through the modulation of GPX4 and lipid peroxidation [2, 3], however, the role of Drp1 in ferroptosis has not been clarified.
In this study, we investigated the effect of Drp1 knockout in neuronal HT22 cells challenged with the ferroptosis inducers erastin and RSL3. Fluorescence-activated cell sorting measurements were conducted after respective cell labelling to detect cell death (Annexin V/Propidium iodide), mitochondrial membrane potential (TMRE) and mitochondrial superoxide formation (MitoSox). Mitochondrial morphology was assessed by fluorescent microscopy after staining the cells with MitoTracker Deep Red, and Seahorse XF Analyzer was used for detecting mitochondrial respiration. Stable knockout of Drp1 was achieved in immortalized mouse hippocampal HT22 cells using CRISPR/Cas9 technology and Western blot analysis verified complete decline of Drp1 protein levels in different Drp1 KO colonies. Analysis of mitochondrial morphology revealed significantly enlarged mitochondria in Drp1 KO cell lines in comparison to wildtype HT22 cells, confirming reduced mitochondrial fission. Further, Drp1 KO significantly abolished cell death as well as loss of mitochondrial membrane potential induced by erastin or RSL3. Mitochondrial ROS formation and mitochondrial respiration were preserved in Drp1 KO cells during ferroptotic stress. The findings from this study suggest that excessive mitochondrial fission mediated by Drp1 is a key process to execute cell death in ferroptosis. This process can be impeded by the knockout of Drp1. Further investigation is needed to elucidate the detrimental impact of Drp1 in mitochondrial pathways of ferroptosis as well as mechanisms underlying cellular resilience against ferroptosis in the Drp1 KO cell lines.

References:
1. Grohm,et al.: Cell Death Differ, 2012, 19 (9): 1446-1458.
2. Gao, et al.: Mol Cell, 2019, 73 (2): 354-353.
3. Wu, et al.: Life, 2021, 11 (3).

116

LPS-induced changes in immunometabolism and the role of the psychiatric risk gene *Cacna1c* in microglia

S. Michels[1,2], J. Eichberg[1], F. Picard[3], M. Braun[4], T. Kisko[4], R. Schwarting[4,2], M. Wöhr[4,2,5,6], H. Garn[3], J. Alferink[7], C. Culmsee[1,2]
[1]University of Marburg, Institute of Pharmacology and Clinical Pharmacy, Marburg, Germany
[2]Center for Mind, Brain and Behavior, Marburg, Germany
[3]University of Marburg, Translational Inflammation Research Division, Marburg, Germany
[4]University of Marburg, Faculty of Psychology, Experimental and Biological Psychology, Behavioral Neuroscience, Marburg, Germany
[5]KU Leuven, Faculty of Psychology and Educational Sciences, Research Unit Brain and Cognition, Laboratory of Biological Psychology, Social and Affective Neuroscience Research Group, Leuven, Belgium
[6]KU Leuven, Leuven Brain Institute, Leuven, Belgium
[7]University of Münster, Department of Mental Health, Münster, Germany

Psychiatric disorders such as major depression, bipolar disorder, schizophrenia, and autism are highly prevalent chronic diseases, but their underlying pathophysiological mechanisms are still largely unknown. During the past decade, several genome-wide association studies (GWAS) have identified *CACNA1C* as one of the most replicable genetic risk factors for all of these major psychoses. Furthermore, multiple lines of evidence indicate the involvement of neuroinflammation and its primary mediators, the brain-resident microglia, in the neurobiology of psychiatric diseases. Central elements coordinating the adaptive processes of microglial activation include changes in energy metabolism and an increase in intracellular calcium levels. Here, recent studies suggest the involvement of L-type calcium channels (LTCC).

In the present study, we investigated the effects of modified *Cacna1c* gene expression as well as pharmacological LTCC blockade on neuroinflammatory responses upon lipopolysaccharide (LPS) stimulation in different model systems. Primary microglial cells were obtained from neonatal *Cacna1c+/-* Sprague Dawley rats. Moreover, we used the microglial BV2 cell line and microglia isolated from rats that received one dose of LPS (5mg/kg) intraperitoneally. Cellular bioenergetics were assessed using a XFe96-Analyzer. Nitric oxide (NO) and pro-inflammatory cytokine release were determined in the culture supernatants.

In microglia, both *Cacna1c* haploinsufficiency and treatment with the LTCC blocker nimodipine were associated with reduced glycolytic metabolism upon LPS stimulation. The LPS-evoked shift from oxidative phosphorylation towards glycolysis seems essential for the inflammatory response, since the downstream release of NO, IL-1β, IL-6, and TNF-α was also decreased in the *Cacna1c* haploinsufficient as well as nimodipine-treated microglial cells. Overall, these results suggest that the GWAS-confirmed psychiatric risk gene *CACNA1C* plays a significant role in the neuroinflammatory activation of microglia, thereby adding to a better understanding of the intracellular processes likely involved in the pathophysiology of *CACNA1C*-associated disorders.

This work is funded by DFG FOR2107, CU43/9-1, and CU43/9-2.

121

Effects of LOX inhibition on hemin-induced cell death in neuronal HT22 cells

M. Merkel[1], C. Culmsee[1], D. Steinhilber[2]
[1]Philipps-Universität Marburg, Institut für Pharmakologie und Klinische Pharmazie, Marburg, Germany
[2]Goethe-University, Pharmaceutical Chemistry, Frankfurt, Germany

Ferroptosis is a form of caspase-independent regulated cell death mediated by iron-dependent accumulation of reactive oxygen species, predominantly through lipid peroxidation and mitochondrial ROS formation. In particular, decrease in GSH levels and reduced GPX4 activity, and enhanced activation of lipoxygenases (LOX) are regarded as key trigger mechanisms in ferroptosis [1,2]. More recently, hemin, the oxidized product of hemoglobin, has been linked to ferroptotic cell death, and therefore, this study aims to clarify the contribution of LOX activity and mitochondrial ROS formation in the hemin-induced ferroptosis with particular focus on the role of 5-LOX and 12/15-LOX.The HT22 cell line of immortalized mouse hippocampal neurons was treated with micromolar concentrations of erastin and hemin to induce oxidative cell death. Effects of 5- and 12/15-LOX inhibitors, e.g. Zileuton, ST1853 and PD146176, respectively, were analyzed using fluorescence-activated cell sorting for detecting mitochondrial ROS formation, mitochondrial membrane potential, and cell death. Furthermore, we determined cell viability through MTT- and ATP-assays, and xCELLigence based real-time impedance measurements.Our data revealed a dose-dependent decrease in metabolic activity after 16 to 24 hours of treatment with hemin or erastin. Co-treatment of erastin with the 5- and 12/15-LOX inhibitors resulted in protection of the neuronal cells. When treated with hemin, only co-treatment with 5-LOX inhibitors Zileuton and ST1853 were able to prevent cell death, mitochondrial ROS formation, and mitochondrial membrane potential, whereas the 12/15-LOX inhibitor PD146176 failed to protect from oxidative death. Additionally, the iron chelator Deferoxamine prevents metabolic activity after hemin treatment, whereas the mitochondrial ROS scavenger Mitoquinone reduced mitochondrial oxidative damage in the erastin model of ferroptosis but failed to protect it from hemin toxicity. Further, Metformin and Phenformin, the mitochondrial complex I inhibitors of the respiratory chain, also failed to protect against hemin-mediated cell death.These results suggest, that on one hand, hemin-mediated cell death is iron-dependent, whereas mitochondria do not seem to play a major role. On the other hand, hemin-induced oxidative damage in HT22 cells depends predominantly on 5-LOX activity, whereas erastin-induced ferroptosis seems to depend on both, 5- and 12/15-LOX activity, and mitochondrial ROS formation.

1. Dixon, et al: Cell.2012,149(5):1060-1072
2. Dixon, and Stockwell. Nature Chemical Biology.2014,10(1)9-17

130

The SARS-CoV-2 main protease M^{pro} causes microvascular brain pathology by cleaving NEMO in brain endothelial cells

J. Lampe[1,2], J. Wenzel[1,2], H. Müller-Fielitz[1], Ü. Özorhan[1,2], M. Zille[1,2], M. Krohn[1,2], M. Schwaninger[1,2]
[1]Institute of Experimental and Clinical Pharmacology and Toxicology, University of Lübeck, Lübeck, Germany
[2]DZHK, Hamburg-Lübeck-Kiel, Germany

Introduction: SARS-CoV-2 has infected more than 260 Mio people worldwide. Besides respiratory symptoms, up to 84% of patients with severe disease show neurological symptoms including anosmia, epileptic seizures, strokes, loss of consciousness and confusion. Some studies indicate SARS-CoV-2-induced damage of the brain microvasculature, but the pathogenesis is still unknown.

Objectives: This study describes structural changes in cerebral small vessels of patients with COVID-19 and elucidates the underlying mechanisms.

Materials & methods: We analysed brain sections from SARS-CoV-2-infected patients and animal models to investigate the effect of the virus on the brain vasculature. Moreover, we determined the expression of membrane receptors and enzymes known to facilitate the entry of SARS-CoV-2 in brain endothelial cells (BEC) by immunohistochemistry and single-cell RNA sequencing. We performed cell culture experiments, immunoblotting and mass spectrometry to investigate cleavage of the essential modulator of nuclear factor-κB (NEMO) by the main protease of SARS-CoV-2 (M^{pro}). To explore the function of M^{pro} *in-vivo*, we employed the adeno-associated viral vector AAV-BR1. In addition, we used a mouse model of inducible *Ikbkg* (*Nemo*) deletion in BEC. Finally, we used genetic and pharmacological approaches to interfere with M^{pro}-induced microvascular pathologies.

Results: We found an increased number of empty basement membrane tubes, so-called string vessels, in the brains of SARS-CoV-2-infected individuals and animal models. Further investigations showed that string vessels were associated with vessel rarefaction and interruptions of the blood-brain barrier. In addition, our study hints that BEC are infected and that M^{pro} cleaves NEMO. This event leads to endothelial cell death, presumably guided by receptor-interacting protein kinases (RIPK). Ablation of RIPK3 and pharmacological inhibition of RIPK1 prevented vessel loss and blood-brain barrier disruption due to NEMO deficiency.

Conclusion: Our study shows that SARS-CoV-2 can cause microvascular pathologies due to M^{pro}-induced cleavage of NEMO and thus, might induce neurological symptoms. Moreover, we suggest RIPK as a potential therapeutic target to treat the neuropathology of COVID-19.

Published in Nat Neurosci. 2021;24(11):1522-1533; "The SARS-CoV-2 main protease M^{pro} causes microvascular brain pathology by cleaving NEMO in brain endothelial cells."; Wenzel J, Lampe J, Müller-Fielitz H, et al.

Fig. 1

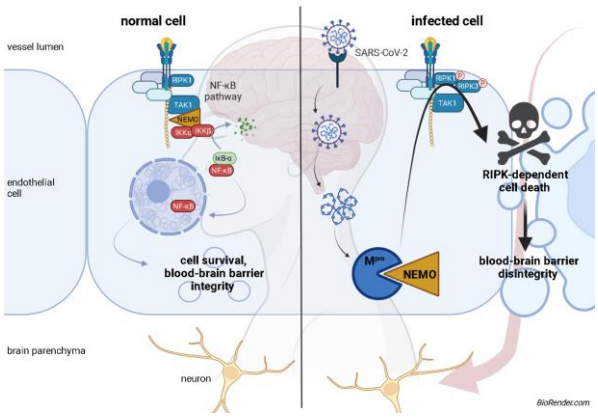

131

Hyaluronan matrix in bone marrow adipose tissue: implications for the development and progression of insulin resistance

K. Wegener[1], L. M. Lahu[1], O. Steinhoff[1], U. Flögel[2], M. Grandoch[1]
[1]Institute of Pharmacology and Clinical Pharmacology, UKD, Düsseldorf, Germany
[2]Institute of Molecular Cardiology, UKD, Düsseldorf, Germany

Bone marrow (BM), consisting of the red hematopoietic BM adipose tissue (rBMAT) and the yellow constitutive BMAT (cBMAT), accumulates under pathological conditions such as obesity and type 2 diabetes mellitus (T2DM). Due to their location bone marrow adipocytes (BMAds) contribute to energy metabolism but also hematopoiesis1.

Hyaluronan (HA), a major component of the extracellular matrix, is synthesized by three HA-synthases (HAS-1, -2, -3) as a non-sulfated glycosaminoglycan. Increased HA synthesis directly impacts on white and brown AT functions2 and massive HA deposition is observed in white AT and skeletal muscle in T2DM3. The role of the HA in BMAT has yet not been elucidated.

Aim of the present study is to verify HA expression in BMAT, to analyze changes in the BMAT HA matrix during the development of obesity and glucose intolerance in a murine model of diet-induced obesity and insulin resistance and to investigate related changes in energy metabolism and hematopoiesis.

Methods: Male C57BL/6J mice were fed a diabetogenic diet (DD) or matching chow diet for 9 weeks. Lipid deposition was measured by 1H-MR-Spectroscopy in skeletal muscle and BM. Effects on circulating and BMAT immune cell subsets were analyzed by flow cytometry and BMAT metabolic activity was examined via seahorse analyzer. Gene expression was evaluated by quantitative real-time PCR and BMAT-HA was investigated by histological stainings. *In vitro*, effects of HA on adipogenic differentiation was studied in primary BMAds.

Results/Conclusion: Feeding DD lead to early lipid accumulation in skeletal muscle and BM and promoted a chronic inflammatory response, leading to neutrophilia and monocytosis. Increased monocyte numbers were observed in cBMAT. Further, cBMAT of DD-fed mice exhibited lower maximal respiration compared to respective controls.

Histological stainings revealed specific HA signals in rBMAT. HA expression increased during adipogenic differentiation, while inhibition of HA synthesis by 4-methylumbelliferone suppressed adipogenic differentiation. In sum, our data show that (i) HA is expressed in BMAT and drives adipogenic differentiation and (ii) is regulated in the course of obesity and impaired glucose homeostasis thereby, resulting in altered hematopoietic response and metabolic activity.

1 Scheller E. L. *et al.* Trends in Endocrinol. Metab. 27(6): 392-403, 2016 **2 Grandoch M. *et al.*** Nat. Metab. 1: 546-559, 2019 **3 Jiang D., Liang J.,Noble P. W.** Physiol. Rev. 91(1): 221-64, 2011

153

Transcriptomic analysis of an idiopathic pulmonary fibrosis model using human precision-cut lung slices

P. Vaccarello[1], S. Engelhardt[1], D. P. Ramanujam[1], C. Staab-Weijnitz[2], R. Rad[3], C. Beck[1]
[1]Technical University of Munich, Institute of Pharmacology and Toxicology, Munich, Germany
[2]Helmholtz Zentrum München, Comprehensive Pneumology Center, München, Germany
[3]Technical University of Munich, Institute of Molecular Oncology and Functional Genomics, Munich, Germany

Idiopathic pulmonary fibrosis (IPF) is a life-threatening interstitial lung disease characterized by progressive inflammation and fibrotic remodeling, for which there is currently no cure. With the aim of providing a human ex-vivo model that recapitulates IPF and can be used for gaining insights into the mechanisms of disease and developing treatments, we established a model based on the one presented by Wagner *et al.* and studied the resemblance to IPF at the whole-transcriptome and miRnome level.

For this, we generated human precision-cut lung slices (PCLS) from tumor-free sections of lungs from patients undergoing resection, and treated them with a control cocktail (CC) or a fibrosis cocktail (FC) containing known fibrosis activators, namely TGF-β (transforming growth factor beta), TNF-α (tumor necrosis factor alpha), PDGF-AB (platelet-derived growth factor AB) and LPA (lysophosphatidic acid). The cocktails were administered on day 0, 2 and 5, and on day 7, RNA was isolated from the PCLS for RNA and microRNA sequencing.

Differential expression analysis showed that over 1500 genes were differentially expressed (p-adj<=0.05, |log2FoldChange|>=0.5, mean expression>=20) in FC-treated PCLS compared to CC-treated, including the upregulation of ECM genes such as COL10A1, COL1A2 and LUM, as well as inflammation markers like CCL11 and STAT1. In addition, gene ontology analysis identified relevant enriched biological processes such as "cytokine-mediated signaling pathway" and "extracellular matrix organization". Furthermore, comparison of our data to two publicly available datasets from IPF patients and donors revealed over 100 commonly up or downregulated genes with each dataset.

At the miRnome level we also found a high correlation between our fibrosis model and IPF patients, with 8 out of the 10 most abundant microRNAs in IPF lungs being also the most abundant in FC-treated PCLS. In particular, miR-21-5p, a microRNA that we previously found to be upregulated and highly expressed in IPF, appears also increased in our PCLS fibrosis model.

In conclusion, we identified important similarities at the whole transcriptome and miRnome levels between our PCLS model of pulmonary fibrosis and IPF lungs, providing a promising ex-vivo human disease model for therapy testing.

160

Development of human hair cells and sensory neurons in otic Bioengineered Neuronal Organoids (oBENOs)

A. Koufali[1,2,3], A. Müller[1], M. P. Zafeiriou[1,4,2]
[1]Universitätsmedizin Göttingen, Pharmacology and Toxicology, Göttingen, Germany
[2]Multi-Scale Bioimaging Excellence Cluster (MBExC), Göttingen, Germany
[3]International Max Planck Research School for Genome Science, Göttingen, Germany
[4]German Center for Cardiovascular Research (DZHK), Göttingen, Germany

iPSC-derived hair cells and sensory neurons can be used to model and study human otic development *in vitro*. 3D modelling of inner ear could enable the generation of diverse cell types found in the inner ear and serve as a platform to understand the mechanisms of sensorineural hearing impairment. This form of hearing loss can be caused by the loss of hair cells that may in turn lead to the death of spiral ganglion neurons. However, even the most renowned protocols have a rather low efficiency and high variability. Our work reports the establishment of a reproducible inner ear organoid protocol based on an established brain organoid model termed Bioengineered Neuronal Organoid (BENO, Zafeiriou et al, 2020). Pluripotent stem cells (iPSCs) embedded in a collagen matrix are differentiated by the addition of small molecules and growth factors. In our study, otic vesicles, sensory and non-sensory inner ear cell types were successfully generated by manipulating and fine-tuning BMP, TGF, WNT and RA signalling in a stepwise manner analogue to *in vivo* development. Gene expression analysis on day 20 revealed high expression of otic progenitor genes *PAX8*, *PAX2* and *FBOX2* (10-fold, 27-fold and 8-fold increase relative to iPSC respectively, N=3, n=4-5). After 40 days in culture mRNA levels of hair-cell specific markers *ATOH1* and *MYO7A* were significantly elevated (8.2-fold, 3.2-fold higher abundance relative to iPSC respectively, N=3, n=4-5). On day 60 *ATOH1* mRNA levels decreased (6.8-fold relative to iPSC respectively, N=3, n=4-5), while *MYO7A* transcripts were upregulated (7.3-fold increase relative to iPSC respectively, N=3, n=4-5), highlighting the otic fate induction of sensory cells. Wholemount immunofluorescence data (N=3, n=3) validated the qPCR findings. PAX8 positive otic progenitors developed into MYO7A/ATOH1 positive hair cell-like cells (in 8/9 organoids) and BRN3A/PV positive spiral ganglion neuron-like cells found around vesicular structures after 60 days in culture. Taken together, human iPSC-derived oBENOS can reproducibly express cell types found in the human inner ear. In the future, oBENOs will serve as preclinical models for gene and cell therapies approaches.

184

Itaconate inhibits succinate dehydrogenase and mediates protection against oxidative cell death

M. Günther[1], S. Schütte[1], C. Culmsee[1]
[1]Philipps-Universität Marburg, Klinische Pharmazie, Marburg, Germany

Oxidative stress and reactive oxygen species (ROS) are increasingly linked to many age-related diseases, such as diabetes, stroke or neurodegenerative processes.

ROS arise from several external sources including UV radiation, chemicals and pollution, however they are also produced through enzymatic reactions in the body. Oxygen metabolism in the mitochondria is predominantly responsible for ROS in a cell. This study reports how mitochondrial complex II activity contributes to ROS production and that a reduced mitochondrial metabolism is able to mitigate oxidative cell death.

Under oxidative stress conditions, itaconate was applied to neuronal HT22 cells for inhibition of succinate dehydrogenase (complex II) in the mitochondria. After an itaconate incubation of 16 hours, oxidative stress markers such as lipid peroxidation, mitochondrial ROS formation, loss of mitochondrial membrane potential, and cell death were analysed using fluorescence-activated cell scanning (FACS). Effects of itaconate on the mitochondrial respiratory chain were evaluated through measurement of the oxygen consumption rate (Seahorse) in permeabilized HT22 cells.

In HT22 neurons, itaconate reduced erastin- and glutamate-induced cell death. The investigation of cell membrane and mitochondrial lipid peroxidation demonstrated protective effects of itaconate against the formation of lipid ROS. Further, itaconate preserved mitochondrial membrane potential, an indicator of functional capability. These effects were similar to malonate, a specific inhibitor of succinate dehydrogenase.

In conclusion, itaconate reliably protected mitochondria from oxidative stress, and thus also prevented ferroptotic cell death. These results provide evidence that moderate succinate dehydrogenase (CII) inhibition could be a potential therapeutic approach for treating oxidative stress related diseases.

191

Modelling transcriptional loss and re-storation of *Krüppel-like factor 15* in stressed engineered human myocardium to halt cardiomyocye remodeling

E. Schoger[1,2,3], R. Kim[1,2], L. Priesmeier[1,2], G. L. Santos[1,2], S. Lutz[1,2], M. Tiburcy[1,2], L. Cyganek[2,4], W. H. Zimmermann[1,2,3], L. C. Zelarayán[1,2,3]
[1]University Medical Center Göttingen, Institute of Pharmacology & Toxicology, Göttingen, Germany
[2]Deutsches Zentrum für Herz-Kreislauf-Forschung, Partner site Göttingen, Göttingen, Germany
[3]Cluster of Excellence "Multiscale Bioimaging", Göttingen, Germany
[4]University Medical Center Göttingen, Clinic for Cardiology & Pneumology, Göttingen, Germany

Upon myocardial stress, cardiomyocyte remodeling is accompanied by transcriptional changes with repression of genes necessary for cardiac homeostasis. One well-characterized gene in this context is the transcription factor *Krüppel-like factor 15* (*KLF15*), an anti-hypertrophic factor expressed in the adult heart and lost in cardiomyopathies. We hypothesize that transcriptional re-storation of *KLF15* prevents cardiomyocyte remodeling in myocardial stress conditions. To test this, we used human induced pluripotent stem cell derived cardiomyocytes (hiPSC-CM) which were combined with fibroblasts and collagen to derive ring-shaped engineered human myocardium (EHM) cultured on flexible silicone poles (flex) for four weeks. We mimicked acute afterload increase by transferring tissues to non-flexible (fix) poles and cultured EHM for seven days resulting in tissue deterioration. We confirmed transcriptional reduction of *KLF15* mRNA levels by ~50% in fix compared to flex EHM. This was accompanied by transcriptional activation of genes associated with cardiomyocyte remodeling including *ACTA2* and *BMP4* (n=6-9 per group from 2 independent experiments). Increased expression of ACTA2 was confirmed on protein level (n = 4 EHM from 2 independent experiments). ACTA2 expression was confirmed in TNNT2 expressing cells when we provoked *KLF15* transcriptional loss in 2D hiPSC-CM upon TGFB1 exposure in a dose dependent manner. To re-store *KLF15* expression, we employed a CRISPR/dCas9-based endogenous gene activation (CRISPRa) system by recruiting enzymatically inactive Cas9 fused to transcriptional activators to the *KLF15* transcriptional start site by guide RNAs (gRNA). Lentiviral delivery of gRNAs (targeted to the *KLF15* promoter region and non-targeted gRNA used as control) into hiPSC-CM was sufficient to induce *KLF15* expression and to re-store *KLF15* mRNA levels in CRISPRa fix EHM comparable to expression levels in control flex EHM (n=6-9 per group from 2 independent experiments). This resulted in significantly reduced *ACTA2* and *BMP4* expression in CRISPRa fix EHM compared to controls in line with our *in vivo* data using the same CRISPRa system in a murine pressure overload model and single cell transcriptome analyses. These data demonstrate 1.) EHM as a suitable model for stress associated *KLF15* reduction *in vitro*, 2.) highlight *KLF15* as a potential target to halt cardiomyocyte remodeling and 3.) demonstrate CRISPRa as a potential novel tool to restore transcription factor expression.

201

Lutein rescues a *nlg-1*-mediated synaptic defect in a *C. elegans* mitochondrial complex I deficiency model

S. Maglioni[1], A. Schiavi[1], M. Melcher[2], V. Brinkmann [1], Z. Luo [3], A. Laromaine [3], N. Raimundo[4], J. N. Meyer [5], F. Distelmaier[2], N. Ventura[1,6]
[1]IUF-Leibniz Institute for Environmental Medicine, Düsseldorf, Germany
[2]University Children's Hospital, Heinrich-Heine-University Düsseldorf, Department of General Pediatrics, Neonatology and Pediatric Cardiology, Düsseldorf, Germany
[3]Institut de Ciència de Materials de Barcelona, ICMAB-CSIC, Bellaterra, Spain
[4]Penn State College of Medicine,, Hershey, United States
[5]Nicholas School of the Environment, Duke University, Durham, NC, United States
[6]Heinrich Heine University Düsseldorf, Düsseldorf, Germany

Question: Complex-I deficiency represents the most frequent pathogenetic cause of human mitochondria-associated diseases (HMAD). Therapeutic options for these devastating disorders, which in most cases present with neurodevelopmental defects, do not exist, in part due to the scarcity of appropriate model systems to study them. Can the model organism *Caenorhabditis elegans* be exploited to create reliable disease models and search for new therapies?

Methods: We used the nematode *C. elegans* to generate new HMAD models and we focused on two complex-I genes associated with Leigh Syndrome, *nuo-5*/NDUFS1- and *lpd-5*/NDUFS4, which were systematically characterized with different neurometabolic assays. Moreover, we exploited a phenotypic-based microscopy platform to screen a small library of compounds in search of disease suppressors.

Results: Our *C. elegans* models nicely recapitulated biochemical, cellular and neurodevelopmental defects of the human diseases. Most notably, our suppressor screening identified lutein, among a library of natural compounds, for its ability to rescue the developmental arrest and neuronal deficits observed upon *nuo-5* and *lpd-5* depletion. We specifically found that lutein exerts its beneficial activity by rescuing a neuroligin-mediated synaptic defect we disclosed for the first time upon *nuo-5* depletion.

Conclusions: Our work pointed to possible novel pathomechanistic targets for the human disease (neuroligin*/nlg-1*) and confirmed the usefulness to exploiting our disease models to further screen FDA-approved library or selected neuroactive compounds in search of diseases therapeutics.

210

Modelling Pelizaeus-Merzbacher disease in Bioengineered neuronal organoids

M. K. Schreiber[1], A. Sebe[2], Z. Ivics[2], W. H. Zimmermann[1], M. P. Zafeiriou[1]
[1]University Medical Centre Göttingen, Institut for Pharmacology & Toxicology, Göttingen, Germany
[2]Paul-Ehrlich Insitute, Langen, Germany

Introduction: Although animal research has greatly contributed to understanding neurodegenerative diseases, translational research faces limitations due to the lack of functional studies on human tissue. For many neurodegenerative diseases, effective treatments are missing – hypomyelinating Pelizaeus-Merzbacher disease (PMD) represents one of them. PMD is commonly caused by mutations or duplications in the proteolipid protein 1 gene (*PLP1)* leading to impaired myelin sheath formation and axonal degeneration.

Objectives: To support PMD animal model research with studies on functional human tissue, we developed a protocol for bio-engineered neuronal organoids (BENOs) derived from human induced pluripotent stem cells (iPSCs). BENOs display self-organisation, normal cortical layering, excitatory and inhibitory neuron as well as glia development. Furthermore, BENOs demonstrate axonal myelination mediated by oligodendrocytes from day 90 of differentiation. We hypothesise that BENOs are suitable human models to monitor myelination and to serve as screening platforms.

Results: We investigated BENOs derived from two PMD patients with a mutation (c. 98G-A), Patient A, and a duplication in PLP1 gene (Xq22.3), Patient B, in comparison with a well-characterised control GMP iPSC line (TC1133, Lonza) and a CRISPR/Cas9 generated isogenic control of c. 98G-A in three independent experiments.

At day 120, both PMD BENOs (Patient A and B) demonstrate reduced gene expression of oligodendrocyte marker *Olig2* (A: 314 fold, B: 217 fold), and myelin proteins *CNP* (A: 1.8 fold, B: 5.5 fold), *PLP1* (A: 57 fold, B: 53 fold) and *MBP* (A: 314 fold, B: 217 fold) compared to control BENOs. Immunofluorescence supports this data by depicting reduced numbers of Olig2-positive oligodendrocytes, decreased neuronal innervation, lower levels of axonal myelination, and signs of neuronal damage. Isogenic control BENOs exhibit a similar phenotype, suggesting that the mutation c. 98G-A is not solely responsible for the observed phenotype but further additional mutations in the *PLP1* gene were not identified.

Conclusions: In future experiments, we aim to: (1) identify the causing mutations (e.g. whole exome sequencing), (2) understand the pathomechanism underlying the disease phenotype and (3) develop therapeutic approaches for PMD in BENOs such as screening platforms to identify factors that ensure enhanced myelination, or oligodendrocyte survival and proliferation.

212

MicroRNA-21 as a novel therapeutic target for COVID-19.

C. Beck[1,2], D. P. Ramanujam[1,2], P. Vaccarello[2], F. Widenmeyer[2], M. Feuerherd[3], J. Schädler[4], J. P. Sperhake[4], K. Püschel[4], M. Graw[5], S. Safi[6], H. Hoffmann[6], U. Protzer[3], S. Engelhardt[1,2]
[1]DZHK (German Centre for Cardiovascular Research), partner site Munich Heart Alliance, München, Germany
[2]Technische Universität München, Medizinische Fakultät, Institut für Pharmakologie und Toxikologie, München, Germany
[3]Technische Universität München, Medizinische Fakultät, Institut für Virologie, München, Germany
[4]UKE Hamburg, Institut für Rechtsmedizin, Hamburg, Germany
[5]Ludwig-Maximilians-Universität München, Medizinische Fakultät, Institut für Rechtsmedizin, Munich, Germany
[6]Technische Universität München, Klinikum rechts der Isar, Thoraxchirurgie, München, Germany

Recent studies have identified alveolar macrophages to be of key importance for the progression of severe lung damage caused by infection with SARS-CoV-2 and for its long-lasting consequences such as pulmonary fibrosis (Melms, Johannes C et al., 2021). Laboratories worldwide developed several effective vaccines against COVID-19. However, an antiviral therapy for severe COVID-19 courses is still missing.

MicroRNAs, a class of small non-coding RNAs, are implicated in many diseases. Thus, make them suitable targets for therapeutic intervention. Here, we report on therapeutic inhibition of microRNA-21 (miR-21) in pulmonary macrophages as a therapeutic strategy to modulate pulmonary inflammation caused by infection with SARS-CoV-2.

To dissect the immune response in COVID-19, we carried out sequencing (long and small RNA-seq) and histological analysis of lung tissue obtained upon autopsy from 10 COVID-19 patients and 10 control subjects. We found macrophage activation-associated signature genes to be significantly enriched in COVID-19. Genetic deconvolution analyses revealed significant increase in macrophage numbers. Small RNA sequencing identified miR-21 to be the single strongest upregulated microRNA in lung tissue in COVID-19. Furthermore, quantitative analysis of all mRNAs revealed a repression of miR-21 targets indicating increased miR-21 activity in these tissues. Using in-situ hybridization, we could confirm an enrichment and upregulation of miR-21 in COVID-19 patients compared to controls.

These findings encouraged us to test the therapeutic efficacy of a macrophage-specific antimiR-21 molecule that was recently developed in our lab. As a human model system for COVID-19, we established human precision-cut lung slices (hPCLS) infected with SARS-CoV-2. Fluorescently labelled antimiR-21 indicated the cellular uptake of ligand-conjugated antimiR molecules by macrophages. Small RNA sequencing together with in-situ hybridization showed a strong reduction of miR-21 by ligand-coupled antimiR-21. Preliminary data indicate that miR-21 inhibition was effective in preventing SARS-CoV-2-induced pathology in hPCLS.

In conclusion, our data indicate microRNA-21 in pulmonary macrophages as a promising target for therapeutic intervention in COVID-19.

214

Characterization of a human midbrain organoid containing dopaminergic neurons

K. Schmoll[1,2], O. Jensen[3], J. Brockmöller[3], W. H. Zimmermann[1,4,2,5,6], M. P. Zafeirou[1,4,2,7]
[1]University Medical Center Goettingen, Pharmacology/Toxicology, Goettingen, Germany
[2]International Max Planck Research School for Genome Science, Göttingen, Germany
[3]University Medical Center Goettingen, clinical pharmacology, Göttingen, Germany
[4]Multiscale Bioimaging Excellence Cluster, Göttingen, Germany
[5]German Center for Neurodegenerative Diseases (DZNE), Göttingen, Germany
[6]Fraunhofer Institute for Translational Medicine and Pharmacology (ITMP), Göttingen, Germany
[7]German Center for Cardiovascular Research (DZHK), Göttingen, Germany

Parkinson"s Disease (PD) is an incurable neurological disease affecting 1% of the population above 60 years of age. The main pathological hallmark of this disease is the degeneration of dopaminergic neurons in the substantia nigra in the midbrain, leading to lack of dopamine in the human forebrain. This may be triggered by insoluble aggregates of misfolded alpha-synuclein which have been shown to have prion-like transmission. Although *in vivo* experiments in rodent models have been instrumental for the identification of the pathological hallmarks of PD, the underlying cause remains unknown rendering regenerative treatment impossible. Human induced pluripotent stem cells (hiPSCs) derived organoids offer new opportunities to investigate and treat neurological diseases.

To decipher the molecular mechanisms underlying the pathophysiology of PD, we aimed to generate human organoids containing ventral midbrain dopaminergic (mDA) neurons, based on a previously established model, the bioengineered neuronal organoid (BENO). Midbrain BENOs (mBENOs) are generated from hiPSCs embedded in a collagen hydrogel. Patterning into ventral midbrain was achieved by supplementation with growth factors and small molecules over a time course of 30 days. On day 62 mBENOs were analysed for floor plate (LMX1a, FOXA2), midbrain (EN1) and mDA neuron (TH) markers. Real time PCR analysis demonstrated a six-fold higher expression of TH, a 180-fold higher expression of EN1, a seven-fold higher expression for LMX1a and a 24-fold higher expression for FOXA2 compared to undifferentiated hiPSCs (n=4). Wholemount immunofluorescence analysis validated the high abundance of midbrain dopaminergic neurons marked by FOXA2 and TH expression. Finally, we quantified the dopamine content of mBENO via liquid chromatography mass spectrometry and detected 0.86 ± 0.25 pmol/mg of tissue by day 62 of differentiation (n=4), which was significantly higher compared to dopamine levels in BENO (0.05 ± 0.01 pmol/mg).

In conclusion, mBENOs represent a novel human midbrain organoid model enriched in ventral dopamine producing neurons. In the future, we will explore the mBENO potential in modelling PD by patient and transgenic lines or as mDA source for cell replacement therapy.

227

Synergy: Key for the pharmacology of herbal medicinal products used in gastrointestinal disorders

O. Kelber[1], M. T. Khayyal[2], K. Nieber[3]
[1]Steigerwald Arzneimittelwerk GmbH, R&D Phytomedicines, Phytomedicines Supply and Development Center, Bayer Consumer Health, Darmstadt, Germany
[2]Cairo University, Department of Pharmacology, Faculty of Pharmacy, Cairo, Egypt
[3]University of Leipzig, Institute of Pharmacy, Leipzig, Germany

Introduction: Synergy is key in the pharmacology of medicinal products containing more than one active molecule. This applies also to herbal medicinal products, which contain hundreds of phytochemical compounds. Gastrointestinal disorders are an important therapeutic area of these products, so that toe role of synergy in their action needs to be elucidated.

Methods: Studies on combination effects of herbal medicinal products used in gastrointestinal disorders were reviewed. Focus were studies that, following the work of Berenbaum and Chou and Talalay, included systematic investigation and evaluation of several concentrations, as only those allow a quantification of synergistic, additive and antagonistic effects [1].

Results: Pharmacological studies are available for STW 5 and STW 5-II, combinations of plant extracts with clinically proven efficacy [2]. Synergistic, additive and antagonistic effects of the combination partners were proven and quantified. For example, chamomile and peppermint extracts acted synergistic with Iberis extract on Il-8 release in an esophageal epithelial cell line, and a combination of chamomile and Iberis extracts contributed synergistically to the LPS-induced TNFα release in CaCo-2 cells. Synergistic effects have also been shown with regard to the inhibition of acetylcholine (ACh) -induced contractions on the ileum of rats in vitro for combinations of Iberis and peppermint or caraway extracts.

Conclusion: Overall, little synergy research has been carried out to date on preparations used in gastrointestinal diseases. Quantitative data that can serve as proof of synergistic effects are available for combination partners of two herbal preparations with clinically proven effectiveness in functional dyspepsia and irritable bowel syndrome, STW 5, which, in accordance with the pharmacological profile of its components [2], is preferred for acute and motility-related complaints, and STW 5-II, which is preferred for long-term complaints, according to the calming, anti-inflammatory and mucosal protective profile of its components. It seems plausible that the described synergistic, additive and antagonistic interactions are involved in the clinically proven effectiveness of these preparations in functional dyspepsia and irritable bowel syndrome, which confirmes the concept of a multi-target therapy in these indications.

1. Chou TC and Talalay P 1984, Adv. Enzyme Regul., 22: 27-55. 2. Abdel-Aziz H et al. 2017, Planta Med 83: 1130-1140

229

Improving transungual permeation studies with bovine hoof membranes *in vitro*: impact of thickness and infection with *Trichophyton rubrum*

S. Kappes[1], T. Faber[1], L. Nelleßen[1], T. Yesilkaya[2], U. Bock[3], A. Lamprecht[1,4]
[1]University of Bonn, Department of Pharmaceutics, Bonn, Germany
[2]Bayer Vital GmbH, Leverkusen, Germany
[3]Bock Project Management, Tawern, Germany
[4]University of Burgundy/Franche-Comté, PEPITE EA4267, Besançon, France

Introduction: The human nail can be considered as a dense hydrophilic keratinous matrix. Thus, delivery of antifungal agents is hindered. Membranes of bovine hoof sheets (BHS) have been established as human nail surrogates in permeation experiments. However, no standards have been decided regarding thickness of these BHS and unphysiologically thin BHS have been used. Additionally, infection status of the nail and impact on drug permeation is hardly studied.

Objectives: In vitro testing of ungual drug delivery systems using Franz diffusion cells (FDC) was to be improved by increasing BHS thickness from 100 to 400 µm and subsequent infection with *Trichophyton rubrum*. Multiple ungual formulations including semisolids, solution, patch and lacquer were investigated.

Materials & Methods: All dosage forms contained 1% (*w/w*) Bifonazole (BFZ). Ethanolic solution (SOL), patch (PAT) and lacquer (LAC) were prepared in lab scale. Commercial products Canesten® Extra Salbe (SAL) with 40% urea, Creme (CRE) and urea free SAL (SAL w/o) were used as semisolid references. BHS were prepared with a thickness of 100 µm and 400 µm. Infection was performed by incubating BHS with *T. rubrum* for 9 d. Permeation experiments were conducted with vertical FDC. BHS were incubated for 6 d with dosage forms and samples taken daily for HPLC-DAD analysis.

Results: Flux, normalized to a thickness of 100 µm, was significantly different between 100 and 400 µm BHS for immediate release dosage forms: SOL (47.6 ± 12 - 11.9 ± 10.6 µg/cm²), SAL (14 ± 2.7 - 10.3 ± 1.8 µg/cm²), SAL w/o (14 ± 1.4 - 2.7 ± 1.6 µg/cm²) and CRE (13.7 ± 2.5 - 4.5 ± 1.4 µg/cm²), respectively. No differences could be observed between semisolid SAL, SAL w/o and CRE in the 100 µm setup, while increasing BHS thickness revealed higher flux of SAL over SAL w/o and CRE. Infection of 400 µm BHS resulted in similar permeation of SAL (10.9 ± 1.8 µg/cm²) compared to the non-infected model. However, permeation of CRE was increased (7.3 ± 3.3 µg/cm²). Furthermore, daily exchange of SAL donor removed superficial infected nail substance.

Conclusion: Increasing BHS thickness increased sensitivity of the FDC setup for distinguishing semisolid dosage forms including permeation enhancing effects of urea. Infection of BHS with *T. rubrum* retained increased sensitivity in comparison to 100 µm membranes, however enabled further evaluation of formulation effects such as nail ablation that was also observed *in vivo* (Lahfa et al., 2013).

232

Why are phytopharmaceuticals so successful in functional gastrointestinal disorders? Anti-inflammatory effects as a joint mechanism of action

O. Kelber[1], K. Nieber[2], M. T. Khayyal[3]
[1]Steigerwald Arzneimittelwerk GmbH, R&D Phytomedicines, Phytomedicines Supply and Development Center, Bayer Consumer Health, Darmstadt, Germany
[2]University of Leipzig, Institute of Pharmacy, Leipzig, Germany
[3]Cairo University, Department of Pharmacology, Faculty of Pharmacy, Cairo, Egypt

Question: Is the irritable gut an inflamed gut? This question, for the first time raised in 1992 by S.M Collins from McMaster University [1], suggests that functional gastrointestinal diseases might be often caused by slightly increased concentrations of inflammatory mediators interfering with the enteric nervous system. Given that the astonishing number of 43 medicinal plants have been rated for the therapy of gastrointestinal disorders by the HMPC of the EMA, the question comes up whether anti-inflammatory effects could be their common denominator.

Methods: In order to pursue this assumption, database research [Medline] on anti-inflammatory effects of these and further herbal products was carried out.

Results: For all these herbal products, anti-inflammatory properties could be identified. In contrast to the NSAIDs, herbal products have been shown to have protective effects on the mucosa of the gastrointestinal tract, associated with an increase of mucosa protective prostaglandins [2, 3, 4], as well in *in vitro* as *in vivo* models.

Conclusions: Herbal drugs and preparations used in functional gastroenterological disorders have anti-inflammatory properties that can counteract functional disturbances – presumably an important reason for their success in the treatment of functional gastrointestinal disorders.

References: [1] Collins SM 1992 Scand J Gastroenterol Suppl 192:102-5; [2] Michael et al., Phytomedicine. 2009, 2-3 :161-71. [3] Kinscherf et al. Phytomedicine 2013, 20:691-8. [4] Khayyal et al., Phytomedicine 2006, 13 SV, 56-66.

234

Functional and metabolic effects of remdesivir on cardiac and kidney cells in vitro

K. Merches[1,2], L. Breunig[1], J. Fender[1], V. Bätz[1], S. Idel[3], L. Kollipara[3], Y. Reinders[3], A. Sickmann[3,4,5], A. Mally[1], K. Lorenz[1,3]
[1]Universität Würzburg, Institut für Pharmakologie und Toxikologie, Würzburg, Germany
[2]Landesamt für Gesundheit und Lebensmittelsicherheit (LGL), Erlangen, Germany
[3]Leibniz-Institut für Analytische Wissenschaften – ISAS – e.V., Dortmund, Germany
[4]College of Physical Sciences, University of Aberdeen, Department of Chemistry, Aberdeen, United Kingdom
[5]Medizinisches Proteom-Center (MPC), Ruhr-Universität Bochum, Bochum, Germany

The nucleoside analog remdesivir is the first antiviral therapeutic approved for Coronavirus disease (COVID-19). In the light of safety concerns due to reports on cardiac toxicity and acute kidney injury, a better characterization of remdesivir toxicity is desired. Nucleoside analogs are known for their potential to induce mitochondrial toxicity, to which cardiomyocytes and proximal tubule cells are highly sensitive.

Here, we assessed adverse effects of remdesivir on cell-viability and mitochondrial function of H9c2 rat cardiomyoblasts and neonatal mouse cardiomyocytes (NMCM) as well as rat NRK-52E cells and human RPTEC/TERT1 cells as *in vitro* models to study cardiotoxic and nephrotoxic effects, respectively. Additionally, the influence of remdesivir on the beating behavior of NMCM was analyzed.

Cell-viability of H9c2 and NRK-52E cells was adversely affected by short-term treatments (24 h) with remdesivir by impairment of proliferation as determined by significantly decreased 3H-thymidin uptake. Remdesivir impaired mitochondrial function, as evident by significantly decreased oxygen consumption rates in H9c2 and RPTEC/TERT1 cells and increased lactate secretion in both cardiac cell types treated with 1.6 - 3.1 µM of remdesivir for 24 - 48 h. Mitochondrial toxicity was also supported by early proteomic changes in NMCM treated with 9 µM (cmax in patients) remdesivir for 12 h. Beating behavior of NMCM was affected by 6.25 µM remdesivir, as shown by altered beat rate and beat amplitude.

In conclusion, adverse events of remdesivir in cardiac and kidney cells were evident at clinically relevant concentrations, suggesting a potential risk of therapeutic use in patients susceptible to cardiovascular or kidney disease.

240

Generation of mouse models with genetic modifications using a fast and precise CRIPSR-based knock-in technology

R. Medert[1], M. Freichel[1]
[1]Heidelberg University, Institute of Pharmacology, Heidelberg, Germany

The development of mouse models with precisely targeted integration of DNA mutations are a key technology in experimental pharmacology. Advancements of CRISPR-based genome editing technologies facilitate the modification of DNA sequences in the genome. CRISPR-Cas9 induced double strand breaks are repaired by non-homologous end joining (NHEJ), which is the dominant DNA repair mechanism resulting in small insertions and deletions or by homology-directed repair (HDR) which enable the integration of defined DNA sequences. However, HDR occurs with low efficiency and precise insertion of longer sequences remains challenging, given that donor DNA templates preferentially multimerizes in the cell by building tandem junctions that integrate in the genome as DNA concatemers.

We set out to generate conditional alleles to establish mouse models that allow time-dependent and cell type-specific gene deletions. Therefore, we developed a modified heiCas9 with boosted editing activity and used a long donor DNA template containing a loxP-flanked exon. To avoid multimerization of donor molecules we 5" biotinylated DNA donor templates and injected them into mouse embryos. Since donor concatemer integration events cannot be detected by conventional genotyping, we developed a diligent PCR strategy that allow us to distinguish intended single-copy integration (scHDR) from multimeric integration events of donor DNA molecules in the mouse genome. Quantitative droplet digital PCR (ddPCR) demonstrated that a donor modification by 5"biotinylation efficiently prevents multimerization in mouse embryos. Thereupon, we found that injecting 5"biotinylated donor DNA in mouse embryos at the two-cell stage leads to efficient and precise single-copy integration of donor DNA. Our dedicated genotyping strategy showed that these precisely modified alleles occurred with a frequency of up to 26%, at different gene loci, indicating that scHDR is dramatically boosted by 5"biotinylation.

Our fast and precise CRISPR-based genome engineering strategy enables the generation of preclinical genetic mouse models with targeted integration of defined DNA sequences within 3 months and allows an early characterization of mutant mice. Robust preliminary data can thus be generated within 12 months, whereas this is not possible with conventional gene targeting methods, as the efficiency for precise integrations by these methods is below 1% and the required screening period is very time-consuming.

250

Metabolic changes by *Cimicifuga racemosa* extract Ze 450 improve cellular resilience to oxidative stress and prolong lifespan in C.elegans

M. Günther[1], M. Rabenau[2], V. Butterweck[2], J. Drewe[2], G. Boonen[2], C. Culmsee[1]
[1]Philipps-Universität Marburg, Klinische Pharmazie, Marburg, Germany
[2]Max Zeller Söhne AG, Romanshorn, Switzerland

An imbalance in energy metabolism is a critical component in the development of age-related metabolic disorders such as obesity or diabetes, and may also contribute to the development of menopausal symptoms. Extracts prepared from the rhizome of *Cimicifuga racemosa* have been shown to mitigate antidiabetic effects in a mouse model of obesity [1], and these effects were linked to changes in energy metabolism. Our previous findings in different cell types revealed that Ze 450 exerted a metabolic shift from mitochondrial oxidative phosphorylation to glycolysis and thereby protected neuronal cells and liver cells from oxidative damage [2].

The aim of this study was to further elucidate the molecular mechanisms underlying the metabolic changes induced by Ze 450 in conditions of oxidative stress. We investigated whether Ze 450 directly affected the respiratory chain function in isolated cortical mitochondria, in cultured neuronal cells *in vitro*, and in the nematode C. elegans *in vivo*. The effects of Ze 450 on mitochondrial respiration and its protection against oxidative cell death were further compared to metformin and estrogen receptor stimulation. High-resolution respirometry and extracellular flux analysis revealed that Ze 450 mediated a direct effect on mitochondria, i.e. inhibiting the electron transport chain complex I, thereby shifting the cellular energy metabolism towards glycolysis, and this was associated with cMyc and HIF1α regulation. Importantly, the effects of Ze 450 were mediated independently of estrogen receptor

activation and distinct from effects exerted by metformin. Furthermore, Ze 450 increased the life span of *C. elegans* and protected the organism from the mitochondrial toxin paraquat [3].

These findings shed light on Ze 450-mediated metabolic mechanisms promoted through a metabolic shift to glycolysis via direct effects on mitochondria and altered cellular signalling pathways. In conclusion Cimicifuga extract Ze 450 enhances resilience against oxidative stress *in vitro* and promotes longevity *in vivo*.

[1]Moser C et al. Antidiabetic effects of the Cimicifuga racemosa extract Ze 450 in vitro and in vivo in ob/ob mice. Phytomedicine [2]Rabenau M et al. Metabolic switch induced by Cimicifuga racemosa extract prevents mitochondrial damage and oxidative cell death. Phytomedicine [3]Rabenau M et al. Cimicifuga racemosa extract Ze 450 re-balances energy metabolism and promotes longevity. Antioxidants

281

Effects of a sodium channel *SCN5A* mutation with associated proton leakage in 3-dimensional engineered heart tissue

B. Pan[1,2], B. M. Ulmer[1,2], A. Shibamiya[1,2], J. Rössinger[1,2], M. Schweizer[3], G. Höppner[1], J. Stenzig[1,2], T. Eschenhagen[1,2]
[1]University Medical Center Hamburg-Eppendorf, Department of Experimental Pharmacology and Toxicology, Hamburg, Germany
[2]DZHK (German Center for Cardiovascular Research), partner site Hamburg/Kiel/Lübeck, Hamburg, Germany
[3]University Medical Center Hamburg-Eppendorf, Department of Morphology and Electron Microscopy, Center for Molecular Neurobiology, Hamburg, Germany

Introduction: The voltage-gated sodium channel encoded by *SCN5A* plays an essential role in cardiac electrophysiology. *SCN5A* mutations are associated with cardiac arrhythmias, conduction disorders and dilated cardiomyopathy (DCM). Here we identified a DCM patient carrying a *SCN5A* R219H mutation previously described to cause a proton leakage current and intracellular acidosis.

Objectives: To assess the effects of the mutation in induced pluripotent stem cell (iPSC)-derived 3-dimensional engineered heart tissue (EHT) as a basis for screening for therapeutic molecules in a near-physiological human heart environment.

Materials & Methods: The iPSC lines from the patient (ERC011) and a healthy donor (ERC001) were differentiated into cardiomyocytes (three batches each) and cast into fibrin-based 24-well format EHTs. Contractility was assessed by video-optical recording, and action potentials (AP) were recorded by sharp microelectrode under 2 Hz electrical stimulation. PH challenge experiments were performed by increasing atmospheric CO_2 concentration from 7% to 14%. EHTs were treated with the Na^+/H^+ exchanger inhibitor (cariporide 2 µM) for 4 days. After culture, EHTs were harvested for histology and gene expression analysis.

Results: ERC011-EHTs carrying the R219H mutation developed lower force and more irregular contractions than control ERC001-EHTs. ERC011-EHTs displayed depolarized resting membrane potential (-69.9 ± 1.9 mV in ERC011 vs -77.8 ± 2.5 mV in ERC001, n=8/8) and strong triangulation (95.6± 5.5 ms in ERC011 vs 67.6 ± 3.7 ms in ERC001, n=8/8). Confocal and electron microscopy showed sarcomeric disorganization. The gap junction protein connexin 43 was lower expressed as well. Under pH challenge, ERC011-EHTs tended to be more susceptible to an acidic environment showing more frequent arrhythmic behaviour or loss of spontaneous contraction. Cariporide had no apparent effect on any parameter.

Conclusion: We successfully established a patient-specific *SCN5A* mutation EHT model and characterized the EHTs regarding morphology, contractility and electrophysiology. ERC011-EHTs exhibited altered contractile functions, sarcomere structure and APs. The easily assessable pathological phenotype in combination with a multiplexable EHT assay should allow successful screening for therapeutic molecules in the future.

Toxicology – Biogenic toxins

9

Cell type-selective protein transport system based on receptor-redirected protective antigen of *Bacillus anthracis*

N. Stadler[1], H. Barth[1], P. Papatheodorou[1], M. Fellermann[1]
[1]Institute of Pharmacology and Toxicology, University of Ulm, medical centre, Ulm, Germany

Common cancer therapies are often prone to side effects due to limited cell type and tissue specificity. Therefore, transport systems for the targeted, cell type-selective delivery of pharmacologically active (macro)molecules are urgently required and one promising approach is the exploitation of modified bacterial protein toxins. Here, a transporter based on *Bacillus (B.) anthracis* protective antigen (PA) was used for cargo delivery into the cytosol of defined cell lines. Due to two point mutations, PA lost its ability to bind to its native cellular receptors while preserving its transporter properties. The mutated PA (mPA) was genetically fused to human epidermal growth factor (EGF) to redirect its receptor specificity to the EGF receptor (EGFR), which is overexpressed on most breast cancer cells. The resulting mPA_EGF delivered the enzymatically active domains of diphtheria toxin (DTA) or *Clostridium botulinum* C2 toxin (C2I), each linked to the non-toxic N-terminal domain of *B. anthracis* lethal factor (LFN), into EGFR-positive cell lines (A431, MDA-MB231) but not into cells with low to no EGFR expression (MDA-MB543, HeLa, CaCo-2, CHO). Thereby, it was irrelevant whether the cargo was fused to LFN genetically (LFN_DTA) or by chemical crosslinking via a thiol-maleimide bond (LFN_m_C2I). A transport of these cargos by mPA_EGF into the cytosol resulted in altered cell morphology (e.g. cell rounding) and a decrease in cell viability by up to 50 % in EGFR-positive cell lines. This cell type selectivity is a major advantage compared to conventional pharmacological tumor therapies and can be extended.

16

Inhibition of the *Clostridioides difficile* toxins TcdA and TcdB by the human peptide α-defensin-6

L. Barthold[1], P. Papatheodorou[1], H. Barth[1], S. Fischer[1]
[1]Institute of Pharmacology and Toxicology, University of Ulm Medical Center, Ulm, Germany

Infections with *Clostridioides (C.) difficile* are increasing in incidence and morbidity. Clinical manifestations of *C. difficile* associated disease (CDAD) range from mild diarrhea to life-threatening pseudomembranous colitis and represent the leading cause of nosocomial and antibiotic-associated diarrhea in developed countries. The main virulence factors causing CDAD are the exotoxins A (TcdA) and B (TcdB). Both protein toxins enter target cells by receptor-mediated endocytosis. Due to the acidification of endosomes, the toxins form trans-membrane pores in endosomal membranes, which serve for translocation of their enzyme domains into the cytosol. After release by auto-proteolytic cleavage, the latter glucosylate Rho-GTPases, which results in inhibition of Rho-mediated signal transduction and breakdown of the cytoskeleton with loss of epithelial barrier integrity *in vivo*. Because treatment of CDAD is limited to a few antibiotics so far, pharmacological inhibitors of TcdA/TcdB are urgently needed.

In the past, we and others reported that human α-defensins, antimicrobial peptides capable of inhibiting bacteria, are also potent inhibitors of bacterial toxins. Here, we investigated the effect of the α-defensin-6, an important factor of the innate immune system in the human intestine, against TcdA and TcdB.

Human α-defensin-6 inhibited both toxins in a time- and concentration dependent manner and protected cells from intoxication, as analyzed in terms of cell-rounding, intracellular substrate modification and changes in the trans-epithelial electrical resistance. To investigate the mechanism underlying the interference of α-defensin-6 with the toxins´ cytotoxic effects in detail, a series of assays was performed to examine individual steps during the toxins´ uptake pathway. The results suggest that the inhibitory effect resulted from the formation of biologically inactive toxin-inhibitor complexes. Incubation with α-defensin-6 showed no inhibition of toxin binding to cells, the intrinsic autoproteolytic cleavage, or the enzyme activity of the toxins.

In conclusion, the human peptide α-defensin-6 represents a potent inhibitor of *C. difficile* toxins TcdA and TcdB. Given its endogenous human origin, this peptide might represent an attractive candidate for novel therapeutic options against CDAD.

46

Oral bioavailability and organ-specific metabolism of the hepatotoxic pyrrolizidine alkaloid senecionine

J. Buchmueller[1], A. M. Enge[1], F. Kaltner[2], C. Gottschalk[1], A. These[1], A. Thuenemann[3], A. Braeuning[1], B. Schaefer[1], **S. Hessel-Pras**[1]
[1]German Federal Institute for Risk Assessment, Food Safety, Berlin, Germany
[2]Justus-Liebig-Universität Gießen, Gießen, Germany
[3]Bundesanstalt für Materialforschung und -prüfung (BAM), Berlin, Germany

Introduction: Pyrrolizidine alkaloids belong to the secondary plant metabolites synthesized by many plants as protection against herbivores. These plants can occur as contamination of foodstuffs such as honey, herbs or tea, or animal feed. Acute intoxication with 1,2-unsaturated pyrrolizidine alkaloids (PAs) can lead to severe liver toxicity, and chronic ingestion of these genotoxic compounds has been associated with carcinogenic effects observed in rats. By now, many mechanisms leading to the development of liver toxicity are known, but there are still large gaps in our knowledge regarding oral bioavailability and organ-specific metabolism.

Objective: In this study, we investigated the hepatotoxic PA senecionine (Sc) in relation to its chemical modification during the digestion process in the mouth, stomach and intestine, the passage of the intestinal barrier and the uptake into hepatocytes, as well the organ-specific metabolism using human microsomal fractions for intestine, liver and lung.

Material and Methods: Sc content was analyzed in digestion liquids, Caco-2 and HepaRG cells as well as after using microsomal organ fractions or supersomes via LC-MS/MS.

Results: Using an artificial digestion system, the passage of Sc through the mouth, stomach, and intestine was simulated *in vitro*. After LC-MS/MS analysis, we conclude that the substance arrives chemically unchanged in the intestine. Analysis on the passage of Sc across the differentiated Caco-2 monolayer as a model for the human intestinal epithelium showed a transfer of 60 % after 24 h. Analysis of the uptake of Sc in the HepaRG cells as a model for human hepatocytes showed a reduction of Sc of

around 100 % in the cell culture medium after 24 h. If we simulate the intracellular metabolism of the main metabolic or target organs using human microsomal fractions, in the intestine about 25 %, in the liver about 40-50 % and in the lung about 20-30 % of the applied amount of Sc is degraded after 4.5 hours of incubation. Using special recombinant enzymes prepared from insect cells, we were able to show that human CYP3A4 appears to be primarily responsible for metabolization.

Conclusion: Our results show that the passage of barriers and organ-specific metabolism can substantially influence the amount of PA parent compound. It would be essential at this point to analyze different structures of PAs in order to draw conclusions on possible amounts and potencies in the individual target organs (liver, lung).

61

The potency to promote aneugenic effects *in vitro* may depend on the chemical structure of the Pyrrolizidine alkaloide

J. Buchmüller[1], A. M. Enge[1], A. Peters[1], J. H. Küpper[2], B. Schäfer[1], A. Braeuning[1], S. Hessel-Pras[1]
[1]Bundesinstitut für Risikobewertung, Lebensmittelsicherheit, Berlin, Germany
[2]Brandenburgische Technische Universität Cottbus Senftenberg, Molekulare Zellbiologie, Senftenberg, Germany

Question: Pyrrolizidine alkaloids (PA) are synthesized as secondary metabolites by many plant species around the world. The altogether more than 660 representatives identified so far were, according to their chemical structure, attributed to four different subclasses. Due to their known acute and subchronic toxicity and their genotoxic and carcinogenic effects, 1,2-unsaturated PA were regarded as relevant plant toxins contaminating food and feed of plant origin. The primary target organ is the liver, since the toxic effects require a bioactivation of the 1,2-unsaturated representatives by cytochrome P450 enzymes. PA are known to induce cytotoxic, carcinogenic and genotoxic effects. In experiments mainly using lasiocarpine and riddelliine the induction of mutations but also sister chromatid exchanges and chromosomal aberrations were observed in several cell culture systems after metabolic activation.

Methods: In this study, we used two different human liver cell lines (HepG2h3A4 and HepaRG) as well as the Chinese hamster cell line V79h3A4 to investigate whether there is a structure-dependency in the potential aneugenic effect of different PA. We therefore used a set of different PAs representing the main structure classes (monoesters, open-chained diester and cyclic diesters). We investigated potential aneugenic effects by flow-cytomeric detection of micronuclei and centromere-specific fluorescent in situ hybridization (FISH) respectively, and tested for DNA damage by the comet assay. We further performed detection of the chromatid status with flow cytometry for cell cycle analysis as well as cytotoxicity analysis and detection of phosphorylated H2Ax histone as an indicator for cellular stress.

Results: The results showed clear structure-dependent and consistent effects in all assays. Monoesters showed only slight effects, whereas open-chained diesters and cyclic diesters induced stronger effects. Of all investigated PAs, none induced DNA strand breaks. Moreover, micronuclei were detected in HepG2h3A4 cells and additionally in V79h3A4 cells by flow cytometry. Furthermore, the centromere-specific FISH showed signals of centromeres in the investigated micronuclei of V79h3A4 cells and HepG2h3A4 cells, indicating an aneugenic origin of the micronuclei.

Conclusion: In conclusion, our study point to an aneugenic effect of PA with consistent structure-dependency.

69

Ambroxol inhibits *Clostridioides difficile* toxins TcdA and TcdB

S. Heber[1], L. Barthold[1], J. Baier[1], P. Papatheodorou[1], G. Fois[2], M. Frick[2], H. Barth[1], S. Fischer[1]
[1]Institute of Pharmacology and Toxicology, Ulm University Medical Center, Ulm, Germany
[2]Institute of General Physiology, Ulm University, Ulm, Germany

Clostridioides (C.) difficile is the most frequent pathogen accountable for nosocomial infections. *C. difficile* infections (CDI) of the gut manifest in a range of symptoms from mild diarrhea to life-threatening pseudomembranous colitis. The major virulence factors of *C. difficile* are the two secreted exotoxins toxin A (TcdA) and toxin B (TcdB). Both toxins share structural similarities and are taken up by receptor-mediated endocytosis after binding to their cellular receptors. Acidification of early endosomes leads to conformational changes within the toxins and translocation of the toxins" enzymatically active glucosyltransferase domain (GTD) into the host cell cytosol. After release, the GTD mono-glucosylates and thereby inhibits small GTPases of the Rho/Ras superfamily. The inhibition of these molecular switches leads to the reorganization of the actin cytoskeleton resulting in gut epithelial barrier breakdown and inflammation. Here, we identified ambroxol (Ax) as a novel and potent inhibitor of TcdA and TcdB induced cytotoxicity.

To investigate protective effects of Ax, different cell lines were incubated with TcdA, TcdB or the combination of both in the presence or absence of Ax. Inhibition of cytotoxicity was monitored by changes in cell morphology and intracellular substrate modification (Rac1 glucosylation). To analyze the mechanism of inhibition, effects of Ax on TcdB stability, cell binding, auto-proteolytic processing and enzyme activity were checked *in vitro*.

Ax protected cells from intoxication with TcdA, TcdB and the medically more relevant combination of both toxins. The underlying molecular mechanism is most likely based on direct inactivation of the toxins" glucosyltransferase activity by Ax, whereas no influence of Ax on toxin stability or intracellular processing was observed. Interestingly, the inhibitory effect of Ax is specific for the glucosylating toxins TcdA and TcdB, while no effect was seen on the ADP-ribosylating *Clostridium botulinum* C2 toxin.

The two exotoxins TcdA and TcdB from *C. difficile* are the predominant virulence factors responsible for the development of clinical symptoms of CDI. Besides antibacterial therapy, pharmacological strategies to target these exotoxins are urgently needed. We identified Ax, an approved small molecular drug with well-established safety and pharmacological profile, as a potential candidate to directly inhibit TcdA and TcdB. Ax might be taken into account as a promising therapy option.

94

Human Peptides α-Defensin-1 and -5 Inhibit Pertussis Toxin

C. Kling[1], A. Pulliainen[2], H. Barth[1], K. Ernst[1]
[1]Universitätsklinikum Ulm, Ulm, Germany
[2]University of Turku, Turku, Finland

Pertussis toxin (PT) is a major virulence factor of the bacterium *Bordetella pertussis*, causing the severe childhood disease whooping cough. As a bacterial protein AB5-type toxin, PT consists of the enzymatically active A-subunit PTS1 and five B-subunits, responsible for binding to cells and transport of PTS1 into the cytosol. In the cytosol, PTS1 ADP-ribosylates α-subunits of inhibitory G-proteins (Gαi), leading to disturbed cAMP signaling [1]. PT is a central factor in promoting disease pathogenesis of pertussis [2] and current therapeutic options are limited to antibiotic therapy, which only relieves symptoms when applied in an early stage of disease. Therefore, we aim to identify new inhibitors against PT to provide starting points for novel therapeutic strategies.

Thus, we studied the effect of human antimicrobial peptides α-defensin-1 and -5 as well as β-defensin-1 on PT [3]. In an *in vitro* enzyme activity assay, based on detection of ADP-ribosylated Gαi via Western blotting, we investigated the direct effect of the defensins on PTS1 enzyme activity. With a sequential ADP-ribosylation assay, we determined the amount of ADP-ribosylated Gαi in CHO cells, intoxicated with PT in the presence of defensins, by detection via Western blotting. Additionally, we employed a novel luminescence-based bioassay, measuring cAMP levels in living sensor cells, to investigate the effect of defensins on the PT-mediated interference in Gαi-mediated signal transduction (iGIST assay) [4].

We showed, that α-defensin-1 and -5 but not β-defensin-1 inhibit enzyme activity of PTS1 *in vitro* in a concentration-dependent manner. Moreover, in the presence of α-defensin-1 and -5 the amount of ADP-ribosylated Gαi was significantly reduced in PT-treated cells. Furthermore, we showed that both α-defensins decrease PT-mediated effects on cAMP signaling.

In conclusion, we identified α-defensin-1 and -5 as inhibitors of PT activity. This suggests that these human peptides bear promising potential for developing novel therapeutic strategies against the life-threatening disease whooping cough.

1. Locht et al. The Ins and Outs of Pertussis Toxin. *FEBS J.* 2011

2. Scanlon et al. Association of Pertussis Toxin with Severe Pertussis Disease. *Toxins* (Basel) 2019

3. Kling et al Human Peptides α-Defensin-1 and -5 Inhibit Pertussis Toxin. *Toxins* 2021

4. Paramonov et al. IGIST-A Kinetic Bioassay for Pertussis Toxin Based on Its Effect on Inhibitory GPCR Signaling. *ACS Sens* 2020

98

***Clostridioides difficile* TcdB impairs lysosomal function**

C. Schneider[1], D. Henkel[1], H. Tatge[1], M. Sandmann[1], M. Mangan[2], **R. Gerhard**[1]
[1]Medizinische Hochschule Hannover, Hannover, Germany
[2]University of Bonn, Institute of Innate Immunity, Biomedical Center, Bonn, Germany

Clostridioides difficile toxin B (TcdB) is a potent cytotoxin that inhibits Rho GTPases by mono-glucosylation. TcdB enters cells via receptor-mediated endocytosis and the N-terminal glucosyltransferase domain (GTD) evades the late endosomes by pH-mediated conformational changes. Thereafter, the GTD is released by the toxin inherent cysteine protease domain. To learn about the uptake, localization and degradation of TcdB we followed the fate of intracellular TcdB by immunochemistry. TcdB entered the cell by the endosomal-lysosomal route and colocalized with the lysosomal marker protein LAMP1. TcdB was rapid degraded as shown by pulse assays, where endocytosed TcdB declined to a limit of detection within two hours. In contrast, the released GTD further accumulated for up to eight hours. To elucidate the different intracellular kinetics of the cleaved GTD and the intra-endolysosomal trunk of TcdB, we compared TcdB with the non-cleavable mutant C698S. We observed that lysosomal degradation of autoproteolytic deficient TcdB C698S happened significantly

faster than wildtype TcdB. Obviously, autoproteolytic cleavage of TcdB triggered interference of TcdB with the lysosomal degradation process. We confirmed that TcdB reduced lysosomal degradation of endosome cargo as tested with DQ-Green BSA. Dysfunction of lysosomes correlated with perinuclear accumulation of LAMP1. Lysosomal dysfunction did not result from toxin-induced membrane damage since galectin-8 or galectin-3 were not recruited to lysosomes. Changes in the autophagosomal marker LC3B furthermore indicated that TcdB-induced impairment of lysosomes indirectly effects the autophagic flux. Previous reports revealed that TcdB induces Ca2+-signaling during endocytotic uptake leading to early ROS dependent cell death. Since impairment of lysosomes was not sensitive to nifedipin, a calcium channel blocker that can prevent TcdB-induced early cytotoxic effect, we identified a novel, glucosyltransferse-independent effect of TcdB and also of other large clostridial glucosyltransferases.

101

Cell intoxication by *Clostridioides difficile* toxins TcdA and TcdB is inhibited by the compound U18666A

P. Papatheodorou[1], S. Kindig[1], A. Badilla-Lobo[2], S. Fischer[1], K. Aktories[3], E. Chaves-Olarte[2], C. Rodríguez[2], H. Barth[1]
[1]Ulm University Medical Center, Institute of Pharmacology and Toxicology, Ulm, Germany
[2]Universidad de Costa Rica, Centro de Investigación en Enfermedades Tropicales and Facultad de Microbiología, San José, Costa Rica
[3]Albert Ludwig University Freiburg, Institute of Experimental and Clinical Pharmacology and Toxicology, Freiburg, Germany

Question: The human gut pathogen *Clostridioides (C.) difficile* is a major cause of diarrhea in hospitals and non-hospital settings in industrial countries. *C. difficile*-associated diseases (CDADs), such as antibiotics-associated diarrhea and the severe, life-threatening pseudomembranous colitis, are directly attributed to the action of two large exotoxins produced by this bacterium, namely TcdA (toxin A) and TcdB (toxin B). Both toxins are single-chain, multidomain proteins, which are taken up into host eukaryotic cells via receptor-mediated and clathrin-dependent endocytosis. TcdA and TcdB target host Rho and/or Ras proteins for inactivation by glucosylation, which eventually results in cell death.

A previous study has shown that membrane cholesterol is required for membrane insertion and/or pore formation of TcdA and TcdB in endosomal membranes, which are key steps during the translocation of the glucosyltransferase domain of both toxins from endocytic vesicles into the cytosol of host cells (Giesemann et al., 2006, J Biol Chem). More recently, we found that the sterol regulatory element-binding protein 2 (SREBP-2) pathway, which regulates cholesterol content in membranes, is crucial for the intoxication of cells by TcdA and TcdB (Papatheodorou et al., 2019, FASEB J). Therefore, we were wondering whether the compound U18666A, an established inhibitor of cholesterol biosynthesis and/or intracellular transport, could serve as inhibitor of TcdA and TcdB intoxication of cells *in vitro*.

Methods: Various mammalian cell lines (HeLa, Vero, CaCo-2) were preincubated for 24 h with U18666A and then challenged with TcdA or TcdB. Cell intoxication by the toxins was monitored either by analyzing the cell morphology microscopically, by probing the glucosylation status of the toxin-substrate Rac1 with glucosylation-sensitive antibodies or by assaying the trans-epithelial electrical resistance of epithelial cell monolayers.

Results: In the current study, we demonstrate that intoxication by TcdA and TcdB is diminished in cultured cells preincubated with the compound U18666A. U18666A also protected cells from TcdA and TcdB variants produced by the epidemic NAP1/027 *C. difficile* strain, which is of particular clinical relevance.

Conclusions: Our study corroborates the crucial role of membrane cholesterol for cell entry of TcdA and TcdB and provides a valuable basis for the development of novel antitoxin strategies in the context of CDADs.

109

AB_5 toxins as tools for diagnostic and therapeutic applications using eukaryotic cell-free systems

F. Ramm[1], L. Jack[1], A. Zemella[1], S. Kubick[1]
[1]Fraunhofer Institute for Cell Therapy and Immunology, Branch Bioanalytics and Bioprocesses IZI-BB, Cell-free and Cell-based Bioproduction, Potsdam-Golm, Germany

A large variety of highly complex proteins is continuously produced by bacterial strains, but some of these proteins can exert toxic effects in human beings. Such bacterial toxins can be correlated with food-associated diseases. One class of pathogenic proteins are AB_5 toxins. These toxins are characterized by their structural composition. The A subunit, which is the catalytic subunit and therefore induces the toxic effect, can be split into two parts. The A1 subunit containing the catalytic domain and the A2 subunit can be separated by a furin cleavage site. The A2 subunit acts as an anchor to the B subunit and recruits the A1 subunit through a disulphide bridge. The B subunit forms a pentameric ring, which is the receptor-binding domain and attaches to the cell surface. Here we present the cell-free protein synthesis and functional characterization of two AB_5 toxins, namely the cholera toxin (Ctx) and the heat-labile enterotoxin (LT). Using eukaryotic cell-free systems the formation of the pentameric B ring could be shown via autoradiography. Cell-based assays in CHO-K1 cells showed that cell-free synthesized AB_5 toxins induced characteristic morphological elongation of cells at lower concentrations and led to cell-death in higher concentrations. Strikingly, complex toxin structures were only active after a co-expression of the A and the B subunits but not when mixing the subunits together after their individual syntheses. This highlights the importance of the formation of disulphide bridges between the A1 and A2, the A2 and B as well as B subunits themselves. With regard to the pathogenicity of these toxins, the detection and characterization are of utmost importance. Nonetheless, years of research have shown that toxic moieties can be used for therapeutic entities as well. Hence, we demonstrate that the individual subunits can be modified and labeled thereby facilitating intercellular trafficking and the design of targeted toxins.

111

Qualifying cell-free systems for the characterization of toxic proteins

F. Ramm[1], S. Kubick[1]
[1]Fraunhofer Institute for Cell Therapy and Immunology, Branch Bioanalytics and Bioprocesses IZI-BB, Cell-free and Cell-based Bioproduction, Potsdam-Golm, Germany

Cell-free systems use a cell-lysate rather than viable cells therefore circumventing toxic effects on the host organism. As a result high laboratory standards as needed for the generation of GMOs can be avoided. This allows for the fast and efficient synthesis of proteinaceous toxins in eukaryotic systems. Cell-free systems are open systems and therefore the individual reactions can be adapted to the individual protein"s need and radioactively labeled amino acids can be added for quantitative and qualitative analysis. As eukaryotic cell-free systems do not harbor endotoxins, assays for investigating the functionality of the toxins can directly be performed without the need of purification steps.

Here, we present the utility of cell-free protein synthesis to study bacterial enterotoxins. The tripartite pore-forming proteins from bacillus cereus Nhe and Hbl were synthesized in a CHO based cell-free system. 5% sheep blood agar plates, cell based assays on Caco2 cells as well as electrophysiological measurements were performed to study the toxins functionalities. We showed that cell-free synthesized multicomponent toxins were functionally active and subunit interactions could be characterized. This demonstrates that cell-free protein synthesis is a fast and efficient set up for toxicological applications.

Fig. 1

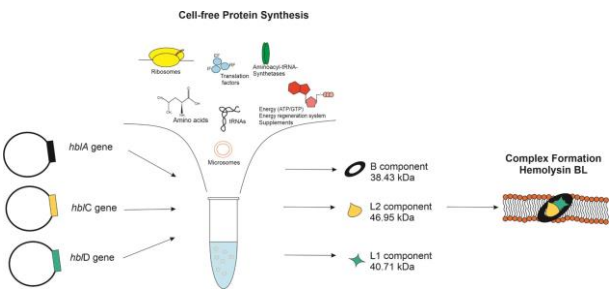

122

Clostridial C3 toxins modulate physiologically relevant functions in dendritic cells

M. Stemmer[1], M. Fellermann[1], H. Barth[1], S. Fischer[1]
[1]Institute of Pharmacology and Toxicology, Ulm University, Medical Centre, Ulm, Germany

C3 toxins are singe chain proteins of about 25 kDa that mono-ADP-ribosylate the GTPases RhoA, -B and -C thereby inhibiting Rho-mediated signal transduction in cells. This results in depolymerisation of F-actin and inhibition of actin-mediated processes such as migration, altered cell morphology and functionality. C3 toxins are internalised into the cytosol of monocytic cells via endocytosis, but not efficiently taken up into the cytosol of other cell types.

Assuming that other immune cells originating from monocytic precursor cells are also target cells of C3 toxins, human dendritic cells (DCs) have recently been identified as new target cells of C3 toxins (Fellermann et al. 2020). DCs are professional antigen-presenting cells, which connect the innate and the adaptive immune systems. They initiate and regulate antigen-specific immune responses and thus play a major role in host immune defence. Since Rho regulates the actin-dependent migration and phagocytosis, all central processes and physiological functions of DCs in immune defence, the consequences of C3 toxin uptake for these DC functions were investigated in more detail.

The effects of clostridial C3 toxins on the migratory, endocytic, and phagocytic activities of DCs were investigated by different approaches such as scratch assays and live-cell-imaging combined with immunohistochemistry and flow cytometry analyses, using an immortalised human dendritic cell line.

C3-treated DCs showed significantly reduced migratory activity and motility.

Currently, the phagocytic uptake of fluorescent *E.coli* particles into C3-intoxicated cells is investigated via flow cytometry, as well as the effect of C3-treatment on primary DCs. However, we were already able to show that C3 toxins efficiently inhibit the endocytosis of a His_eGFP-labelled vaccine carrier (His_eGFP-CRM197) in DCs.

In conclusion, the results revealed that C3-treatment down-modulates central actin-mediated functions in human DCs controlled by Rho-signalling, such as migration and endocytosis. This supports the hypotheses that a pathophysiological role of C3 toxins might be the specific inactivation of important immune cell functions, which should provide an evolutionary advantage for C3 toxin producing bacteria.

Reference: Fellermann M, Huchler C, Fechter L, et al (2020) Clostridial C3 Toxins Enter and Intoxicate Human Dendritic Cells. Toxins (Basel) 12:. doi:10.3390/toxins12090563

129

Non-toxic variants of the C3 toxin from *Clostridium botulinum* enter human macrophages and dendritic cells and can be used as carriers for drugs or vaccines

M. Fellermann[1], M. Stemmer[1], F. Wondany[2], D. Mayer[3], S. Stenger[3], J. Michaelis[2], S. Fischer[1], H. Barth[1]
[1]Ulm University, Medical Center, Institute of Pharmacology and Toxicology, Ulm, Germany
[2]Ulm University, Institute of Biophysics, Ulm, Germany
[3]Ulm University, Medical Center, Institute of Medical Microbiology and Hygiene, Ulm, Germany

Macrophages and dendritic cells (DCs) are the most important antigen-presenting cells (APCs) and play a major role in the innate and adaptive immune defense. Monocytes, macrophages and DCs are known to specifically internalize clostridial C3 mono-ADP-ribosyltransferase toxins (C3bot or C3lim) (Fahrer et al. 2010; Fellermann et al. 2020). These C3 toxins are known to specifically modify the GTPases Rho-A, -B, or -C in the cytosol of their target cells and thereby inhibit Rho-mediated signal transduction, and important APC-functions. Here we investigate the use of the enzymatically inactive and therefore non-toxic C3bot mutant $C3bot_{E174Q}$ as cell type-selective transporter system into APCs. We demonstrated that $C3bot_{E174Q}$ strongly enhanced the uptake of the cargo model eGFP into human macrophages as well as immature and mature DCs. By using stimulated emission depletion (STED) super-resolution microscopy localization of the internalized eGFP-labeled $C3bot_{E174Q}$ (^{His}-eGFP_$C3bot_{E174Q}$) into early endosomes was confirmed. In contrast, the cargo model ^{His}-eGFP alone was not efficiently internalized in the same timeframe. Moreover, it was confirmed that eGFP-labeling did not inhibit release of enzymatically active C3bot into the cytosol of APCs indicating that the cargo does not interfere with the uptake process. Finally, cytosolic release of the cargo was verified in a digitonin-based cell fractionation assay. Hence, $C3bot_{E174Q}$ can be used as APC-selective drug delivery tools. Finally, two modular systems were generated, which allow the fast attachment of different functionalized cargo molecules to $C3bot_{E174Q}$. Loading of these transport systems with proteins or peptides was confirmed and cytosolic release of cargo molecules will be further investigated. Based on these results $C3bot_{E174Q}$ seems to be an interesting candidate for specific drug- or vaccine-delivery specifically into macrophages or DCs.

Fahrer J, Kuban J, Heine K, et al (2010) Selective and specific internalization of clostridial C3 ADP-ribosyltransferases into macrophages and monocytes. Cell Microbiol 12:233–247. https://doi.org/10.1111/j.1462-5822.2009.01393.x

Fellermann M, Huchler C, Fechter L, et al (2020) Clostridial C3 Toxins Enter and Intoxicate Human Dendritic Cells. Toxins (Basel) 12:. https://doi.org/10.3390/toxins12090563

166

The enzymatically inactive transport subunit C2IIa of the binary *Clostridium botulinum* C2 toxin down-modulates the chemotaxis of human polymorphonuclear leukocytes

J. Borho[1], J. Eisele[1,2], S. Schreiner[1], S. Fischer[1], S. Heber[1], M. Fellermann[1], M. Huber-Lang[3], G. Fois[2], M. Fauler[2], M. Frick[2], H. Barth[1]
[1]Ulm University Medical Center, Institute of Pharmacology and Toxicology, Ulm, Germany
[2]Ulm University, Institute of General Physiology, Ulm, Germany
[3]Ulm University Medical Center, Institute of Clinical and Experimental Trauma Immunology, Ulm, Germany

The C2 toxin of *Clostridium botulinum* consists of two individual proteins: C2I (enzyme subunit) and C2II (binding/translocation subunit). Proteolytically activated C2II (C2IIa) forms ring-shaped heptamers that bind to carbohydrate receptors which are universally expressed on mammalian cells. Following binding of C2I, C2I/C2IIa-complexes are taken up by receptor-mediated endocytosis. Inside endosomes, C2IIa heptamers form trans-membrane pores through which C2I translocates into the cytosol. There, C2I ADP-ribosylates G-actin, resulting in a breakdown of the cytoskeleton, cell rounding and eventually cell death. So far, no effects on cells were observed after incubation with the single subunits, only for complete C2 toxin. However, there is increasing evidence that the transport subunits of binary actin ADP-ribosylating toxins exhibit cytotoxic effects on certain cells by their own. Therefore, the effect of C2IIa on various cell types was investigated in more detail.

Morphological effects of C2 toxin and its single subunits on cells were examined by phase contrast and fluorescent microscopy, effects on cell viability by MTS assay. Chemotaxis of primary human polymorphonuclear leukocytes (PMNs) was investigated using porous cell culture inserts with and without a tight monolayer of co-cultured endothelial cells.

C2IIa alone induced changes in the morphology and actin cytoskeleton of primary human PMNs, while it had no effect on other cell types including macrophages, endothelial and epithelial cells. These effects are most likely caused by pore formation of C2IIa in the cytoplasmic membranes of PMNs. Furthermore, application of C2IIa inhibited chemotactic PMN translocation *ex vivo* in the absence and presence of an endothelial barrier.

PMNs are part of the innate immune system and recruited to sites of infection by chemoattractants to eliminate pathogens. However, excessive invasion of PMNs into injured tissue can worsen the outcome of traumatically injured patients. Therefore, pharmacological down-modulation of excessive PMN recruitment after traumatic injuries might be beneficial. Hence, the findings that C2IIa selectively acts on PMNs and inhibits their chemotaxis, while it has no effect on other cell types, deepens the understanding of the role of C2 toxin in pathophysiology and provides a starting point for the pharmacological exploitation of C2IIa to down-modulate excessive PMN recruitment in the context of inflammatory and (post)traumatic diseases.

215

Exploring the underlying mechanism of pertussis toxin-induced cell clustering in the model cell line CHO

M. Braune-Yan[1], L. Kwapich[2], U. Rupp[3], H. Barth[1], O. Marti[2], C. Read[3,4], K. Ernst[1]
[1]Ulm University, Medical Center, Institute of Pharmacology and Toxicology, Ulm, Germany
[2]Ulm University, Institute of Experimental Physics, Ulm, Germany
[3]Ulm University, Central Facility for Electron Microscopy, Ulm, Germany
[4]Ulm University Medical Center, Institute of Virology, Ulm, Germany

Pertussis toxin (PT) is one of the main virulence factors of *Bordetella pertussis* which causes whooping cough. PT is an AB5-toxin composed of a binding and an enzyme subunit (PTS1) and follows a receptor mediated endocytosis to the endoplasmatic reticulum. There PTS1 is released, unfolded and transported to the cytosol where it ADP-ribosylates the inhibitory alpha subunit of G proteins leading to a disturbed cAMP signaling[1]. PT causes characteristic morphological changes in CHO cells that are described as cell clustering[2].

CHO cell clustering assay is used as a qualitative endpoint to detect PT activity in intoxication experiments and for testing residual PT activity in acellular pertussis vaccines. The underlying mechanisms of PT-induced cell clustering are still unclear. Here, we investigated the effect of PT on the cytoskeleton and the ultrastructure of organelles like mitochondria in CHO cells.

Fluorescence and light microscopy revealed a reduced cell size after incubation of CHO cell with PT. Quantification confirmed a significant smaller cell area of PT-treated cells compared to untreated control cells. Deformability cytometry revealed that PT-treated CHO cells show an increase in elongation and deformation compared to untreated cells. Immunofluorescence staining for F-actin resulted in a significant increase in signal intensity if cells were treated with PT. The effect of PT on CHO cells was analyzed by transmission electron microscopy. Besides the reduction in size of PT-treated cells, preliminary results indicate an effect of PT on mitochondria of CHO cells. In PT-treated cells, mitochondria were densely packed in the cytosol. Moreover, swelling of mitochondria and reduction of cristae was observed in these cells. Quantitative analysis of mitochondria showed an increase in mean volume of mitochondrion as well as in volume fraction of mitochondria per cell in PT-treated cells.

PT leads to reduction of size of CHO cells, altered cell mechanics and an increase of F-actin signal intensity suggesting that the actin cytoskeleton is involved in cell clustering. Furthermore, PT leads to morphological changes in mitochondria and an increase in mitochondria volume. Future investigations will clarify whether these morphological changes also lead to an impairment of mitochondria function by PT.

1 Locht, C., et al. *FEBS J.* (2011). 2 Hewlett, E. L., et al. *Infect. Immun.* (1983).

255

The Role of Organic Anion Transporters in the toxicity of Aristolochic Acid

H. Bastek[1], **G. Mucic**[1], T. Zubel[1], A. Mangerich[1], S. Beneke[1], D. Dietrich[2]
[1]Universität Konstanz, Biologie / Molekulare Toxikologie, Konstanz, Germany
[2]Universität, Biologie / Human & Ökotoxikologie, Konstanz, Germany

The phytotoxin Aristolochic Acid I (AAI), found in various traditional medicines and contaminated grain products, is considered to be the major cause of Chinese Herbal Nephropathy (CHN) and Balkan Endemic Nephropathy (BEN). Both diseases are associated with renal fibrosis and upper urothelial cancer. The mechanism how the nephrotoxicity of AAI occurs is still under debate, however, the carcinogenic potential is attributed to the formation of AAI-DNA adducts. Renal fibrosis is thought to be attributed to the AAI-induced sustained loss of renal proximal tubular epithelial cell (RPTEC). Organic anion transporters (OAT) found on the basolateral side, OAT1 and OAT3, and OAT4, potentially expressed on the luminal side, are assumed to be

responsible for the increasing concentration of AAI inside the PTECs. As HEK293 cells do not express OATs they are a well suited system for investigation of the individual properties of each single channel. The aim of this work was to overexpress OAT1, 3 and 4 in HEK293 cells, respectively, and investigate their transport activity towards a subset of different substrates, especially AAI, by competition analysis. For this, HEK293 cells were transfected successfully with expression plasmids containing the specific OAT variant coupled to a fluorescent protein, which was confirmed by western blot analysis. Functional transport was investigated using 6-carboxyfluorescein as reporter substrate, which was tested singly and in competition with probenecid, estrone sulphate and aristolochic acid. OAT1 and OAT3 show a high affinity for AAI in comparison to other common OAT substrates, resulting in IC50 values for 6-CF uptake of 1.9 and 1.2 µM, respectively, while probenecid and estrone sulphate were less effective. OAT4 displayed a lower transport activity for 6-CF. Ongoing competition experiments data suggest that estrone sulphate is well transported by OAT4, whereas probenecid is not. The high affinity of AAI to OAT1 and OAT3 could indicate that even AAI minimal exposures of RPTECs could result in a site specific accumulation and thus lead to toxic concentrations.

258

Machine Learning Prediction of Cyanobacterial Toxin (Microcystin) Toxicodynamics in Humans

R. Fotler[1], S. Altaner[1], S. Jäger-Honz[2], I. Zemskov[3], V. Wittmann[3], F. Schreiber[2], D. Dietrich[1]
[1]Universität Konstanz, Biologie / Human & Ökotoxikologie, Konstanz, Germany
[2]Universität Konstanz, Bioinformatik, Konstanz, Germany
[3]Universität Konstanz, Bioorganische Chemie, Konstanz, Germany

Microcystins (MC) represent a family of cyclic peptides with approx. 250 congeners, some of which were demonstrated to be toxic to humans. The toxicological profile of MC is characterized by the active cellular uptake of MC via organic anion transporting polypeptides (OATPs), and the subsequent irreversible inhibition of primarily ser/thr protein phosphatases (PPP) amongst a number of cellular proteins. Although a comparison between rodents and humans demonstrated that rodents are poor surrogates for humans with regard to the i) type of OATP expressed in the various tissues, ii) the affinity and iii) capacity of expressed OATPs for specific MC congener transport, risk assessment is still based on a single MC congener and a 90-day toxicity study in mice. The observation that humans demonstrate major differences in OATP expression and thus susceptibility to MC only compounded the fact that current risk assessment premises could severely underestimate the potential toxicities of MC due to their congener-specific kinetics. In view of the ever-increasing number of identified MC congeners, yet lacking the ability to synthetize these in sufficient purity and amounts for *in vitro* or *in vivo* testing, an *in silico* approach using toxicodynamic data could provide a first step towards a better toxicity assessment of uncharacterized MCs with relevance for humans. Accordingly, the aim of this study was to develop a comprehensive dataset of toxicodynamics, i.e., the PPP inhibitory capacities of a limited number of MC congeners. These *in vitro* data were then used as a comparative basis driving an *in silico* approach using machine learning (ML). The inhibition of PPP1, PPP2A and PPP5 by 18 structurally different MC was determined and demonstrated MC congener-dependent inhibition activity and a lower susceptibility of PPP5 to inhibition than PPP1 and PPP2A. The data were employed to train a ML algorithm that allows prediction of PPP inhibition (toxicity) based on 2D chemical structure of MC. IC50 values were classified into three toxicity classes, and three ML models were used to predict the toxicity class, resulting in 80-90% correct toxicity predictions, thereby providing an initial step towards in silico hazard predictions for MC and thus a basis for improved risk assessment.

Toxicology – Biokinetics

38

Miniaturized Method for the Measurement of total Cytochrome P450 Content

E. Fabian[1], L. Thibol[2], B. Wareing[3], S. Kolle[3], D. Funk-Weyer[3], R. Landsiedel[3]
[1]BASF, Experimental Toxicology and Ecology, Ludwigshafen, Germany
[2]TU Kaiserslautern, Food Chemistry and Toxicology, Kaiserslautern, Germany
[3]BASF SE, Experimental Toxicology and Ecology, Ludwigshafen, Germany

Cytochrome P450 (CYP) form a superfamily of heme-containing monooxigenases which are found all around nature. They are key enzymes in many metabolic pathways including biosynthesis of steroid hormones and xenobiotic metabolism. The expression of individual CYP gene, the amount of enzymes and their activity vary between different species as well as interindividually and tissue-specific; moreover CYP activity can be altered by enzyme inducers and inhibitors. While mRNA, protein and activity can be analyzed to quantify specific enzymes (or groups of enzymes), the total amount of CYPs can be quantified by photometry of the Soret band. The total CYP content is quantified by its absorbance at 450 nm after reducing the iron of the prosthetic group and forming an enzyme-carbonmonoxide as described by Omura and Sato in 1964 [1]. This well-established method is performed in cuvettes in a spectrophotometer; it requires relatively large volumes, is is laborious and with a low throughput. To overcome these limitations, Choi et al. [2] developed a method which prepares and measures the samples in 96 well plates.

The goal of the current project was to establish and optimize this miniaturized method and evaluate the results by comparing to results of classical Omora and Sato measurements. Microsomes of induced rat liver were incubated in a chamber with constant CO-flow, followed by heme-iron reduction with a solution of sodium hydrosulfite. The samples were measured in a TECAN plate reader. The experimental procedure was optimized in respect of the sequence of reduction and CO incubation, protein amount per sample, concentration of the sodium hydrosulfite solution and CO incubation time. Best results were obtained, when the well plate was first incubated with CO for 3 min, then reduced with 15 µL of 0.5 mM sodium hydrosulfite solution and then measured within 30 min in a TECAN plate reader. The CYP content measured by this miniaturized method was 1.24 ± 0.15 [nmol/mg protein] and was therewith comparable to the CYP content obtained with the classical Omura and Sato method of of 1.32 ± 0.11 [nmol/mg protein].

References

[1] Omura and Sato (1964) J. Biol. Chem. 239, 2370-8.

[2] Choi et al. (2003) Journal of Biochemistry and Molecular Biology 36, 332-5.

39

Study on intestinal Absorption of Microplastics *in vitro* using the EpiIntestinal™-human 3D Model

E. Fabian[1], B. Birk[1], T. Gründling[2], S. Woelk[1], P. Walter[2], S. Kolle[1], W. Wohlleben[2], J. Markus[3], D. Funk-Weyer[1], R. Landsiedel[1]
[1]BASF SE, Experimental Toxicology and Ecology, Ludwigshafen, Germany
[2]BASF SE, Central Analytics, Ludwigshafen, Germany
[3]MatTek In Vitro Life Science Laboratories, Pratislawa, Slovakia

The goal of the current project was to investigate potential absorption of microplastic through the intestinal barrier. The EpiIntestinal™ is a 3D model based on human primary cells from the small intestine, it incorporates enterocytes, paneth cell, M cells, tuft cells and intestinal stem cells into a highly differentiated, polarized epithelium. The chosen microplastic can be regarded as worst case: particle size between 100 and 200nm, negatively charged surface, individualized acrylic copolymer particles.

The EpiIntestinal™ model was cultivated in membrane inserts, the apical side was exposed for four hours to a suspension of acrylic copolymer microplastic particles (1 mg/mL in HBBS). The nominal dose was 200 µg particles / model. After exposure, the test substance preparation was removed and the model was washed twice with 400 µL HBBS solution. After washing, defined models were used for a cytotoxicity test (MTT-assay; triplicates each for the test substance, negative control and positive control). For absorption measurements, samples of three models each were pooled for analysis (washing solution, tissue models, receptor medium as well as test-substance preparation and blanks). Quantitative analysis for acrylic copolymer in the samples was performed by GC-MS for defined fragments after pyrolysis (Py-GC-MS) after sample preparation including concentration steps by ultracentrifugation.

The microplastic did not induce cytotoxicity in the EpiIntestinal™ model after four hours of exposure under the test conditions used. The total recovery of the microplastic was 93%. In the receptor medium, the amount of microplastic was below the limit of quantification (< 0.1 % of dose). These data demonstrate that even worst case microplastic particles did not induce cytotoxicity in a 3D small intestine model and no quantifiable absorption was detected in the absence of cytotoxicity.

89

Consideration of *in vitro* dose metrics: concentration in cytosol

D. Dimitrijevic[1], E. Fabian[2], B. Nicol[3], D. Funk-Weyer[2], R. Landsiedel[2]
[1]Freie Universität Berlin, Berlin, Germany
[2]BASF SE, Experimental Toxicology and ecology, Ludwigshafen, Germany
[3]Unilever U.K., Safety & environmental assurance centre, Sharnbrook, Bedford, United Kingdom

The nominal concentration (C_{Nom}) is a common dose metric in cell-based assays although it may not reflect the actual exposure of cells to the test substance, hence hampering meaningful concentration-response relations and *in vivo* extrapolations. Free concentration in medium or in the cells may be closer to the actual biologically effective doses (BED). Yet, the measurement of cytosolic or cellular concentrations is challenging. The aim of this work was to test two techniques for cell lysis and to measure total concentration in medium (C_{Med}), cells and cellular cytosol (C_{Cell} and $C_{Cytosol}$) of four chemicals. Measured C_{Cell}, $C_{Cytosol}$ and C_{Med} were related to results from an established computational prediction model (Armitage et al. 2014, Kramer et al., 2012, Fischer et al., 2017).

Balb/c 3T3 cells were incubated with Acetaminophen (APAP, 60 µM), Caffeine (CAF, 160 µM), Flutamide (FLU, 10 µM) and Ketoconazole (KET, 15 µM). The concentrations were confirmed to be subtoxic. After 48 hours of incubation, the medium and cells were collected, cytosol extracted from cells and analyzed by HPLC-MS/MS to obtain C_{Med}, C_{Cell}, and $C_{Cytosol}$. Cytosol was harvested from the cells by two different methods: digitonin treatment (Deusser et al., 2020, Kaiser et al., 2009), trypsination followed by thawing and freezing cycles.

Both methods provided comparable results within factors of 1.2-3.2.The lipophilic chemicals FLU and KET were present in higher concentration (17 and 30fold, respectively) in cells and cytosol compared to C_{Med}. Comparable $C_{Cytosol}$, C_{Cell} and C_{Med} were yielded for CAF and APAP. C_{Cell} of APAP was 4.5times that of C_{Med} or $C_{Cytosol}$. The computational model predicted C_{Cell} of KET but overpredicted C_{Cell} of the other substances by factors of 5–7.Computational prediction model may need refinement to better predict effective *in vitro* concentrations.

The biological relevance of concentrations should increase from C_{Nom} > C_{Med} > C_{Cell} > $C_{Cytosol}$ but ultimate proof for this is still missing. Considering protein-binding and measuring unbound fractions may further approximate the ultimately effective concentration *in vitro*.

Armitage, J.M. et al. 2014, https://doi.org/10.1021/es501955g.

Deusser, H. et al. 2020, https://doi.org/10.1007/s40495-020-00242-5.

Fischer, F. et al. 2017, https://doi.org/10.1021/acs.chemrestox.7b00023.

Kaiser, E. et al. 2009, https://doi.org/10.1111/j.1462-5822.2009.01291.x

Kramer, N. I. et al. 2012, https://doi.org/10.1021/tx200479k.

91

Comparison of different methods to determine the unbound fraction of chemicals in human plasma

D. Dimitrijevic[1], E. Fabian[2], D. Funk-Weyer[2], R. Landsiedel[2]
[1]Freie Universität Berlin, Berlin, Germany
[2]BASF SE, Experimental Toxicology and Ecology, Ludwigshafen, Germany

Plasma protein binding (PPB) is diminishing the free, unbound fraction of chemicals in plasma (f_u). The unbound fraction is often regarded as the effective concentration (Groothuis et al., 2015, Henneberger et al., 2021). Different methods allow quantifying PPB. In this project, twelve chemicals ($LogP_{OW}$ ranged from -0.1 to 6.8) were selected to determine f_u using three methods.

Human plasma was incubated with test chemicals at a nominal concentration of 5 µM. The plasma protein fraction was separated by rapid equilibrium dialysis (RED), ultrafiltration (UF) and ultracentrifugation (UC). Test chemical"s concentration were measured in different matrices by HPLC-MS/MS.

Hydrophilic chemicals (3/12, $LogP_{OW}$ < 2) had a high fu (> 70%) measured after RED and UF whereas lipophilic chemicals a low f_u (<33 %). In contrast, lower f_u were found for lipophilic chemicals after UC. Low recoveries (<50%) - probably due to non-specific binding to the devices - were found after UC and UF which could distort the f_u quantifications. RED and UF resulted in f_u consistent with published references. Less accordance was found with UC: f_u derived after UC were overpredicted for five of the 12 test chemicals above a factor of 2. Overpredictions of f_u were observed for Flutamide in RED and Ketoconazole in UF experiments. Underpredictions were found for Colchicine in UF and UC data. For data assessment, it should be kept in mind that most reference data were obtained with RED.

In conclusion, not all of described methods are suitable for all chemical and the criteria for a method to be applicable to a substance need to be described. Until now, UF was suitable for polar molecules while RED provided the highest recovery and reproducibility.

Groothuis et al., 2015. https://doi.org/10.1016/j.tox.2013.08.012.

Henneberger et al., 2021. https://doi.org/10.1021/acs.chemrestox.1c00037.

93

Refinement of *in vitro to in vivo* extrapolation (IVIVE) of potential endocrine disruptors based on *in vitro* dosimetry approaches

D. Dimitrijevic[1], E. Fabian[2], C. Gomes[2], D. Funk-Weyer[2], R. Landsiedel[2]
[1]Freie Universität Berlin, Berlin, Germany
[2]BASF SE, Experimental Toxicology and Ecology, Ludwigshafen, Germany

Physiologically based toxicokinetic models (PBTK) can support the translation of *in vitro* effect concentrations to *in vivo* doses by so-called IVIVE (*in vitro* to *in vivo* extrapolation). In cell-based assays, nominal concentrations (C_{Nom}) are often used to describe concentration-effect relationships although C_{Nom} may significantly differ from the effective concentration in the cells. This could over- or underestimate the corresponding *in vivo* doses obtained by IVIVE. We performed *in vitro* dosimetry and used IVIVE to predict doses causing endocrine effects *in vivo* of seven chemicals published by Fabian *et al.*, 2019. For this purpose, total concentrations in medium (C_{Medium}) and cells (C_{Cell}) were measured in yeast estrogen and androgen screening assays (YES/YAS, Kolle *et al.*, 2010) and steroidogenesis assay in H295R cells (OECD TG no. 456, 2011).

Yeast cells were incubated for 48 hours with Acetaminophen, Bisphenol A, Caffeine, Flutamide, Genistein and H295R cells with Fenarimol and Ketoconazole at the lowest observed effect C_{Nom}. C_{Medium} and C_{Cell} were analytically measured by LC-MS. The *in vitro* derived estimated lowest observed effect doses (est. LOELs) were obtained from C_{Medium} and C_{Cell} by reverse dosimetry using a PBTK 8 compartment model. These est. LOELs were compared to the *in vivo* LOELs.

Using total C_{Medium} and plasma concentrations, est. LOELs were comparable (within a factor of 10) to *in vivo* LOELs for four of the seven chemicals. For three chemicals, Genistein, Flutamide and Ketoconazole, est. LOEL and *in vivo* LOEL did not correlate. For FEN, correlation even increased when free C_{Medium} instead of total C_{Medium} was used. When using C_{Cell} and tissue concentrations, est. LOEL and *in vivo* LOEL correlated for five of the seven chemicals with Flutamide and Ketoconazole not correlating.

This study demonstrates how *in vitro* dosimetry can improve the prediction of *in vivo* effect concentrations but also points out the limits of this approach. Further improvement of the methodology and/or a better definition of the applicability of the existing method is advised.

Fabian, E. et al., 2019, https://doi.org/10.1007/s00204-018-2372-z.

Kolle, S. N., et al. 2010, https://doi.org/10.1016/j.tiv.2010.08.008.

OECD 2011.,https://doi.org/10.1787/9789264122642-en.

Toxicology – Computational toxicology

13

Reliability of published QSAR models for the prediction of developmental and reproductive toxicity – a case study on pesticides

A. Weyrich[1], M. Joel[2], G. Lewin[2], T. Hofmann[1], M. Frericks[3]
[1]BASF SE, Experimental Toxicology and Ecology, Ludwigshafen am Rhein, Germany
[2]Preclinical Science – Föll, Mecklenburg & Partner GmbH, Münster, Germany
[3]BASF SE, Agricultural solutions – Toxicology CP, Limburgerhof, Germany

Introduction: The importance of in silico methods for predicting toxicity has increased significantly in recent years due to the 3 R principle. In addition to read across approaches, quantitative structure-activity relationship (QSAR) models play a major role. These use existing experimental toxicity data for a range of chemicals to create a model that relates experimentally observed toxicity to molecular descriptors or fingerprints to predict the toxicity of other chemicals. In addition to these statistical models, expert rule-based methods (structural alerts) are available. QSARs are also increasingly required for evaluations of substances that are toxic to development and reproduction.

Objectives: Aim of the study was to analyse freely available and commercial developmental and reproductive toxicity QSAR tools regarding their performance in a database with approx. 300 pesticides.

Materials & Methods: A database of 342 pesticides, which are or were approved in the EU, with information about their structure, pesticide class, mode of action and GHS classification by ECHA was prepared. The developmental and/or reproductive potential of the pesticides was predicted with different in silico tools: VEGA, OECD (Q)SAR Toolbox, Leadscope Model Applier and CASE Ultra by MultiCASE. The results were subsequently compared to the GHS classification by ECHA.

Results: In all models, a large proportion (up to 77 %) of all pesticides was classified as outside the applicability domain of the model. The evaluation of the prediction of the remaining pesticides resulted in a balanced accuracy of the models between 0.48 and 0.66.

Conclusion: The results show that the models' predictions are not fit for purpose, yet. A meaningful prediction of the toxicity of the tested pesticides was provided only rarely, often due to incompatibility of the chemical spaces. For the correct assessment of the prediction, all information in the underlying database must be considered, as well as potential modes of action and metabolism.

The models can be improved by expanding the existing, underlying databases with experimental standardized data. In addition, it would be necessary to generate an endpoint-specific database to allow for an in-depth evaluation of data.

205

Comparison of different Derek Nexus and Sarah Nexus software versions for the prediction of bacterial mutagenicity of pesticide compounds

J. König[1], K. Bech[1], B. Fischer[1], C. Kneuer[1], K. Herrmann[1]
[1]German Federal Institute for Risk Assessment (BfR), Pesticides Safety, Berlin, Germany

The use of (Q)SAR models plays an increasingly important role in risk assessment of pesticides. While experimental data on various toxicological endpoints is mandatory for active substances (a. s.), data requirements for metabolites and impurities are less strict and comprehensive. In this context, toxicological evaluation using (Q)SAR predictions is gaining importance. I*n silico* based predictions for bacterial mutagenicity using statistical and rule-based tools in combination show good performance. However, (Q)SAR models are continuously updated and new software

versions are released regularly. It should be noted that current software versions may lead to better or worse predictions for certain compounds.

The aim of the present study was to compare different software versions of Derek Nexus as rule-based and Sarah Nexus as statistical model. In particular, it was to clarify whether the prediction of bacterial mutagenicity has been improved in current software versions for compounds from the pesticide sector.

A balanced data set containing 15 mutagenic and 15 non-mutagenic compounds was selected, including a. s., metabolites and impurities. Experimental data was obtained from studies performed in compliance with OECD TG 471. *In silico* predictions were conducted using Derek Nexus 4.1.0, 6.0.1, 6.1.0 and 6.1.1 as well as Sarah Nexus 1.2.0, 3.0.0, 3.1.0 and 3.1.1. Specific acceptance criteria were defined to decide whether a prediction is "*mutagenic"*, "*non-mutagenic"* or *"not evaluable"*.

The second most recent versions Derek Nexus (6.1.0) and Sarah Nexus (3.1.0) correctly predicted 9/15 mutagenic substances. No compounds were evaluated as false-negative. In contrast, up to 2 compounds were evaluated as false-negative in previous versions.

Of the non-mutagenic compounds, 13/15 were correctly predicted with Derek Nexus (6.1.0) and Sarah Nexus (3.1.0), respectively. For one compound, the prediction was not verifiable and one substance was predicted as a false-positive. With earlier software versions, no reliable prediction could be made for up to 9 compounds and one additional compound was predicted as false positive.

Overall, the more recent Derek Nexus and Sarah Nexus versions performed better in identifying mutagenic and non-mutagenic compounds from the pesticide sector. Outdated analyses should thus always be reviewed before using them for regulatory purposes.

206

***In silico* prediction of clastogenic properties of pesticide metabolites and impurities – comparison of predictions and experimental data sets**

B. Fischer[1], K. Bech[1], K. Herrmann[1], A. Sonnenburg[1], S. Juling[1], C. Kneuer[1], J. König[1]
[1]German Federal Institute for Risk Assessment (BfR), Pesticides Safety, Berlin, Germany

Introduction and Objective: Prior to authorisation of plant protection products, biocides, and chemicals, applicants need to prove that their products are safe regarding human health. This is usually based on experimental data. However, *in silico* models may be used when technically justified, *e.g.* due to the instability or non-availability of the test compound or when there is no explicit legal requirement for experimental data. The latter applies, for example, to impurities and residues of metabolites in food. Interestingly, regulatory acceptance of (Q)SAR predictions varies depending on the toxicological endpoint. While *in silico* predictions for bacterial mutagenicity show a good performance and are therefore well accepted, the reliability for clastogenicity seems to be limited. It is assumed that predictions of clastogenicity exhibit a comparably low accuracy, possibly due to a higher number of false-positive results in the underlying data sets.

A pilot study recently conducted in our group, aimed to investigate the applicability of (Q)SAR tools to correctly predict potential bacterial mutagenicity of pesticide active substances, metabolites, and impurities. The present study now focusses on clastogenicity.

Methods and results: We have developed a database based on the OECD test guideline criteria to compile and curate experimental data from *in vitro* micronucleus tests (OECD TG 487) and to provide a concise, yet detailed extract of the respective study. A balanced test data set of 10 clastogenic and 10 non-clastogenic active substances, metabolites, and impurities was selected from this data to analyse in detail the respective (Q)SAR predictions of the expert system Derek Nexus and the statistical models of the Leadscope Model Applier. Furthermore, we have compared our experimental data with publicly available data from the EFSA genotoxicity data set.

Conclusion: A structured database was developed to collect data on clastogenicity. Data on clastogenic and non-clastogenic compounds collected according to OECD TG 487 was compiled. We present a comparison of *in silico* prediction performance. We assume that the use of curated test datasets is of key importance when evaluating the applicability of *in silico* models for clastogenicity of pesticides.

272

***Ab initio* assessment of interaction between nucleotide base pairs and anthocyanins of *Prunus serotina* Errh.**

O. Szczepaniak[1], **J. Brózdowski**[2]
[1]Poznań University of Life Sciences, Department of Gastronomy Science and Functional Foods, Poznań, Poland
[2]Poznan Univeristy of Life Sciences, Department of Chemical Wood Technology, Poznań, Poland

The aim of the study was to investigate the interactions of two anthocyanins found in fruits of *Prunus serotina* Errh.: cyanidin and malvidin with DNA base-pairs to vaidate it potential docking activity. There were the long-range interactions and hydrogen bonds that were compaired between the dsDNA and the studied anthocyanins. Simple base pairs AMP-TMP and GMP-CMP were adopted as the model for dsDNA. Moreover, an interaction study was performed for the 1R3Z structure.

To calculate the interaction energies, the RHF self-consitent field method was applied, along with STO-3G functional base. Optimizations and calculations were performed for the gas phase models, without taking into account the influence of the solvent. For calculation Gaussian software was used.

Based on the analyzed models, it can be concluded that anthocyanins have better binding with the guanine-cytosine pair than with the adenine-thymine pair. The models for GMP and CMP were characterized by more favorable interaction energies, the lowest value of which was achieved for the MGC model - describing the optimal interaction of malvidin with this pair of mononucleotides. Models using AMP and TMP were characterized by less favorable interaction energies. Moreover, these were positive values, indicating that their hypothetical formation would be unlikely. Excluding base superposition error, the models were characterized by the interaction energy lower than zero (Table 1). In addition, the excess electrons in the guanine and cytosine models accumulate on the aromatic C ring, which is electron deficient. This stabilizes the resulting complex also electrostatically. In the case of A-T models, the negative charge is mainly accumulated next to the interacting atoms, which favors its accumulation rather than dispersion. Interaction also resulted with changes in distance and angle between the nucleotides. These changes were most visible for the CAT and MGC models, for which the CMP changed from *anti* to *syn* conformation.

Fig. 2

Table 1. Total energy (E_b) values, base superposition error (E_{BSSE}) values, total energy values of individual monomers (E_m) and interaction energy values presented for each of the analyzed models

Model	E_b [4)]	E_{BSSE} [4)]	E_m [4)]	E_i [1)3)]	E_i [1)3)]
CAT	-3873.10	0.01	-3873.09	-15.89	-8.88
CGC	-3872.95	0.02	-3872.97	-4.34	9.61
MAT	-4006.97	0.02	-4006.99	-2.02	12.22
MGC	-4024.29	0.02	-4024.22	-54.47	-41.94
1R3Z+C	-13329.98	0.58	-13331.95	871.72	1235.93
1R3Z+M	-13479.55	0.60	-13481.20	662.82	1037.04

1) given in kcal/mol;
2) interaction energy with no E_{BSSE} corrections;
3) interaction energy with E_{BSSE} corrections;
4) given in Hartrees. 1 Hartree = 630 kcal/mol

CAT – cyanidin and adenosine-thymine base pair; CGC – cyanidin and guanosine-cytosine base pair; MAT – malvidin and adenosine-thymine base pair; MGC – malvidin and guanosine-cytosine base pair; 1R3Z+C – 1R3Z nucleotide with cyanidin; 1R3Z+M - 1R3Z nucleotide with malvidin

278

Chlorpyrifos kinetics in pregnant and non-pregnant women using physiologically-based kinetic (PBK) modeling

E. Algharably[1], R. Kreutz[1], U. Gundert-Remy[1]
[1]Charité – Universitätsmedizin Berlin, Institute of Clinical Pharmacology and Toxicology, Berlin, Germany

Question: PBK modeling is a valuable tool to evaluate internal exposures to chemicals in situations where information on the kinetics is sparse. This applies particularly to special populations, e.g. pregnant women. Epidemiological studies have suggested that in utero exposure to Chlorpyrifos (CPF), an organophosphate insecticide, is associated with developmental neurotoxic effects in children later in life. In those studies daily dose of CPF are not given, but only blood concentrations in the pregnant women/cord blood. We aimed 1. to evaluate pregnancy-related kinetics and 2. to model the doses, based on the measured blood concentrations.

Methods: A PBK model for CPF in non-pregnant women and pregnant women was developed in PkSim ® using pregnancy-specific physiological data. We preformed population-based simulations for CPF plasma concentration-time profiles after oral intake in pregnant women at term (38 weeks of gestation) and compared the model output to non-pregnant women. By a reverse dosimetry (RD) approach, we calculated the dose of CPF in pregnant women that would result in the CPF concentration in blood measured at term. We established a dose-effect relationship between maternal dose and neurobehavioral/neurodevelopment findings in their offspring.

Results: The mean AUC in pregnant women was 3.3 fold higher than that obtained in non-pregnant women. The predicted oral doses were 6.4, 1.3 and 0.6 µg/kg/day corresponding to blood levels of 0.56 ng/ml, 10.6 pg/g, 5 pg/g measured at term in previous studies (Rauh et al. 2006; Rauh et al. 2011; Silver et al. 2017). Neurodevelopmental adverse effects were reported at predicted doses (pd) above 1.3 µg/kg/day. The plausibility of the established kinetic model was confirmed by

comparing the pd with the low adverse effect level from rat developmental neurotoxicity studies, showing a margin of safety as the conventional uncertainty factor.

Conclusion: Systemic exposure to CPF in pregnant women is lower compared to non-pregnant women due to pregnancy-related changes in physiological parameters including higher volume of distribution and decrease in protein binding in pregnancy.

Toxicology – Emerging topics

15

Identification of the EGF receptor extracellular domain as a cell-surface sensor for dioxins and structurally related persistent organic pollutants

C. Vogeley[1], N. Sondermann[1], S. Woeste[1], A. Momin[2], A. Rossi[1], S. Arold[2], **T. Haarmann-Stemmann**[1]
[1]IUF - Leibniz-Research Institute for Environmental Medicine, Düsseldorf, Germany
[2]King Abdullah University of Science and Technology, Division of Biological and Environmental Sciences and Engineering, Thuwal, Saudi Arabia

Background: Chloracne, a persistent acne-like skin eruption, is the hallmark of an acute intoxication with dioxins and related halogenated aromatic hydrocarbons. The underlying pathomechanisms are not well understood but may involve alterations in the proliferation and differentiation of sebocytes and epidermal keratinocytes. The fact that in contrast to dioxin-like compounds (DLCs) some chloracnegenic agents do not bind to the aryl hydrocarbon receptor (AHR) implies the involvement of other cellular effector molecules. Preliminary data of our group point to an involvement of the epidermal growth factor receptor (EGFR), an important regulator of keratinocyte biology.

Objective: To investigate whether the EGFR serves as a cell-surface sensor for dioxins and polychlorinated biphenyls (PCBs).

Material & methods: Human HaCaT keratinocytes, Western blot analyses, *in silico* docking analysis, EGFR internalization assay, site-directed mutagenesis, CRISPR/Cas-based AHR knockout, BrdU incorporation assay.

Results: Western blot analyses revealed that a treatment of HaCaT keratinocytes with DLCs inhibits the growth factor-stimulated phosphorylation of EGFR. Results from EGFR internalization assays confirmed that DLCs, i.e. 2,3,7,8-tetrachlorodibenzo-*p*-dioxin and PCB126, interfere with the EGF-induced internalization of the receptor tyrosine kinase. *In silico* docking analyses predicted that DLCs interact with the extracellular domain (ECD) of EGFR in its extended conformation in close proximity to the EGF binding site. A mutational exchange of the ECD amino acid residues predicted to be essential for DLC-binding (Q8A, Q408A) and subsequent Western blot analyses confirmed that the EGFR ECD serves as a cell-surface receptor for DLCs. Further experiments assessing the effect of various DLCs as well as non-dioxin-like PCBs on EGFR ligand-induced DNA synthesis in genetically-modified HaCaT keratinocytes revealed that the chloracnegens inhibit EGFR function independently of AHR.

Conclusion: Dioxins and PCBs, including non-dioxin like congeners, are capable of binding to the EGFR ECD to attenuate growth factor-induced signal transduction and DNA synthesis in human keratinocytes. These data may enhance our understanding of the pathogenesis of chloracne and other diseases associated with an exposure to ubiquitous halogenated aromatic hydrocarbons.

40

Oral exposure to cyclic siloxanes from silicone-made food contact materials – is there a risk?

E. Galbiati[1], T. Tietz[1], C. Lorenz[1], S. Merkel[1], A. Luch[1], **S. Zellmer**[1]
[1]German Federal Institute for Risk Assessment (BfR), Department of Chemical and Product Safety, Berlin, Germany

Introduction: Silicone bakeware products are widely used in both industrial and consumer applications as alternative to metal or single-use paper bakeware. Residues of cyclic volatile methyl siloxanes (cVMS) used for and formed during the production of silicone-based polymers can migrate into food and food simulants, and thus raising some concerns on potential adverse health effects. Octamethylcyclotetrasiloxane (D4), decamethylcyclopentasiloxane (D5) and dodecamethylcyclohexasiloxane (D6) are listed as Substances of Very High Concern (SVHC) for authorization due to their properties as being persistent, bioaccumulative and toxic (PBT) and very persistent and very bioaccumulative (vPvB). D4 is classified as toxic to reproduction (cat. 2). Toxicological data on the other oligomers are scarce or missing. Migration levels depend on the type and composition of food(simulants). Mean concentrations of D3 to D9 were 11.4 mg/kg (ranging from 0.09 to 53.5 mg/kg) in cake samples [1]. Toxicological effects resulting from the intake of cVMS via food have not been assessed yet. Publicly available toxicological data were used to estimate a temporary tolerably daily intake (tTDI) for cVMS, in order to set the basis for future risk assessment.

Materials & methods: A comprehensive literature review was performed to establish a Point of Departure (PoD) for the cVMS risk assessment. The tool PROAST was used to derive a PoD via BMD-modelling. Inhalation-to-oral extrapolation was conducted by applying default physiological parameters. From the corresponding tTDI, acceptable migration into food was calculated assuming a body weight (bw) of 60 kg and food consumption of 1 kg food/day.

Results: Inhalative exposure studies in rats with D4 and D5 showed increased kidney weight, associated with chronic nephropathy in both sexes, as the most sensitive effect. Modelling the non-adaptive absolute kidney weight increase after 24 months in male rats gave a BMDL05 of 84 ppm. The BMDL05 corresponds to a tTDI of 0.21 mg/kg bw/day, resulting in an acceptable migration of 13 mg/kg food.

Conclusion: Due to missing data for higher cVMS, a read-across approach was applied. Correspondingly, the tTDI should apply to the sum of D3 to D13, resulting in an acceptable overall migration of 13 mg/kg food. Several sources of uncertainty were identified, which should be addressed in the future.

[1] DOI: 10.1016/j.envint.2019.01.081

Fig. 1

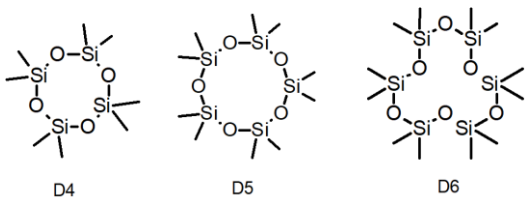

60

PAHs induce AKR1C3 expression through a non-canonical AHR signaling pathway: Implications for prostaglandin metabolism and Th2-related skin inflammation

C. Vogeley[1], S. Kress[1], S. Woeste[1], A. Rossi[1], D. Lang[2], M. Nakamura[1,3], J. Krutmann[1], T. Schikowski[1], T. Haarmann-Stemmann[1]
[1]IUF - Leibniz-Research Institute for Environmental Medicine, Düsseldorf, Germany
[2]Bayer AG, Pharmaceuticals, Wuppertal, Germany
[3]Nagoya City University, Department of Environmental and Geriatric Dermatology, Nagoya, Japan

Background: In the skin, activated mast cells release prostaglandin D_2 (PGD_2) which subsequently stimulates type 2 T helper (Th2) cell-driven inflammation. PGD_2 is unstable and spontaneously dehydrates to anti-inflammatory 15Δ-PGJ_2 or is reduced by aldo-keto reductase (AKR) 1C3 to 9α,11β-PGF_2. The metabolite 9α,11β-PGF_2 is less potent in activating Th2 cells than PGD2 but metabolically stable and thus prolongs allergic inflammation. Interestingly, recent studies reported that an exposure to polycyclic aromatic hydrocarbons (PAHs) and PAH-rich particulate matter (PM) fosters the worsening of Th2-related atopic diseases.

Objective: To mechanistically assess whether PAHs are capable of inducing AKR1C3 expression and associated PGD2 reduction in human keratinocytes and to elucidate its clinical relevance for atopic dermatitis (AD).

Material & methods: Human immortalized and primary keratinocytes, qPCR and Western blot analyses, LC-MS analysis, CRISPR/Cas-based gene knockouts, gene-environment interaction study.

Results: Treatment of keratinocytes with PAHs, i.e. benzo[a]pyrene and benzo[k]fluoranthene, elevated AKR1C3 gene and protein expression and the associated 11-ketoreduction of PGD_2 in an aryl hydrocarbon receptor (AHR)-dependent manner. Further mechanistic studies revealed that the PAH-induced and AHR-mediated upregulation of AKR1C3 occurred independently of ARNT and involved a sequential activation of tyrosine kinase c-Src, protein kinase C and metalloproteases. The resulting ectodomain shedding of the cell surface-bound growth factors amphiregulin and transforming growth factor-α led to an auto-/paracrine activation of the epidermal growth factor receptor (EGFR), downstream MEK/ERK signal transduction, and AKR1C3 transcription. The potential clinical relevance of the PAH-dependent induction of AKR1C3 was demonstrated by conducting a gene-environment interaction study with two German birth cohorts. This analysis, including land-use regression modelling and genotyping, showed that a "gain-of-function" polymorphism in the coding region of AKR1C3 interacts with the exposure to PAH-rich airborne PM in childhood AD.

Conclusion: Exposure to free and PM-bound PAHs may worsen the symptoms of AD by enforcing the AKR1C3-mediated production of Th2-stimulatory 9α,11β-PGF_2.

67

Impact of *in vitro* digested zinc oxide nanoparticles on Caco-2/HT29-MTX cocultured cells

A. Mittag[1], A. Singer[1], C. Hoera[2], M. Westermann[3], A. Kämpfe[2], M. Glei[1]
[1]Institute of Nutritional Sciences / Friedrich Schiller University Jena, Department of Applied Nutritional Toxicology, Jena, Germany
[2]German Environment Agency, Swimming Pool Water, Chemical Analytics, Bad Elster, Germany
[3]Friedrich Schiller University Jena, Electron Microscopy Centre, Jena, Germany

Introduction: Zinc oxide nanoparticles (ZnO NP) offer favourably characteristics for numerous applications, especially in the food sector. As part of the human food chain, they are presumably taken up orally. Data about the toxicological effects of orally ingested ZnO NP are still controversial and incomplete. Moreover, the properties of ZnO NP can change during the digestion process, which leads to a modified biological behaviour.

Objectives: The aim of our investigations was to examine the fate of digested ZnO NP and their effects on a model system of the intestinal barrier.

Materials & methods: ZnO NP were *in vitro* digested including a mouth, gastric and intestinal phase. Proportions of free zinc ions and bound zinc were investigated using inductively coupled plasma optical emission spectrometry. ZnO NP morphology was visualized via transmission electron microscopy during digestion. Caco-2 enterocytes and HT29-MTX goblet cells were cultured under coculture conditions (ratio 3:1) in a Transwell system for 23 days. They were incubated with 123–614 µM digested ZnO NP (<50 nm; <100 nm) or $ZnCl_2$ as salt control for 24 h. The cellular zinc uptake and zinc permeation through the monolayer were measured using inductively coupled plasma mass spectrometry. The barrier integrity was investigated by measuring the transepithelial electrical resistance (TEER) and permeability using FITC-dextran. The metabolic activity and mitochondrial membrane potential (MMP) of cocultured cells as well as the generation of reactive oxygen species (ROS) were quantified to examine the cytotoxic effects of digested ZnO NP.

Results: ZnO NP went through morphological changes during *in vitro* digestion with about 70% free zinc ions after the intestinal phase. There was a dose-dependent cellular zinc uptake after treatment with digested ZnO NP. The internalized zinc resulted in increased ROS amounts but showed no impact on the metabolic activity and MMP. Less than 1% zinc reached the basolateral area, which can be explained by the unmodified TEER and permeability.

Conclusions: The physicochemical properties of ZnO NP are changed during digestion, which should be taken into account when investigating the effects of orally ingested ZnO NP. *In vitro* digested ZnO NP have no toxic impact on differentiated Caco-2/HT29-MTX cocultured cells at concentrations of 123–614 µM.

76

Investigation of the cost-effective degradation of anti-inflammatory drugs using UV-C radiation with and without oxygen supply and the biological effects of anti-inflammatory drug residues on *C. elegans*

O. Krings[1], S. Raabe[2], B. Schumann[2], S. Kamalakkannan[2], F. Glahn[1], K. Krüger[2], H. Foth[1]
[1]Institute of Environmental Toxicology, Medical Faculty of Martin Luther University Halle-Wittenberg, Halle, Germany
[2]GMBU e.V., Department of Environmental Biotechnology, Halle, Germany

The aim of the project is to develop an innovative process for removing problematic substances from municipal and industrial wastewater by using UV-C radiation with or without oxygen supply and to test its efficiency in the model organism of Environmental Toxicology *C. elegans*. Anti-inflammatory drugs and their metabolites are difficult to remove in wastewater treatment plants due to their persistence and high water-solubility. For active pharmaceutical ingredients, however, the goal is to have remaining levels without biological effects. In previous investigations the anti-inflammatory drug Ibuprofen (2.5; 10; 25 µM) did not lead to toxic effects in *C. elegans*.

To investigate possible biological effects, the model organism *C. elegans* was cultivated in NGM (Nematode Growth Medium) with different concentrations of anti-inflammatory drugs (Diclofenac, Ibuprofen, Naproxen and Acetaminophen) without and with UV-C radiation or UV-C radiation with additional oxygen supply. Subsequently, studies of acute and chronic toxicity (life span assay, locomotion) and studies of reproductive toxicity (progeny assay) were established and conducted.

In studies on the chronic toxicity of Naproxen (2.5; 10; 25 µM), the life span of *C. elegans* is not shortened at any concentration compared to the untreated control. During the locomotion assay we could not observe any differences between groups exposed to Naproxen and controls. Moreover, Naproxen in NGM did not show effects in the progeny assay. Same observations were made for the samples with UV-C irradiation under oxygen supply.

In an initial assessment, Naproxen and it´s metabolites after irradiation show no toxicity, despite the selection of approximately 6000-fold higher concentrations than runoff waters from wastewater treatment plants previously analyzed (BLAC, 2003). Further investigations will be carried out on the biological effects of mixtures of the drugs investigated and their metabolites that arise after applying UV-C radiation under oxygen supply.

82

Investigation of the biological response of Acetaminophen and its residues after using UV-C radiation under oxygen supply on the model organism *Euglena gracilis*

S. Kamalakkannan[1], O. Krings[2], S. Raabe[1], B. Schumann[1], F. Glahn[2], H. Foth[2], K. Krüger[1]
[1]GMBU e.V., Department of Environmental Biotechnology, Halle, Germany
[2]Institute of Environmental Toxicology, Medical Faculty of Martin Luther University Halle-Wittenberg, Halle, Germany

A whole range of pharmaceutically active compounds (PACs) have been detected in waste water. As it is one of the most commonly used analgesic compounds in OTC-drugs Acetaminophen was selected for this study. The aim of this project is to examine the impact of the analgesic compound, Acetaminophen on the model organism *E. gracilis*. Since this analgesic compound is water-soluble and thus transportable in water, the aquatic ecosystem is of particular interest.

In order to understand the various possible biological responses of the micro-algae *E. gracilis* to analgesic compounds multiple levels of exposure were analysed. The micro-algae were cultured as a stationary culture at room temperature with 12 h of light/dark cycle to induce the combination of the auxotrophic and heterotrophic pathways. In our studies we used concentrations of 0.5, 1 and 2 mM of Acetaminophen and concentrations of 0.5, 1 and 2 mM of Acetaminophen's metabolites after irradiation, as well as after combination of irradiation and oxygen supply and negative controls, in total 10 groups of the analgesic compound were used for an exposure period of 7 days. Cell density, growth rate and chlorophyll content were measured.

The highest concentration group (2 mM) of Acetaminophen with UV-C irradiation and oxygen supply showed a 294.6% increase in cell density compared to the negative control after 168 h. The highest concentration group (2 mM) of Acetaminophen with UV-C irradiation showed a similar increase (292.2%) in cell density after 168 h. Whereas, the highest concentration (2 mM) of Acetaminophen shows only a 9.5% increase in cell density. The chlorophyll content shows no difference among the different dose groups. Further investigations will be carried out to measure induction of oxidative stress and use of Acetaminophen metabolites by *E. gracilis* as possible food source.

84

Effects of genetic or pharmacological Nrf2 activation on aldosterone-induced kidney damage in mice

R. Brinks[1], C. Wruck[2], N. Schupp[1]
[1]Institute of Toxicology, Medical Faculty, Heinrich Heine University of Düsseldorf, Düsseldorf, Germany
[2]Institute of Anatomy and Cell Biology, RWTH Aachen University, Aachen, Germany

Question: The blood pressure regulating mineralocorticoid aldosterone (Ald) is known to cause kidney damage and oxidative stress. As a protection against the induced damage, kidney cells upregulate key regulators of the antioxidant defence, such as nuclear factor erythroid 2-related factor 2 (Nrf2). The aim of the present study is to investigate the influence of pharmacological or genetic Nrf2 activation on aldosterone-induced kidney damage and oxidative damage in mice.

Methods: Male wildtype (WT) and transgenic Keap1 hypomorph ($Nrf2^{\uparrow}$) mice received Ald combined with 1% NaCl in the drinking water. In $Nrf2^{\uparrow}$ mice it could been shown that Nrf2 is already upregulated. Additionally, WT mice were treated with an Nrf2 activator (sulforaphane) alone and in combination with Ald (WT Ald+Nrf2 activator). After 4 weeks the kidneys were isolated for further analysis.

Results: Ald-exposed WT mice showed a significantly changed blood pressure compared to the WT control whereas the blood pressure of the $Nrf2^{\uparrow}$ Ald mice did not change compared to their control. Kidney weights were significantly higher in Ald-treated mice and in the WT Ald+Nrf2 activator group. Additionally, kidney weights of control $Nrf2^{\uparrow}$ mice were higher compared to the WT control. The kidney function of both Ald-infused groups (WT Ald and $Nrf2^{\uparrow}$ Ald) was impaired, as detected by elevated levels of albumin in urine. WT mice treated with Ald and the Nrf2 activator revealed lower albumin levels compared to WT Ald mice. The tubular damage marker neutrophil gelatinase-associated lipocalin (NGAL) in urine was not increased in $Nrf2^{\uparrow}$ Ald mice, but in WT-Ald and WT Ald+Nrf2 activator mice. Increased systemic oxidative damage as reflected by urinary 8-OHdG and 15-isoprostane F_{2t} excretion was measured in the Ald treatment groups, but not in the WT Nrf2 activator group. Surprisingly, the excretion was also significantly higher in the combination treatment.

Conclusion: Aldosterone infusion increased oxidative stress and kidney damage in WT mice. Whereas treatment with the Nrf2 activator in WT-Ald mice reduced the marker of glomerular damage, albumin, in $Nrf2^{\uparrow}$ Ald mice a reduction of the marker for tubular damage, NGAL, was observed. Surprisingly, the induced oxidative damage by Ald was also neither prevented by genetic nor pharmacological activation of Nrf2.

110

Transcriptional responses to genotoxic and non-genotoxic compounds in the liver model HepaRG and the blood cell model TK6

K. Kreuzer[1], H. Sprenger[1], A. Braeuning[1]
[1]Federal Institute for Risk Assessment, Food Safety, Berlin, Germany

To evaluate the genotoxic and carcinogenic potential of chemicals, a battery of in vitro (and sometimes also in vivo) tests is applied as standard regulatory practice. In the last decade, transcriptomics approaches demonstrated that genotoxic (GTX) compounds can be distinguished from non-genotoxic (NGTX) compounds based on transcriptomic response. However, omics techniques are not yet accepted for regulatory purposes.

We identified a 33-gene transcriptomic signature for food-relevant GTX carcinogens in the metabolically competent human liver cell line HepaRG by RNA sequencing. To verify whether the signature can be transferred to another cell line, the treatment and sequencing were repeated as similarly as possible in the p53-competent blood cell model TK6.

A simple comparison of the two RNA sequencing experiments showed clear differences between HepaRG and TK6 cells in the regulation of the published 33-gene signature of HepaRG cells. Only six of the genes from the signature were also significantly altered in TK6 cells, three of which were not consistent with the direction of change observed in HepaRG. It was also remarkable that there was no difference between GTX and NGTX effects in the mapped genes in TK6 cells, contrasting previously published results using the HepaRG model. Previous analyses of transcriptomic data with the software Ingenuity Pathway Analysis (IPA) showed that GTX-affected cellular functions in HepaRG cells share a high degree of similarity. For TK6 cells, IPA analyses revealed that the response was substantially different among GTX compounds at the level of pathway and regulator predictions. Thus, a different strategy had to be chosen to establish criteria for a clear separation between GTX and NGTX compounds in TK6 cells. With a Partial Least Squares Discriminant Analysis, it was possible to derive a gene signature from the RNA sequencing data of the TK6 cell line.

In conclusion, the data show that transcriptomic responses may vary widely in different cell models. Nonetheless, a transcriptomic GTX signature was derived in the blood cell model. This suggests that gene expression analyses of blood samples could be a valuable approach to assess responses to toxic exposure in target organs such as the liver.

114

A multisystemic approach to investigate the role of polystyrene nanoparticles on neurodegeneration

L. Schröter[1], A. Limke[1], A. von Mikecz[1], S. Maglioni[1], L. Jentsch[1], N. Ventura [1]
[1]IUF – Leibniz-Institut für umwelt- medizinische Forschung gGmbH, Düsseldorf, Germany

Objectives: Nano plastic particles (NPs) derived from the degradation of all sorts of disposable plastics can be found in the air, water, the food and in several day-to-day products. We are thus continuously confronted with these small particles and recent investigation could show their internalization into human cells thus raising the concern about their possible toxic effects for organismal health. The aim is to assess the effect of different NPs (non-modified and aminated polystyrene particles, PS/PS-NH2) on different readouts primarily of relevance for the nervous system, through a multisystemic approach.

Material & Methods: The effect of NPs (50 nm) acute exposure was investigated *in vitro* (in undifferentiated and differentiated SH-SY5Y cells) by assessing cytotoxicity, neuronal like differentiation and secretion of Alzheimer"s Disease related protein Aß (ß Amyloid). Moreover, the particle effect was evaluated upon chronic exposure *in vivo* (in *C. elegans*) looking at animals" development (4 days of exposure) and health-span (~20 days of exposure).

Results: Experiments in undifferentiated cells treated with PS and PS-NH2 revealed a significant reduction in cell viability induced by PS-NH2 (> 5 µg/cm²) but not by PS. Moreover, Aβ ELISA assays indicated an increase in Aβ 1 – 42 secretion after exposure to PS-NH2. Particle treatment in differentiated cells could show a degeneration of neurite outgrowth with very low concentrations of PS-NH2 (2 µg/cm²). Worms" lifespan and movement was not altered when animals were treated with particles on solid agar plates, compared to liquid exposure, likely due to differences in particle availability and absorption. Instead, treatment with 50 µg/mL PS-NH2 in liquid culture starting from embryo lead to a strong delay in animals" development and a sick phenotype, whereby treatment from young adult decreased the lifespan up to 20% compared to control. PS only slightly decreased lifespan at much higher (100 µg/mL) doses.

Conclusion: My results show aminated particles have toxic effects in both *in vitro* and *in vivo*. First investigations suggest a correlation of NPs exposure with neurodegeneration, by increasing Aß secretion and impairment of neuronal outgrowths. Further work is planned to evaluate additional parameters of relevance for the nervous system *in vitro* as well as *in vivo* and to investigate the molecular mechanisms underlying their toxic effects.

167

SEMO-1 (Y37A1B.5), a novel selenium-binding protein ortholog and hydrogen sulfide source, mediates selective stress resistance in the model organism *C. elegans*

V. A. Ridolfi[1], T. M. Philipp[1], W. Gong[1], J. Priebs[1], H. Steinbrenner[1], L. O. Klotz[1]
[1]Friedrich-Schiller-Universität Jena, Nutrigenomik, Jena, Germany

Question: The *Caenorhabditis elegans* ortholog of human selenium-binding protein 1 (SELENBP1), Y37A1B.5 (Y37), is a pro-aging factor. Knock-down of Y37 resulted in elevated lifespan and better resistance against oxidative stress [1]. SELENBP1 catalyzes the conversion of methanethiol to hydrogen sulfide (H_2S), hydrogen peroxide (H_2O_2) and formaldehyde, thus acting as methanethiol oxidase (MTO). Here, we tested whether Y37 has MTO activity, whether it is involved in selenium homeostasis, and whether energy metabolism is involved in the observed modulation of lifespan by Y37.

Methods: MTO activity was measured using a coupled assay based on *in situ*-generation of methanethiol as catalyzed by a bacterial recombinant L-methionine gamma-lyase, followed by detection of MTO-generated H_2S and H_2O_2 [2]. Lifespan analyses were performed using standard *C. elegans* culture. For stress resistance analyses, nematodes were exposed to toxic concentrations of selenite or paraquat. Worms employed included N2 wildtype and mutant strains deficient in Y37 or in the AMPK ortholog, AAK-1/-2.

Results: Like SELENBP1, isolated recombinant Y37 has MTO activity. While MTO activity was detected in lysates from wild-type nematodes, the Y37-deficient strain was devoid of it. A Y37-deficient mutant strain generated through CRISPR/Cas technology exhibited an extended lifespan, similar to the previously reported worms exposed to Y37-specific RNAi. Moreover, resistance against the redox-cycler paraquat was also improved in the Y37-deficient strain. In contrast to paraquat, selenite was more toxic in the Y37-deficient strain, as compared to wild-type worms. Lifespan extension following Y37 depletion was abrogated in a mutant strain deficient in both isoforms of the catalytic AAK subunit, while Y37 depletion through RNAi appeared to enhance AAK phosphorylation in wild-type worms.

Conclusions: (1) Y37 acts as MTO in *C. elegans*; thus, we named it SEMO-1 (SELENBP1 ortholog with MTO activity). (2) SEMO-1 mediates selective stress resistance. It renders worms susceptible to oxidative stress but also serves as selenium buffer, protecting against high doses of selenite. (3) SEMO-1 is involved in the AAK-mediated regulation of energy metabolism, thereby affecting organismal lifespan and stress resistance.

Support: Deutsche Forschungsgemeinschaft (DFG, Bonn, Germany) RTG 2155, "ProMoAge".

[1] Köhnlein *et al.*, Redox Biol. 28:101323 (2020), [2] Philipp *et al.*, Redox Biol. 43:101972 (2021).

175

Pilot monitoring Lübeck Bay – A two-year monitoring study on the release of explosive compounds from dumped munitions, and pharmaceuticals in the marine environment

T. H. Bünning[1], J. S. Strehse[1], E. Maser[1], C. Böttcher[2]
[1]University Medical School Schleswig-Holstein, Institute of Toxicology and Pharmacology for Natural Scientists, Kiel, Germany
[2]Ministry of Energy, Agriculture, the Environment, Nature and Digitalization, Schleswig-Holstein, Sonderstelle Munition im Meer, Kiel, Germany

Question: In the period after the Second World War, about 1.6 million tons of munitions were dumped in German waters, of which an estimated share of 300,000 tons is located in in the Baltic Sea, especially in the three former dumping grounds "Kolberger Heide", "Kleiner Belt" and "Lübecker Bucht". In contrast to the Kolberger Heide, where large-scale ordnance such as naval mines and torpedo heads are piled up in places, and which has been extensively studied in the UDEMM project, in the Lübeck Bay mainly smaller munitions like rifle ammunition, artillery shells and hand grenades, packed in ammunition boxes, were sunk in an estimated total amount of 65,000 tons. The ecotoxicity of explosives such as TNT and its metabolites to the marine environment has been researched and documented in numerous studies in recent years. It is also known that pharmaceuticals in the sea are of ecotoxicological concern. Therefore, analytical methods for these substances should be integrated into existing monitoring efforts in the North and Baltic Seas.

Methods: In cooperation with the Ministry of Energy, Agriculture, the Environment, Nature and Digitalization (MELUND) and the State Agency for Agriculture, the Environment and Rural Areas (LLUR) of Schleswig-Holstein a two-year pilot monitoring program was run. Monthly water samples were taken at four designated sampling stations as part of LLUR's routine monitoring in Lübeck Bay. In addition, blue mussels, accompanied by passive samplers, were deployed a total of six times at four locations within the dumping areas and recovered after two to nine months. Water samples were also taken directly from dumped munitions objects.

Results and Conclusion: The samples were processed in the lab and analyzed by GC-MS/MS for their concentrations of the munition compounds 1,3-DNB, 2,4-DNT, TNT, and its metabolites 2- and 4-ADNT. All of them have been detected in the low

nanogram range in all water samples tested to date (08.2019 – 08.2020), as well as in the passive samplers, and in traces below the quantification limit also in the mussels. The measured values are thus significantly lower than those found in the Kolberger Heide. Further, the five human and veterinary pharmaceuticals diclofenac, carbamazepine, imidacloprid, cypermethrin and diazinon were also measured by GC-MS/MS and LC-MS/MS in the taken samples.

239

Beyond microplastics: First investigations on submicron- and nanoplastic particles *in vitro*

M. Paul[1], A. Braeuning[1], H. Sieg[1]
[1]German Federal Institute for Risk Assessment, Berlin, Germany

Due to continuously increasing plastic production and waste, microplastics became a very intensively discussed topic. Published data regarding orally absorbed microplastics, especially polystyrene, show that particles smaller than 1.5 µm might be bioavailable and cross the gastrointestinal barrier. With regard to the risk assessment of smaller nanoplastic particles, hardly any data on toxicological endpoints and gastrointestinal absorption are available. Due to its small size, nanoplastics might be able to overcome the gastrointestinal barrier more effectively than microplastics and thus show increased bioavailability.

This study aims to investigate possible toxic effects of food-relevant materials in submicron or nanoscale ranges after oral uptake *in vitro*. Therefore, polymethyl metacrylate (25 nm), melamine resin (366 nm), polylactic acid (250 nm and 2 µm) particles were used.

Particles were characterized using electron microscopy, dynamic light scattering and different viability assays. By using *in vitro* Transwell® systems, studies on the uptake and transport of submicron- and nanoplastics via the gastrointestinal tract were conducted. To this end, Caco-2 cells were cultivated alone or in co-cultures with Raji B or HT29-MTX cells. Afterwards, uptake of particles in liver cells (HepG2) was examined using flow cytometry.

All particles were taken up by Caco-2 cells in different amounts and a very low fraction was transported through the gastrointestinal barrier. Liver cells were also able to take up all types of particles. Especially for the PLA250 and MF366 particles, different accumulation of particles in cells was detected, indicating various ways of uptake mechanisms. However, the particles showed cytotoxicity in Caco-2, HepG2 and HepaRG cells only at unphysiologically high concentrations.

This study provides evidence for gastrointestinal uptake of submicron- and nanoplastics and points towards differences of oral bioavailability between microplastics and smaller plastic particles.

277

Snake venom - an emerging challenge in cosmetology

D. G. Moisă[1], F. G. Gligor[1], L. L. Rus[1], C. Morgovan[1], A. Frum[1], A. M. Juncan[1]
[1]Lucian Blaga University of Sibiu, Sibiu, Romania

Questions: *Regnum Animalae* represents a valuable source of compounds with potential applications in cosmetology. Nowadays, there were reported various bioactive compounds (1), including proteins from the venom of insects and reptiles with a therapeutic potential (2). The objective of this study was the identification of proteins and peptides from snake venom which have benefical effects for human use and which confer the possibility to be incorporated in cosmetic products with various claims.

Methods: 1) Identification of actual studies in order to evaluate the snake venom composition; 2) Identification of cosmetics from online media based on specific keywords (*"snake venom", "snake", "viper venom", "SYN-AKE", "analogues of snake venom"* or *"synthetic snake venom")* and their comparative analysis.

Results: The snake venomous contain a mixture of different families of enzymatic (phospholipase A2, hyaluronidase, proteinases, L-amino acid oxidase) and non-enzymatic proteins (disintegrines, proteinase inhibitors and Three finger toxins) which represent 90-95% of dry weight of venom (2,3). In cosmetology, the use of snake venom represents an emerging domain like the development of neurocosmetics, because of its skin benefits and cosmetic claims. Thus, this products contain different peptides (e.g., neurotoxins) with anti-aging effect, by relaxing facial muscles, minimizing wrinkles (4). There were analyzed 140 cosmetics (51 manufacturers). The snake venom, namely viper venom was identified in 26 of the total analyzed products (18.6%). In 104 products (81.4%) the synthetic analogue of Waglerin-1, a peptide from the viper venom (SYN®-AKE), was present in different concentrations, from 0,01-4%.

Conclusions: In the last years, there was observed a great interest in the research of bioactive compounds used in cosmetic formulation, as well as for biotechnologies in order to obtain their structural analogues, with a lower price compared to that of natural venom.

References:

1) Juncan AM et al. Advantages of Hyaluronic Acid and Its Combination with Other Bioactive Ingredients in Cosmeceuticals. *Molecules*. 2021; 26(15):4429;

2) Utkin YN. Animal venom studies: Current benefits and future developments. *World J Biol Chem* 2015;6(2):28–33;

3) El-Aziz TMA et al. Snake Venoms in Drug Discovery: Valuable Therapeutic Tools for Life Saving. *Toxins* 2019, 11, 1–25;

4) Casewell NR et al. Complex Cocktails: The Evolutionary Novelty of Venoms. *Trends Ecol Evol* 2013, 28, 219–229.

Pharmacology – Pharmacological education

10

Rudolf Buchheim

H. Greim[1,2]
[1]Technical University of Munich, Toxikologie und Umwelthygiene, Freising-Weihenstephan, Germany
[2]University, Toxicology, Freising-Weihenstephan, Germany

Rudolf Buchheim (1820-1879) was born in Bautzen as a son of a physician. As a medical student in Leipzig, he started his research in the Dept. of Physiology (Ernst Heinrich Weber) where his supervisor the physiological chemist Karl Gotthelf Lehmann (1812-1863) introduced him to the chemical aspects of medicine. His German translation of the popular book "*The Elements of Materia Medica and Therapeutics"* made him familiar with pharmacology. Based on his research work he concluded that modern pharmacology needs to adopt methods of physiology and pathology to understand the mechanisms of action of a particular drug and its effects on organs and he supplemented each drug chapter with the experimental data headed by "Mode of Action". And, in 1849 he stated: "The investigation of drugs is a task for the pharmacologist and not for a chemist or pharmacist, who until now have been expected to do this."

Due to the recommendation of the physiologist Friedrich Bidder, Dean of the Medical Faculty in Dorpat he moved to Dorpat (Tartu) as chairman of *Materia Medica, Dietetics and History and Encyclopaedia of Medicine*in 1847. There he established a pharmacological laboratory in the basement of his house, which in 1860 has been moved into the new and spacious Institute of Pharmacology, which served his successors Schmiedeberg (1867), Boehm (1872), Meyer (1882) and Kobert (1886). After 20 years in Dorpat in 1867 he accepted the chair of Pharmacology in Giessen where the construction of a spacious department has been promised. However, the building was still under construction when he died in 1879.

In his publication *Über die Aufgaben* und *die Stellung der Pharmakologie* an den deutschen *Hochschulen. Arch. exper. Path. Pharmak. 5 (1876) 261-278* Buchheim defined the new role of pharmacology in research and education of students. Since pharmacology is no longer based on simple observations of the patient"s reaction to drug treatment, it is a theoretical discipline close to physiology and needs to be presented to the students with the same intensity as physiology. With this, the basic competence of a pharmacologist in research and teaching needs to be chemistry and physiology.

11

PubPharm – Platform for pharmacology, toxicology & pharmacy-specific literature search

C. Draheim[1], D. Eckweiler[1], H. Kroll[2], J. Ohms[1], J. Wawrzinek[2], S. Wulle[1], W. T. Balke[2], K. Stump[1]
[1]Technische Universität Braunschweig, Universitätsbibliothek, Braunschweig, Germany
[2]Technische Universität Braunschweig, Institut für Informationssysteme, Braunschweig, Germany

The drug-centred search platform PubPharm (www.pubpharm.de) comprises more than 55 million pharmacology-, toxicology- and pharmacy-specific publications, including the complete Medline/PubMed and additional life science resources: Journal articles, preprints, information on clinical trials, patents, books, e-books and dissertations. The location-based availability check supports a direct access option for many electronic resources. In addition to the text-based search function, PubPharm offers a structure search capability. If possible, search results are linked to relevant pharmaceutical and bioinformatical sources, e.g. KEGG, Uniprot, and DrugBank.

PubPharm is the central service of the "Fachinformationsdienst Pharmazie", which aims to sustainably improve the supply of literature for academic pharmaceutical research in Germany (1). In this project, the cooperation between the University Library and the Institute for Information Systems at TU Braunschweig results in innovative services for PubPharm such as: Listing contextualized substances, diseases or genes when searching for a drug substance or disease, and the visualisation of drug-disease associations in interactive network views (2). The latest development is a novel prototype providing a narrative information access (3). Todays

researchers often look for scientific narratives, i.e. short stories talking about the interaction of pharmaceutical entities such as drugs, diseases or targets. When being restricted to keyword-based search, formulating precise narratives can be exhausting. Therefore, the prototype supports the precise formulation of short narratives consisting of entities (drugs, diseases, targets, etc.) and interactions between them (treats, inhibits, etc.). On the one hand, narrative queries result in precise document hits. On the other hand, narrative queries feature placeholders that provide an entity-structured literature overview.

Acknowledgments: The project is funded by the Deutsche Forschungsgemeinschaft.

1. Draheim C, Keßler K, Wulle S. PubPharm – die Rechercheplattform. PZ Prisma 2019; 26(2):68-74.
2. Wawrzinek J, Pinto J M G, Balke W-T. Linking Semantic Fingerprints of Literature – from Simple Neural Embeddings Towards Contextualized Pharmaceutical Networks. TPDL. Springer, Cham, 2019; 33-40.
3. Kroll H, Nagel D, Balke W-T. Modeling Narrative Structures in Logical Overlays on Top of Knowledge Repositories. International Conference on Conceptual Modeling. Springer, Cham, 2020.

28

Advantages and disadvantages of a blended PbL approach – students' views obtained by qualitative content analysis

U. Servos[1], **J. Matthes**[1]
[1]Universität zu Köln, Zentrum für Pharmakologie, Köln, Germany

Introduction: Problem-based Learning (PbL) is a widely used format for small group teaching in medical studies. In a pre-pandemic study, we compared a conventional on-site PbL (cPbL) with a variant where the first PbL meeting takes place via a written internet chat (blended PbL or bPbL).

Objectives: To obtain anticipated and perceived advantages and disadvantages of the blended PbL approach from the students' point of view.

Materials & methods: During summer term 2018 and winter term 2018/2019, 3rd-year students attended a mandatory course consisting of 2x1h PbL, 3x1h lecture, a two-hour exercise and a final summative written exam. Some were randomised to the bPbL variant. The main difference to the conventional PbL approach was that the first PbL appointment took place as a purely written internet chat instead of an on-site meeting. At the end of the second PbL appointment, which took place on site for all groups, the students were asked to name advantages and disadvantages of the bPbL approach. Interviews were audio-taped, transcribed and analysed according to qualitative content analysis as described by Mayring.

Results: The content analysis resulted in 49 categories. 21 of the categories were associated with at least one mention of an advantage of bPbL and 34 with a disadvantage. Both the cPbL and bPbL groups saw the following aspects as advantages of bPbL: no need to travel, free choice of learning location and the comfortable learning environment (probably mostly: at home). The following aspects were seen as disadvantages of bPbL by both the cPbL and bPbL groups: typing to communicate, lack of communication forms, language reduction, lack of depth of discussion, and lack of social, direct interaction. More cPbL groups felt that meeting via chat was time-saving, while more bPbL groups stated that it was time-consuming, e.g. because of the need to type. Although the same number of groups were interviewed, the content analysis revealed more different arguments both for and against bPbL from the bPbL groups.

Conclusion: Both cPbL and bPbL groups see advantages and disadvantages in running one of two PbL meetings in the form of a written chat. The more differentiated feedback of the bPbL groups indicates that some advantages and disadvantages are only recognised through their own experiences. Overall, the qualitative data, as well as the quantitative data presented earlier, show that our blended PbL can be a suitable and accepted variant of PbL.

124

Eight Pharmacologic – Historical Forum: Scope, development and perspectives

A. Philippou[1], H. Greim[1]
[1]University of Innsbruck, Pharmacology and Toxicology, Innsbruck, Austria

The "Pharmakologie - Historisches Forum" was established nine years ago. Aim of the Forum is to honour personalities of Pharmacology, Clinical Pharmacology and Toxicology of the various Universities of Germany who, with their research, have greatly contributed to the development of their scientific disciplines. Further scope of the Forum is to inform young pharmacologists and toxicologists about the achievements of our famous predecessors. The first Forum was initiated by Roland Seifert. It was organized by Brigitte Lohff and Athineos Philippou and was held 2014 during the 80th Annual Meeting of the DGPT in Hannover. Theme was the life and scientific work of Marthe Vogt and Edith Bülbring. The following Forums have been organized by Athineos Philippou. The second one (Kiel, 2015) was dedicated to Heinz Lüllmann. The third Forum (Berlin 2016) was dedicated to the Pharmacologists of Berlin who worked there after the Second World War (Hans Herken, Friedrich Jung, Helmut Coper, Helmut Kewitz) including the years that Wolfgang Heubner has spent in Berlin. The fourth Forum (Heidelberg 2016) was honouring Wolfgang Heubner and Franz Gross, both Professors and Heads of the Pharmakologisches Institut. The fifth Forum" (Göttingen, 2018) was dedicated to Ludwig Lendle who, besides his scientific work, also founded the second Chair for Pharmacology and Neuropharmacology. The sixth Forum (Stuttgart, 2019) was dedicated to Clinical Pharmacology. Ulrich Klotz and Helmut Greim spoke about the history of the Dr. Margarete Fischer-Bosh Institute for Clinical Pharmacology and Emil Starkenstein, Prague. The seventh Forum, held in Leipzig 2020 was dedicated to Fritz Hauschild, Reinhard Ludewig and the Papyrus Ebers presented by the historian of the Leipzig University Reinhold Scholl. Due to covid-19, the eight Forum is held in Bonn 2022 instead of 2021. Gunther Hartmann will honour Hans J. Dengler and Paul Martini, Eberhard Schlicker and Ivar von Kügelgen Manfred Göthert and Helmut Greim Rudolf Richard Buchheim.

152

Manfred Göthert - life and work - Symposium Pharmakologie-historisches Forum

E. Schlicker[1], I. von Kügelgen[1]
[1]University of Bonn, Department of Pharmacology, Bonn, Germany

Late Professor Manfred Göthert was a leading scientist in pharmacology, who published nearly 300 original and review articles. He was born in 1939 in Braunschweig and studied medicine in Hamburg, Freiburg, Innsbruck, Wien and Göttingen. In 1967 he joined the Institute of Pharmacology at the University of Hamburg where he identified nicotinic and 5-HT_3 receptors as targets of general anaesthetics. Although those findings represented an important modification of the Meyer-Overton hypothesis, they were not appreciated at that time and the relevance of ligand-gated ion channels in the effects of general anaesthetics was generally recognized only 10 years later in 1984. In 1971 he completed his habilitation thesis and in 1976 he became Professor at the University of Hamburg. In Essen (1978-1985) he started to identify presynaptic receptors including autoreceptors for serotonin, together with Eberhard Schlicker; he was the first to identify presynaptic somatostatin receptors (Göthert M, *Nature* 288, 86, 1980) and ACTH receptors. In Bonn (1985-2006) he was director of the Institute of Pharmacology and Toxicology. (i) Together with Gerhard J. Molderings, he studied more than 20 types of presynaptic receptors and became one of the most prolific investigators in this area. (ii) Together with Klaus B. Fink, he showed that ethanol interferes with the transmitter release evoked by N-methyl-D-aspartate (NMDA); in the same year (1989), another group, using an electrophysiological technique, reached the same conclusion. (iii) Together with Heinz Bönisch, Michael Brüss and Martin Barann, he studied naturally occurring mutants of 5-HT receptor subtypes and found altered pharmacological properties of the Arg219Leu 5-HT_{1A} receptor (shown to be associated with major depression) and the Phe124Cys 5-HT_{1B} receptor (probably related to sumatriptan-induced vasospasm). (iv) *In vivo* studies dedicated to presynaptic receptors and ion channels were carried out with Barbara Malinowska (Medical University of Białystok). M. Göthert served as the managing editor of Naunyn-Schmiedeberg´s Archives of Pharmacology (1995-2002) and President of the Federation of the European Pharmacological Societies (2004-2006) and the German Society of Experimental and Clinical Pharmacology and Toxicology (DGPT; 1997-1999). He was member of the National Academy Leopoldina and received honorary doctorates from the medical universities of Białystok (2003) and Katowice (2004).

193

On Futurology of Pharmacology and Toxicology: Ethics, International Education and Research

E. Neu[1], M. C. Michailov[1], M. Sharma-Kaune[1,2], S. K. Gupta[1,3], C. Luetge[1,4], G. Weber[1,5], D. G. Weiss[1,6]
[1]Inst. Umweltmedizin (IUM) c/o ICSD/IAS e.V., POB340316, 80100 M. (Int.Council Sci.Develop./Int.Acad.Sci. Berlin-Innsbruck-Paris,etc.), Muenchen, Germany
[2]All India Inst. Med. Sci., Dept. Pharm., & c/o German & Indian ICSD-IAS Sections, New Delhi, India
[3]All India Inst. Med. Sci., Dept. Pharm., New Delhi, India
[4]Techn. Univ., Inst. Ethics (Dir.), Muenchen, Germany
[5]Univ. Lxbg. and Vienna, Fac.Psychology (Ex-Dean), Vienna, Austria
[6]Univ., Fac. Biol., Inst. Cell Physiology (Dir.a.D.), Rostock, Germany

Introduction: Pharmacology is a basic medical science incl also classical toxicology. In the last decades is founded also an environmental toxicology conc effects of chemicals. For the future it is necessary to constitute a really united *integrative pharmaco-toxicology* in context of an holistic&multidimensional medicine&ecology (ref).

Conception-Results: The best way for realization of this idea would be the foundation of an *International Institute of Pharmacology and Toxicology (IIPT)* via a permanent network of selected institute from some selected countries (e.g. anglo-, franco-, germanophone,etc) in context of interaction of scientific and cultural level as paradigm for future sciences. The IIPT could be related to the projects of the *ICSD* about the foundation of an *International Medical Academy and Hospital* (pharmacology) as well as *International Centre for Ecology* (toxicology).

Aims of this international institute could be to promote 1. International educational programmes for post graduate training in pharmacology & toxicology (physicians, biologists, chemists,etc incl also 2. philosophical fundamentals (human & bioethics, epistemology) as well as 3. interdisciplinarity, i.e. relation to the basic sciences physiology, morphology, genetics, pathology, psychology,etc. Further, 4. foundation of international institutes by association of existing national ones.

Conclusion: Foundation of IIPT under participation of 1-3 universities of selected countries could promote some scientists as *employees of UNO* with possibility for whole life work (acc to Immanuel KANT) incl recognition for intern. professors,

doctors,etc (after 65years - hon dir, scientists,etc), working temporary at univ of countries,e.g. in Athens-Berlin-Bonn-London-Moscow-Madrid-Paris-Rome-Sofia or Amman-Beijing-Cape Town-Jerusalem-New Delhi-Rio de Janeiro-Tokyo-Washington,etc. This way could be supported UNO-Agenda21, leading to better health, education, economy,etc on global level (ref).

see also Michailov,Neu et al (this Congr incl dedication).

References: *Policy:* Intern. Conf. Güstrow-Rostock: Umwelt, Gesundheit, Bildung in Kontext der Agenda21. Regierung Meck.-V. & ICSD-IAS, S.7,235,247,259,279,299. ISBN 300007218-7

Philosophy:FISP2018 Peking Abs-Book 1348-1350,1374-5,1420.

Bioethics:IAB2016 Edinburgh AB 93-95.

Psychology:IUPsyS2021 Prag, Int.J.Psychol.

*Chemistry:*IUPAC2017 São Paulo AB 121, Po-No 2181. IUPAC 2013 Istanbul, AB 224,611,613,1534.

267

Learning Behaviour and Attitude of Medical Students in Clinical Pharmacology at Ulm University – COVID-19 Pandemic-related Changes

S. Hafner[1], O. Zolk[2], H. Barth[1,3]
[1]Institute of Pharmacology of Natural Products and Clinical Pharmacology, University Hospital Ulm, Ulm, Germany
[2]Hochschulklinikum der Medizinischen Hochschule Brandenburg Theodor Fontane, Rüdersdorf bei Berlin, Germany
[3]Institute of Pharmacology and Toxicology, University Hospital Ulm, Ulm, Germany

Introduction: In March 2020, the German government decided a nationwide lock-down in order to contain the COVID-19 pandemic. Schools and universities faced the challenge to establish online education.

Objectives: Within the clinical part of medical studies, clinical pharmacology is a subject with a high study load. The pandemic-related changes of university teaching might affect students' learning habits and needs.

Methods: We conducted regular surveys to identify students' learning behaviour, attitude and needs from winter term 2019/2020 (before the pandemic) to summer term 2021. Coding facilitated the correlation of survey data with the examination mark as an indicator of learning success while preserving participant anonymity.

Results: Overall, 884 students answered the survey (107 – 237 in each semester). 61.1% were female, 38.7 % were male, 0.2% diverse. Over time, the usage of learning materials in print form constantly decreased. While 64.5% of students used paper-based learning scripts in the pre-pandemic cohort, this was true for only 34.5% in summer term 2021. This trend was even stronger for text books with a drop from 35.5% (pre-pandemic) to 13.3% (summer 2021). In turn, the use of digital learning scripts increased and most students used the e-learning tools provided by the institute consisting of medication tasks and comprehension questions (both 68%). Most students stated that their learning habits had changed in comparison to the pre-pandemic period, and that they would prefer a mixture of online and classroom teaching for the future. Learning scripts were considered the most useful learning aid. Video lectures for time-independent attendance were preferred over scheduled lectures.

To identify determinants of learning success, the survey data were correlated with students' grading in the written exams of clinical pharmacology. In the first online semester (summer term 2020), the use of paper-based learning scripts was correlated with better exam grades. No correlation with grade was found for any other learning materials. Age was inversely correlated with exam grading.

Conclusions: The survey shows that learning habits and preferred learning media of medical students have changed in comparison to the pre-pandemic time. In pharmacology teaching, a mixture of online and classroom elements appears didactically appropriate. However, additional efforts are required to implement and optimize alternative teaching formats.

270

Comparison of learning success in pharmacological education between face-to-face and online teaching during the COVID pandemic

E. Moritz[1], T. Kohlmann[2], F. Aschenbrenner[3], M. Wiemann[3], S. Engeli[1], M. V. Tzvetkov[1]
[1]University Medicine Greifswald, Institute of Pharmacology, C_DAT, Greifswald, Germany
[2]University Medicine Greifswald, Institute for Community Medicine, Greifswald, Germany
[3]University Medicine Greifswald, Fachschaftsrat Medizin, Greifswald, Germany

Introduction: The SARS-CoV-2 pandemic has led to a rapid introduction of digital formats into academic teaching. The question remains open to what extent digital formats should be a permanent part of academic teaching after the pandemic. To answer this question, a direct and measurable comparison of the two teaching formats "face-to-face versus online" is missing so far.

Objectives: Following the current regulations in our institution of 50% occupation of the available seats in the seminar rooms (so called "chessboard pattern"), we are performing pharmacological seminars alternating between face-to-face and online via Zoom.

In this study, we took advantage of this close to "cross-over" design between face-to-face and online seminars to analyze the impact of the teaching format on both the subjective and objective learning success in pharmacological education.

Participants & methods: The target population comprises 80 students, which are for pharmacological education divided into two groups (group 1 + group 2). The two groups will alternate between face-to-face and online teaching with each group completing half of the topics in face-to-face and the other half in online seminars (see Figure 1).

The subjective learning success of the students in face-to-face versus online seminars will be assessed by questionnaires at two time points (time point 1: in the course of the semester; time point 2: after the exam). The questionnaires consist of baseline characteristics, e.g. age, gender, previous grades, and questions, e.g. on comprehension, knowledge gain, promotion of interest in the subject. As primary outcome we define the question "Which teaching format was the most helpful in preparing for the exam?"

The objective learning success will be assessed by comparison of the individual results in the pharmacology exam (in total 30 multiple-choice questions for 11 topics). We will compare the correctness of the questions between the topics taught face-to-face and the topics taught online.

The study was approved by the institutional ethics committee. Prior to admission to the study, each student must provide a written informed consent.

Results: The here described study is conducted during the ongoing winter semester. As the pharmacology exam will take place in January, we are looking forward to presenting our results at the 7th German Pharm-Tox Summit in March.

Fig. 1

Figure 1: Pharmacological education in "Chessboard pattern"

Topic (4 h / week)	Group 1	Group 2
1	face-to-face	online
2	online	face-to-face
3	face-to-face	online
4	online	face-to-face
5	face-to-face	online
6	online	face-to-face
7	face-to-face	online
8	online	face-to-face
9	face-to-face	online
10	online	face-to-face
11	face-to-face	online
Exam	30 MC questions	

Toxicology – Toxicological education

36

Development of a Digital Toxicology Lab for high school students within the framework of two Master theses in Educational Sciences (MEd)

J. Ruszkiewicz[1], N. Hettich[1], E. Lorse[1], J. Huwer[1], **A. Mangerich**[1]
[1]University of Konstanz, Molecular Toxicology Group, Department of Biology, Konstanz, Germany

Toxicology is of fundamental social and environmental significance, since it helps us to understand the harmful effects that diverse agents can have on people and the environment and provides information and evidence to reduce the risk of adverse outcomes on human health and the environment. Several educational programs have been established in Germany to account for the need to train professional toxicologist (e.g., Master and PhD study programs and professional certificate programs), however up to now, in schools teaching of basic toxicological principles is largely missing. To approach this issue, we performed an educational pilot project with two Master of Education (MEd) students (i.e., N.H. and E.L.) to put high school students in touch with basic toxicological principles (e.g., dose-response relationship) and to give them first experimental insight into toxicological research. We chose a digital teaching approach by preparing, conducting, and evaluating two complementary digital lessons at a local high school for students of the 11th grade. In preparation of the lessons, N.H. and E.L. conducted experimental wet-lab projects, which provided original scientific data and video material. One project dealt with the analysis of (neuro-)toxic effects of ethanol in *C. elegans* and the other project focused on the cytotoxicity of the chemotherapeutic chlorambucil in HeLa cells. From the videos and experimental data obtained, interactive media were prepared using the H5P software, which was then - together with introductory information, quizzes, and student work assignments - integrated in an all-digital course framework using the Moodle educational platform. The study was accompanied by the evaluation of students" pre- and post-lesson knowledge, intrinsic motivation (KIM test), and school-related self-efficacy expectations (WIRKSCHUL test), as well as individual feedback by students and a high school teacher.

Here, we present an overview on the objectives, overall framework, and evaluation results of this study, which will serve as a starting point for further developments to raise the awareness on the importance of toxicology already at the level of high school students.

Acknowledgements: The project was conducted within the "edu 4.0" program (*Freiräume für die digitale Lehrerinnen und Lehrerbildung*) funded by the *BMBF*. We thank Robert Martena and students the 11th grade of the Humboldt Gymnasium Konstanz for their support and participation.

235

On Application of Angio-Cardiac Fish Preparations in Toxicological Education

M. C. Michailov[1], E. Neu[1], A. Gerdzhikov[1], V. Foltin[1,2], S. Krammer[1,3], J. Foltinova[1,4], G. Stainov[1,5], D. G. Weiss[1,6]
[1]Inst.Umweltmedizin (IUM) c/o ICSD/IAS e.V., POB340316, 80100 M. (Int.Council Sci.Develop./Int.Acad.Sci. Berlin, Innsbruck, Paris, etc.), Muenchen, Germany
[2]St. Elisabeth Univ., of Health and Social Work, Bratislava, Slovakia
[3]IUM c/o ICSD-IAS-Section, Paris, France
[4]Comenius Univ., Med. Fac., Bratislava, Slovakia
[5]Bulg. Acad. Sci., Inst. Systems Engineering & Robotics (ISER), Sofia, Bulgaria
[6]Univ., Fac. Biol., Inst. Cell Physiology (Dir.a.D.), Rostock, Germany

Introduction: Cardio-vascular preparations of frog, rat, rabbit,etc. are till today usual for education&research in toxicology. An essential part of experiments could be replaced by isolated preparations of angio-cardiac fish organs. About various physiological approaches of cardiovascular system incl. blood-pressure is reported [1-6]. Presently are given effects of xenobiotics, esp. motor reactions.

Method: Motor activity (isotonic/isometric rec) of isolated aorta, bulbus as well as atrium, ventriculus cordis of *salmo gairdneri* is registered in Krebs-Henseleit-solution (n=150,p<0.05<0.01)[1].

Results: Bulbus preps. are very sensitive to butanol: threshold concentrations 0.0001%. HgCl2 10-5 mol/l induced contractile responses, contrary to aorta which is insensitive.

Atrium&ventriculus cordis generate spontaneous regular&uniform contractions (6-24°C) (*chronotropic effect*). Ethanol (0.01-0.5%) & butanol (0.001-0.01%) transform regular atrium-contr into burst-like ones. HgCl2 10-8 mol/l also induce similar effect without *inotropic effect*.

Conclusion: Fish angio-cardiac preparations could be used as sensitive indicator for xenobiotics reducing enormous application of various animal organs in education&research, supporting UNO-Agenda21 for better health, education, ecology, economy on global level [6].

Dedication for moral-scientific support 2021-1980/Nobel Laureates (ICSD-IAS members): Austria: K.Lorenz, Australia: Sir J.Eccles, Belgium: I.Prigogine, Canada: G.Herzberg, J.Polanyi, France: J.Dausset, J.-M.Lehn, Germany: M.Eigen, K.v.Klitzing, H.Michel, E.Neher, GB: Sir A.Hewish, B.Josephson, Lord A.Todd, India/USA: S.Chandrasekhar, H.B.Khorana, Japan: K.Fukui, Sweden: S.Bergström, B.Samuelson, USA: P.Anderson, J.Deisenhofer, D.Hubel, L.Pauling, E.Wiesel

Ref. Michailov,Neu et al

physiology: 1. FEPS 2018 London Europhysiol AB:p334P-337P. 2. IUPS-2017-Rio de Janeiro, Abstract-Book ID977,999,1001,1003

pharmacology: 3. IUPHAR 2018 Kyoto Abs.-Book 22093,22127,22330,22335

toxicology: 4. IUTOX 2016 Merida/Mex,Tox.Lett.259S, S109 (2x). 5. EUROTOX 2016 Seville, Tox. Lett.258S, p. S188, 188-189, 304

philosophy: 6. FISP 2018 Peking AB:1348-1350,1374-5,1420.

see also Neu,Michailov et al. (DGPT Congr 2022).

Table

Action of butanol on bulbus cordis:

Isom. contraction (tension in mg)

temp.24°C,n=48,prep.length 7.6±1.4mm

0.0001% 0.1% 1.0%

6.0±8.6 36.6±25.7 153.7±52.9

Author Index